

Alma Mater Studiorum – Università di Bologna

**DOTTORATO DI RICERCA IN  
MECCANICA E SCIENZE AVANZATE DELL'INGEGNERIA  
(DIMSAI)**

Ciclo XXXI

**Settore Concorsuale: 09/B2 – Impianti Industriali Meccanici**

**Settore Scientifico Disciplinare: ING-IND/17 – Impianti Industriali Meccanici**

**GAS DISTRIBUTION: FROM NETWORKS' INTEGRITY MANAGEMENT TO  
NEW SMART METERS' PERFORMANCES TECHNICAL EVALUATION**

**Presentata da:** Dott. Ing. Alessandro Guzzini

**Coordinatore Dottorato**

**Supervisore**

**Prof. Ing. Marco Carricato**

**Prof. Ing. Cesare Saccani**

**Esame finale anno 2019**



## **Abstract**

Safety represents the main goal for Natural Gas (NG) Distribution System Operators (DSOs) that have to operate very complex networks to supply gas to customers. However, the identification of the optimum strategy to manage NG distribution is a very challenging task for decision makers because of the size of the networks. Therefore, priorities have to be identified and many data about the operative conditions of the networks are required. While for the first topic a standardized and internationally accepted procedure has to be identified, for the second one the new NG metering philosophy, i.e. the Smart Metering gas, seems to be appropriate for the scope even if some technical issues have still to be solved.

Consequently, the thesis is divided in two main parts. In the first one, attention is given to the distribution networks and to the proposal of a risk management approach to improve maintenance procedures. Thus, after a brief overview of the sector, existing safety performances of NG distribution sector are analysed. Furthermore, failure causes and consequences are investigated in order to propose a risk assessment approach in NG distribution. A case study is finally examined identifying several positive outcomes respect to the state of the art.

In the second part of the thesis the NG smart metering is analysed with particular attention to the power supply that is one of the technical issues to be overcome for the success of the technology: in fact, because of the use of electrical batteries in smart meters, a limited capacity is now available. Consequently, the estimation of battery supply's operative life is considered an important information for the success of the technology. For this reason, an experimental approach has been proposed and performed to estimate battery's operative life.



# **INDEX**

Introduction to the project .....	7
PART 1: Risk assessment in natural gas distribution networks .....	10
Chapter 1 .....	11
Natural gas: from production to final customer.....	11
1.1 An outlook of international statistics.....	11
1.2 A brief overview of American and European natural gas sectors .....	16
1.3 An insight into Italian natural gas sector .....	19
1.4 Comments.....	31
Chapter 2 .....	32
Technical characterization of NG distribution networks.....	32
2.1 Main components of a natural gas distribution network .....	32
2.2 Installation requirements for natural gas distribution networks .....	59
2.3 Comments.....	61
Chapter 3 .....	63
Risk management of a NG distribution network.....	63
3.1 State of the art.....	63
3.2 Methodologies for risk analysis: ISO 31000 .....	76
3.3 Failure causes of NG distribution networks .....	80
3.4 Consequences of NG distribution accidents.....	130
Chapter 4 .....	142
An innovative method to perform integrity management in NG distribution networks.....	142
4.1 Introduction to the method .....	142
4.2 Step I: Identification of the gas distribution network .....	144
4.2 Step II: Risk identification.....	145
4.3 Step III: Risk analysis.....	148
4.4 Step IV: Risk evaluation.....	153
4.5 Step V: Risk ranking, identification of the priorities and share of the results.....	154
4.6 Application of the proposed risk assessment method to a real case study .....	156
Chapter 5 .....	168
Proposal of a database for NG distribution network failures .....	168
5.1 Reasons for the creation of a failure database .....	168
5.2 Main information required for failure database.....	171
5.3 Future development suggested .....	177
PART 2: Quality and safety performance of smart meters implemented in NG distribution networks .....	180
Chapter 6 .....	181

Natural Gas smart metering: the new philosophy to measure natural gas consumptions.....	181
6.1 Reasons for the introduction of NG smart metering.....	181
6.2 Implementation of the NG smart metering in the Italian market.....	182
6.3 The NG smart meters.....	185
Chapter 7 .....	188
Experimental research about NG smart meters' battery pack performance .....	188
7.1 Reasons and aims of the research activity .....	188
7.2 NG Smart metering communication system description .....	188
7.3 Main technical characteristics of the analysed device .....	191
7.4 Main technical characteristics of the power supply battery pack .....	194
Chapter 8 .....	200
Method and materials .....	200
8.1 Data transmission configurations analysed .....	200
8.2 Instrumentation used during the experimental activity .....	201
8.3 Method.....	205
Chapter 9 .....	209
Results and discussion.....	209
9.1 Available database.....	209
9.2 Electrical loads' characterization.....	210
9.3 Communication characterization.....	211
9.4 Estimation of the batteries' pack capacity .....	223
9.5 Estimation of batteries' operative life .....	225
Conclusions .....	228
References .....	231

## **Introduction to the project**

Natural gas (NG) represents one of the most important source of energy both at the moment and in the next future as reported by available data from several references. As described in the first chapter, many activities have to be performed in order to extract, to transport and to distribute gas to final customers. Furthermore, very complex and large infrastructures have to be managed ensuring the highest level of safety as possible: in order to understand the complexity of these systems, Europe and the United States, where almost 6 million of kilometres of pipelines are operated for the scope, are considered as example. It is therefore immediately clear the human and economic efforts required to reach the maximum level of safety. For the scope, research and development activities are financed by NG operators in order to investigate new solutions able to improve existing performances.

The activities performed in the three years of the PhD course and summarized in the thesis have been financed and supported by the Gruppo HERA S.p.A., the most important Italian energy multiutility distributing more than 1.900.000.000 Sm<sup>3</sup> of gas through the operation of almost 14.000 km of networks and more than 1.4 million of meters installed to the final customers. The project was dedicated to the memory of Simone Messina, a volunteer firefighter, that died with other five people the 24<sup>th</sup> of December 2006 after the gas explosion caused by a gas leakage from the local gas network at San Benedetto del Querceto.

Following this tragic event, many efforts and resources have been spent in order to improve the performances of the gas distribution networks. Collaborations with public authorities have been started in order to exchange information, to increase know-how and to identify critical points. All of these actions ensured a positive improvement of safety performances making always more difficult to reach higher safety levels.

Therefore, many energies have been spent in order to identify the best actions to improve gas distribution sector in the three years. However, two main topics have been identified: the risk analysis of NG distribution networks and the gas smart metering. Following this division, the project activities have been organized in two main parts.

In the first one, the research focused on the possibility to apply risk analysis in NG distribution networks in order to help the Top Management to take decisions. At the moment, in fact, the allocation of the available budget is usually justified on the basis of failure frequency and very poor considerations are made about the possible consequences in case of failure. Furthermore, very poor failure analysis is currently performed making impossible to identify anomalies or trends and so to select the best solutions.

In order to take into account these weak points, integrity management is proposed to NG distributors: in fact, as defined by the Pipeline and Hazardous Materials Safety Administration, integrity management can be defined as a “risk based approach to improve pipeline safety” ensuring also other beneficial outcomes such as the improvement of management, analytical and operational processes, the increase of government’s role in the oversight of operator activities and the improvement of public confidence in pipeline safety.

Unfortunately, no international standard is available in literature about the application of integrity management in NG distribution networks making very difficult the comparison between operators. Moved by this aim, a

procedure is suggested in the first part in order to highlight the potentials but also the criticalities derived from its application. Consequently, the first part of the thesis is organized in the following way:

1. In the first chapter, a brief overview of the NG sector with particular attention to European and American systems is proposed in order to highlight the complexity required to manage NG assets. In order to conclude the chapter an overview of Italian condition is proposed with particular attention to gas distribution.
2. In the second chapter, the main technical characteristics of NG distribution networks are proposed with particular attention to Italian rules that are compared with American ones.
3. In the third chapter the concept of risk management in NG distribution is introduced. In the first paragraphs, an analysis of existing safety trends is performed with available data about international and Italian context. A methodology to perform risk analysis in NG distribution based on available international standards about risk management is proposed in the second paragraph. After that, a review of the possible causes of failure and outcomes following a gas accident is proposed. Because of few data are available in literature, a statistical analysis of accident occurred in American distribution networks is performed finding values that can be used in the integrity management.
4. In the fourth chapter a method to perform integrity management in NG distribution network is proposed. Required steps are defined and explained in the text justifying the importance of each one. In order to show the potential and existing criticalities a case studio about a real network is proposed.
5. In the fifth chapter the creation of a database about gas failures, accidents, and near missing occurred in NG distribution networks is proposed and motivated. For the scope, the main information that should be recorded are identified defining for each one the reasons why it has been selected.

In the second part of the thesis NG smart metering is analysed with particular attention to the technical issue connected to the power supply batteries.

Smart metering can be defined as a new measuring philosophy characterized by a new type of connection between the supplier and the final customer. Respect to the past in which lecturers are present, smart metering requires automatic data communication at predefined time intervals. A great quantity of data is available and can be used in order to improve the safety of NG distribution networks. In fact, new intelligent meters are installed at final customers giving the possibility to create a distributed and organized monitoring system of the gas network especially where the risk is the highest in case of gas leakage.

However, several reasons limit the potentials. The first one is the presence of technical issues that complicate the implementation of the technology. Between them, the operative life of battery power supply represents a challenge for the success of the technology. The second reason is due to the fact that gas smart metering is not a mature technology. The third reason is the few research activities performed until now limiting the beneficial suggestions deriving from the collaborations between sector stakeholders and research centres.

Consequently, the second part of the thesis is divided as follow:

6. In the sixth chapter, the reasons why smart metering has been introduced in NG distribution have been deeper explained proposing a brief outlook of the Italian state of the art with some data and percentages about the implementation. At the end of the chapter, the smart meter has been described reporting main components and functionalities.
7. In the seventh chapter, the research activity about the power supply of smart meters has been reported. In fact, because of many batteries installed in smart meters do not reach the expected operative life, it was decided to start an experimental activity aimed to identify the main factors responsible of the discharge and to suggest new solutions.
8. In the eighth chapter, the material and the method followed in order to perform the experimental activity are detailed described in order to give the possibility to repeat the investigation if of interest.
9. At last, in the ninth chapter, the obtained results for four different configurations of communication are reported and, on this base, suggestions for future research are given.

As clearly stated and repeated through the thesis, even if good results have been obtained thanks to the project, a lot of research is still needed in order to contribute further in the improvement of safety and quality in NG distribution.

# **PART 1: Risk assessment in natural gas distribution networks**

Natural gas (NG) is an odourless, colourless fuel mixture constituted by several substances such as methane (up to the 98%) and hydrocarbons such as ethane, propane and other ones as reported [1] where allowed composition for domestic uses are reported.

That is, being a flammable gas, efforts have to be spent in order to reduce the risk due to a leakage. In fact, the mixture of gas and air can create a flammable atmosphere that start to burn if an ignition source is present and the gas concentration is between the flammability limits (5% and 15%). Therefore, even if NG toxicity is not an issue until CO is formed from a partial combustion, jet flame and explosion represent severe threat to people, buildings and environment.

In order to reduce the probability of gas network failures several actions are planned by NG Distribution System Operators (DSOs) such as the renovation of the oldest and less performant networks, the installation of new ones and the implementation of monitoring and control systems able to identify abnormal conditions and so to generate an alarm. Furthermore, in order to reduce the consequences of failure occurred in the network, inspections are annually planned with the scope to find and to restore failed pipelines, fittings, valves, meters, etc.

However, no standardized rule is present in order to prioritize interventions, especially taking into account that a limited budget is usually available and that it is not usually sufficient for all the networks. Therefore, two possible solutions are present: the first one is the installation of monitoring devices in the networks that constantly monitor the assets while the second one is the optimization of existing procedure. Even if the first one should be preferred, especially in the era of Industry 4.0, more resources than available are required for their implementations such as for the management of data. Therefore, at the moment, priorities have to be identified in order to understand where to install the devices even if in next future an always more implementation of sensors will be possible thanks to the expected reduction of technology costs and to the higher capabilities to manage big data.

Until then, priorities have to be selected. For the scope, a risk based approach has been considered as the most appropriate for the gas distribution networks. For this reason, the main element required to perform risk analysis and to integrate it in integrity management plans are evaluated in this first part. Also the identified lacks, such as the low availability of data about leakages, failures and near missing are discussed introducing potential improvements thanks to their uses.

# Chapter 1

## Natural gas: from production to final customer

Before to analyse safety and quality performances of natural gas (NG) distribution, it is necessary to make a brief introduction about natural gas sector from production to final consumption. For this scope, available data about natural gas reserves, production and consumption are analysed and reported in order to understand social and economic importance of NG nowadays and in future years. After that, the focus is directed to American and the European NG sectors where the penetration of NG in energy sector is becoming always greater. To conclude the first chapter, the analysis of Italian situation is provided. For the scope, a preliminary distinction between transportation and distribution systems is made followed by a more in depth analysis about NG distribution.

### *1.1 An outlook of international statistics*

Despite the increase of renewable sources in order to reach the objectives set out in the Kyoto Protocol and updated with the Paris agreements at the end of 2015 [2], natural gas has still a primary role in energy scenario; in fact, among fossil fuels, natural gas is the preferred ones having the highest heat of combustion [about 50 MJ/kg], being easily conveyed through pipelines for long lengths and being responsible of the lowest environmental impact compared to other traditional fuels in terms of emitted CO<sub>2</sub> [3].

From available predictions, an increase of the U.S consumption of 25% in 2040 respect to the quantity consumed in 2016 is estimated in [4] thanks to a technological improvement and, oil price forecast equal to 109 \$/barrel and an annual growth of energy consumption equal to 2.2%.

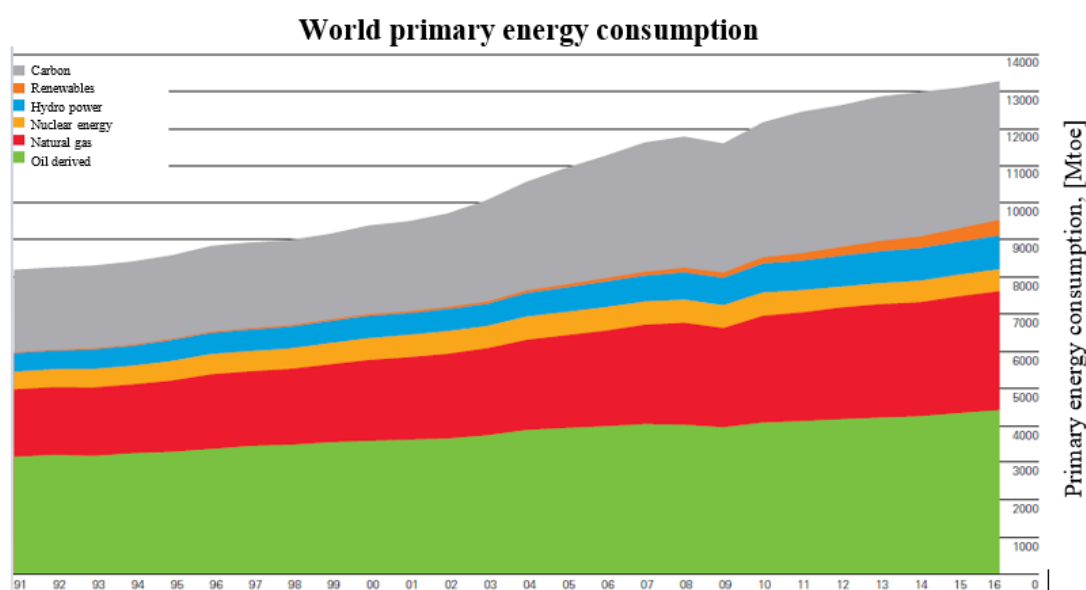
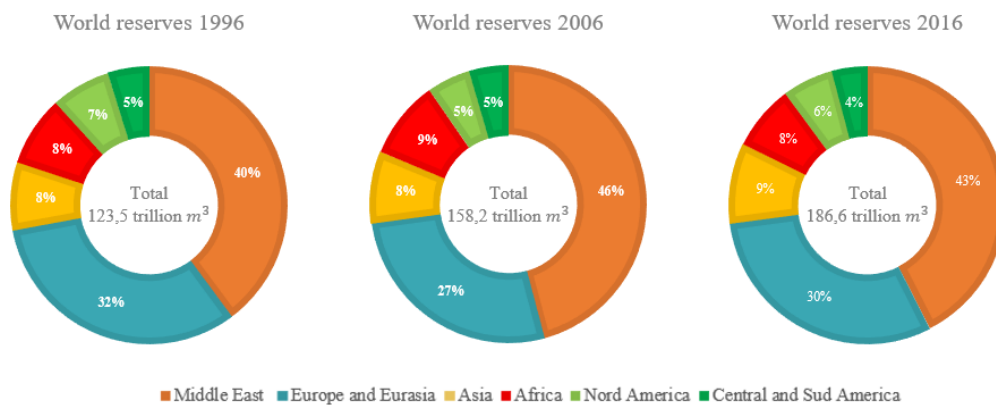


Figure 1. World primary energy consumption by energy source in the period 1991 – 2016. Source [4].

In this scenario, an increase of production longer than 40% is also forecasted. Even if these are only predictions, NG importance appears from available databases. Of the total consumed primary energy in 2016 (13.276

Mtoe), the 24% was supplied by natural gas and the 3% by renewables as reported in Figure 1 were the period between 1991 and 2016 is shown. As shown, NG and renewables were characterized by the highest growth since the beginning of the period even if renewables have still a secondary role considering the supplied quantity.

Therefore, because of it is supposed that NG will still have a primary role in next years, available reserves have to be carefully evaluated. Three different types of reserves are present: conventional, unconventional (shale gas) [5] and methane hydrates reserves [6] that, because of the specific conditions required, are difficult to be commercially exploited. However, considering the other two, only conventional reserves are fully exploited, while shale gas extractions are not. Considering only conventional reserves (Figure 2), the largest reserves of natural gas (42.5% of the total) are located in the Middle East area that is responsible for the 15% of the global gas consumption; Eurasian area with a high density in Russia (central Asia, Siberia, Barents Sea) and in Norway (North Sea) account for the 30.4%.



**Figure 2.** World Natural gas reserves in 1996, 2006 and in 2016; values in percentages. Source [4].

In Figure 3 the estimated gas reserves from 1996 to 2016 are shown. Even if a reduction is reported in 2011 for Russian fields, an annual increasing trend is present reaching a total volume of 186.6 trillion cubic meter in 2016 (+51.1% in 2016 respect to 1996) thanks to the new available extraction technologies.

In Figure 4, instead, the ratio between estimated conventional reserves (R) and production (P) defined as (R/P) is shown finding that Middle East area is characterized by the highest value that is equal to almost 120 years in 2016, two times higher than European and Eurasia area, and almost three times lower than the same value at 1996 because of the increase of extraction activities in the area.

The same conclusion derives from Figure 5 where production is reported for the period between 1996 and 2016. It is interesting to see that Europe and Eurasia are characterized by the highest production followed by the Nord America and that the Middle East area where, however, a great capacity seems to be still unused considering the estimated reserves. In order to reduce the gap, high investments have been made in Middle East in last years. In fact, considering the time derivative of yearly production, it was found that Middle East was characterized by the highest yearly increase of production followed by the North America and the Asiatic area while European production has been almost constant until 2008. To show clearer results a five year moving average is considered in Figure 6.

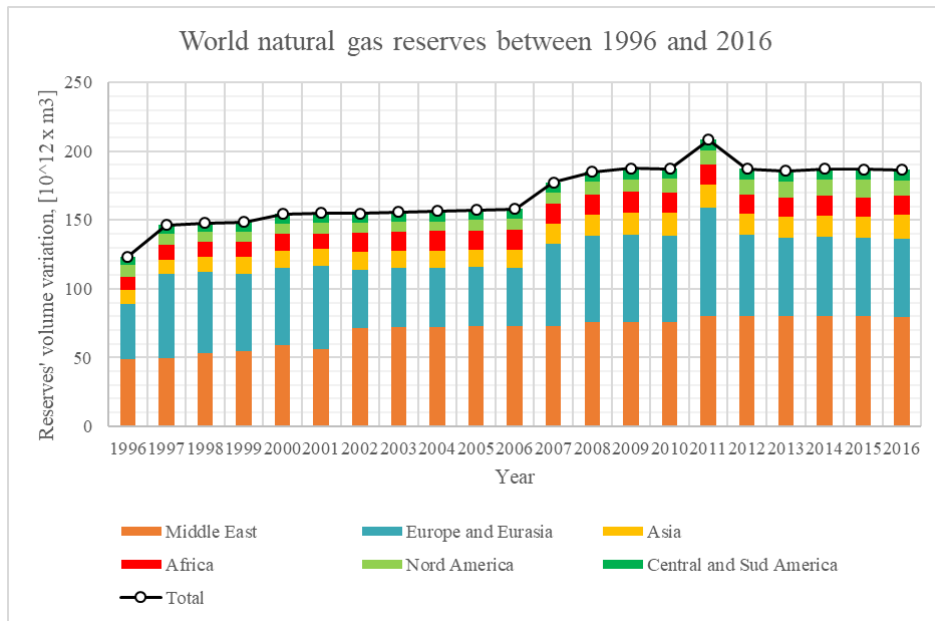


**Figure 3.** Natural gas world reserves respect to 1996.

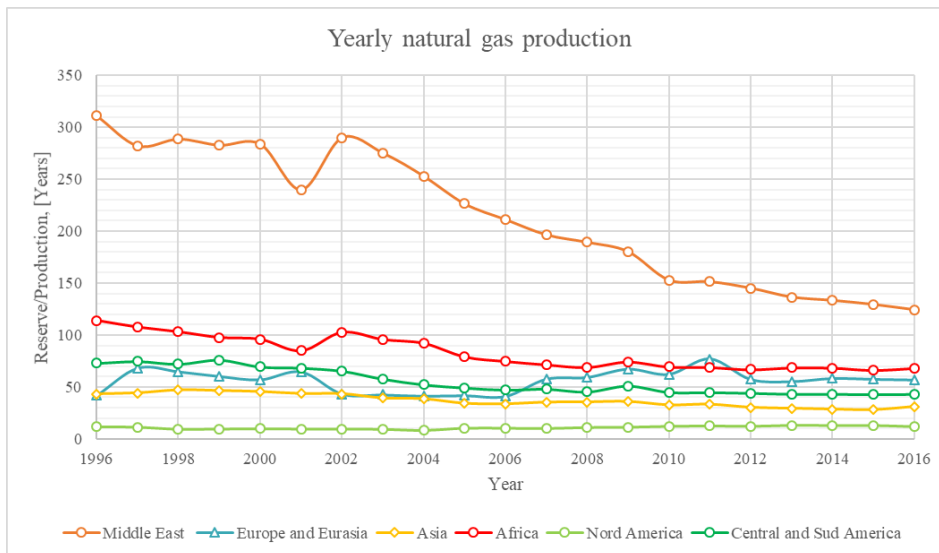


**Figure 4.** Reserves' volumes to Production ratio (R/P) between 1996 and 2016. Only conventional reserves are considered.

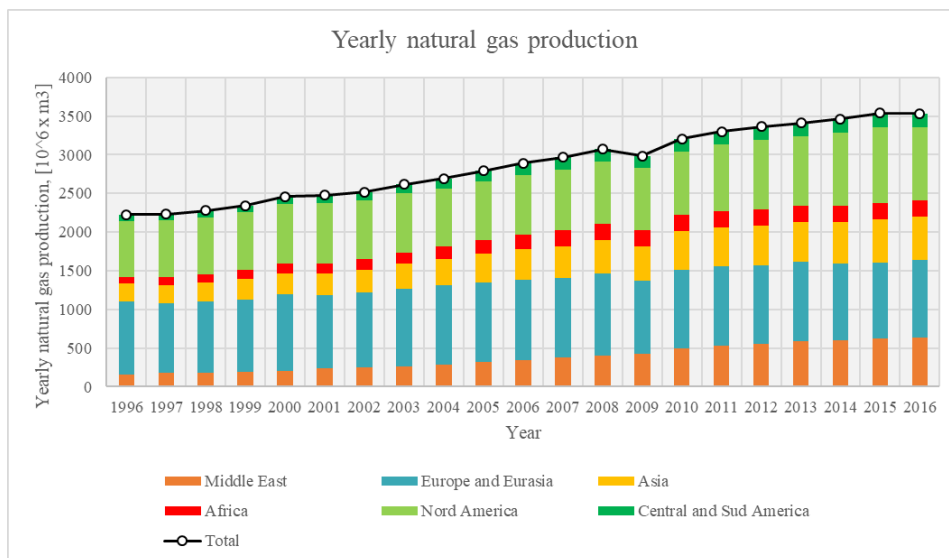


**Figure 5.** Yearly natural gas production from 1996 to 2016.

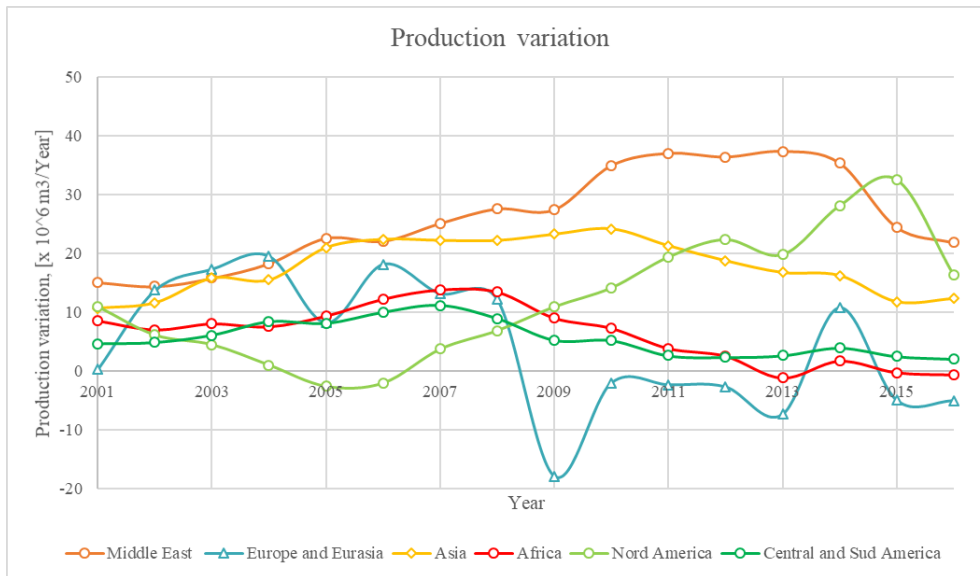


**Figure 6.** Five years' average production variation. Data elaborated from reports published by British Petroleum through the years.

Considering consumption, an increasing trend is observed between 1996 and 2016 with a total increase of almost 55% with a rather constant trend of 2.8%/year as reported in Figure 7. From the figure, the main consumers in the market are North America and Europe followed by Asia.

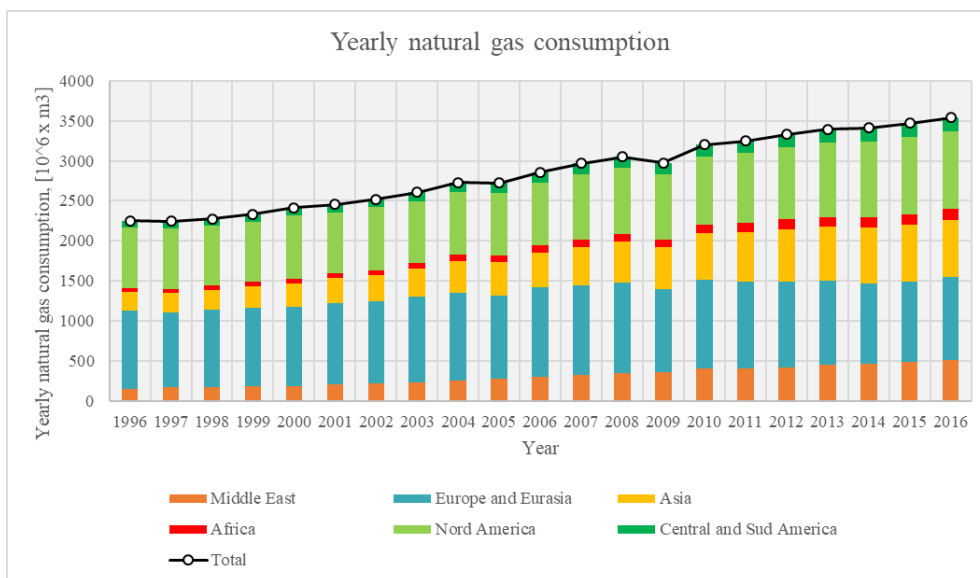


**Figure 7.** Yearly natural gas consumption from 1996 to 2016.

In Figure 8, percentage variation respect to 1996 is reported, it appears that Asia is characterized by the highest increasing trend in the period considered (+204% respect to 1996) while an almost constant consumption is present in Europe and North America, being natural gas an ingrained source of energy with a dedicated and stable infrastructure. Therefore, very high investments are expected in Chinese market to improve gas infrastructure. Consequently, gas sector stakeholders should cooperate and start collaborations in order to create new business and to ensure an exchange of information and resources necessary to assure high quality performances of new systems.

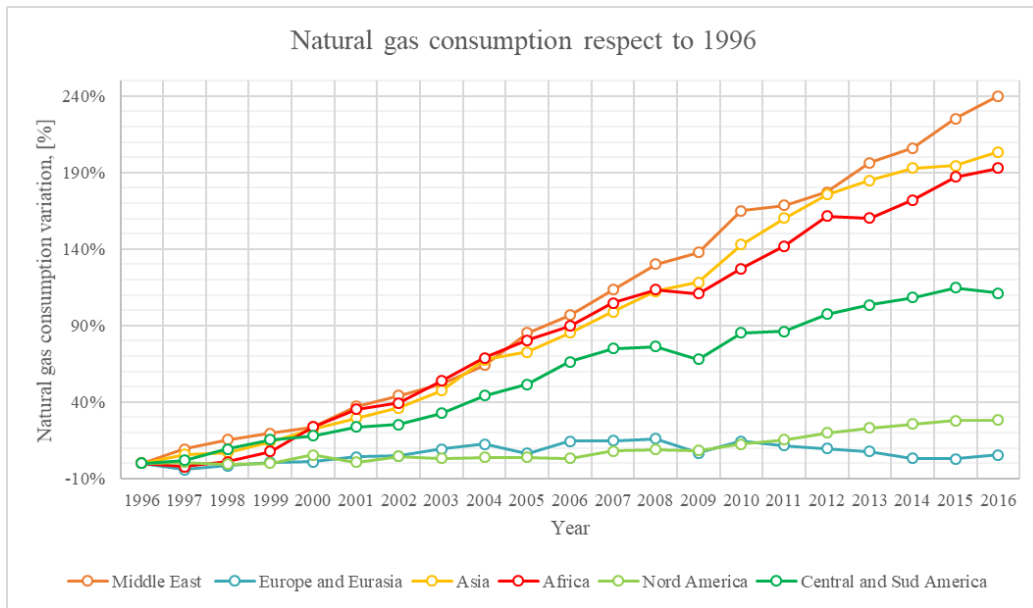


**Figure 8.** Natural gas consumption variation respect to 1996.

To conclude this first section, it has to be noted that long distances separate production to consumption. In fact, not always the produced gas is sufficient to satisfy the internal demand. Furthermore, gas has to be distributed inside the country. For this reason, transportation is necessary.

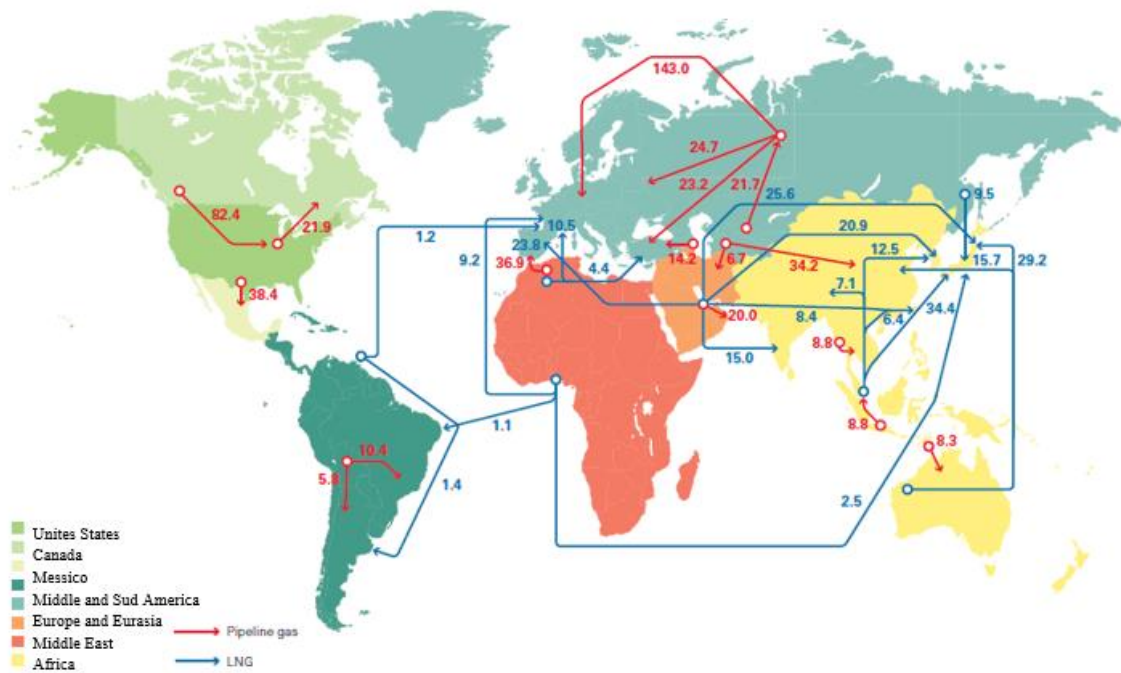


**Figure 9.** Volumes of gas exported in the world through pipelines (red lines) or LNG vessels (blue lines). Source [4].

To convey gas, pipelines or methane tankers are used such as shown in Figure 9 where main world gas exchanges are represented dividing between LNG transportation (blue) and pipeline convey (red). Because of these activities are responsible for a high risk to population, environment and infrastructures, gas companies have to correctly manage all phases from extraction to final distribution for the entire operative life of the system.

## 1.2 A brief overview of American and European natural gas sectors

As shown in previous section, European and North American areas have been characterized by an almost constant consumption since 1996 and therefore it is possible to suppose that they represent a state of the art markets. For this reason, a focus on European and American (i.e. United States) situations is proposed.

Considering Europe, around 500 GSm<sup>3</sup> of gas were consumed in 2016 [4]. Natural gas is the second energy source after oil, covering over a quarter of the final energy consumption since 1996 even if energy policies tend to promote energy efficiency and renewable energies. However, as reported in Figure 10, Germany, United Kingdom, Italy, the Netherlands and Spain were the European countries with the highest natural gas consumption in 2014 with a total of 226.5 Mtoe in 2014. It is interesting to note that France, even if it is one of the main consumer, is less influenced by gas availability thanks to nuclear penetration [7].

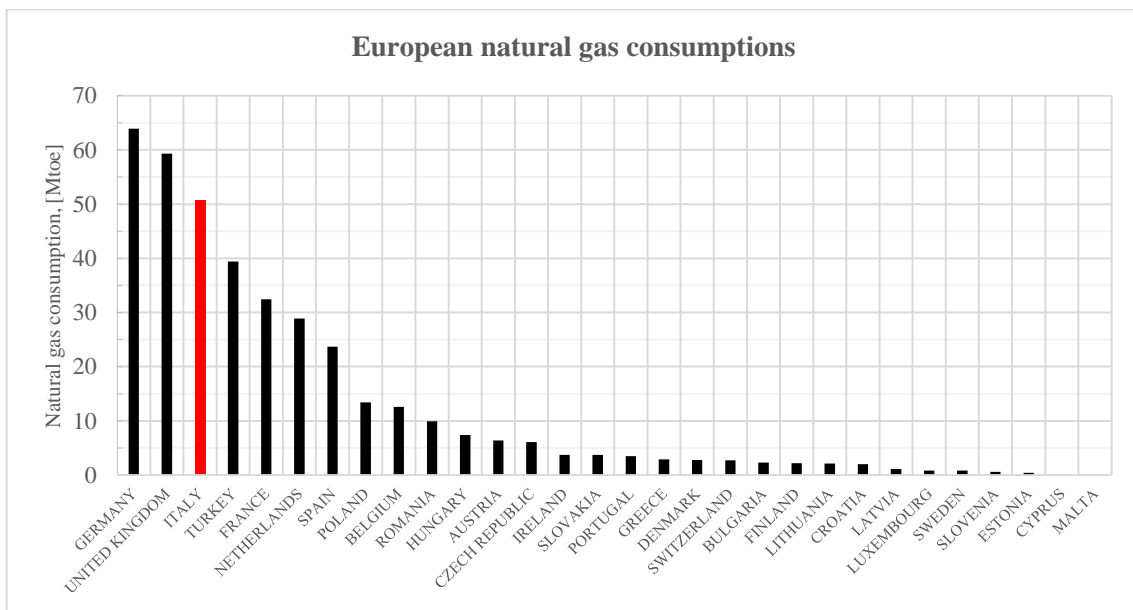


Figure 10. Natural consumption in European countries in 2014. Source [7].

In order to characterize these consumptions, the final use of natural gas has to be analysed. For the scope the following are introduced: residential and commercial sector, industry, power generation, transportation and other uses. That is, the greatest amount of NG consumption is due to residential and commercial sectors as where it is used for heating and cooking purposes (Table 1). So, an almost constant value is reported through the years. In 2014 it represented 41.5% of the total. Industrial sector, instead, has been characterized by a decreasing trend in the period between 2008 and 2014. The reasons can be found in the economic crisis that reduces the productivity and so gas consumption but also in the implementation of more efficient technologies in product cycles. Energy production was responsible for the 22.8% of European total consumption in 2014; it should be noted that a decline occurs from 2008 because of the contemporary reduction of energy demand, the reduction of energy price in the market and the always more production from renewables plants. Last, transport and other uses account for a very low consumption that represents the 2.8% of the total. In fact, very few national markets are characterized by a high use of natural gas for transportation system as occurred, for exemple, in Italy.

**Table 1.** European natural gas consumption for different sectors from 2008 to 2014 [TWh].

Year	2008	2009	2010	2011	2012	2013	2014
<b>Residential and commercial</b>	2066	2069	2260	1793	2050	2160	1852
<b>Industry</b>	1731	1574	1603	1692	1575	1551	1471
<b>Energy production</b>	1555	1406	1659	1481	1242	1130	1016
<b>Transport</b>			16	16	20	20	19
<b>Other use</b>	238	197	112	149	175	135	105
<b>Total</b>	5590	5245	5650	5130	5061	4996	4463

The same analysis is made the United States. Data are reported in Table 2. From these an increasing trend of consumption is observed between 2008 and 2014 (+14.8%) respect to the decreasing trend observed in Europe (-20.2%) in the same period that can be explained by the substitution of carbon to reduce environmental impact.

**Table 2.** American natural gas consumption for different sectors from 2008 to 2015 [TWh]. Source [8].

Year	2008	2009	2010	2011	2012	2013	2014	2015
<b>Residential and commercial</b>	2414	2365	2357	2351	2111	2463	2583	2367
<b>Industry</b>	2369	2230	2426	2486	2585	2679	2767	2767
<b>Energy production</b>	2001	2058	2206	2260	2722	2455	2451	2909
<b>Transport and other use</b>	203	210	211	215	229	260	223	215
<b>Total</b>	6987	6863	7200	7312	7647	7857	8024	8258

However, the main difference respect to Europe is present in energy production and industrial sector. In fact, energy production accounts for the highest consumption in 2015, while industry presents a constant increasing rate through the years (+16.8%). As for European case, residential and commercial sectors present a nearly constant trend that depends on yearly climatic conditions.

Consequently, a different strategy between Europe and Unites States was present in the analysed period. This situation can be justified by the presence of large amount of shale gas in the United States which reserves have been estimated equal to 5.900 billion m<sup>3</sup> [9]. In fact, the exploitation of these has been increased through the years in order to reach an energy independence respect to other foreign countries.

About NG infrastructure similar conditions has been found in the considered areas. To supply gas to final customers (more than 67 million in EU [7] and 70 million in US in 2014 [10]), in fact, transportation and distribution pipelines, that represent the main part of the part of the system, are designed, installed and operated with thousands of devices that are necessary to control and monitor the state of the system.

That is, the total length of European gas networks has increased from 2.044.000 km at the end of 2010 to almost 2.215.000 in 2015 with an increase of 8.4% [7,11]. Unfortunately, no distinction is made between transport and distribution system in the reports and so between high pressure (transportation lines) and low pressure pipelines (distribution networks). Considering the first seven countries in Europe that accounts for the 88.4% of total consumption, a total length of 1.368.931 km has been found for distribution systems at 2014 [12]. However, it is observed a different strategy for each country through the years: for example, the most industrialized ones such as Germany, Italy, France increased the available infrastructure of 14%, 2.4% and 1% respectively between 2008 and 2014; vice versa, Netherlands reduced the total length of the system of 11% in accordance to a consumption reduction equal to 26%.

European natural gas system is reported in Figure 11. Only high pressure transportation pipelines are reported.

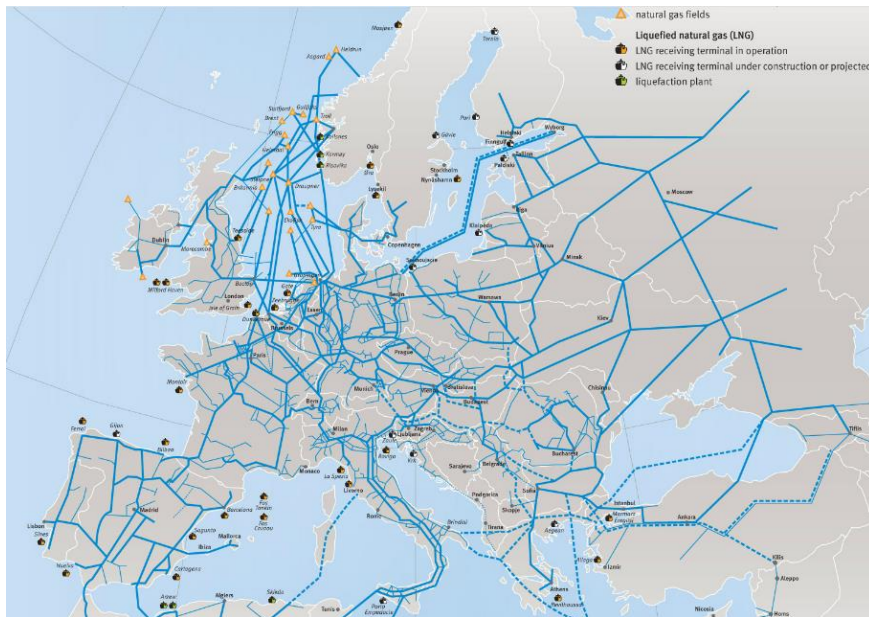


**Figure 11.** European natural gas networks in 2015. Only transport pipelines are shown in the figure. Source [7]. A more detailed map can be find at [13].

Considering the same period, in the United States the overall length of the networks increased from 3.676.340 km to 4.009.349 km with an increase of 9.1% that is similar to European situation; of these 3.524.692 km are low pressure distributed pipelines installed near to end users [14].

In Figure 12 the most strategic pipelines of U.S. natural gas system are reported.

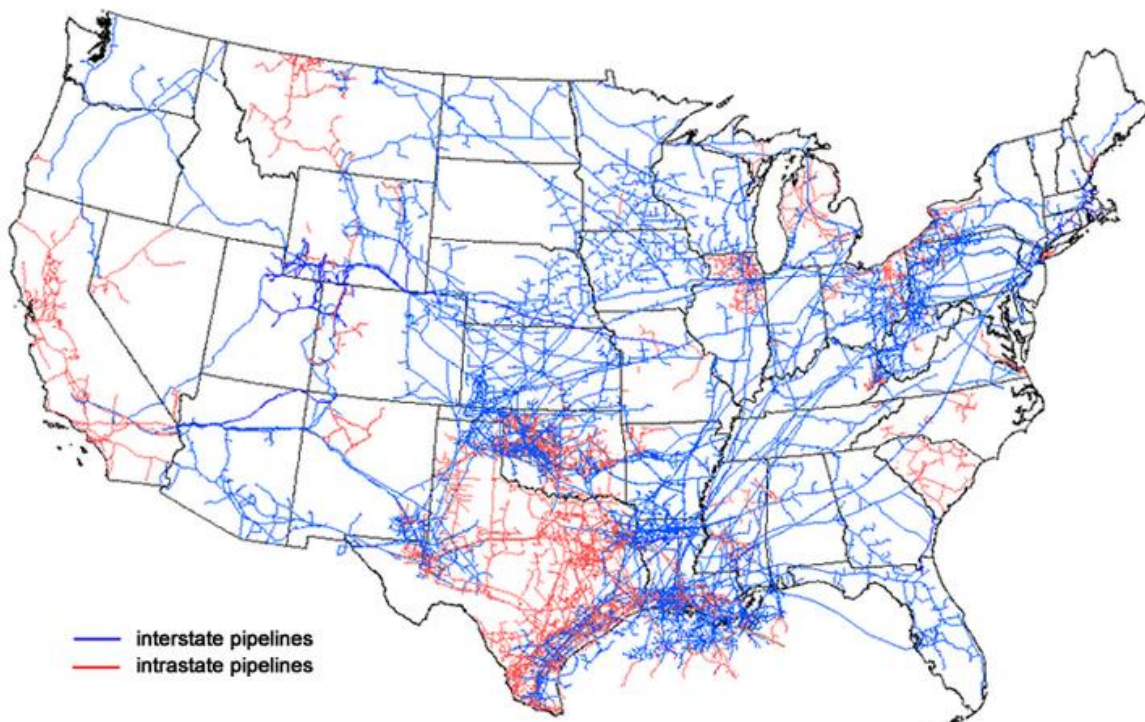


**Figure 12.** U.S. natural gas system. Source [10].

Even if not shown in the figures to make clearer the image, the presence of distribution networks in the territory is responsible for a very branched configuration, increasing the risk to surrounding people and environment in case of failure.

From a technical point of view, different materials can be used in distribution networks in both regions. Statistical data are respectively reported in [12] for EU and [15] for U.S.

Even if data are updated to 2014 and consider only 18 countries, in European distribution mains polyethylene (51.8%) is the most used material, followed by steel (36.8%), cast iron (4.2%) and other materials as for example copper (7.2%). In last years, in fact polyethylene pipes have substituted other materials thanks better performance at low pressures.

Similar percentages are present in the United States distribution mains where plastic pipelines have reached the 57.7% of the total length followed by steel with the 40.6%, iron (1.9%) and other materials (0.10%) in 2017. To compare with European situation percentages at 2014 are reported for plastic, steel, cast iron and other materials as following: 54.5%, 43.0%, 0.1% and 2.4%. If also service pipelines are considered, a higher percentage of plastic can be expected thank to the characteristic lower pressure of this part of the system.

From the reported analysis it appears a very similar technical development of European and American natural gas systems; particularly technologies research and investments have been focused in the same direction in order to substitute old and vintage cast iron pipelines with new and more performant plastic pipes.

In the next paragraph, the attention will move to Italy in order to identify the potential and the issues that all natural gas sector stakeholders have to overcome to operate correctly the system, from the design phase to its abandonment. Also, difference between regions are presented in order to understand in which part of Italy NG is a strategic source of energy.

### ***1.3 An insight into Italian natural gas sector***

Italian NG sector has several affinities with those presented in previous paragraph; however, a more focused analysis seems to be useful for the scope of the thesis.

Considering national energy balance, Italian situation is similar to other main industrialized European countries. Particularly, a reduction of gas consumption has been reported in the period between 2008 and 2016 (-17.4%) with a consequently reduction of import (-15.1%) and of national production (-37.6%) [16]. Energy balances are reported in Table 3 for the considered years.

**Table 3.** Voice of the Italian national energy balance about natural gas [Gm<sup>3</sup>] from 2008 to 2016. Source [16].

Year	2008	2009	2010	2011	2012	2013	2014	2015	2016
<b>National production (P)</b>	9.3	8.0	8.4	8.4	8.6	7.7	7.1	6.8	5.8
<b>Import (I)</b>	76.9	69.3	75.4	70.4	67.7	62.0	55.8	61.2	65.3
<b>Export (E)</b>	0.2	0.1	0.1	0.1	0.1	0.2	0.2	0.2	0.2
<b>Net imports (N = I – E)</b>	76.7	69.1	75.2	70.2	67.6	61.7	55.5	61.0	65.1
<b>Stock changes (S)</b>	1.1	-0.9	0.5	0.8	1.3	-0.6	0.8	0.2	-0.1
<b>Gross consumption (G = P + N – S)</b>	84.9	78.0	83.1	77.9	74.9	70.1	61.9	67.5	70.9
<b>Losses (L)</b>	1.5	1.3	1.8	1.8	2.0	1.9	2.0	2.0	2.0
<b>Available for final consumption (F = G – L)</b>	83.4	76.7	81.3	76.1	72.9	68.2	59.9	65.6	68.9

It has to be noted that losses, which represent the amount of energy consumed or lost during transportation and distribution, have been characterized by an increase reaching the 3% of the net available quantity. This result

is difficult to be justified because a reduction of transported natural gas occurs in the period. So a decrease of transport efficiency has to be considered as possible cause. That is, considering an average selling cost of 24.7 c€/Sm<sup>3</sup> [17], a total yearly economic loss equal to 50 M€ can be estimated.

A reduction of energy consumption is reported in Table 4 where different energy sources are reported. Two reasons are considered in order to justify the reduction of consumption: the technological improvement and the penetration of renewables. The second reason was possible thanks to national incentives that were principally concentrated in energy production where gas presents the highest reduction in the period (-48.3%) as reported in Table 5.

As in other countries, residential and commercial sectors have a nearly constant consumption which annual variations depends on the external climatic conditions. This results from heating demand even if a slightly reduction is expected in future thanks to the increasing implementation of renewable sources such as biomass, solar thermal and heat pumps [18,19].

However, natural gas will still represent a primary source of energy in future as justified by the investments made to improve existing performances. In fact, despite the reported reduction of consumption, Italian gas system increased from 271.978 km in 2008 to 294.922 km in 2014 (+8.4%). Of this improvement the main part was concentrated in distribution networks.

Therefore, the reported conditions clearly highlight the importance of natural gas respect to national strategies.

**Table 4.** Italian primary energy consumption for energy source in [Twh]. Data from Eurogas' reports.

Year	2008	2009	2010	2011	2012	2013	2014
Primary energy consumption, [Mtoe]	2235	2098	2156	2069	2001	1924	1936
Primary energy from natural gas, [Mtoe]	814	743	791	742	714	668	671
Primary energy from other fossil fuels, [Mtoe]	1122	1018	679	998	933	856	824
Primary energy from renewables and hydroelectric, [Mtoe]	197	225	259	285	312	357	411

**Table 5.** Natural gas consumption for different end – customers [TWh]. Data from Eurogas' reports.

Year	2008	2009	2010	2011	2012	2013	2014
Residential and commercial, [TWh]	316.4	338.4	359.8	330.4	330.0	312.3	273.3
Industry, [TWh]	194.3	166.9	171.3	169.2	166.4	161.8	161.6
Energy production, [TWh]	363.0	298.6	320.6	295.9	265.7	228.3	187.6
Transport, [TWh]	24.6	22.1	8.8	9.2	9.6	10.4	11.1
Other, [TWh]			17.5	19.5	21.0	19.8	21.6
Total, [TWh]	898.3	826.0	878.0	824.2	792.7	732.6	655.2

As reported in in previous sections, European countries import large quantities of gas because of the indigenous production is in the most cases insufficient. For the scope, natural gas is transported through pipelines or LNG carriers that connects production sites with different end-users overcoming large distance: for European area, Russia (27% of the total gas that is consumed), Norwegian (24%), North African territories (Algeria, Nigeria and Libya with respectively the 8%, 1% and 1%) and the Middle East (Qatar with the 5%) are the main exporters. In order to ensure NG availability, gas system has to be characterized by the highest performances as possible in terms of quality and supply safety being a flammable gas [20].

To transport and distribute gas, two systems characterized by the different operative conditions are usually identified: the transportation and the distribution systems.

As shown in Figure 13, natural gas is firstly conveyed through national and regional high pressure pipelines. Before to enter into distribution networks, a pressure reduction and flowrate measurement is made in the so called ReMi station (“Regolazione e Misurazione” in Italian standing for Pressure Reduction Stations); also, being the natural gas inodour, odorization is performed to ensure its smelling in case of leakages. After the treatment and the fiscal measurement, natural gas is supplied inside distribution networks to be supplied to final customers at a pressure lower than 5 barg. Successive pressure reductions can be present in the network in order to ensure the correct boundary conditions at customer meter before to enter in the domestic gas plant.

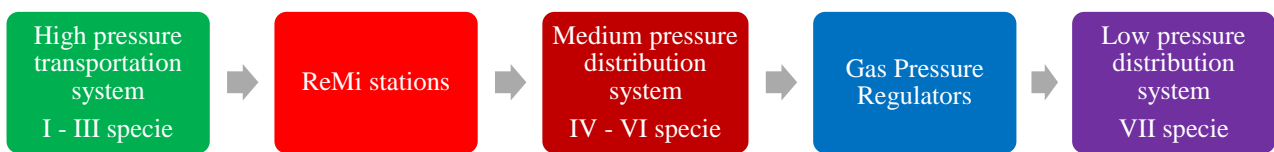


**Figure 13.** Functional diagram of the national gas network considering different classes as reported in Table 6.

That is, different classes (called as “specie” in Italian) are identified in order to characterize different operative pressures and so rules to be respected (Table 6) in Italian gas system.

**Table 6.** Italian natural gas systems as a function of operative pressure. Transportation and distribution systems are highlighted in the third column.

Classes	Operative pressure (relative to atmosphere)	Transportation/Distribution	Definition in accordance to (D.M. 24/11/1984)
<b>I specie</b>	$> 24 \text{ bar}$	Transportation	High pressure
<b>II specie</b>	$\in [24; 12[ \text{ bar}$	Transportation	
<b>III specie</b>	$\in [12; 5[ \text{ bar}$	Transportation	
<b>IV specie</b>	$\in [5; 1.5[ \text{ bar}$	Distribution	Medium pressure
<b>V specie</b>	$\in [1.5; 0.5[ \text{ bar}$	Distribution	
<b>VI specie</b>	$\in [0.04; 0.5[ \text{ bar}$	Distribution	
<b>VII specie</b>	$< 0.04 \text{ bar}$	Distribution	Low pressure

From the brief introduction, it is clear that different owners and responsibilities are recognized depending on the part of the system:

- *Transportation system:* Transportation System Operators (TSOs) are responsible;
- *ReMi stations and distribution system (medium and low pressure):* Distribution System Operators (DSOs) are responsible up to customers’ meter.

To introduce Italian natural gas distribution system, some data about transportation system and ReMi stations are given in next two sections. This is considered very useful by the Author to highlight the technical complexity involved in the convey of gas from import points to final customers.

### 1.3.1 The transportation system

As already reported, only a small percentage of national consumption is produced in Italian fields while the main part is imported from foreign countries. To assure gas import, Italian gas Transportation System is connected to foreign infrastructures at the so called “Import Points” where gas passes through; the following Import Points are in Italy [21]:

- Five Import Points, located at Mazara del Vallo (*Trapani – Sicily*), Gela (*Caltanissetta – Sicily*), Passo Gries (*Verbano Cusio Ossola – Piedmont*), Tarvisio (*Udine – Friuli Venezia Giulia*) and Gorizia (*Friuli Venezia Giulia*), connect national system with foreign transportation pipelines;
- Two Import Points, located at Panigaglia (*La Spezia – Liguria*) and Porto Viro (*Rovigo - Veneto*), ensure the connection with gasification plants;
- Two Import Points, located at Campo Collalto (*Treviso – Veneto*) and Montalfano (*Chieti – Abruzzo*), assure the exchange of gas with existing storage plants;
- Fifty-one Import Points from national extraction fields.

From the operative point of view, Transportation System is operated at a pressure between 24 barg and 75 barg and it is divided into a National System which size is approximately 10.200 km (the "Primary Transportation System") and Regional System which size is approximately 24.700 km (the "Secondary Transportation System"). The main difference between the two system is the end scope.



**Figure 14.** Italian Transportation System: Primary and Secondary Transportation Systems respectively in blue and grey. Source [21].

The Primary Transportation System consists of a main network that connects the North with the South of Italy conveying gas from Import Points to the Interconnection Points with the Secondary Transportation Systems and the storage plants located in the territory. The Secondary Transportation System, instead, is responsible

for the distribution of gas through the national territory and particularly to power plants and to local distribution networks with which is connected through ReMi stations.

For the scope, 20 Interconnection Points (defined as “Nodes”) and 567 ReMi station plants are running in Italy. In Figure 14 only the Transportation System managed by SNAM (in Italian “Società Nazionale Metanodotti), that is the most important Italian Transportation System Operator, is shown. In fact, it should be noted that nine TSOs are present in Italy but the 93.2% of the system is controlled by SNAM [16].

Since a high capacity is required, high operative pressures are necessary to transport gas through Transportation networks that are designed, installed and operated in accordance to existing technical rules [22,23]. Considering a gas flowrate  $G$  in [kg/s], the following equation is used to design it in accordance to the criteria of minimum cost:

$$G = \pi \frac{D^2}{4} \times \rho \times v = \pi \times \frac{D^2}{4} \times \frac{p}{R \times T} \times v \quad (1-1)$$

Where  $D$  is the internal diameter in [m],  $p$  is the operative pressure in [Pa],  $R$  is the methane gas constant equal to 519.6 [J/(kg K)],  $T$  is the gas temperature in [K] and  $v$  is the gas velocity in [m/s]. As reported in the equation, high mass flowrates can be obtained increasing pressure. Usually velocity is not increased to limit pressure drops and so energy consumption due to transportation:

$$\Delta p = \Delta p_{\text{dist}} + \Delta p_{\text{loc}} = \left( \lambda \frac{L}{D} + \xi \right) \rho \frac{v^2}{2} \quad (1-2)$$

Where  $\Delta p_{\text{dist}}$  e  $\Delta p_{\text{loc}}$  are respectively the distributed and local pressure drops in [Pa],  $L$  is the length of the pipeline in [m],  $\lambda$  is the friction factor in [#] that depends on flow and pipeline characteristics,  $\xi$  is the local loss coefficient in [#] that is function of the hydraulic element. To overcome existing pressure drop, gas compression plants are installed along the network. Particularly, 11 compression plants consisting of centrifugal compressors for a total installed capacity of 922 MWe are installed along the Primary Transportation System [21]. These compression plants are characterized by a pressure ratio between 1.4 and 1.5 that require a minimum pressure of 50 barg upstream the compressor considering an operative pressure of 75 barg.

Because of part of the imported gas has to pass through regasification terminals before to be introduced in the Primary Transportation System. Regasification terminals allow the transformation of Liquefied Natural Gas (LNG) and its introduction into the system. In fact, in the case that natural gas cannot be transported through pipelines from production to consumption site, LNG vessels are used: from a supply point of view, LNG importation ensures a greater reliability than pipelines because of vessels do not pass through politically unstable areas as can occur with the pipelines which operation depends on the decisions of the governments of territories crossed.

Last but not least, storage plants are present in order to compensate fluctuations of gas demand and supply in the different periods of the year. Storage plants work as an accumulator when importation is higher than demand or as a source when consumption is higher than importation. In fact, it has to be highlighted that gas

importation is almost constant through the year while the demand has a variable trend with a maximum in winter and a minimum in summer because of the influence of weather on the demand of residential and customer sectors.

### 1.3.2 The pressure reducing and measuring station (ReMi station)

The physical separation between transportation and distribution systems is located at the Pressure Reduction and Metering stations (called in Italian “ReMi” stations that stands for **R**egolazione e **M**isurazione). In ReMi stations the following operations are performed:

- *Natural gas pressure reduction.* In order to convey gas through distribution networks, pressure has to be reduced in accordance to pressure levels defined in technical standards [23]. Valves or turbo-expander generators are usually used for the scope. In both cases, however, a contemporary temperature reduction occurs increasing with the total pressure drop across the ReMi stations. Considering the valve case, an isenthalpic process can be assumed and the following energy balance defined:

$$H_{in} = H_{out} \rightarrow c_p(p_{in})T_{in} = c_p(p_{out})T_{out} \quad (1-3)$$

Where H is the enthalpy of the gas in [J/kg],  $c_p(p)$  is the specific heat of the gas at the pressure p in [J/kgK], T is the temperature in [K] while the subscript in and out represent respectively upstream and downstream condition.

To avoid the formation of hydrates due to excessive temperature reduction because of the increase of  $c_p$  [24], natural gas is pre-heated before pressure reduction in the case upstream pressure is higher than 12 bar because of the accumulation of hydrates in the section of the pipes increases the risk of service interruption. A traditional boiler or a heat pump can be used for the scope.

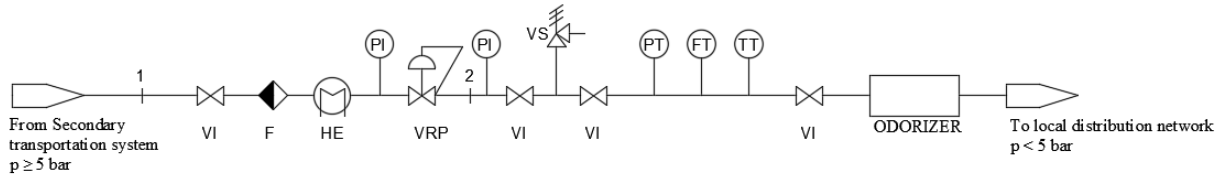
- *Fiscal mass flow rate metering.* Natural gas mass flowrate is measured in accordance to [25] that specify different technologies available for the scope as gas piston, diaphragm, turbine and, for higher flows, Venturi meters ( $G \geq 12,000 \text{ m}^3/\text{h}$ ,  $D \geq \text{DN}100$ ,  $\Delta p \geq 2\text{bar}$ ).
- *Gas odorization.* An odorant is added to the gas flow in the last section of the ReMi station. In accordance to [25], the odorant consists of a mixture of mercaptan or a substance containing tetrahydrothiophene (THT). In fact, being odourless and flammable, leakages of gas can be responsible for very high risk to surrounding people;

Considering plant layout, several configurations have to be considered as a function of the required availability and of the type customers to be supplied. Therefore, different levels of reliability can be achieved simply modifying the design of the plant. However, a general Process Flow Diagram (PFD) is reported in Figure 15. From left to right the following elements are present upstream the pressure reduction element that is represented as a pressure reduction valve:

- A shut off valve to close the line in case of downstream problems;
- A filter to block particles that are present in the flow;
- A heat exchanger can be present if a pressure higher than 12 barg is measured.

- Instrumentation as pressure, temperature and flowrate transmitters are installed to control and to monitor the working conditions.

### Process Flow Diagram (PFD) of a typical ReMi station



*Legend:*

- VI = Shut off valve;
- F = Filter;
- HE = Heat Exchanger (only if  $p_1 > 12$  bar);
- VRP = Pressure Reduction Valve. Also turbo - expander generator can be used;
- PI = Pressure indicator;
- VS = Safety valve;
- PT = Pressure transmitter;
- FT = Flowrate transmitter;
- TT = Temperature transmitter

**Figure 15.** Simplified Process Flow Diagram (PFD) of a typical ReMi station.

The thermodynamic transformation that verifies through the valve is reported in the  $\log(p) - H$  diagram (Figure 16).

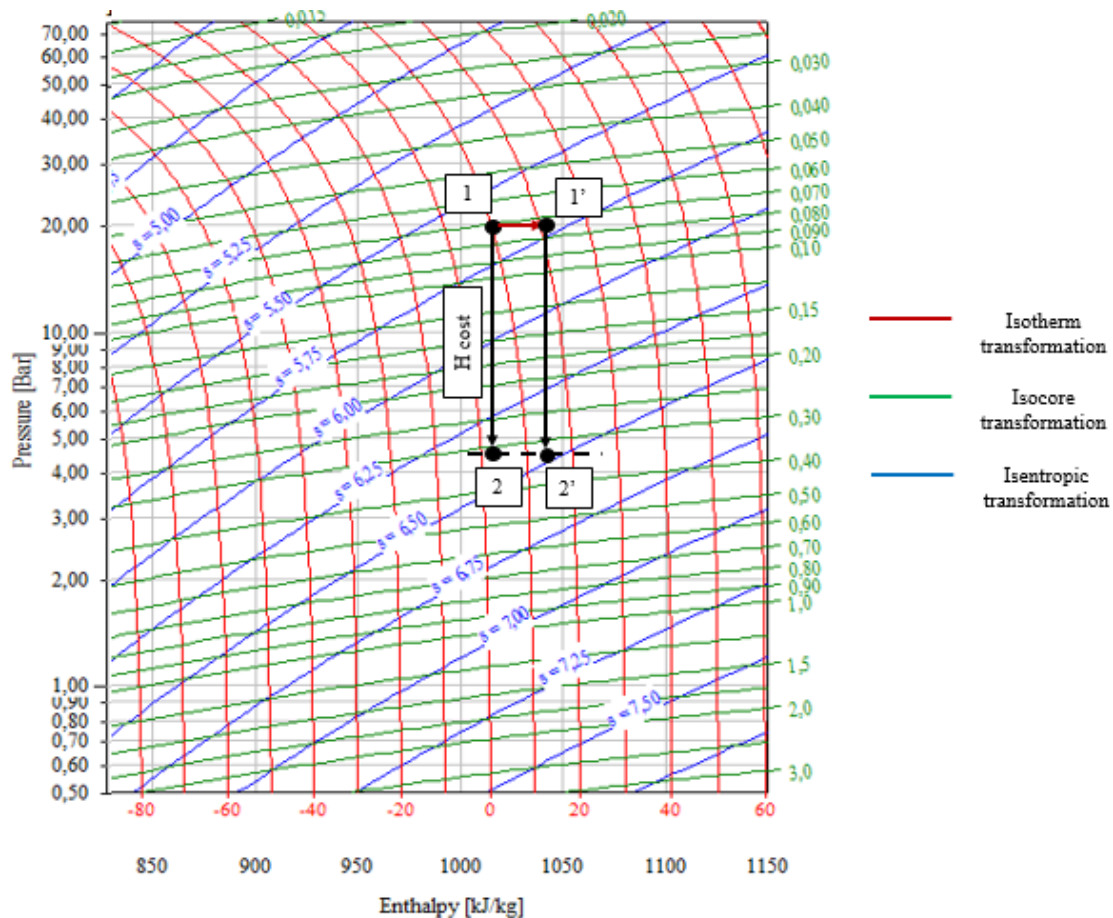


**Figure 16.**  $\log(p) - H$  diagram of the transformation occurring to natural gas through the ReMi station with particular attention to the section of pressure reduction.

As shown, because of the variation of  $c_p$  during the lamination, a temperature reduction occurs. Considering an inlet pressure of 20 bar, gas temperature at the outlet of the plant depends on inlet conditions: in the case a temperature equal to 10 °C is present, a gas temperature near to 0 °C is verified at the outlet with a high risk of hydrate formation. This result justifies therefore the thermal treatment before the pressure reduction section.

The required thermal power to be supplied to the gas flow  $Q_{heat}$  [kW] can be calculated as follow:

$$Q_{heat} = G \times (H_{1'} - H_1) \quad (1-4)$$

Where  $G$  is the gas flowrate though the ReMi station in [kg/s],  $H_{1'}$  is the enthalpy of the methane at the defined temperature in order to avoid hydrate formation after lamination in [kJ/kg] while  $H_1$  is the enthalpy of the gas at the inlet conditions ( $p_1$  and  $T_1$ ) in [kJ/kg].

### 1.3.2 The distribution system

Natural gas distribution networks ensure the supply of natural gas to final customers. Therefore, a brief overview of the natural gas sector is reported before to present the main technical and operative characteristics.

#### 1.3.2.1 Overview of Italian natural gas distribution sector: some data

Almost 30 GSm<sup>3</sup> of natural gas are annually supplied to more than 20 million final customers that are mainly present in the North of Italy and particularly in Lombardy, Emilia Romagna, Veneto and Piedmont that are respectively responsible for the 26%, 13%, 12% and 11% of the total consumption. South and Central Italy, instead, reached together a total consumption equal to 30 thanks to the fact that heating is less critical than in northern regions.

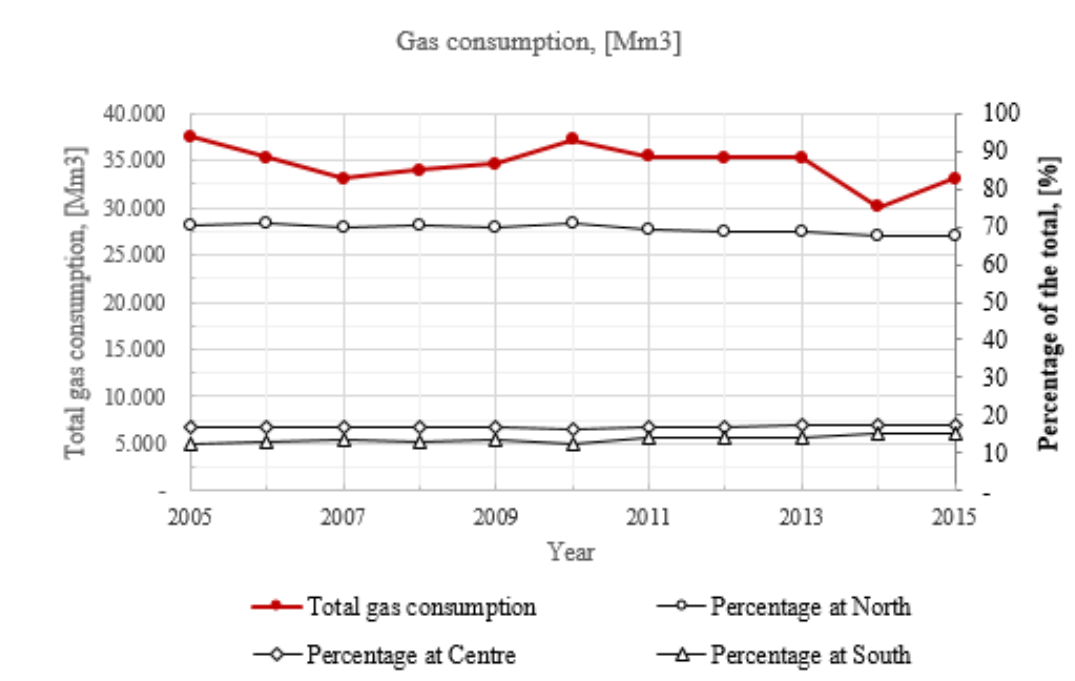
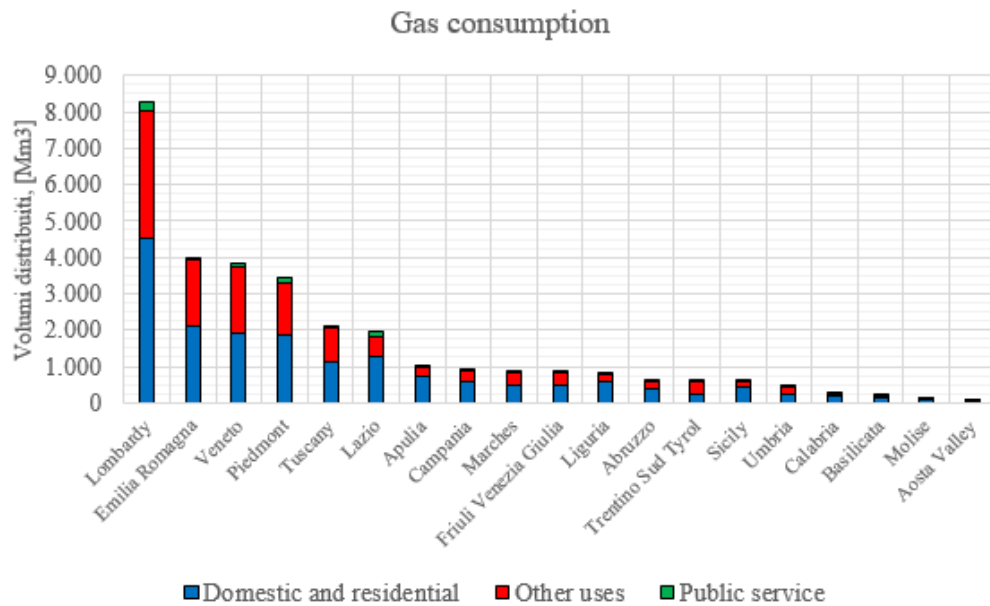


Figure 17. Italian gas consumption divided by areas. Source [16].

For each regions gas consumption is reported as a function of the final scope in Figure 18. As shown, the main part of consumption is due to domestic and residential uses even if other uses are quantitatively simila.



**Figure 18.** Natural gas consumptions divided by Regions and final scope of use. Source [16].

Italian distribution networks are designed and operated to supply a base load for all the year and to ensure peak demands during the heating season. For this reason, distribution network is considered as a possible short term storage for gas produced in local “Power to Gas” application; in fact, since an always higher production of electricity from renewables is expected in the future, natural gas networks can be used as energy storage when demand is lower than production [27]: the excess of energy production is used to produce synthetic methane that can be used in another moment.

Regarding final customers, 23.6 million end-users have been supplied by almost 200 Distribution System Operators (DSOs) in 2016. DSOs are divided in three main groups as a function of the number of supplied customers as reported in Table 7: more than 200.000, between 200.000 and 100.000, and less than 100.000. As shown, the first group (Group 1) is responsible for more than 70% of the market. Therefore, gas market is completely different respect to the electricity one in which a smaller number of Distributors is present.

This complex condition makes difficult to reach common objectives and to identify common development strategies. Furthermore, since several procedures, practices and know-how are property of single companies, a difference of performances between DSOs (particularly between the biggest and the smallest ones) can verify in terms of safety and quality of the service. This condition is highlighted in the era of Industry 4.0, in which new technologies and algorithms are applied to distribution system obtaining effective results if correctly implemented.

Nevertheless, a reduction of the number of DSOs has occurred from 2004 when the total number was double that at the moment. This trend is justified by the necessity of Distributors to obtain always more competence and so by the necessity to merge companies by the acquisition of the smallest companies by the biggest ones.

**Table 7.** Main Italian DSO and number of customers supplied defined as percentage respect to the total. The data have been elaborated considering the information given by each DSO in their website or other documentation.

Group	Main DSOs	Percentage of the market, [%]	Total percentage, [%]
Group 1	Snam	27.9	70.1
	2i Rete Gas	16.6	
	InRete (HERA)	5.9	
	A2A	5.3	
	Toscana Energia	3.4	
	IREN	3.0	
	Ascopiave	2.5	
	Union Fenosa Internacional	1.8	
	ESTRA	1.7	
	Linea Group Holding	1.1	
Ambiente Energia Brianza	0.9		
Group 2	Dolomiti Energia	0.8	4.4
	ACSM-AGAM	0.8	
	Gas Rimini	0.7	
	AGSM Verona	0.6	
	Edison	0.6	
	Aim Vicenza	0.6	
	Energei	0.3	
Group 3	Not available	29.5	25.5

From the data reported by the Authority, the consumption per capita can be calculated as the ratio between total annual consumption and the total number of customers as reported in Table 8 for each Italian region. In the estimation only residential and domestic consumption are considered. As expected the highest values are present at the North because of the longer period in which heating is required as simply described by the Degree Days (DD).

**Table 8.** Yearly and daily per capita consumption. Only domestic and residential uses are considered.

Region	Average degree days, [°C]	Size of the system, [km]	Annual consumption, [Mm <sup>3</sup> ]	Number of customers x 10 <sup>3</sup> , [#]	Annual consumption per capita, [m <sup>3</sup> /#]	Daily consumption per capita, [m <sup>3</sup> /#]
Piedmont	2668	24386	1870	1860	1005	5,5
Aosta Valley	2885	359	24	19	1263	6,9
Lombardy	2472	47922	4520	4454	1015	5,5
Trentino Sud Tyrol	2958	4244	240	250	960	5,2
Veneto	2423	30403	1934	1898	1019	5,6
Friuli Venezia Giulia	2295	7452	489	505	968	5,3
Liguria	1438	6054	557	845	659	4,0
Emilia Romagna	2233	30876	2109	2086	1011	5,5
Tuscany	1753	16879	1146	1505	761	4,6
Umbria	2061	5424	215	328	655	3,6
Marches	1910	9370	500	622	803	4,8
Lazio	1540	15586	1270	2120	599	3,6
Abruzzo	1866	9950	392	581	675	4,1
Molise	1999	2262	85	120	708	4,3
Campania	1219	13009	579	1270	456	3,3
Apulia	1330	12283	731	1272	575	4,2
Basilicata	1962	2642	130	186	699	4,2
Calabria	1180	7053	183	373	491	3,6
Sicily	1021	13888	446	1027	434	3,2

In Table 8, in fact, an average Degree Day (DD) is present for each region. Because of very different locations characterized by different degree days can be present in the same region, the representative value (DD) has been calculated as follow:

$$DD = \frac{\sum_{i=1}^N DD_i \times N_i}{\sum_{i=1}^N N_i} \quad (1-5)$$

Where  $DD_i$  is the Degree Days for the  $i$ -th village of the Italian regions considered [26] and  $N_i$  is the number of customers for the  $i$ -th village. The number of customers is calculated as the ratio between the population of the  $i$ -th village [27] and the number of components of a family as defined by [28]. A total number of 7155 villages are considered for the analysis.

The result can be used as a preliminary estimation for resilience analysis in order to estimate the actions to be done in case of service interruption. The daily consumption has been calculated as the ratio between the annual consumption per capita and the total number of heating days in a year in accordance to the calculated DD. In Figure 19 and Figure 20 the estimated annual and daily consumption per capita are reported as a function of average degree days.

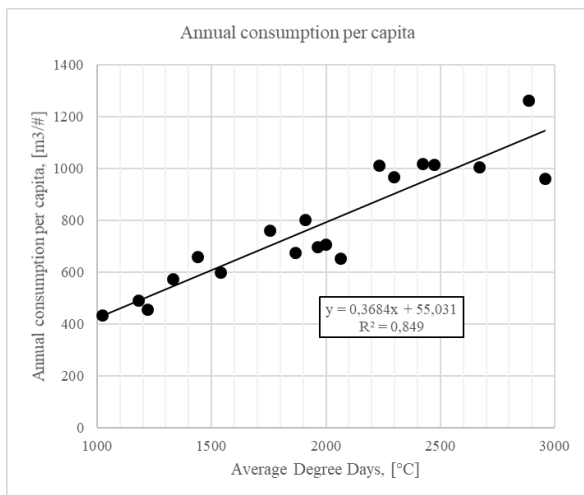


**Figure 19.** Estimated Annual consumption per capita as a function of degree days.

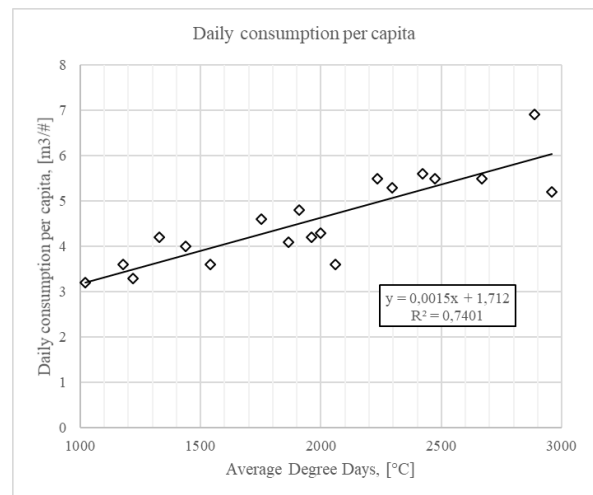


**Figure 20.** Estimated daily consumption per capita as a function of degree days.

Interesting information can be obtained also analysing the development of the distribution infrastructure during the years. Particularly, considering the period between 2010 and 2016, the size increased from 248.688 km to 260.042 km with an average yearly increase of almost 2.700 km/y and a total variation of 4.6% respect to 2010. In the same period gas consumption changed from 36.336 Mm<sup>3</sup> to 30.942 Mm<sup>3</sup> with a reduction of 14.8%; instead connected end-users increased from 22.241.000 to 23.574.000 (+ 6.0%). Considering these data, possible correlations have been investigated.

Respect to previous analysis all consumptions have been considered Figure 21. Because of it is not acceptable to think that a reduction of consumption is responsible for the increase of the total length of the system, the correlation between system size and consumption is not considered. From the analysis it results also a very poor correlation between the variation of system length and of customer number. Consequently, the variation

of the size can be justified by the need of Distributors to improve the quality of the service and particularly to reduce as possible eventual loss of supply conditions.

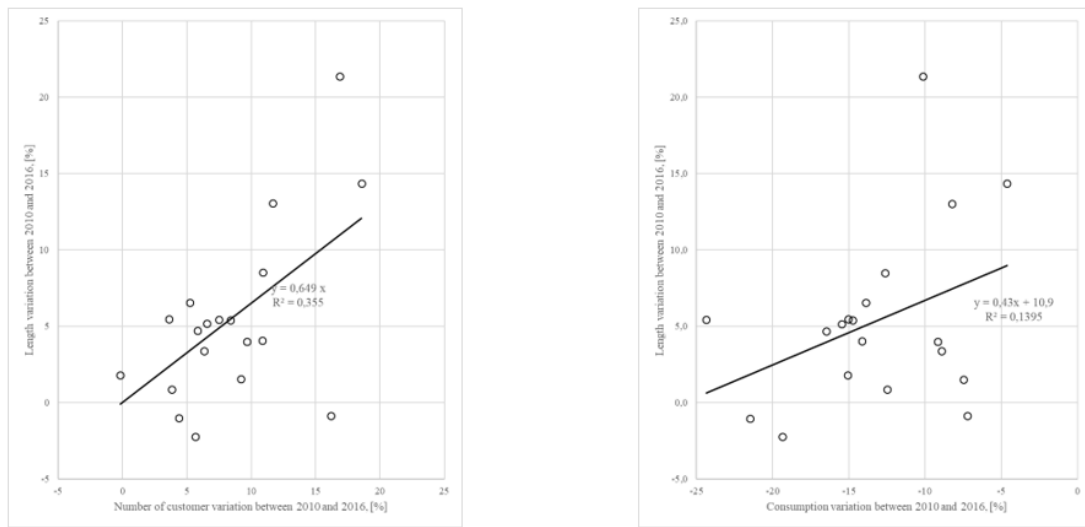


**Figure 21.** Variation of the size of the infrastructure respect to the variation of consumption (left) and of customers (right) between 2010 and 2016 in the Italian Regions.

Even if the variation occurred in last year has not been caused by the variation of national consumption, it should be highlighted that total size is connected with total consumption; in fact, even if annual variation should be considered for domestic and commercial consumption a correlation is present as shown in Figure 22 where total length and consumption for each Italian region is reported for the period between 2010 and 2016. A linear correlation has been found between the two variables. It should be highlighted that the highest consumption in the top right of the figure is due to Lombardy; this region presents a consumption higher than the extrapolated trend so a higher specific consumption [Mm<sup>3</sup>/km]. This can be justified by the highest presence of industrial customers that are locally concentrated in industrial districts.

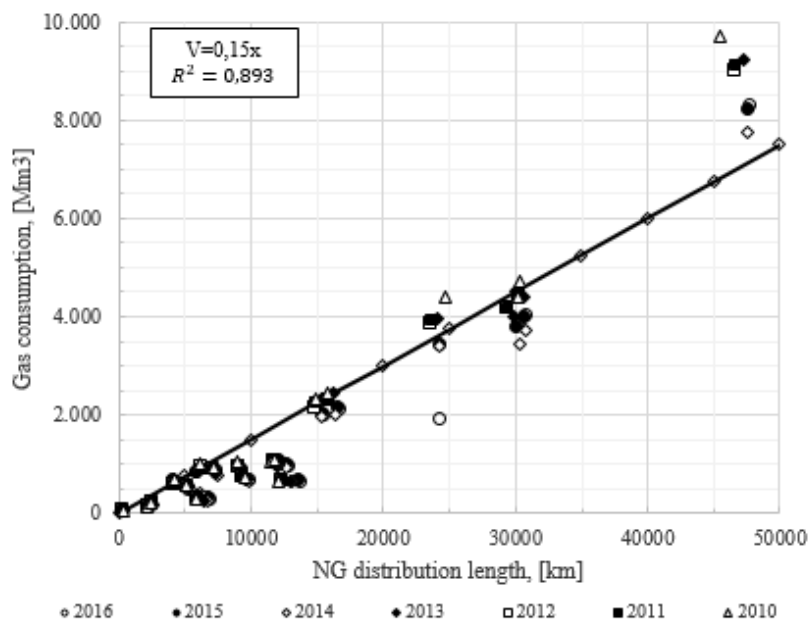


**Figure 22.** Natural gas consumption [Mm<sup>3</sup>] vs infrastructure length for the period between 2010 and 2016.

## ***1.4 Comments***

From the reported data it is evident the importance of natural gas in the international scenario for the next years. Particularly, an increase of production is expected in the Middle East Area while an increase of consumption is estimated in Asia justified by the fast economic growth of emerging Countries such as China.

At the moment natural gas is a deep rooted source of energy both in Europe and in the United States, where large infrastructure in the territory to supply all the existing customers; however, even if more attention will be given in the future to renewable energies gas will be considered a primary source of energy for long times. In fact, nevertheless the always highest penetration of renewables in power generation, it is believed that natural gas will continue to have a predominant role in next future especially in Italy as reported in the National Energetic Strategy (in Italian “*Strategia Energetica Nazionale*”, SEN) where improvements to the whole sector are considered to ensure the transition between carbon and renewables.

Considering Italy, a very complex system has been depicted in the chapter. Three main parts have been identified: transmission, pressure reduction and distribution for a total size of almost 290,000 km and thousands of components. It is therefore intuitive the complexity to operate correctly the gas system ensuring high reliabilities and safety during the operation. Furthermore, differently respect to transmission system where SNAM controls the main part of the system, the distribution activity is performed by several distributors located in different parts of Italy, characterized by different trends and consumptions. Therefore, even if sector standards are present, free exchange of know-how between distributors is very difficult resulting in possible different levels of performance.

For these reasons, a brief analysis of technical characteristics of the natural gas distribution network is proposed in next chapter before to analyse the existing safety performance of natural gas distribution. Particular attention will be given to material, components and installation requirements as reported in existing technical standards.

## Chapter 2

### Technical characterization of NG distribution networks

Natural gas distribution networks are very complex infrastructures. In fact, pipelines of different materials, diameter and thickness are usually present as a function of the operative conditions; furthermore, thousands of other devices such as valves, joints, instruments and several other are installed along the network to ensure operation. For this reason, a technical description of NG distribution networks is suggested before to introduce safety considerations.

However, because of the absence of a common European technical standard, it has been decided to analyse Italian requirements that are considered representative of the European best practice and to compare them with those required in American standards. For the scope, it has been decided to focus only on the most important elements of the networks giving all references to the readers. In fact, the aim of the chapter is not to give an explanation on how to design a network, but to clearly illustrate the elements that constitute it.

#### **2.1 Main components of a natural gas distribution network**

Natural gas distribution networks are responsible for the distribution of natural gas to end-users at a pressure lower than that is required for transportation; consequently, all the components included between ReMi station and customer's meter are part of the distribution system. Furthermore, different operative conditions in terms of pressure and flowrate can be identified along the network in order to satisfy customers' supply conditions. Leaving from the ReMi station, gas is introduced into principal mains which convey gas to several customers in a defined area. Mains are usually installed underground and are characterized by large diameters to convey large quantities of gas. For the scope, they are designed in accordance to [29]. In order to reduce pressure, pressure reduction plants designed in accordance to [30] or to [31] are present along the network.

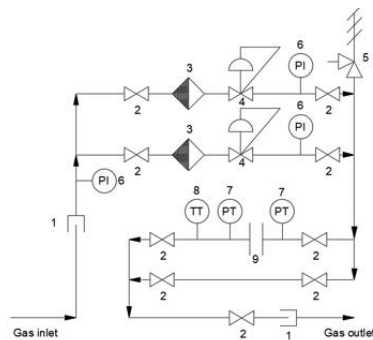


**Figure 23.** Pressure reduction station for the supply of low distribution networks. The following elements are present as reported in the P&ID (in the right): 1 dielectric joint, 2 butterfly valve, 3 filter, 4 pressure regulating valve, 5 pressure safety valve, 6 pressure indicator, 7 pressure transmitter, 8 temperature transmitter, 9 calibrated flanges.

In Figure 23 a final pressure reduction station and corresponding P&ID are reported. As shown, redundancy is present in order to minimize pressure reduction station unavailability.

Natural gas is finally supplied to small groups of customer through service lines designed in accordance to [32] and connected to mains with service tees; two examples used in polyethylene mains are reported in Figure

24. Because of the number of customers supplied by service lines are less than for mains, lower diameter and gas pressure is typically found.

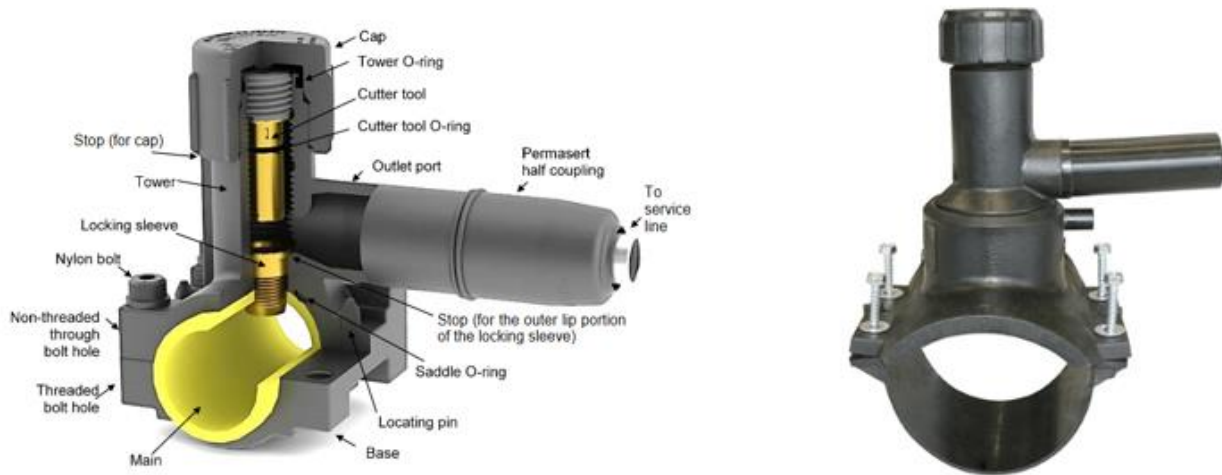


**Figure 24.** Some of the possible service tees for polyethylene mains and services. In this case a PermaLock Mechanical Tapping Tee Assemblies is reported in the right and an electrofusion saddle joint in the left.

From a technical point of view, service lines include all the elements between the service tee and service riser. As reported in Figure 25, other components are present to complete gas supply to final end-users.

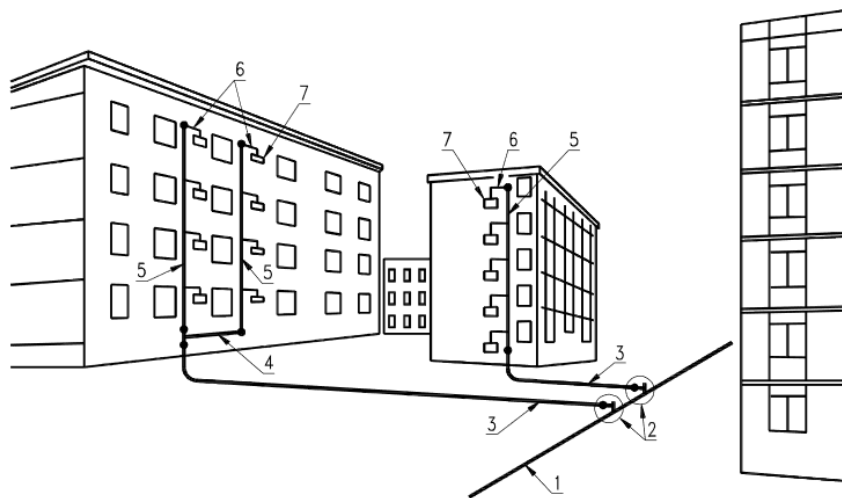


**Figure 25.** Natural gas distribution networks: from the main to final customers. In the case of Liquefied Petroleum Gas (LPG) a slightly different configuration is used. Source [32]. The following elements are reported: 1 main, 2 service tee, 3 service line, 4 horizontal connection line, 5 service riser, 6 gas connection, 7 gas meter.

Distribution networks end at customer's gas meter. This device represents the last part of the distribution network and it measures the consumed gas necessary to calculate fiscal bills: therefore, gas meters represent the physical and legal separation of responsibility between DSO and end user. It should be anticipated that, even if it is considered a simple device, several technical issues are present because of the implementation of the new concept of gas smart metering that represents a new gas measuring philosophy and that will be discussed in the second part of the thesis.

In Figure 26, a schematic representation of the distribution networks is reported.

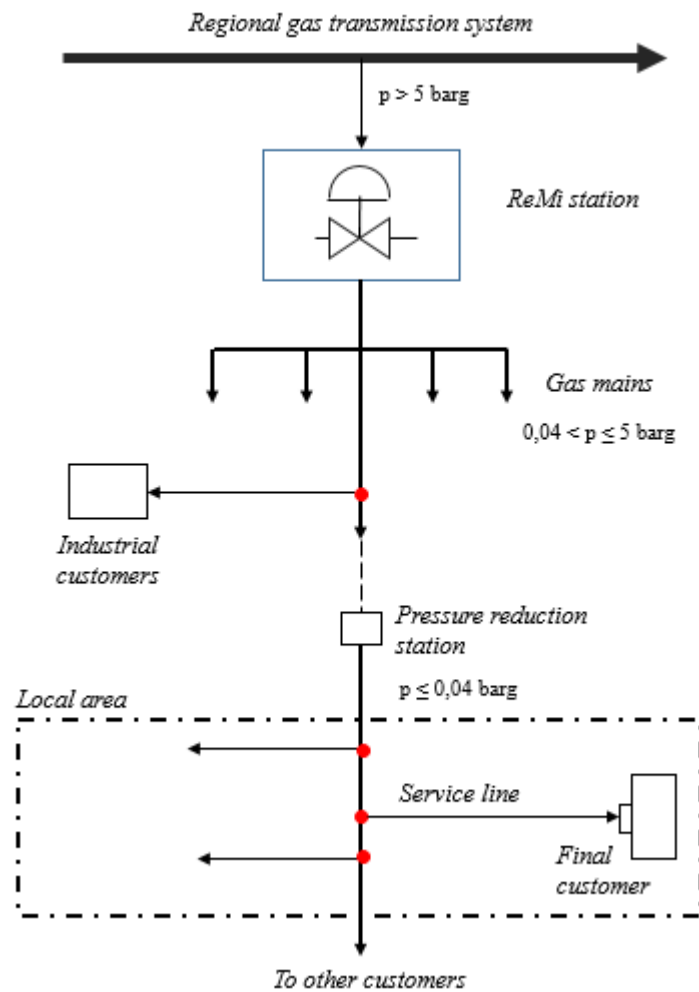


**Figure 26.** NG distribution flowchart. In the figure, the main elements required to distribute NG to final customers are reported.

The introduced elements are only some of the several ones that are present in a typical distribution networks such as valves, joints, transmitters and other ones that are required to ensure gas distribution and are designed in accordance to technical standards.

Because of it is not considered useful to make a list of standards, a more detailed description of the most critical components of NG networks are proposed in next paragraphs. However, it should be highlighted that in 2008 the Italian Minister for the Economic Development (MISE) promulgated a new rule for the design, construction, test, operation and monitoring of gas distribution networks [23] substituting the existing regulations and making for the first time a clear separation between gas transportation and distribution in terms of Maximum Operating Pressure (MOP).

Even if from a technical point of view rules was updated few years ago, the law dated 6/12/1971 and titled “Safety rules for the use of combustible gas” [33] is still the reference safety text for Italian gas operators after 47 years. This situation represents a critical aspect to be considered in next evaluations.

### ***2.2.1 NG distribution pipes: analysis of the materials***

NG pipes are the physical means in which NG flows to reach final end users. While internal diameter depends on gas flowrate, wall thickness is function of several parameters such as material and MOP. However, respect

to natural gas transmission systems in which only steel is allowed, several materials can be used in the distribution in accordance to Italian technical standard [29]. To better understand the main characteristics and expected performances, a focus about allowed materials is proposed in the following sections.

### 2.2.1.1 Steel

Steel is produced adding carbon to iron even if other elements are usually added in the manufacturing process in order to improve its performance against specific phenomenon [34]. Thanks to its mechanical performances and availability in the market, steel is the second most used material in distribution networks.

From a chemical and mechanical point of view it is not correct to speak generically of steel. In fact, several different types are present in the market and can be used for pipeline systems. Five different types can be used for pressure higher than 0.5 barg [35]. Chemical composition is reported in Table 9. As shown, an increase of manganese content is observed from L210 GA to L360 GA increasing the strength and the hardness of the material. A similar carbon content is present except for L235 in which a high content of manganese is present. In fact, the simultaneous presence of a high carbon and manganese content induces embrittlement behaviour that should be avoided in natural gas systems. No other differences are present as shown by the same content of silicon, phosphorus and sulphur.

**Table 9.** Chemical composition of different types of steel for gas distribution networks with pressure higher than 0.5 barg.

Nomenclature	C content, [%] of the mass	Si content, [%] of the mass	Mn content, [%] of the mass	P content, [%] of the mass	S content, [%] of the mass
L210 GA	0.21	0.40	0.90	0.30	0.30
L235 GA	0.16	0.40	1.20	0.30	0.30
L245 GA	0.20	0.40	1.15	0.30	0.30
L290 GA	0.20	0.40	1.40	0.30	0.30
L360 GA	0.22	0.55	1.45	0.30	0.30

Considering mechanical performances, yield strength, tensile (or ultimate) strength and elongation are reported in Table 10. Yield strength represents the load up to which elastic behaviour is ensured by the material. Tensile or ultimate stress, instead, represents the load that is responsible for the fracture of the specimen. Lastly, the elongation, is the measure of the ductility of the material.

**Table 10.** Mechanical properties of different types of steel pipelines for gas distribution networks with pressure higher than 0.5 barg.

Nomenclature	Yield strength, [MPa]	Tensile strength, [MPa]	Elongation, [%]
L210 GA	210	355-475	25
L235 GA	235	370-510	23
L245 GA	245	415-555	22
L290 GA	290	415-555	21
L360 GA	360	460-620	20

Analysing the data reported in the table, an increase of yield and tensile strength and a reduction of ductility is observed in accordance to the increase of carbon and manganese content reported in the chemical composition. Because of pipeline failure is considered for stress higher than yield strength, a preliminary ranking list of the material is consequently possible as a function of the mechanical properties.

Chemical and mechanical characteristics are not the only elements to be considered. In fact, attention has to be given also to pipe manufacturing process and particularly to the presence or absence of welds. The following types can be present in the market: seamless (S), electric welded (EW), submerged arc-welded (SAW) and continuous welded (BW) pipes. As reported by [34], a seamless pipe is “a wrought tubular product made without a welded seam” that is made through hot rolling or hot rolling and cold finishing processes starting from an ingot or a billet (Figure 27). In electric welded pipes two strips are welded together by the pressure impressed and the heat that is transferred by the passage of an electric current through the material (Figure 28); in this case no filler material is added in the Heat Affected Zone (HAZ). It should be highlighted that since 1970 high frequency currents have been used substituting low frequency ones obtaining higher quality welds: in fact, it has been observed low frequencies ones are more susceptible to selective seam corrosion, hook cracks and inadequate bonding and so to failure. Submerged arc welding consists in the presence of an arc that is realized between the bare metal and the electrode; the fusion zone is protected from atmospheric contamination by the melting flux (Figure 29). Last, the continuous welding or butt welding procedure is typical used to produce low cost carbon pipes.



**Figure 27.** Seamless pipes. As reported in the figure no seam is present in the length of the pipe reducing the risk due to a failure of the weld.



**Figure 28.** Electric Resistance Weld during formation.



**Figure 29.** Submerged arc welding process. An helical seam is reported in the figure.

Furthermore, considering welded pipes, longitudinal and circumferential welds can be present even if higher hoop residual stresses are present in longitudinal respect to circumferential welds [36]. Even if welds represent a critical point respect to safety, quality tests are performed in the pipes before the installation and strictly quality performance are required to manufacturers in accordance to [35].

Very few works are present in literature about the performance of the different types of weld. For example, 49 failures occurred at a stress lower than 50% of yield strength have been identified in [37]. It results that the

larger number of failures occurred in EW pipes and especially in low frequency ones as reported in Figure 30. In the figure it is also shown that the failed low frequency welds are principally made in the period between 1940 and 1960: therefore, priority should be given to these pipes in case of substitution. SAWs seem to be the most performant welds even the best performance is offered by seamless pipelines.

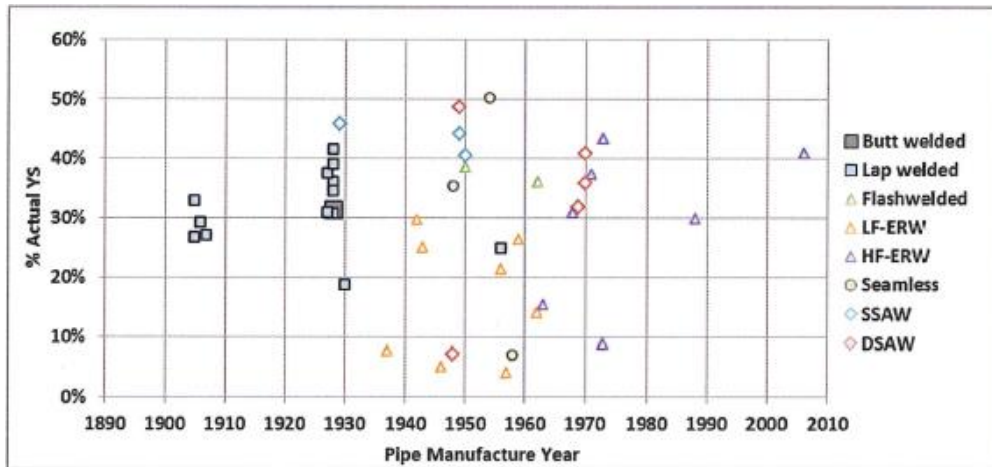


Figure 30. Failure stress vs manufacture year. Source [37].

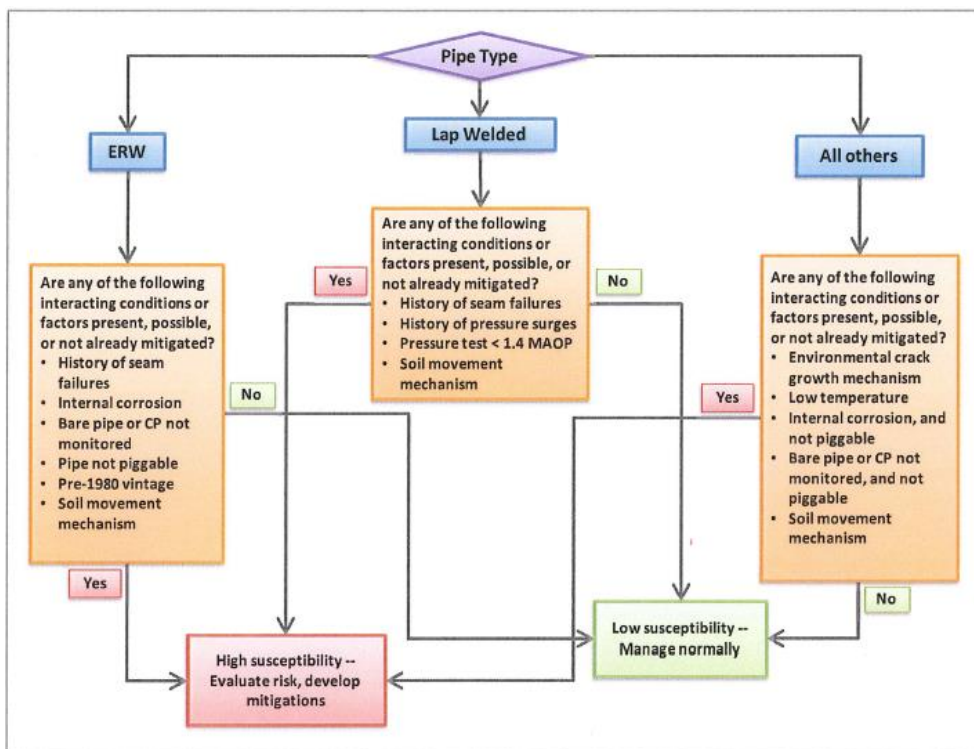


Figure 31. Risk decision tree about the performances of pipe welds. Source [37].

Always in the study, main causes of failure are analyzed resulting that selective seam weld corrosion has been the main reason finding a corrosion rate higher than that is typical for pitting corrosion in similar environment conditions. Consequently, from the reported results it is evident that attention should be given to bare pipelines, where no corrosion monitoring is present or in those cases where protective coatings can disband as reported in the decision tree for failure risk evaluation (Figure 31).

In the case of pressure lower than 0.5 barg, pipelines has to be designed in accordance to [38]. As reported, seamless tube have to be used for buried and unburied installations even if longitudinal welded in accordance to [35] are accepted. Main chemical and mechanical characteristics are reported in Table 11. Respect to those previously introduced, a similar chemical composition is present even if a higher content of manganese that increases the limit strengths of the material but reduces the ductility is present.

**Table 11.** Chemical and mechanical characteristics of steel pipes for pressure lower or equal to 0.5 barg [38].

Nomenclature	C content, [%] of the mass	Mn content, [%] of the mass	P content, [%] of the mass	S content, [%] of the mass	Yield strength, [MPa]	Tensile strength, [MPa]	Elongation, [%]
S 195 T	0.20	1.40	0.035	0.030	195	320-520	20

Before to introduce another material, diameter and thickness sizing is discussed. In fact, pipes are designed in order to resist external and internal loads and to supply the desired flowrate to final end users. Minimum wall thickness is defined as a function of the external diameter or of the nominal diameter depending on the operative pressure of the system as reported in Table 12 and Table 13.

**Table 12.** Minimum wall thickness for pressure higher than 0.5 barg in accordance to Italian technical standard.

External diameter, [mm]	Minimum wall thickness taking into account manufacturing negative tolerance, [mm]
$\leq 30$	1.8
$30 < D_{ext} \leq 65$	2.3
$65 < D_{ext} \leq 160$	2.6
$160 < D_{ext} \leq 325$	3.5
$325 < D_{ext} \leq 450$	4.5
$450 < D_{ext}$	1% of $D_{ext}$

**Table 13.** Minimum wall thickness for pressure lower or equal than 0.5 barg in accordance to Italian technical standard.

Nominal diameter, [DN]	Minimum wall thickness required, [mm]
$10 \leq DN \leq 20$	2.1
$25 \leq DN \leq 40$	2.6
$50 \leq DN \leq 65$	2.8
DN = 80	3.2
DN = 100	3.5

However, while for pressure higher than 0.5 barg negative tolerance should be considered, for lower pressure no clear requirement is present even if they impact the effective resistance of the pipe.

- *EN 10208:1*:
  - Seamless pipes:
    - $T \leq 4$  mm, between +0.6 mm / -0.5 mm;
    - $4 \text{ mm} < T < 25$  mm, between +15% / -12.5%;
    - $T \geq 25$  mm, between +3.75 mm / -3.0 mm or  $\pm 10\%$  (whichever the greater);
  - Welded pipes:
    - $T \leq 10$  mm, between +1.0 mm / -0.5 mm;
    - $10 \text{ mm} < T < 20$  mm, between +10% / -5%;
    - $T \geq 20$  mm, between +2.0 mm / -1.0 mm
- *EN 10255*:

- Welded pipes:
  - $\pm 10\%$  for M, H series and Type L;
  - $-8\%$  with the plus tolerance limited by the mass tolerance, for Types L1 and L2.
- Seamless pipes:
  - $\pm 12.5\%$

To understand the importance of dimensional tolerances, the tangential stress due to internal pressure is introduced:

$$\sigma = p \times \frac{D_{ext} - t}{2 \times t} \quad (2-1)$$

Where  $D_{ext}$  is the external diameter in [m],  $p$  is the internal pressure in [Pa] and  $t$  is the average wall thickness in [m] as commercially available; therefore, and hyperbolic trend is present between stresses and wall thickness. Considering the minimum thickness  $t_{min}$  due to manufacturing tolerances the following maximum stress is calculated:

$$\sigma_{max} = p \times \frac{D_{ext} - t_{min}}{2 \times t_{min}} \quad (2-2)$$

Therefore, an intensification factor  $F_i$  can be calculated as the ratio between  $\sigma_{max}$  and  $\sigma$ :

$$F_i = \left( \frac{\sigma_{max}}{\sigma} - 1 \right) \times 100 = \left( \frac{D_{ext} - t_{min}}{D_{ext} - t} \times \frac{t}{t_{min}} - 1 \right) \times 100 \quad (2-3)$$

Results are reported in Figure 32.

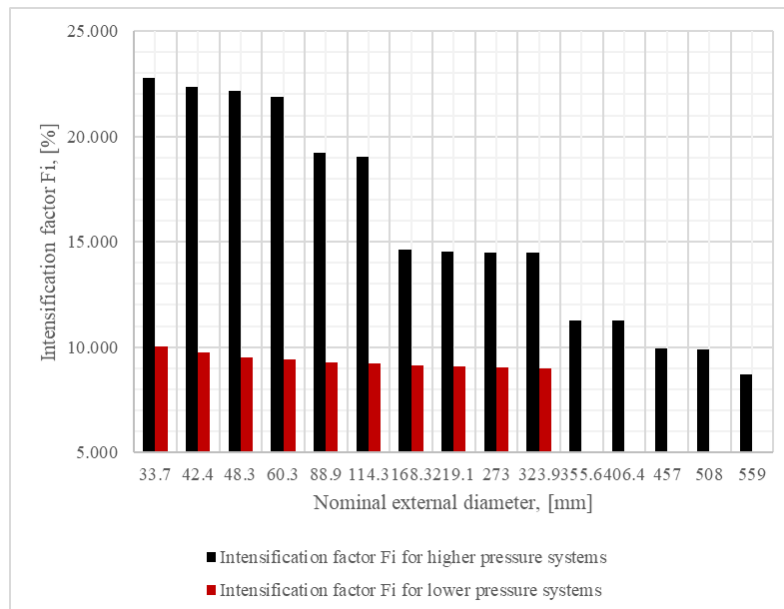


**Figure 32.** Intensification factor  $F_i$  for steel pipelines considering manufacturing tolerances. In the calculation dimensional tolerances about external diameters are not reported. Values have been taken from [35,38].

A decreasing trend with diameter is present. Therefore, from a stress point of view and considering manufacturing tolerances, a higher intensification of stress is expected for pipelines with smaller diameters.

From the reported analysis, tolerances are most critical for small diameter pipelines being responsible for a high intensification of stresses.

In Figure 33 main information required to characterize steel pipelines are reported. These questions can be used not only to create a simple and immediate database but also to easily identify the characteristics of failed pipes and so to evaluate trends. It should be noted that for the scope more detailed information about surrounding environment is necessary but will be introduced in next chapters.

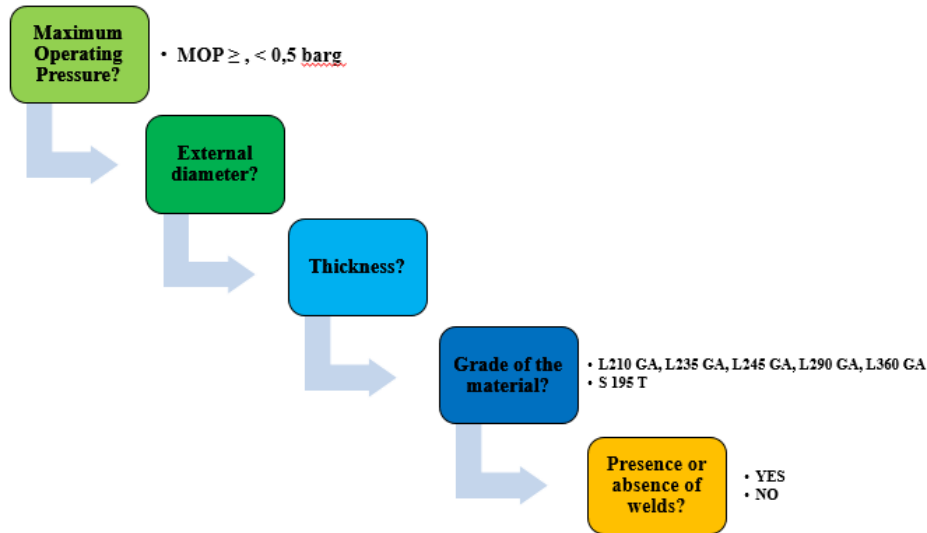
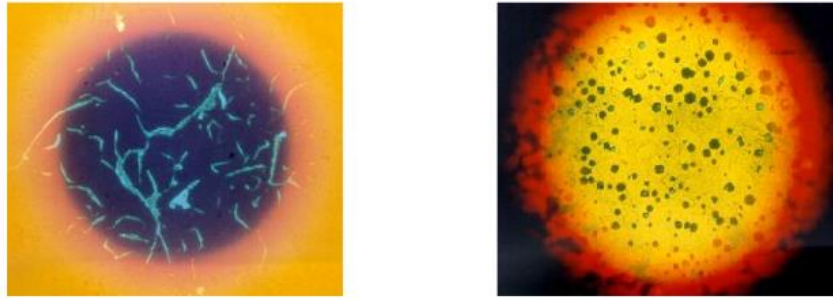


Figure 33. Main information required to characterize steel pipes.

### 2.2.1.2 Cast iron

Cast iron is a carbon – iron alloy with a low percentage of carbon between 2.11% and 6.67%. During the time different manufacturing procedures have been performed. Cast iron was the most used material in the past decades since the introduction of steel pipeline systems during the growth of cities at the end of the 19<sup>th</sup> century. As reported in [39] the first application was found in 1562 at Langensalza (Germany); cast iron pipes were also installed in 1664 to supply water to a fountain even if the first application for distribution has been reported for water distribution at Versailles palace. However, many other cast iron systems were designed and installed worldwide and used for the distribution of various fluids including pressurized natural gas after these pioneering systems.

Two types of cast iron are available in the market: gray and ductile cast iron. The first one is the most diffuse and it is obtained by the fusion of iron, steel and other elements as silicon (between 1% and 3% in weight). A lamellar structure is present causing a brittle behaviour of the material. Ductile iron, instead, is characterized by the presence of distribute spherical graphite that are responsible of lower loads concentration in the material and so greater resistance against cracks propagation is achieved. The different microstructure of the two is reported in Figure 34.



**Figure 34.** Microstructure of gray cast iron (left) and ductile iron (right).

Furthermore, a better performance is achieved by ductile iron pipes that are usually characterized by a tensile strength and an elongation higher than 420 MPa and 10% respectively. That is, material mechanical performances such as the minimum tensile strength and the elongation are reported in Table 14 in accordance to [40]. As shown in the table, respect to available steels a lower tensile strength and ductility is present, making therefore cast iron more brittle and less resistant to applied external loads.

**Table 14.** Material characteristics of cast iron in accordance to [40].

Type of casting	Tensile strength, [MPa]	Elongation, [%]
Pipes centrifugally cast	420	10
Pit casting pipe, fittings and accessories	420	5
The 0.2% proof stress ( $R_p 0.2$ ) may be measured. It shall not be less than: <ul style="list-style-type: none"> <li>• 270 MPa when elongation is <math>\geq 12\%</math></li> <li>• 300 MPa in other cases.</li> <li>• A maximum Brinell hardness equal to 230 HBW is allowed for pipes.</li> </ul>		

That is, only ductile iron is allowed in new Italian NG distribution systems even if gray cast iron was allowed for the lowest pressure part of the network in the past. Minimum thickness is defined as a function of the nominal diameter and of the manufacturing process in the identified standard. Such as for low pressure steel systems, the wall thickness  $t$  is defined in accordance to nominal diameter (DN):

$$\begin{cases} t = 4.5 + 0.009 \times DN & \text{if } DN \geq 250 \\ t = 5.8 + 0.003 \times DN & \text{if } DN < 250 \end{cases} \quad (2-4)$$

Because of commercial pipes can be produced with different manufacturing processes, a minimum wall thickness is defined as a function of the manufacturing process and nominal diameter:

$$\begin{aligned} t_{\min} &= t - (1.3 + 0.001 \times DN) && \text{Centrifugally cast} \\ t_{\min} &= t - (2.3 + 0.001 \times DN) && \text{Other} \end{aligned} \quad (2-5)$$

As shown, more stringent conditions are required for centrifugal cast pipes due to the possible higher dispersion obtained during manufacturing. Furthermore, geometrical tolerances are not clearly defined in the selection of the minimum wall thickness as already found in low pressure steel pipelines. That is, tolerances for commercial cast iron pipes are the following:

- *Pipe centrifugally cast:*
  - Nominal wall thickness  $\leq 6.0$  mm, limit deviation on the nominal thickness: -1.3 mm;

- Nominal wall thickness > 6.0 mm, limit deviation on the nominal thickness:  $-(1.3+0.001 \text{ DN})$  mm.
- *Pipe not centrifugally cast:*
  - Nominal wall thickness  $\leq 7.0$  mm, limit deviation on the nominal thickness:  $-2.3$  mm;
  - Nominal wall thickness > 7.0 mm, limit deviation on the nominal thickness:  $-(2.3+0.001 \text{ DN})$  mm.

As made for steel pipelines, intensification factors  $F_i$  of hoop stress considering available tolerances is calculated for iron pipelines as a function of external diameters.

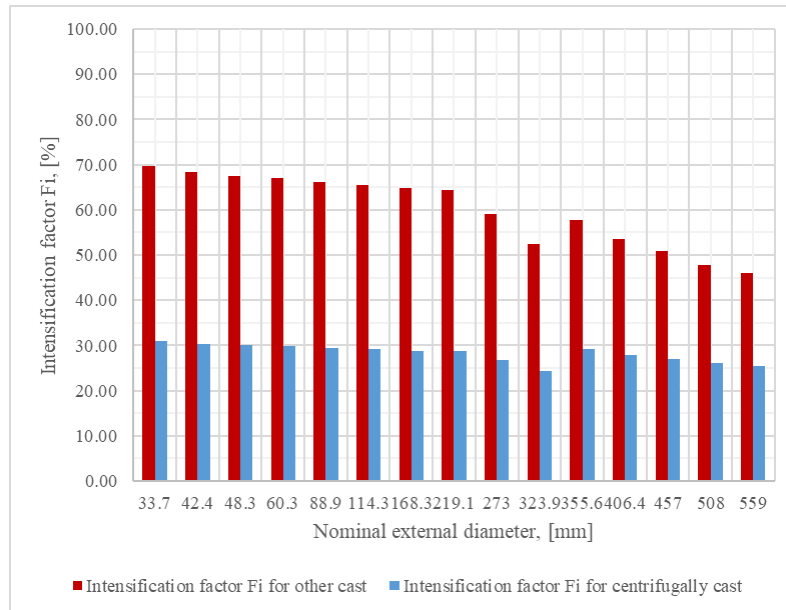


**Figure 35.** Intensification factor for cast iron pipelines. In the calculation dimensional tolerances about external diameters are not reported. Values have been taken from [40].

As shown in Figure 35, intensification factors calculated considering maximum negative manufacturing tolerances are higher than the value obtained for steel. Therefore, from a stress point of view, cast iron pipes are more critical respect to steel ones not only for the lower mechanical performances but also for the higher intensity factors that can be present because of the higher negative tolerances obtained during manufacturing processes.

As made for steel, a flowchart is proposed for the characterization of cast iron pipes as shown in Figure 36. Between the reported data, the identification of class designation is useful to estimate the resistance offered to longitudinal bending moments  $M$  that can be caused by ground subsidence or soil settlement. Only for explanation purpose, bending moments  $M$  are calculated as follow:

$$M = 0.785 \times t \times R_f \times (D - t)^2 \quad (2-6)$$

Where  $t$  is the wall thickness in [mm],  $R_f$  is the bending stress in [MPa] and  $D$  is the external diameter in [mm]. As shown in the technical standard, two classes are available in the market: K9 and K10. K10 class pipes are characterized by higher minimum moment resistance for diameter bigger than DN 125. Furthermore, being

characterized by a higher stiffness  $S$  [kN/m<sup>2</sup>], K10 pipes undergo smaller ovalization caused for example by the weight of the soil or traffic live loads:

$$S = 1000 \times \left( \frac{E \times I}{(D - t)^3} \right) = 1000 \times \frac{E}{12} \times \left( \frac{t}{D - t} \right)^3 \quad (2-7)$$

Where  $E$  is the modulus of elasticity of the material equal to 170.000 MPa,  $I$  is the second moment of area of the pipe wall per unit length [mm<sup>3</sup>].

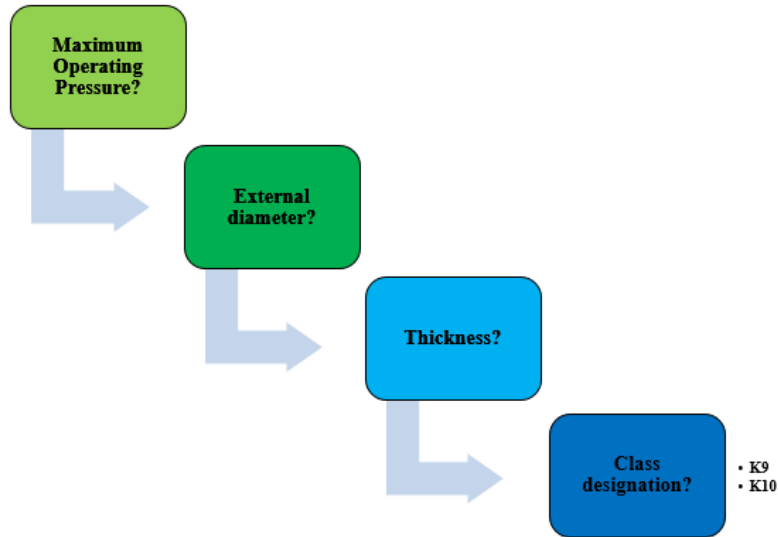


Figure 36. Main information required to characterize cast iron pipes.

### 2.2.1.3 Polyethylene

Polyethylene (PE) has become the most used material in low pressure natural gas distribution networks thanks to its properties and the continuous improvement of performances. Polyethylene is a thermoplastic polymer that consists of smaller units, the monomers, joined together to create a long chain and produced from ethylene, a colourless gas composed of two double – bounded carbon atoms and four hydrogen atoms. Depending on density, molecular weight and molecular weight distribution different characteristics can be achieved as briefly explained below:

- *Density*: since the begin, the main difficulty was to achieve a very tight branched structure of monomers. Therefore, first products were characterized by low densities while only in the recent years high densities were achieved by the development of new manufacturing processes. The different types of polyethylene available in the market are reported in Table 21. Increasing density, a higher crystalline structure can be obtained corresponding to a higher yield strength and stiffness.

Table 15. Density classification of polyethylene pipes as a function of density in accordance to ASTM D 3350.

Type	Density, kg/m <sup>3</sup>	Classification
I	0.910 – 0.925	Low density
II	0.926 – 0.940	Medium density
III	0.941 – 0.959	High density
IV	> 0.960	High and homopolymer

- *Molecular weight*: as reported in [41], the size of a polymer molecule is represented by the molecular weight that gives also information about physical and mechanical properties such as the long term strength, toughness, ductility and fatigue-endurance that increase with the molecular weight.
- *Molecular weight distribution*: it gives indication about the statistics distribution of the size of polymers in the material. Because of a polymer with a broad range of chain length from short to long offers a good resistance to phenomenon such a Slow Crack Growth (SCG) or to impact, the last generation of products, called as high performance materials, are produced from bimodal resins that consist of both very long and very short monomers.

In Table 16 the effects of the three parameters on material characteristics are reported. From the table it is clear that a proper selection of the material is required to ensure the best performance during the operative life.

**Table 16.** Properties variation as a function of density, molecular weight and molecular weight distribution. Source [42].

Property	As density increases, property	As molecular weight increases property	As molecular weight distribution broadens, property
<b>Tensile strength</b>	+	-	
<b>Stiffness</b>	+	-	-
<b>Impact strength</b>	-	-	-
<b>Low temperature brittleness</b>	+	+	-
<b>Abrasion resistance</b>	+	-	
<b>Hardness</b>	+	-	
<b>Softening point</b>	+		+
<b>Strass Crack Resistance</b>	-	-	+
<b>Chemical resistance</b>	+	-	
<b>Gloss</b>	+	+	-
<b>Haze</b>	-	-	
<b>Shrinkage</b>	+	-	+

Respect to metals, polyethylene acts as a viscoelastic material. In the case of an exerted load a small instantaneous elastic strain appears (elastic response) followed by a time dependant increasing strain (viscous response). In Figure 37 the qualitative trend of strain and stress is reported.

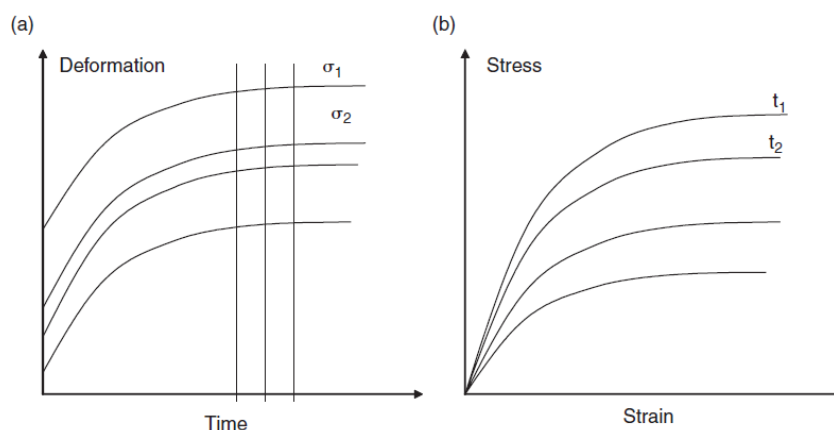


**Figure 37.** Viscoelastic response of polyethylene in the case of an applied load. In (a) deformation is given as a function of stress and time, while in figure b stress in the material is defined as a function of strain and time. Source [42].

As shown in the left, an instantaneous strain appears simultaneously and proportionally to the load followed by an asymptotic trend to a value that depends on the applied stress. In the right stress is reported as a function of strain and time. The presence of a constant strain causes a reduction of stresses with time. Another difference

with metals is that a new state is reached different from the initial after the load is removed as shown in Figure 38: an instantaneous strain recovery verifies followed by a delayed recovery. In the final state a permanent deformation is however present in the material respect to initial conditions. This particular behaviour of plastic material is usually defined as stress relaxation.

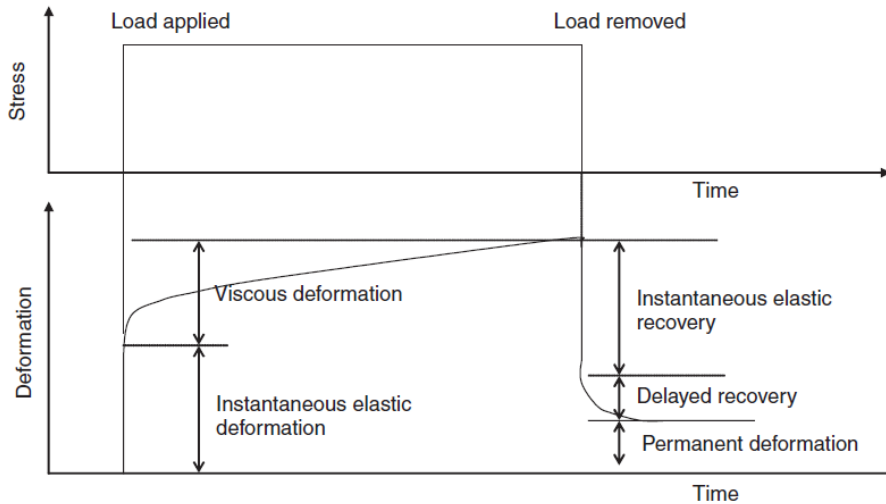


**Figure 38.** Viscoelastic behaviour of polyethylene. Source [42].

Consequently, it is not possible to define an unambiguous modulus of elasticity as made for metals. For this reason, an *apparent modulus of elasticity under tension* is usually defined. To correctly identify the value, type of stress (uni-axial or multi-axial), magnitude, duration and temperature have to be defined. An example of apparent modulus of elasticity for polyethylene of the class PE 3XXX is reported under uni-axial stress at 23.0 °C in Figure 39.

In the case of pressurized pipes, the reported values should be multiplied for a factor equal to 1.25 in order to take into account the presence of bi-axial stress condition characterized by the circumferential hoop stress and the axial stress due to the restraint given by the surrounding soil. Also in the case of compressive stress a slightly higher value is found respect to those reported in the figure. The apparent modulus of elasticity for different types of polyethylene is reported in Table 17.

Because of different possible characteristics, a nomenclature procedure is required. Polyethylene is identified in accordance to AST F412 with four digits. The first one can assume a value between 1 (low) to 5 (high) and represents the density of the polyethylene. The second one identifies the Resistance to Slow Crack Growth and can be a number between 4 (poor quality) to 7 (excellent quality), the last two digits instead represent the Hydrostatic Design Stress for water at 23 °C in units of 100 psi. For example, PE 3608 is representative of a polyethylene with a density between 0.940 and 0.947 kg/m<sup>3</sup>, an excellent resistance to SGC and a hydrostatic design pressure of 800 psi. According to [43] another designation is usually used for polyethylene pipes consisting of two digits that represent the Minimum Required Strength (MRS) of the material that is defined

as the value of lower confidence limit of predicted hydrostatic strength  $\sigma_{PL}^1$  at 20 °C and 50 years in [MPa] multiplied by ten.

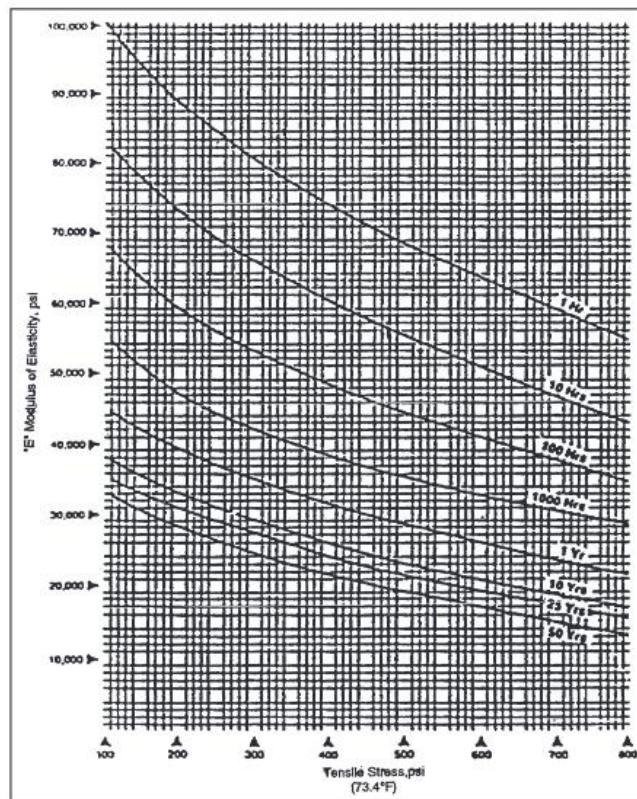


**Figure 39.** Apparent modulus of elasticity for PE3XXX material evaluated under uni-axial stress in air at 23 °C. Source [41].

As reported in the table a reduction of the apparent modulus of elasticity with time is present, even if it is lower for higher density materials. Series “4” present a value that is almost 130% higher than series “2” and 105% than series “3”. This is very important because of material fracture can be due to localized concentration of stress with following crack propagation or to an excessive deformation.

**Table 17.** Apparent modulus of elasticity [MPa] for different type of polyethylene calculated at 23 °C. The values reported can be considered conservative in the case of multi-axial stresses and can be applied conservatively for stresses up to 400 psi. Source [41].

Duration of sustained load, [h]	PE 2XXX	PE 3XXX	PE 4XXX
0.5	428	538	565
1	407	510	538
2	393	490	510
10	345	428	448
12	331	414	434
24	317	393	414
100	290	359	379
1000	241	303	317
8760 (1 year)	207	262	276
87600 (10 years)	179	221	234
438.000 (50 years)	152	193	200

Regarding natural gas distribution, polyethylene pipes can be installed only in buried systems because of the mechanical degradation due to the exposition to solar radiation; to improve it, however, stabilizers such as

<sup>1</sup> The lower confidence limits is the quantity with the dimensions of stress, which represents the 97.5% lower confidence limit of predicted hydrostatic strength at a temperature T and time t [43].

carbon black or other ones are introduced during the manufacturing. In accordance to Italian technical standard wall thickness  $t$  [mm] is calculated as follow:

$$t = \frac{D_e \times p}{20 \times \sigma + p} \quad (2-8)$$

Where  $D_e$  is the external diameter [mm],  $p$  is MOP [bar] and  $\sigma$  is the design stress [bar] that is calculated as:

$$\sigma = \frac{MRS}{K} \quad (2-9)$$

In which  $K$  is a safety coefficient equal to 3.25 and  $MRS$  has to be greater or equal to 8.0 MPa. However, minimum wall thickness is defined as a function of the external diameter as shown in Table 21. Furthermore, dimensional tolerances are not expressly required for the selection of the pipe even if they are reported in material standards [44]. At any point the wall thickness has to be in accordance to manufacturing standard:

$$t_{min} \leq t \leq t_{min} + c \quad (2-10)$$

Where  $t_{min}$  is the minimum wall thickness as a function of Standard Dimension Ratio (SDR) (

Table 19) and  $c$  is the permitted wall thickness tolerance as a function of the minimum wall thickness (**Errore. L'origine riferimento non è stata trovata.**). SDR in [#] is defined as the ratio between the external diameter and the wall thickness ( $SDR = D_{ext} / t$ ):

$$SDR = \frac{D_{ext}}{t} \quad (2-11)$$

As shown in the table, up to DN 50 only SDR11 pipes can be used in accordance to Italian standard.

Therefore, a higher MOP is obtained reducing SDR. Considering the available pipeline in the market, a SDR 11 pipe can be used at a MOP that is 1.6 times higher than allowed by a SDR 17 pipe. Higher mechanical performances are expected reducing SDR. However, even if a lower SDR ensures better performance against structural stability such as occurring in the case of high surcharge loads, other considerations should be made for wall buckling and ring deflection.

The MOP can be calculated as:

$$MOP = \frac{20 \times \sigma}{SDR - 1} \quad (2-12)$$

Wall buckling involves the presence of a longitudinal wrinkling in the pipe wall due to the presence of a higher vertical pressure; ring deflection, instead, is the change in the vertical diameter due to the presence of external loads. Such as for static loads, lower SDR is responsible for a better performance respect to wall buckling while in the case of ring deflection a worst behaviour is found because of the allowed ring deflection reduction.

**Table 18.** Minimum required wall thickness as a function of external diameter. Source [29].

External diameter, [mm]	Minimum wall thickness, [mm]
$\leq 50$	3.0
$50 < D_e \leq 63$	3.6
$63 < D_e \leq 75$	4.3
$75 < D_e \leq 90$	5.1
$90 < D_e \leq 160$	6.2
$160 < D_e \leq 180$	7.0
$180 < D_e \leq 200$	7.7
$200 < D_e \leq 225$	8.7
$225 < D_e \leq 250$	9.7
$250 < D_e \leq 280$	10.8
$280 < D_e \leq 315$	12.2
$315 < D_e \leq 355$	13.7

**Table 19.** Minimum required wall thickness as a function of external diameter and SDR. Source [44].

Nominal size DN/OD	SDR 17.6	SDR 17	SDR 11
16	2.3	2.3	3.0
20	2.3	2.3	3.0
25	2.3	2.3	3.0
32	2.3	2.3	3.0
40	2.3	2.4	3.7
50	2.9	3.0	4.6
63	3.6	3.8	5.8
75	4.3	4.5	6.8
90	5.2	5.4	8.2
110	6.3	6.6	10.0
125	7.1	7.4	11.4
140	8.0	8.3	12.7
160	9.1	9.5	14.6
180	10.3	10.7	16.4
200	11.4	11.9	18.2
225	12.8	13.4	20.5
250	14.2	14.8	22.7

**Table 20.** Tolerance on wall thickness. Source [44].

Nominal wall thickness, [mm]	Tolerance, [mm]
$\leq 2.0$	0.3
$2.0 < t \leq 3.0$	0.4
$3.0 < t \leq 4.0$	0.5
$4.0 < t \leq 5.0$	0.6
$5.0 < t \leq 6.0$	0.7
$6.0 < t \leq 7.0$	0.8
$7.0 < t \leq 8.0$	0.9
$8.0 < t \leq 9.0$	1.0
$9.0 < t \leq 10.0$	1.1
$10.0 < t \leq 11.0$	1.2
$11.0 < t \leq 12.0$	1.3
$12.0 < t \leq 13.0$	1.4

In order to compare polyethylene pipes, allowed MOP is calculated as a function of diameter and SDR. Results are reported in Figure 40 considering a MRS equal to 8 MPa.

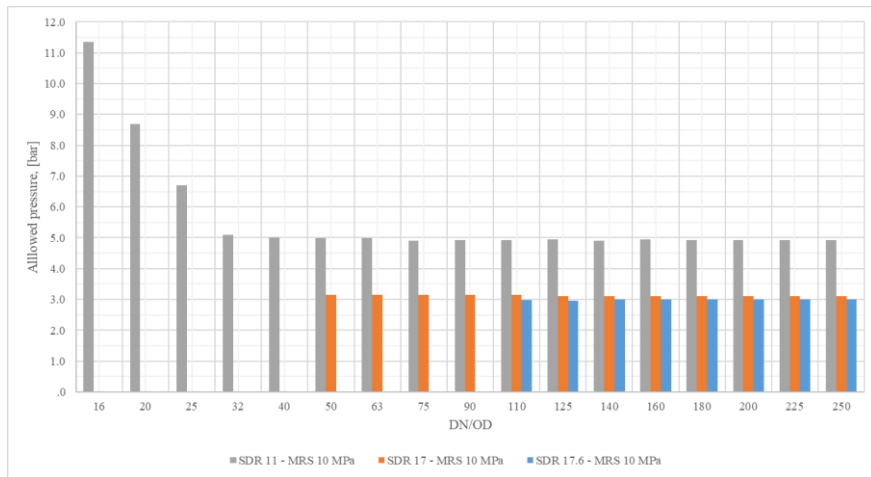


**Figure 40.** Maximum allowed pressure considering the minimum wall thicknesses in accordance to [44].

As shown, for diameters higher than DN 25 allowed MOP is not influenced by diameter but only by SDR.

Respect to steel and cast iron, tolerance is not considered. In fact, the use of minimum wall thickness is conservative in accordance to the definition of tolerance in manufacturing standards.

However, information required in order to characterize plastic systems are proposed. In fact, very poor information is often present about polyethylene pipes in available database where the classification consists only of the term polyethylene without further specification. As shown, more information should be collected.

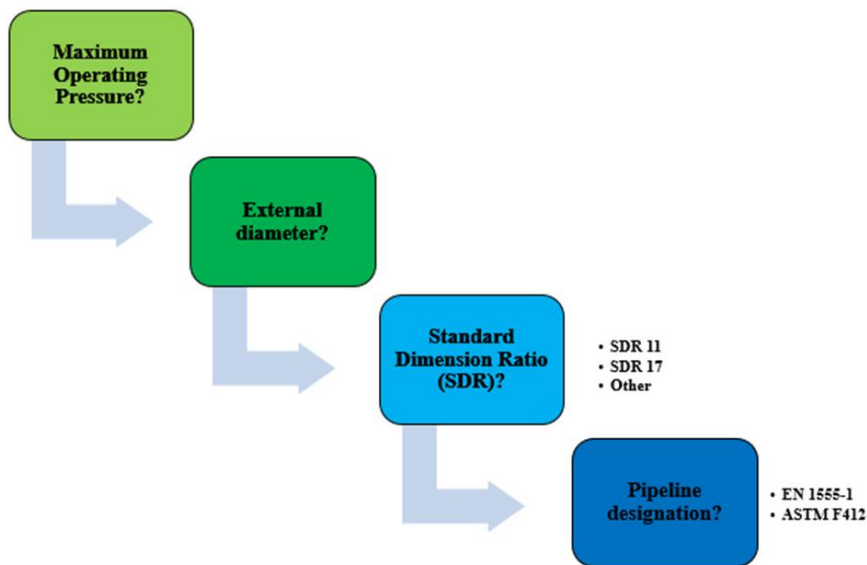


**Figure 41.** Main information required to characterize polyethylene pipes.

#### 2.2.1.4 Copper

The use of copper in gas distribution networks is limited only to service lines with a MOP lower than 0.04 barg with a maximum external diameter of 108 mm and in accordance to [45]. The following chemical composition is allowed:

$$Cu + Ag: \text{ min } 90.9\% \quad (2-13)$$

$$0.015\% \leq P \leq 0.040\%$$

About mechanical properties, lower performances are available respect to previous other material as reported in Table 21. However, a higher ductility is present except for R290 type (hard).

**Table 21.** Mechanical properties of copper pipes in accordance to international standards.

Material condition	Nominal outside diameter, [mm]	Tensile strength, [MPa]	Elongation, [%]	Hardness (indicative) HV 5
R220 (annealed)	6 – 54	220	40	40 – 70
R250 (half hard)	6 – 66.7 6 – 159	250	20 30	75 – 100
R290 (hard)	6 – 267	290	3	Min. 100

As for other materials, minimum thickness is required to convey gas as reported in Table 22. As shown, as for high pressured steel distribution pipelines, negative tolerance has to be considered during the design of copper systems. Considering the available product on the market, the following tolerance are allowed in [45]:

- *Nominal outside diameter* < 18 mm:
  - Nominal wall thickness < 1.0 mm:  $\pm 10\%$ ;
  - Nominal wall thickness  $\geq 1.0$  mm:  $\pm 13\%$ .
- *Nominal outside diameter*  $\geq 18$  mm:
  - Nominal wall thickness < 1.0 mm:  $\pm 13\%$ ;
  - Nominal wall thickness  $\geq 1.0$  mm:  $\pm 15\%$  (some exception should be considered for R250 tubes).

**Table 22.** Minimum wall thickness copper pipes. Source [29].

External diameter, [mm]	Minimum wall thickness taking into account manufacturing negative tolerance, [mm]
$\leq 18$	1.0
$18 < D_{ext} \leq 42$	1.5
$42 < D_{ext} \leq 64$	2.0
$64 < D_{ext} \leq 88.9$	2.5
$88.9 < D_{ext} \leq 108$	3.0

Furthermore, a simple survey form is suggested to characterize copper systems as reported in Figure 42. No more information that those required seems to be useful for the scope.

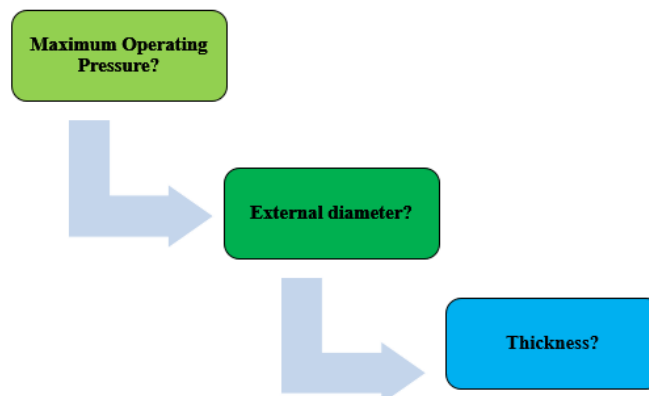


**Figure 42.** Main information required to characterize copper pipes.

### 2.2.1.5 Comparison with ASME B31.8

Respect to Italian condition, some differences have been identified in the American technical standard [46]. First of all, it should be note that requirements both for distribution and transportation systems are present in the same document. That is, the same materials are identified even if in addition to polyethylene other plastic materials are allowed such as PVC. In order to make a comparative analysis between the two standards, the available materials are analysed one by one as follow starting from steel.

In the case of steel pipes, American standard defines wall thickness as a function of seven parameters that take into account hoop stress, mechanical performance and the risk induced in case of leakage:

- *Nominal external diameter* of the pipe  $D_{ext}$  [in];
- *Longitudinal joint factor*, E, that takes into account the production process of the pipe such as if it is seamless, electric resistance welded, etc. [#];
- *Design factor*, F, that depends on the location class and so on the population density [#];
- *Minimum yield strength of the material*, S [psi];
- *Temperature derating factor*, T [#];
- *Maximum Operative Pressure (MOP)*, p [psi].

Therefore, wall thickness t can be defined as:

$$t_{ASME\ B31.8} = f(D_{ext}, E, F, S, T, p) = \frac{p \times D_{ext}}{2SFET} \neq t_{UNI\ 9034} = f(D_{ext}) \quad (2-14)$$

In order to explain American formulation, an insight in the definition of E, F is necessary. Temperature derating factor is not considered because it assumes a value equal to 1 for operative temperature lower than 120 °C. The longitudinal joint factor E takes into account the manufacturing process used for steel pipelines and so the presence or absence of welds. From the table, it results that seamless pipes have the best performances followed by Submerged Arc Welded, Electric Fusion Arc Welded and Continuous Butt Welded. Basic design factor instead takes into account the risk to surrounding environment and so a bigger wall thickness is required for most dense areas as reported in Table 24.

**Table 23.** Longitudinal Joint Factor E in accordance to ASME B31.8.

<b>Spec. No.</b>	<b>Pipe class</b>	<b>Longitudinal joint factor, E</b>
ASTM A 106	Seamless	1.00
ASTM A 134	Electric Fusion Arc Welded	0.80
ASTM A 135	Electric Resistance Welded	1.00
ASTM A 211	Spiral Welded Steel Pipe	1.00
API 5L	Seamless	1.00
	Electric Resistance Welded	1.00
	Electric Flash Welded	1.00
	Furnace Butt Welded	0.60
	Submerged Arc Welded	1.00

**Table 24.** Basic design factor F in accordance to ASME B31.8.

Location class	Design factor, F
Location class 1, Division 1 <sup>(a)</sup>	0.80
Location class 1, Division 2 <sup>(a)</sup>	0.72
Location class 2 <sup>(b)</sup>	0.60
Location class 3 <sup>(c)</sup>	0.5
Location class 4 <sup>(d)</sup>	0.4

<sup>(a)</sup> Any 1-mile section with 10 or fewer buildings for human occupancy;  
<sup>(b)</sup> Any 1-mile section that has more than 10 but fewer than 46 buildings intended for human occupancy;  
<sup>(c)</sup> Any 1-mile section that has 46 or more buildings intended for human occupancy except when a Location Class 4 prevails;  
<sup>(d)</sup> Areas where multistore buildings are prevalent, where traffic is heavy or dense, and, where there may be numerous other utilities underground.

Nevertheless, considering same operative conditions a thicker wall is considered by Italian rules. Particularly, considering the most hazardous location (class 4), a seamless grade B welded pipe in accordance to API 5L the pressure required to reach the same thickness required by Italian standard is reported as a function of the external diameter. Results are reported in Figure 43.

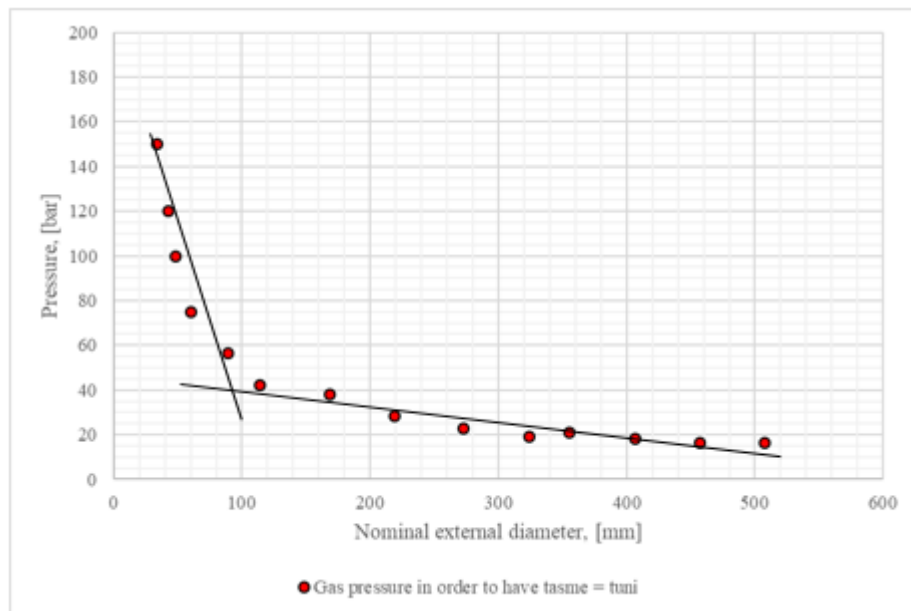


**Figure 43.** Gas pressure [bar] required in order to have the same minimum wall thickness as calculated by American and Italian standard.

As shown, a pressure higher than that allowed in distribution is required to reach the same thickness especially for low diameters pipelines and, furthermore, higher than that allowed in NG distribution. As shown in the figure, a hyperbolic trend is found for MOP that tends to plus infinite for external diameter that tends to zero, and to zero for external diameter that tends to plus infinite. However, omitting the theoretical extreme values, a critical point is found for external diameter in the range of 100 mm beyond which a small variation of MOP is present for great variation of external diameter.

Regarding cast iron, no mathematical correlation is present in American standard. Thickness is identified as a function of nominal diameter, burial depth and laying condition even if only nominal diameter should be

considered for NG distribution as for Italian standard. In Figure 44 the ratio between the calculated values is reported.

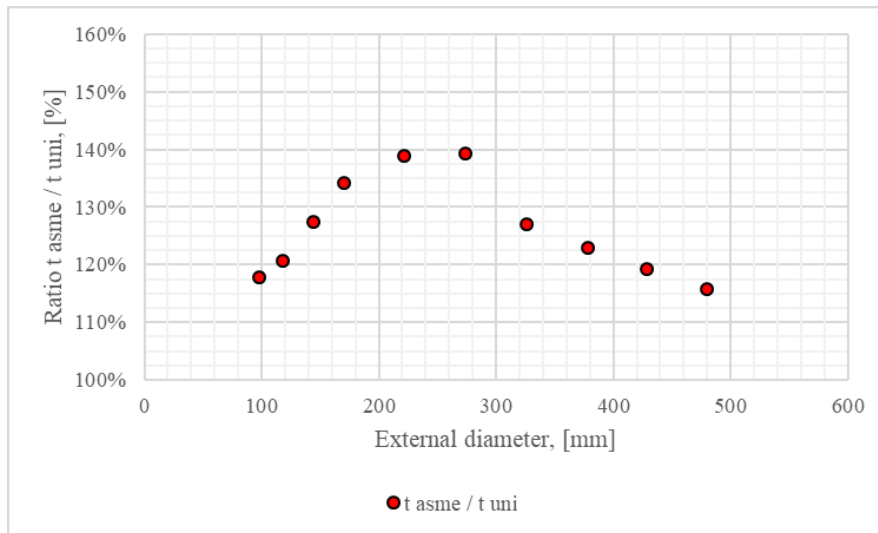


**Figure 44.** Ratio between thickness required by American and Italian technical standard for cast iron.

As shown, more stringent requirements result in American standard with a maximum equal to 140% is found for external diameters in the range between 200 mm and 300 mm. This result can be justified because the standard is also valid for MOP (250 psig) higher than those allowed in Italian standard.

Regarding polyethylene, no specification is present in American standard where the term plastic is generally used. Therefore, also polyvinyl chloride, more commonly known as PVC, is included in this section while in Italian distribution systems cannot be used for gas distribution. That is, plastic pipes are allowed for MOP lower or equal to 100 psig, corresponding to 6.9 barg, and thickness is calculated as a function of hoop stress similar to Italian requirements. Therefore, very poor differences are present for polyethylene pipes between the two standards.

Last but not least, copper pipes can be implemented in American network only if MOP does not exceed 100 psig and if hydrogen sulphide concentration is lower than 0.3 grains per 100 standard cubic feet of gas in order to reduce possible corrosion. Also a minimum wall thickness of 0.065 in (1.65 mm) is required.

In order to conclude the comparison, considerations about tolerances between American and Italian technical standards have to be made; in fact, also in the American standard it is stated to not consider the negative tolerances as explicitly reported at the point 804.222:

*“Nominal wall thickness,  $t$ , is the wall thickness computed by or used in the design equation ... .., pipe may be ordered to this computed wall thickness without adding allowance to compensate for the underthickness tolerance permitted in approved specifications”.*

That is, the main difference between the two documents regards steel pipelines, where requirements seem to be more stringent in Italian text. This condition can be justified by the fact that American standard can be applied also to other part of NG systems, as transportation system where steel is the most used material. Therefore, being a common document for gathering, transmission and distribution, it is necessary to define

wall thickness as a function of the effective hoop stress in order to avoid oversizing. However, safety coefficients such as basic design factor are introduced in order to take into account failure risk in American system.

### 2.2.2 Fittings and joints used in NG distribution

Several fittings and joints are used in NG distribution ensuring the connection of accessories and pipes in accordance to [29,32]; the main ones are reported in Table 25. As reported, the allowed connection depends on the material of the pipe. Considering steel, three main types are identified: welded, flanged and threaded connections. In the first case, continuity between the pipe and the fitting is ensured by the weld. For connection such as flanges or threads, instead, an element between the pipe and the fitting is required to ensure gas tightness: a gasket is installed as sealing material between the two faces of the flanges while a sealing material is usually installed between the two screw profiles in threaded connections to improve gas tightness.

Regarding ductile iron, three main types of connection between pipe and fittings can be used: flanged ones, sockets and spigots. For each one, sealing device has to be installed to ensure gas tightness.

In polyethylene pipes, electrofusion, butt fusion and mechanical fittings can be used in accordance to [40]. While electrofusion and butt fusion fittings ensure continuity between the pipe and the fitting, a sealing material is required in mechanical fittings. That is, between the connections cited, electrofusion and butt welding are the most common. In the first case surfaces to be connected are melted together thank the heat generated by current flows through wiring submerged inside the material as reported in Figure 45. In the second case, instead, the surfaces to be connected are heated and pressed together.

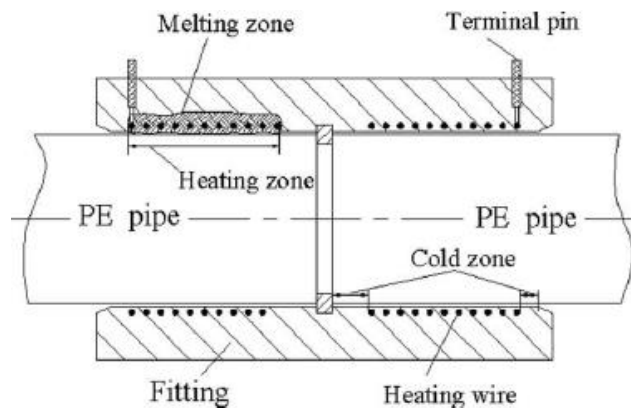


**Figure 45.** Schematics of an electrofusion joint of two polyethylene pipes.

To conclude, brazing is the preferred connection process for fittings in copper pipes. In this case melting process is substituted by capillarity. An additional alloy is liquefied and enters by capillarity in the interstitial voids inside the two piece to be connected. As a function of the liquefaction temperature different mechanical performances are achieved: for example, material annealing occurs with temperature increases reducing consequently the allowed mechanical stresses of the pipe. However, a threshold limit equal to 450 °C can be considered for the phenomenon. Furthermore, no ageing effects are present in modern brazing processes even if in the past failures occurred because of the alloys used in the process (such as lead base alloys) that typically deteriorated during the time.

**Table 25.** Types of fittings and joints used in NG distribution as a function of the pipeline material.

Type of fitting and joints \ Material	Steel	Polyethylene	Ductile iron	Copper
Welds	✓			
Flanges	✓		✓	
Threads	✓			
Socket or spigot			✓	
Electrofusion fittings		✓		
Mechanical fittings		✓	✓	
Butt fusion fittings		✓		
Brazed				✓

The rules defined above regards the situation in which the material of fittings and pipe is the same; however, also connection between different materials is possible but no detail is proposed in this thesis.

Even if it seems not particularly useful to proceed in a more detailed description of the available fittings in the market, a survey form should be however introduced by DSOs to correctly characterize failed fittings and joints and so to identify trends as made by American Authorities. Attention should be given to the information required in the questionnaire in order to not complicate its compilation. A proposed form is reported in Figure 46 where very few information is required for a good characterization.

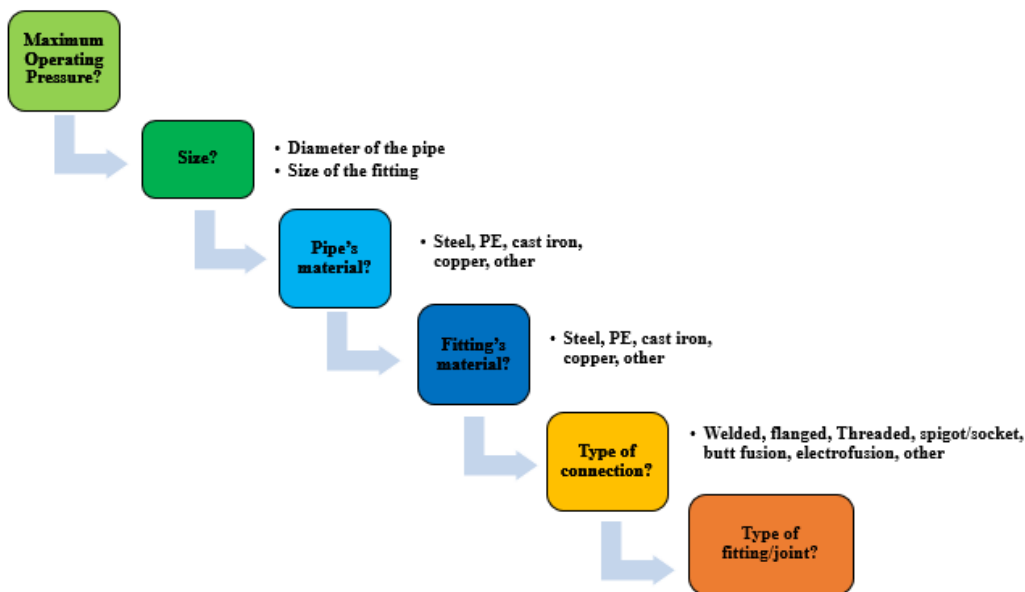


**Figure 46.** Main information required to characterize fittings and joints in NG distribution networks.

Continuing the comparison between American standard, it is found that similar types are allowed as in Italian network (Table 26). As shown, more configurations are allowed for copper where also threaded and mechanical fittings are allowed. Brazing connection is allowed also in steel systems and compression fittings are clearly identified as possible method for the connection of different parts of the system.

**Table 26.** Types of fittings and joints used in NG distribution as a function of the pipeline material.

Type of fitting and joints \ Material	Steel	Polyethylene	Ductile iron	Copper
Welds	✓			
Flanges	✓		✓	
Threads	✓			✓
Socket or spigot			✓	
Electrofusion fittings		✓		
Mechanical fittings	✓	✓	✓	✓
Butt fusion fittings		✓		
Brazed	✓			✓

### 2.2.3 Valves used in natural gas distribution networks

Several types of valves can be installed in gas distribution networks in order to regulate pressure, flow or discharge overpressure in the case of system failure. That is, isolation valves are of primary importance because of they have to ensure the interruption of gas supply as required in the shortest time as possible. However, no mandatory inspection frequency is identified in [47] leaving the decision to DSOs. In American standard, instead, it is required to inspect and partially operated those valves that should be operated during an emergency at least one a year. In fact, time delays are usually responsible for the increase of consequences in the case of an emergency. Another difference between Italian and American standards is request to install isolation valves in all new or replaced American service lines, while the decision is leaved to DSO in Italy. That is the following types of valves can be installed depending on material of the piping (Table 27).

**Table 27.** Valve allowed in accordance to [29].

Pipeline material	Allowed material for valves
<b>Steel</b>	<ul style="list-style-type: none"> <li>• Steel;</li> <li>• Cast iron. Forbidden grey cast iron;</li> <li>• Bronze;</li> <li>• Brass;</li> <li>• Polyethylene (only for service lines with pressure lower or equal than 0.04 barg).</li> </ul>
<b>Cast iron</b>	<ul style="list-style-type: none"> <li>• Steel;</li> <li>• Cast iron. Forbidden grey cast iron.</li> </ul>
<b>Polyethylene</b>	<ul style="list-style-type: none"> <li>• Polyethylene;</li> <li>• Steel;</li> <li>• Brass;</li> <li>• Bronze.</li> </ul>
<b>Copper</b>	<ul style="list-style-type: none"> <li>• Brass;</li> <li>• Bronze;</li> <li>• Steel (only for unburied systems).</li> </ul>
Different types of valve are available on the market as a function of the material: <ul style="list-style-type: none"> <li>○ Steel: Butterfly valves (UNI 9245), ball valve (UNI 9734), cone valves (API 599);</li> <li>○ Cast iron: API 599;</li> <li>○ Polyethylene: EN 1555:4;</li> <li>○ Brass: EN 331;</li> <li>○ Bronze: DVGW VP305</li> </ul>	

Among valves, Excess Flow Valves (EFV) ensure the automatically interruption of gas supply in the case that flowrate exceeds a defined threshold (Figure 47). The implementation of this valve is evaluated in [48] in order to protect downstream systems in the case of pipeline rupture following soil movement, earthquakes, ground

settlement. The working principle of an EFV is very simple because of it is based on the pressure drop caused by the increase in the flowrate through the valve. When the flowrate is higher than a predetermined level, a higher pressure drop occurs. The pressure difference between the valve becomes higher than the force exerted by the spring automatically closing the valve.

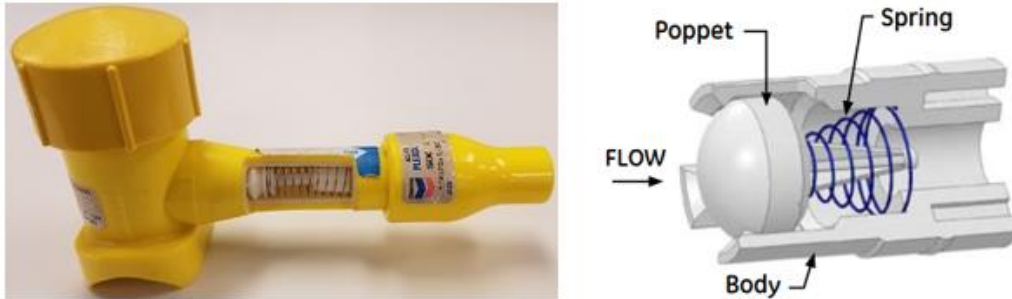


**Figure 47.** Excess Flow Valve for natural gas service lines. Images are from Atlanta Gas Light (right) and Dresser (left).

Two types exist on the market: EFV with and without bypass. The first one has a small bypass in order to ensure the automated re-opening of the valve when pressure is stabilized upstream and downstream the valve. The second one require manual intervention to return in open position.

Because of EFVs intervene only in the case of high flowrate leakages, the implementation in existing network is still slow. Some cases are reported:

- *France*: the law requires the use of Excess Flow Valve from a government order dated July 2000;
- *Italy*: no requirements is present for distributors so the installation is decided by the single distributors;
- *Germany*: excess flow valves are required to be installed on all new service lines;
- *Japan*: no excess flow valve but intelligent meters in the house (the smart meters) that identify abnormal consumption.
- *Iran*: they use EFV to avoid higher consumption than those allowed, to protect customers in the case of third party damages or of earthquake;
- *USA*: A number of Operators have published articles stating their position to voluntarily install EFVs under the regulation 49 CFR 192.383. Furthermore, California building code requires the installation of excess flow valves or other acceptable devices to isolate the flow of natural gas in the event of a line rupture downstream of the meter. Additionally, other cities such as Frisco, Texas and Houston, Texas also have ordinances requiring the installation of excess flow valves downstream of the gas meter.

That is, the National Transportation Safety Board (NTSB), an independent federal agency charged with determining the probable cause of transportation accidents including accidents occurred in transportation systems such as natural gas networks, identifies some accidents occurred in natural gas distribution networks which consequences could be lower in the case that an excess flow valve was installed in the network. An example is schematically reported:

- Gas explosion destroyed an apartment (Figure 48):



**Figure 48.** Damaged service pipe (right) and destroyed building (left).

- i. **Date:** 13/12/2005;
- ii. **Damages:** an apartment completely destroyed, three residents were killed and five people were injured;
- iii. **Gas system:** 1" ¼ steel natural gas service line operated at 11.5 psig (0.8 bar);
- iv. **Cause:** During the excavation of a buried structure, soil collapsed reducing the supporting capacity. No sufficient shoring of the trench was performed and a break at the threaded end of the steel pipeline occurs. During the emergency response the isolation valve implementing in the plant was blocked and does not shut off immediately the gas supply;
- v. **Comment:** As reported by NTSB, the presence of an EFV would have stopped gas flow before the minimum concentration to ignite was achieved.

As made for other components of the system, a questionnaire is proposed to characterize valves.

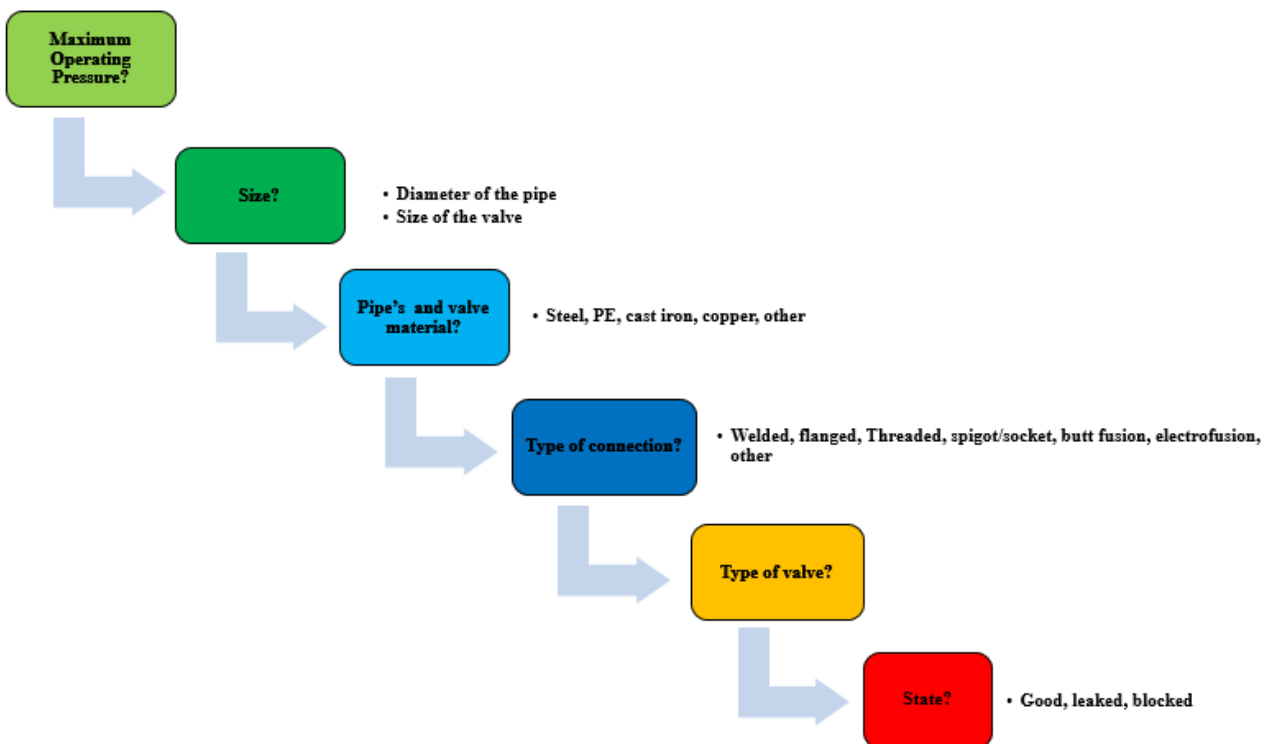


**Figure 49.** Main information required to characterize fittings and joints in NG distribution networks.

This survey can be made in case of failure in order to evaluate trends. However, respect to those proposed for pipes, fittings and joints, in the case of valves also blockages should be considered in addition to leakages. The information required will be therefore helpful to plan inspection based on the effective risk in case of system failure.

## 2.2 Installation requirements for natural gas distribution networks

To conclude the brief description of NG distribution networks, some requirements about installation are introduced. Several parameters have to be taken into consideration such as the installation depth, the distance from other infrastructure or buildings, and trench filling materials in the case of buried pipelines.

In Italian standards installation depth is defined as a function of the destination use of the area and of system MOP principally in order to reduce the risk due to excavation damages and transmitted surface loads. A different design philosophy is present in American standard where cover depth is defined as a function of population density. Therefore, a load base design is present in Italian standard (Table 28) while a risk based design is present in American one (Table 29).

Regarding distances from buildings and other infrastructures, soil permeability and gas pressure are considered for the identification of distances even if no considerations are present for pressures lower than 0.5 bargas shown in Table 30.

**Table 28.** Installation depth in accordance to Italian standard.

Laying condition	$1.5 < P_e \leq 5$	$0.5 < P_e \leq 1.5$	$0.04 < P_e \leq 0.5$	$P_e \leq 0.04$
Street	0.9	0.9	0.6	0.6
Areas not subjected to vehicular traffic	0.4	0.4	0.4	0.4
Land installation	0.9	0.9	0.6	0.6
Rocky land	0.4	0.4	0.4	0.4

**Table 29.** Installation depth in accordance to American standard.

	Normal excavation	Rock excavation	
		NPS $\leq 20$	NPS $\geq 21$
Class 1	0.61	0.30	0.46
Class 2	0.76	0.46	0.46
Class 3, Class 4	0.76	0.61	0.61
Drainage ditch	0.91	0.61	0.61

**Table 30.** Minimum distance [m] from buildings for mains as function of operative conditions and laying environment. Source [49].

Category	Laying conditions	MOP, [barg]			
		[5; 1.5[	[1.5; 0.5[	[0.04; 0.5[	> 0.04
A	<ul style="list-style-type: none"> <li>Impermeable superficial layer;</li> <li>Higher permeability in lower layers than in superficial ones.</li> </ul>	2	2	No requirements	
B	<ul style="list-style-type: none"> <li>No impermeable layer for at least 2 m coaxially to the axis of the pipe;</li> <li>Same permeability in lower layers than in superficial ones.</li> </ul>	1	1		
C	<ul style="list-style-type: none"> <li>Same conditions as reported in category A but with drainage solutions for gas implemented.</li> </ul>	No requirements			
D	<ul style="list-style-type: none"> <li>Same conditions as reported in category A but with protection solutions implemented.</li> </ul>				

About gas migration in the soil, very few studies and experimental activities are present in literature; from these, it has been found that the main parameter that affects gas migration is soil permeability followed by gas pressure [50]. Furthermore, it was found that explosion very rarely occurred at a distance of more than 15 m from leak source.

An occurred accident is reported as example to make more clear the risk due to gas migration through the soil:

- *Natural gas explosion destroyed a house* (Figure 50):
  - i. **Date:** 5/3/2008;
  - ii. **Damages:** a house was completely destroyed, one man killed;
  - iii. **Gas system:** a 2” and an 8” carbon steel carbon steel pipelines are present. Pipelines were installed in 1961 and operated at 10 psig (0.69 barg). Coal tar enamel was used as coating;
  - iv. **Consideration:** The porous material used in the sewage trench (that is perpendicular respect to gas line) caused the gas to flow in a preferred diction inside the home.

In this case, even if distances from buildings and other buried lifelines were respected, gas migrated through the present sewage trench becoming a preferred path to the home. Technical solutions should be implemented to reduce gas migration such as the installation of impermeable layers, gas drainage paths and sealing devices at the connection between lifelines and supplied homes.



**Figure 50.** Gas accident occurred in Pennsylvania the 5<sup>th</sup> March 2008.

A minimum distance equal to 0.5 m is also required in the case that other buried services are present near to the pipeline both in Italian and American standards even if the requirement is valid only for pressure higher than 0.5 barg in Italian case. The importance of distance is reported citing an occurred accident caused by the closeness between a plastic pipes and an electric cable:

- *Natural gas explosion destroyed a house* (Figure 51):



**Figure 51.** Damaged service pipe (right) and destroyed building (left). In the polyethylene pipe is evident the ductile rupture due to the softening of the material caused by an electric arc from the electric cable.

- i. **Date:** 7/7/1998;
- ii. **Damages:** a house was completely destroyed, one woman died, one man was seriously injured and two children received minor injuries;
- iii. **Gas system:** a 3/4" polyethylene service pipe;
- iv. **Cause:** a failure in the electrical cable system produce overheating of the polyethylene pipe that reached the Vicant softening temperature (this is defined as the temperature at which a flat ended needle of 1 mm<sup>2</sup> circular cross section will penetrate a thermoplastic specimen to a depth of 1 mm under specified load using selected rate of temperature rise equal to 119 °C in the case). A leaking hole after produce the leaking hole and gas flowed out enter the building or through the lifelines penetration paths or through small cracks in the foundations.

### **2.3 Comments**

As reported in the chapter, a detailed description of NG distribution networks is very difficult because of the several components that are required to convey natural gas to final customer. For this reason, main components have been identified such as pipes, joints and fittings and valves and a brief description was reported considering Italian situation that can be considered as a state of the art for the gas distribution sector.

From the analysis of standards, it results that system design depends on operative conditions and used materials that can be steel, plastic, cast iron, copper or also other ones in the case of existing networks. It was found that steel has the highest mechanical performances even if very high performance can be achieved by polyethylene. Furthermore, priorities of interventions can be identified for each materials considering design and specific characteristics. Main differences respect to American conditions were also analysed. It should be immediately reported that, while dedicated standards are present for Italian gas distribution, gathering, transmission and distribution are together reported in American technical rule. Nevertheless, similar requirements are present in the two standards even if the concept of Location Class present in the American part gives more attention to a risk based design increasing the requirements in high density areas.

Considering fittings and joints, similar connection techniques are allowed in American and Italian gas distribution; it should be noted that American document is less organized respect to Italian one making the identification of the components very difficult. Another important difference is about valves. While Italian DSOs are responsible for the definition of inspection frequency, American standard defines minimum inspection frequency for emergency valves leaving instead the definition for service valves to DSOs. Furthermore, while many American DSOs are going to install Excess Flow Valves in new service lines to reduce the risk in case of gas emergency, no suggestion is present in Italian standard.

Minimum installation requirements are finally evaluated with particular attention to installation depths, distance from buildings or other buried lifelines evaluated. Installation depth is defined as a function of pressure and soil permeability in the case of Italian standard while as a function of Location Class in the American case. Also in this case the design philosophy is different because of while Italian standard tends to reduce the accident probability, American one is finalized to the minimization of outcomes in case of leakages.

A similar condition resulted for distance from buildings and other buried lifelines. In this case, however, both rules don't suggest solutions to reduce the gas permeation through the soil or through the trench of other services as for example the presence of impermeable layers between the services, gas drainage path or other possible solutions. The introduction of more stringent requirements for new networks in order to reduce underground gas permeation seems necessary because of several accidents occurred in the past caused by the explosion of gas introduced into buildings.

Thanks to the brief description of NG distribution networks, risk management applied to gas distribution introduced in next chapter. Particular attention will be given to the state of the art and existing solutions. Furthermore, the actual safety performances will be analysed in order to justify the importance of the proposed solution.

## Chapter 3

### Risk management of a NG distribution network

Before to proceed in risk analysis some considerations an overview of the state of the art is required. For this reason, the chapter is divided as follow. In the first part risk and maintenance procedures used in NG distribution networks are reported. After that, the procedure for risk management described ISO 31000 [51] is reported. Finally, possible accident causes and consequences are described and characterized.

#### **3.1 State of the art**

NG distribution asset management derives from a critical balance between economic and safety considerations. Every year thousands of failures occur in networks posing a risk to surrounding targets such as human, environment and buildings. That is, the importance of risk analysis and management firstly appear in the work of [52] in which a historical and preliminary analysis of 131 gas accidents occurred in transportation of natural gas is made; even if the work not specific to distribution, it is immediately clear their importance.

A very complex activity is required in the case of NG distribution because of network size and specific boundary conditions that characterize each part of the system. Several methods are present in literature about the optimization of maintenance activities such as that proposed in [53] based on cost optimization: even if several voices of cost are considered such as the acquisition cost, the cost of maintenance, the cost of opportunity of the capital, the cost of decommissioning, the benefit of depreciation, and other economic variables resulting in a very accurate analysis from an economic point of view but very poor attention is given to risk; furthermore, the risk is considered only as failure probability not considering possible outcomes and so not making difference between pipelines installed in different populated areas.

Several other methods are based on stress – resistance balance. In this case the intervention is planned in order to reduce the probability that stresses are higher than resistance. However, only time dependent causes are considered. [54] used First Order Reliability Method (FORM) to calculate the failure probability of L290 GA pipes considering a constant corrosion rate and the limit state proposed by ASME that, as evaluated by [55], gives conservative results respect to those obtained by structural models. [56] applied Monte Carlo simulation to analyse pitting corrosion depth and rate using data collected over a three-year period from 250 excavated pipeline sites located across southern Mexico. [57] proposed a model to estimate the localized corrosion damage based on Gumbel probability distribution without considering coating. Markov method is applied by [58] to evaluate pit corrosion rate and so to evaluate remaining life. A review of structural deterioration of water cast iron is proposed considering several loads such as inside pressure, traffic, soil and thermal loads in [59]. In [60] a methodology to estimate remaining service life of grey cast iron water mains is proposed based on an iterative procedure starting from an estimation of corrosion rate. In [61] Artificial Neural Network (ANN) is applied to assess conditions of an offshore transmission pipeline; in the work, even if several parameters have been considered, only corrosion is considered to assess the condition of the pipelines.

Furthermore, training dataset is given to the algorithm thanks an inspection activity on the pipeline. In this case, a limited number of possible treats has been considered making difficult the application to distribution networks where, as already said, several loads can be present.

Other methods to plan maintenance are based on the results from inspection. [62] proposed a method based on costs and pipeline inspection data. In [63] corrosion depths measured by in line inspections are used to design a Bayesian analysis applied for the identification of optimum maintenance strategies.

That is, several concerns appear for the application of the identified methods in NG distribution networks. Firstly, in the economic based models no considerations of possible consequences in case of gas leakage are present. In the stress – resistance models it is very difficult to evaluate all the possible loads for each part of the system because of the high uncertainty in real cases; furthermore, inputs are often not available in existing databases. Finally, in case of distribution networks inspection activities gives poor information not sufficient to identify the real state of the pipeline respect to what happen in transportation systems.

However, the most important lack is the absence of consequences evaluations in the proposed models. In fact, after the accident occurred at San Bruno (California) in 2011 that was responsible for the fatality of eight people and the injury of fifty-eight, more attention was given to risk in distribution networks by the Authorities. For the scope, the American National Transportation Safety Board suggested the application of Integrity Management (IM) programs by gas operators. By its application it is possible to have information to improve prevention, detection, and mitigation activities resulting in better safety performances. Particularly the following elements should be considered in the definition of an integrity management program:

- *To understand system design and material characteristics, operating conditions and environment, and maintenance and operating history;*
- *To identify existing and potential treats;*
- *To evaluate and rank risks;*
- *To measure IM program performance, monitor results and evaluate effectiveness;*
- *To periodically assess and improve the IM program;*
- *To report performance results to Authorities.*

In [64] main principles are reported even if they are applicable only to ferrous materials. Therefore, improvements should be proposed for the application in distribution networks. That is, very few works are present in literature about the application of IM plans in NG distribution systems. In [65] a review of different strategies is reported highlighting the principal steps required for the application. In [66] a review of integrity management programs supported by in line inspection data is made. In [67] the state of the art of integrity management practice in gas distribution systems is proposed; in the paper a practical example dealing with a gas utility located in the South East of Asia is given identifying the following steps: data collection, remaining life assessment, life extension program, cost/risk/benefit analysis. In [68] an integrity management program is proposed for gas distribution being constituted of: asset and threats identification, prioritizing of the risks, identification of corrective actions, results monitoring. In [69] an integrity management programs for pipelines

transporting hydrocarbons and operated by ENI is shown. Interesting results are also presented by [70]; in the paper a decision model for risk assessment based on multi attribute utility theory is proposed. The model classifies different sections of the pipelines considering three possible targets (human, environment and financial) in case of gas accident. [71] proposed to prioritize the inspection and maintenance procedure using a leak quantification that can be assessed during the repair of leaks even if no considerations are made to identify system characteristics and potential treats to surrounding environment.

A qualitative and quantitative risk assessment method for urban natural gas pipelines is proposed by [72]: while the qualitative assessment introduces a causation index, a consequence index and an inherent index to assess the risk, the quantitative approach estimates the probability and assesses possible consequences; however, a very poor assessment of failure probability is performed using data valid for transmission and not for distribution systems. In [73] a fatal length and a cumulative fatal length are identified for each pipeline; the fatal length means a weighted length of pipeline within which an accident has a fatal effect on a person at a specified location while the cumulative fatal length is representative of a length within which an accident leads to N or more fatalities. In [74] a quantitative risk assessment model is proposed even if a unique value for failure probability is considered without taking into account possible differences between pipelines in the network. In [75] risk analysis of urban gas pipeline network based on improved bow-tie model is proposed to critically analyse causes and consequences of NG failures. The proposed model seems to be useful to a preliminary characterization of the system but it does not allow to quantify the risk so a ranking of the network.

Therefore, even if several methods are present in literature no standardization and so common way to evaluate results is present. No comparison between assets exercised by different DSOs is therefore really possible.

For this reason, it is impossible to evaluate the effective performance of the systems and so a common method has to be proposed. Before this, however, a quick description of existing safety performances in NG distribution networks is proposed.

### ***3.1.1 International NG distribution networks safety performances***

As reported, DSOs have to annually distribute high quantity of gas ensuring high performances in terms of quality and of safety. In order to describe international NG distribution safety performances, safety indexes useful to identify trends are proposed [76].

#### ***3.1.1.1 Available sources of data***

Very few papers or documents that critically analyse the existing performance of NG distribution systems are present in literature although the importance [77]. More results are available for the transportation system as reported by [78] about American one or by the European Gas pipeline Incident data Group (EGIG) that periodically publish reports about the performance of the European transmission system; the last one analysed 1.366 accidents recorded between 1970 and 2016 [79]. Also the Transportation Safety Board (TSB) reports accident occurred in Canadian transmission systems.

Instead very poor information is available for NG distribution. For example, the Comitato Italiano Gas (CIG), that is the Italian gas technical organization, annually reports very basic data about accidents occurred in

distribution gas sector including also failure occurred in domestic plants; some data are also reported by [24] even if very poor organization makes impossible to proceed with statistical analysis. Looking outside Italian borders, the Swiss Gas and Water Industry Association (SGWA) reported some data about NG pipeline length, material and accidents [80]. A more detailed analysis about the Deutschland distribution system is made by the Paul Sherrer Institut (PSI) but has not been updated from the 2002 [81]; other information is present in [82]. Finally, the Technical Association of the European Natural Gas Industry (Marcogaz) published a report about safety performance of the distribution system for the years between 2008 to 2015 in 2017 even if no statistical elaboration is possible because of the low quantity of data [83].

The lack of information represents therefore a barrier to proceed in detailed analysis. A different condition is present in the United States where the Pipeline and Hazardous Materials Safety Administration (PHMSA) requires the record of accidents occurred in distribution systems in accordance to the Part 191 of Title 49 of the Code of Federal Regulations in an open database. In the database, accidents are recorded from 1970 even if a change of the minimum conditions to record an accident changed in 1984; in this date, in fact, PHMSA increased the minimum parameters necessary to record an event.

However, no common definition of accident is present in literature. For example, PHMSA requires the submission of a written report in the case that one of the following conditions verifies:

1. *An event that involves a release of gas from a pipeline, or of liquefied natural gas, liquefied petroleum gas, refrigerant gas, or gas from an LNG facility, and that results in one or more of the following consequences:*
  - (i) *A death, or personal injury necessitating in-patient hospitalization;*
  - (ii) *Estimated property damage of \$50.000 or more, including loss to the operator and others, or both, but excluding cost of gas lost;*
  - (iii) *Unintentional estimated gas loss of three million cubic feet (i.e. 84951 m<sup>3</sup>) or more;*
2. *An event that results in an emergency shutdown of an LNG facility. Activation of an emergency shutdown system for reasons other than an actual emergency does not constitute an incident*

*An event that is significant in the judgment of the operator, even though it did not meet the criteria of paragraphs (1) or (2) of the list.*

Marcogaz instead defines an accident as “*an unintentional event, related to natural gas, which has caused physical injuries or fatalities or big material damage*”, in which the term big material damage stands for “*any damage greater than 100.000€, e.g. to houses, cars, excavators etc, except damage on the gas distribution system itself*”. Furthermore, Marcogaz does not include fatalities and injuries that occurs to internal personal and/or contractors. Therefore, it is immediately evident that the comparison between the two sources of data is a bit forced because of some differences are present in the recording method. Even if this situation could be responsible of errors, safety performance trends can be compared.

### 3.1.1.2 Proposal of safety indexes

Because of no common rules are present, the identification of safety indexes is of primary importance. As proposed in [76] accident failure rate in [accident/km], defined as the ratio between the number of accidents in [#] and the total length of the system [km] is proposed:

$$X = \sum_{z=1}^{N_i} x_z / L \quad (3-1)$$

Where X is the accident failure rate in [accident/km],  $x_z$  is the z-th accident occurred in the year considered in [accident] and L is the total length of the NG distribution system in the year considered in [km]. Accident failure rate gives an immediate information about the hazard of the NG distribution system and could be used to identify future objectives or minimum thresholds by national Authorities.

To evaluate the consequences of a gas accident, injury and fatality rates are introduced [injury/accident] or [fatality/accident]. These indexes are calculated as the ratio between the number of injuries or fatalities occurred in the year considered and the total number of accidents in the year:

$$K_j = \sum_{z=1}^N i_{j,z} / \sum_{z=1}^{N_i} x_z \quad (3-2)$$

Where:

- K is the injury (j=1) or fatality (j=2) rate, expressed in [injury/accident] or [fatality/accident];
- $i_{j,z}$  is the z-th injury or fatality occurred in the year considered, [injury] or [fatality];
- $x_z$  is the z-th accident occurred in the year considered, [accident].

Also F-n curves could be considered for the scope to make an evaluation respect to other source of energy. As reported by [84], “F-n curves are a graphical representation of the probability of events causing a specified level of harm to a specified population” and “show the cumulative frequency (F) at which N or more members of the population that will be affected. High values of N that may occur with a high frequency F are of significant interest because they may be socially and politically unacceptable”. Therefore, F-n curves are “a useful way of presenting risk information that can be used by managers and system designers to help make decisions about risk and safety levels” giving an immediate information of frequency and consequence in an accessible format; for the scope, fatalities are considered as consequence.

That is, it should be immediately highlighted that only the PHMSA database allows at the moment the elaboration of the graph even if it is hoped that in the future other sources will become available for the scope as will be justified by the obtained results.

### 3.1.1.3 Results and discussion

Because only PHMSA data are available, a highlight of American condition is proposed even if a trend comparison is reported with other sources and carefully analysed. Only accidents occurred after 1984 have been considered because a wrong interpretation of statistical trends could verify considering the previous period. In the following figures, elaboration regards mains and service lines considering all possible materials.

As shown in Figure 52, a decreasing trend is present for accident. A different conclusion results for injuries and fatalities for which several peaks are present because of the presence of events characterized by very severe consequences. That is, the results do not take into account networks size as made by the accident failure rate, the injury rate and the fatality rate.

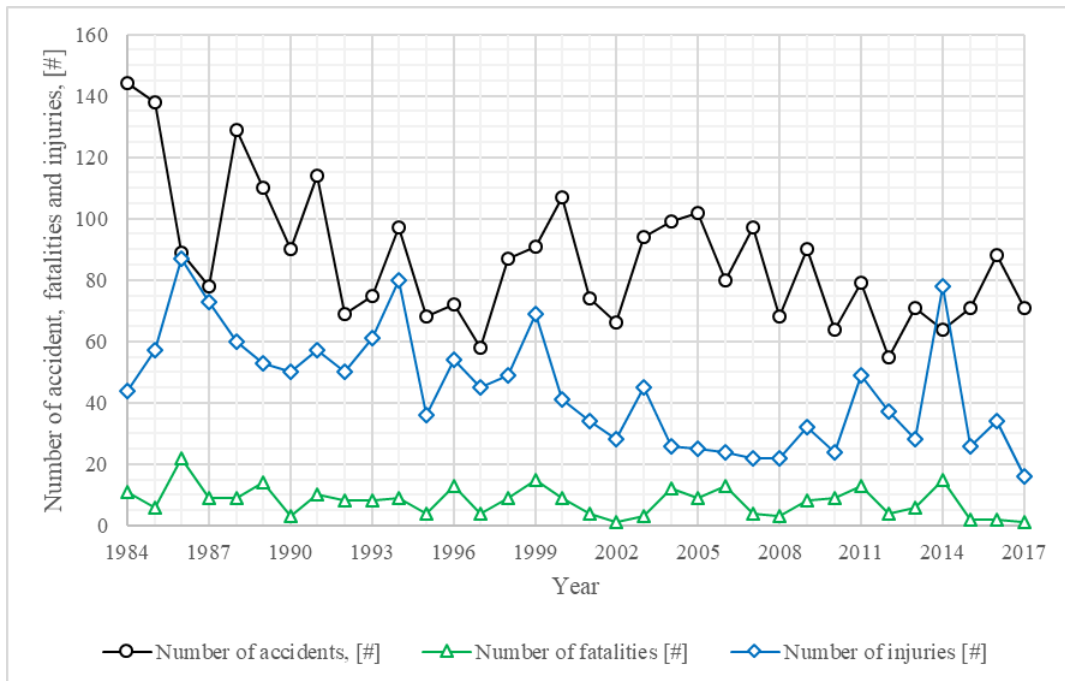


**Figure 52.** Number of accidents, fatalities and injuries that occurred between 1984 and 2015 in mains and service lines of the United States NG distribution system. All materials are considered.

In Figure 53 accident failure rate is reported for American distribution networks. In the same figure, accident failure rate elaborated from other sources are represented for a qualitative comparison. As shown, a reduction of accident failure rate is present in all cases, even if in the last years a low rate is present due to the difficulties to improve the reached performances. The mathematical interpolation is shown for the American system: this is strictly valid for the analyzed period because of the accident failure rate tends to + infinitive for x vanishing (not physically acceptable) and tends to zero for x that tends to + infinitive. This condition is not in accordance with the data because it seems that an asymptotical trend was reached with almost  $2.0 \times 10^{-5}$  accidents/km; considering only steel and plastic an accident failure rate of  $1.6 \times 10^{-5}$  accidents/km has been estimated. Therefore, considering the proposed trend almost 250 years are necessary to reach the goal of  $1 \times 10^{-5}$  accidents/km with the existing trend. A similar trend is reported by the other sources. Of particular interest is the comparison between PHMSA and Marcogaz, because this last is representative of the most industrialized countries in Europe. As shown, a fluctuation is present and higher values are reported in the first part even if American rules are more stringent about the conditions required to record an accident. For this reason, it seems that a higher performance is present in American natural gas distribution systems, even if some doubts are present because of the few number of years available for European infrastructure.

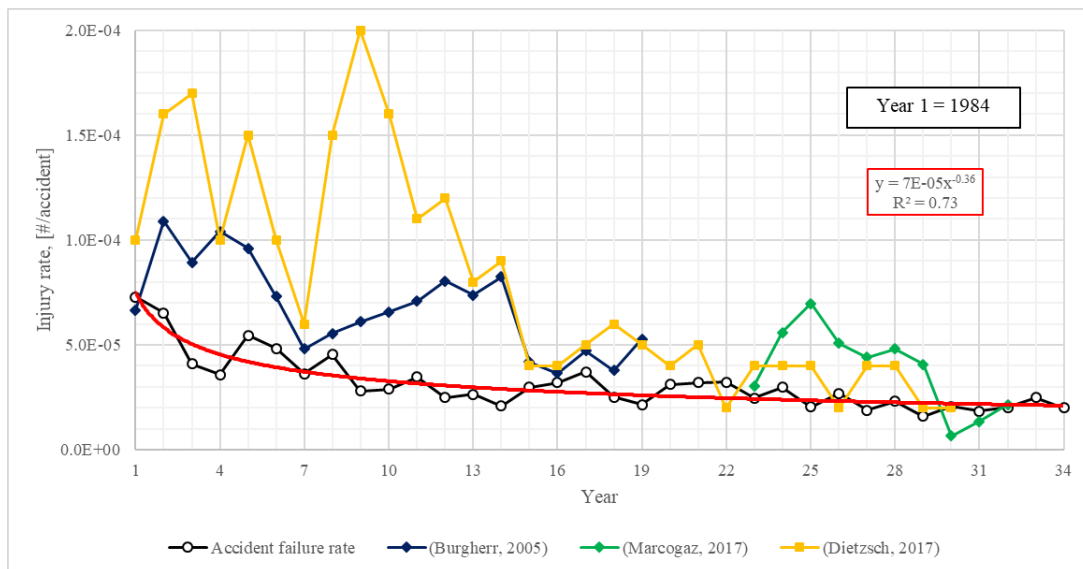


**Figure 53.** Accident failure rate from 1984 to 2017 considering data from several sources.

Injury and fatality rates are shown in Figure 55 and in Figure 54. Considering fatality rate no clear trend through the years is present because of a high dispersion year by year. For this reason, a moving average analysis is considered. Considering a period of ten years for fatalities, a rate between 0.07 and 0.11 fatalities per accident have been calculated. Values of the same order of magnitude have been also found from other sources demonstrating the effectiveness of mitigation and protective equipment to reduce deadly consequences of gas accident.

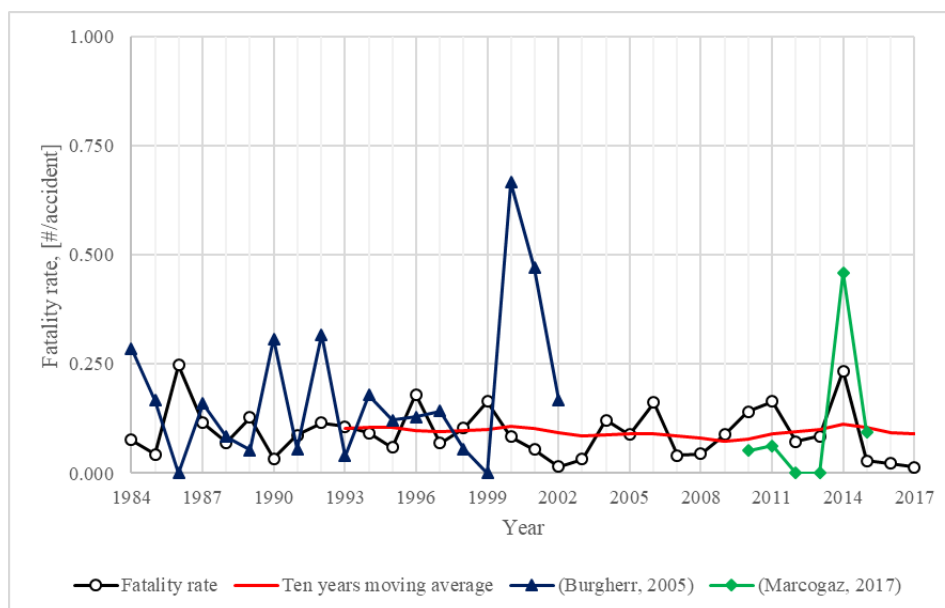


**Figure 54.** Fatality rate in the years between 1984-2017 considering data from different sources.

For injuries, a five-year period is used, finding a minimum in 2008 - 2009 (between 0.2 and 0.3 injuries per accident) and a following slight increase. From the figure, it results a higher number of injuries reported by Marcogaz. Considering that the information does not regard DSO's employers, particular care should be given to analyse the reasons and the possible measure to mitigate the problem. However, this is not possible with the available data and so improvements are suggested about the required information to be recorded.

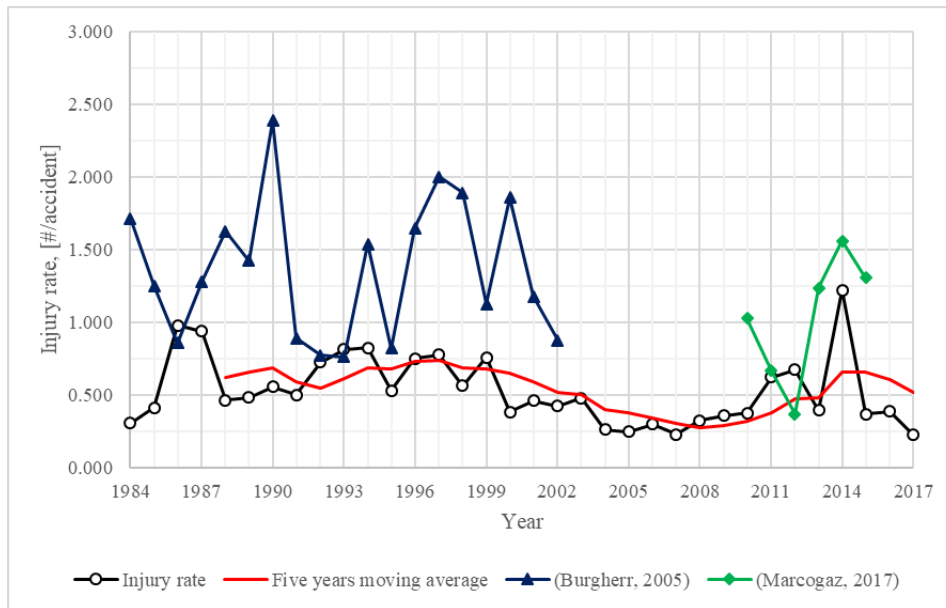


**Figure 55.** Injury rate in the years between 1984-2017 considering data from different sources.

F-n curves about fatalities occurring in the American mains and service lines are shown in Figure 56 where three different regions are identified: the intolerable region (red), the As Low As Reasonably Practicable (ALARP) region (blue) and the broadly acceptable region (green).

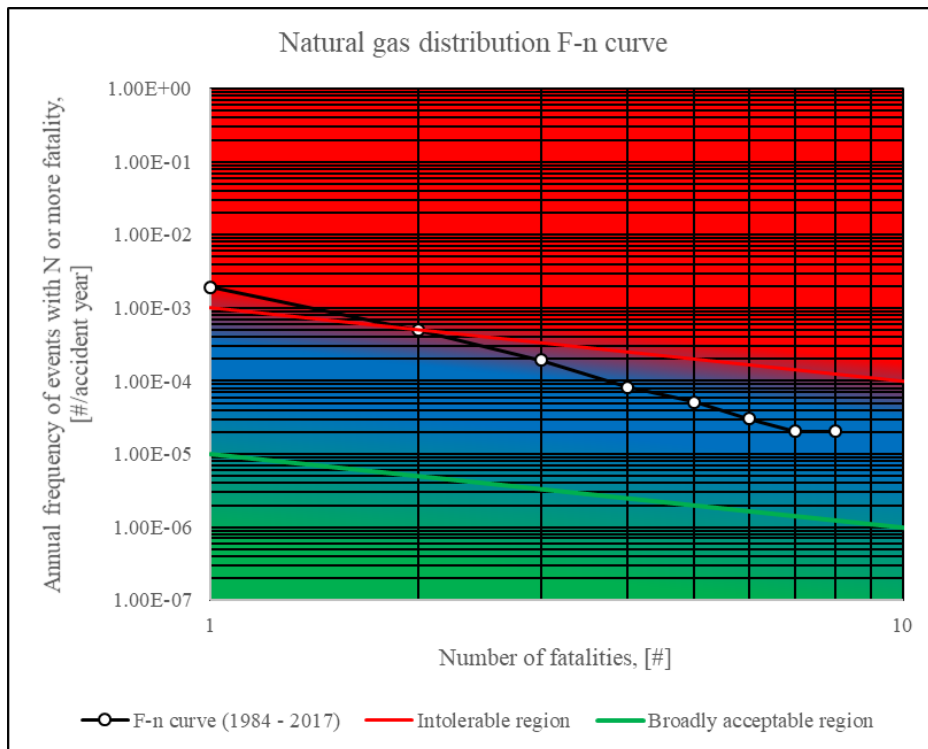


**Figure 56.** F-n curve for the American natural gas distribution system. Data between 1984 and 2015 are considered for the elaboration.

ALARP principle states that risks lower than the limit of tolerability are tolerable only if risk reduction is impracticable or if its cost is grossly in disproportion to the improvement gained. Respect to fatality rate in which a sum of the fatalities occurred are made, in the F-n curves the number of accident with a number higher or equal to N is proposed. That is, considering the total period between 1984 and 2017 part of the curve is intolerable region. Particularly, for the three time periods, i.e. 1984 – 2004, 2004 – 2010 and 2010 – 2015 a

similar behaviour has been found in Figure 57 where the percentage of occurred accident with n fatality is proposed. So, even if corrective actions have effectively reduced the number of accidents, further improvements seems to be required in order to reduce accident consequences.

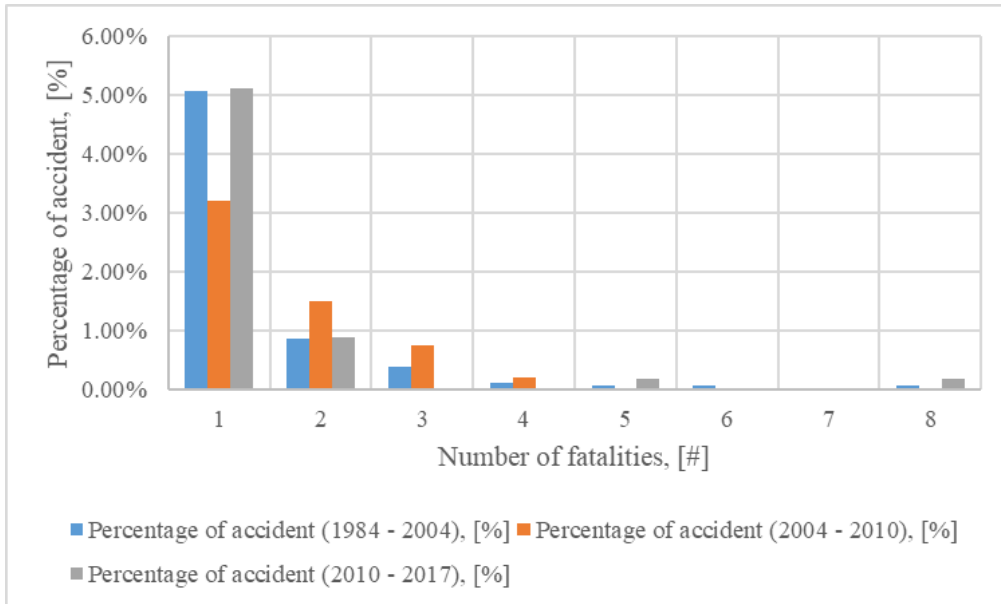


**Figure 57.** Percentage of accident with a defined number of fatalities.

Consequently, it is evident the potential and the importance that a dedicated database could have to drive the best decisions in order to improve safety performance. At the moment, in fact, it results very difficult to understand in which direction actions have to be taken especially in European case. Consequently, it is opinion of the Author that a standardized and worldwide accepted method to records gas accident information have to be introduced (Figure 58).

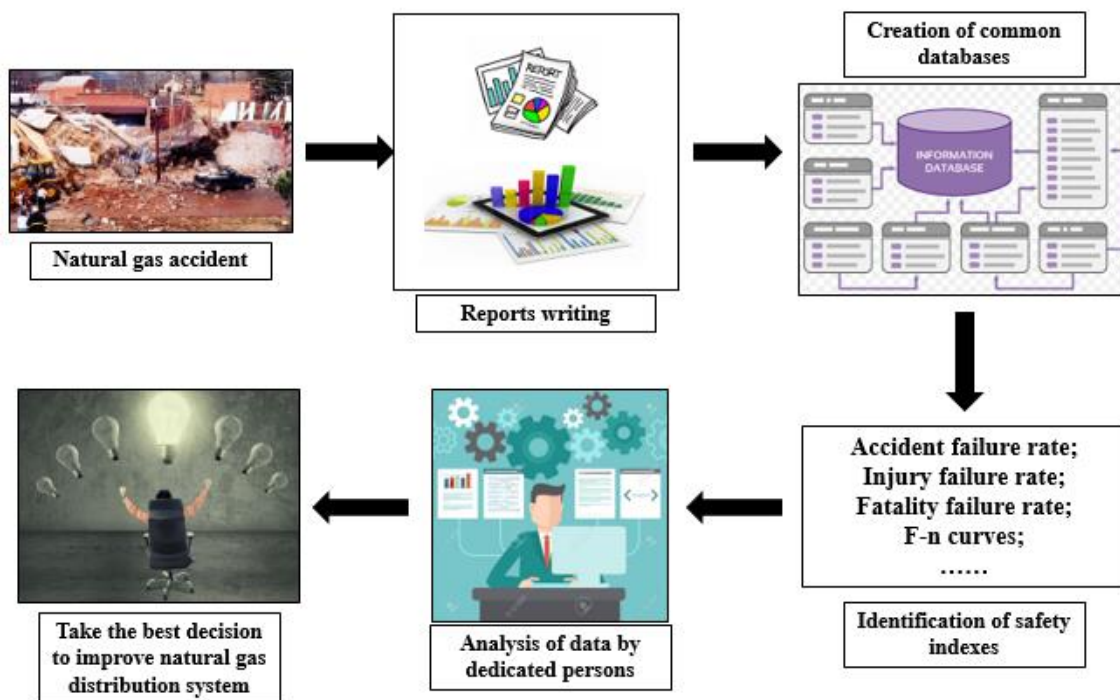


**Figure 58.** Schematic representation of potentials reachable with a dedicated and internationally standardized database.

### 3.1.2 Italian NG distribution networks safety performances

As reported in first chapter, more than 250.000 km of pipelines are installed in Italy with the highest percentage in densely populated areas increasing the risk in case of failure. In fact, since the risk is the product between failure probability and consequences, a higher risk is expected in more populated areas. However, as reported in [47,85] several requirements about quality and safety have to be respected by Italian DSOs such as, for example, the calculation and the reports of the following:

- The percentages of network annually inspected at high, medium and low pressure, defined as the ratio between the inspected length and the total length of the system.
- The number of leakages annually identified during planned inspections and reported by third parties;
- The performance of first aid interventions such as the call response time, the arrival time and the time required to eliminate the leakage.

Consequently, to maintain high safety and quality levels is a very challenging task for DSOs. For the scope, inspection frequency requirements have to be respected in accordance to the following:

- High and medium pressure networks: 100% of the system in 3 years;
- Low pressure networks: 100% of the system in 4 years. More frequent inspection is required for those part of the system made with a material different from cathodic protected steel, polyethylene, restored cast iron, cast iron with joints that does not present hemp and leads material.

Furthermore, an annual report on the assessment of gas leakage risks is required by Italian Authority in accordance to the method proposed by [86]. As reported, DSOs have to report the following:

- A *risk index*,  $I_r$ , estimated as a function of pipe materials, gas pressure and gas leakages identified by third party as follow:

$$I_r = \frac{1}{2} \left[ \frac{\sum_i L_i f_i + \sum_j L_j f_j}{\sum_i L_i + \sum_j L_j} + \frac{1000}{2} \frac{D_t + D_{t-1}}{L_{rs}(\sum_i L_i + \sum_j L_j)} \right] \quad (3-3)$$

Where  $L_i$  and  $L_j$  are respectively the size of the low pressure and middle/high pressure networks,  $f_i$  and  $f_j$  are parameters that depend on pipe material,  $L_{rs}$  is a defined threshold for leakages (=0.1 leak/km) and  $D_t$  are the number of leak identified by third party in the year  $t$ .

**Table 31.**  $f_i$  and  $f_j$  parameters used in the estimation of risk index.

Material	$f_i / f_j$
Polyethylene	0
Cathodic protected steel	0
Unprotected steel	1
Cast iron with lead joints	1.5
Cast iron with other joints	0
Other material	1.5
Renovated cast iron	0

- *Demerit classification* that ranks pipelines or network areas in order to identify intervention priority. The method is used for steel or cast iron with lead joints pipelines. That is, pipe ranking is in accordance to the following:

$$P_i = \sum_k A_k k_k \quad (3-4)$$

Where  $A_k$  and  $k_k$  are the parameters and importance weight respectively as reported below:

- *Cast iron*: diameter, pressure, distance from building and installation depth;
- *Steel*: diameter, pressure, distance from building, installation year and system type.

In the case of an area an average value is calculated:

$$P_{area} = \sum_i P_i \frac{L_i}{L} \quad (3-5)$$

Where  $L_i$  is the length of the  $i$ -th pipe and  $L$  is the total size of the network of the considered area.

Therefore, existing inspection requirements takes into account only probability of failure and no considerations are made about possible consequences of a gas failure and so to the risk induced to surrounding targets.

That is, the percentage of networks annually inspected in Italy is shown in Figure 59. As it is shown, an increasing trend is present from 1997 to 2016 passing from 30.0% to 67.2% with an increase of +124%. Considering the period between 1997 (year = 1) and 2016 (year = 20) a linear trend for inspection activities is proposed; it should be noted that the trend is strictly valid for the period considered because of for  $x$  that tends to infinity a not physically admissible value would result ( $+\infty$ ). However, for  $x$  that tends to infinity the 100% should be reached asymptotically; in fact, this sentence could be justified and reasonably motivated by the always more implementation of sensors and instruments on the networks according to the paradigm of Industry 4.0 that would ensure real-time and continuous monitoring in next years.

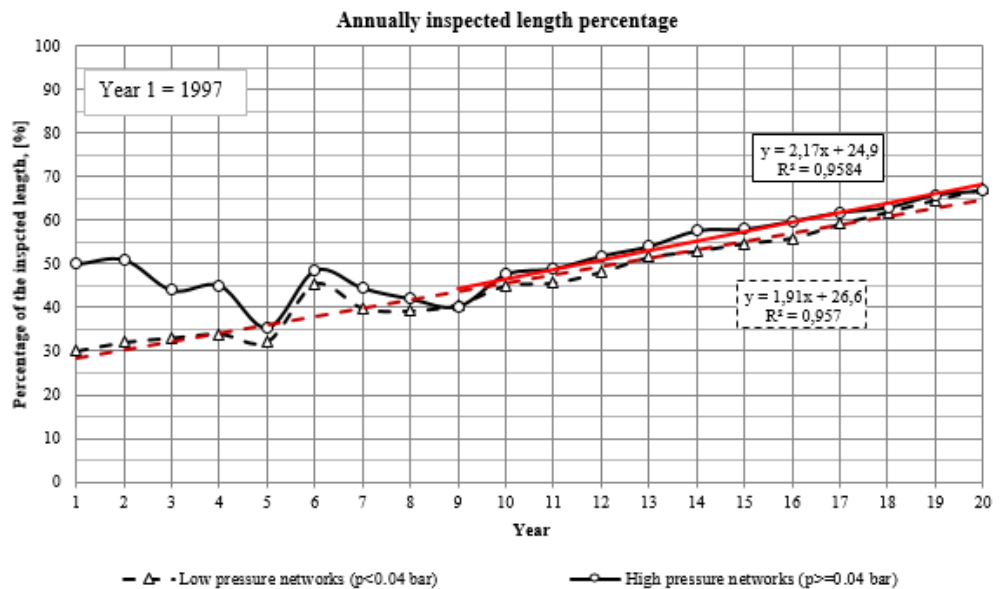


Figure 59. Percentage of annually inspected length of the Italian natural gas distribution networks.

Such as the percentage of inspected networks, also the number of annually identified leakages gives a clear information about the condition of the national systems. However, it should be immediately highlighted an issues to perform the analysis due to existing definition. In fact, no distinction between low, middle and high pressure systems is made:

$$NDI = \frac{DI}{L_{HP+MP} + L_{LP}} \times 100 \quad (3-6)$$

Where DI is the total number of leakages in the considered year [leakage/y] and  $L_{HP+MP}$  and  $L_{LP}$  are the length of high, medium and low pressure systems inspected in [km]. Consequently, a very poor characterization of leaks is possible. Therefore, it is opinion of the Author that distinction between systems should be done not only in terms of MOP but also in terms of design: in this way, it would be easier to identify trends or abnormal conditions and directing future strategies to improve the performance of the existing system.

As shown in Figure 60 a decreasing trend of leakages per km is present from 2002 (year 1) to 2016. Also in this case the trend is strictly valid in the period analysed; in fact, a physically inadmissible condition occurs for x that tends to infinity that would represent the total absence of leaks in the networks that seems to be not possible. However, the reducing trend is justified by the substitution and renovation of old and low performance pipelines with higher performance ones. Considering that at 2016 the inspected length has been 129.334 km (almost the 64.3% of the national system), 7.761 leakages have been found during inspection. If more dedicated and severe recording policies will be required by the Authority, a statistical analysis could be implemented contributing to increase DSOs' know – how and give more information to decision makers in which direction allocate the budget.

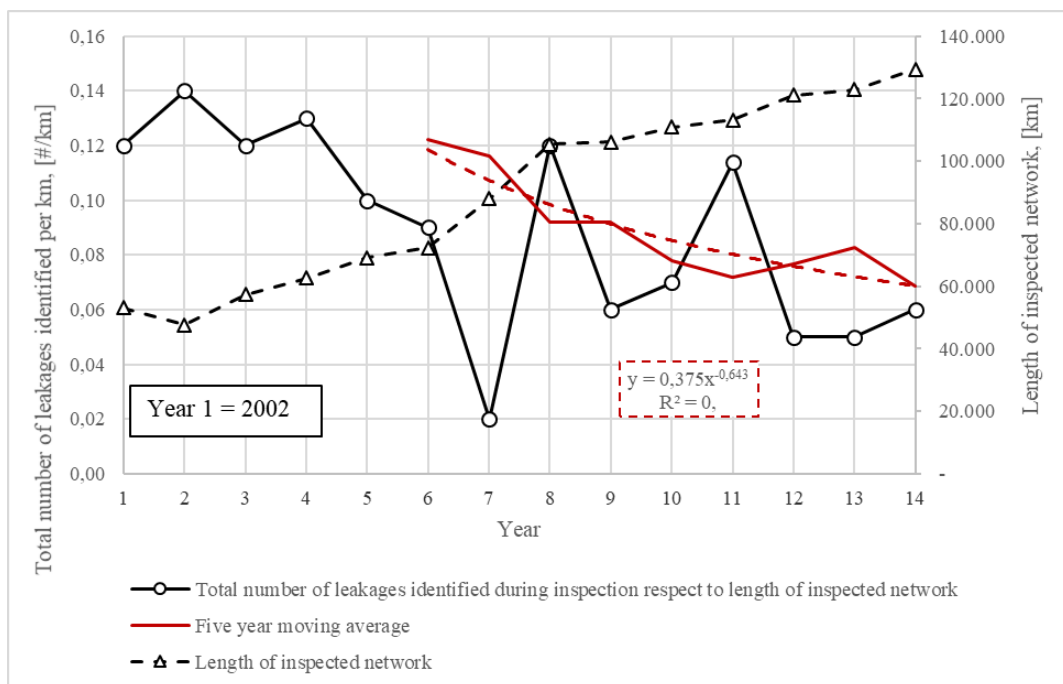


**Figure 60.** Number of identified leakages during inspection activities (continuous black line), total length of inspected pipeline (dashed black line) and five year moving average of identified leaks during inspection (red continuous line).

Another interesting information to is the number of calls to distributors in case of problems; unfortunately, no distinction is made as a function of the call reasons, reducing the impact of the information.

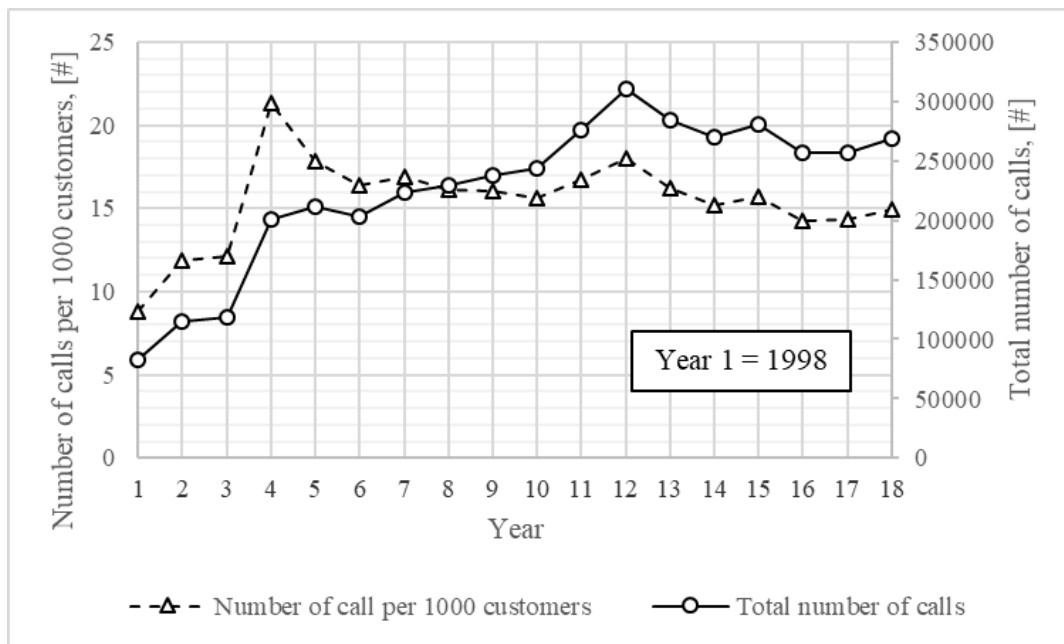


**Figure 61.** Number of calls (per 1000 customers and total) between 1998 and 2016.

As shown, between 1998 and 2010 an increasing trend was present, followed by an almost constant trend with an average of 270.000 call/year in accordance to the number of supplied customers in the same period. Therefore, an asymptotic value of 0.015 call / (year x customer) has been reached.

However, no distinction between causes is made in the available data even if Art. 28 requires to Distributors more specific information respect to those that are publicly available; consequently, it is not possible to proceed to further analysis. With more data, the following considerations would instead be possible:

- *What part or parts of the distribution system is characterized by the highest failure rate?* Specific suggestions would be given to Distributors in order to improve the actual performance of the system;
- *How much existing inspection procedures performant are?* In fact, knowing the number of calls due to gas leakage, it would be possible to evaluate if the increase of the inspection activities in last decades have a positive impact to improve safety the safety performance of the distribution networks.

To conclude the paragraph natural gas emergencies and accidents occurred in Italian gas distribution sector are analyzed. Emergencies are defined as “*an event that is capable to produce serious effects for the security and continuity of the distribution service and that is caused by one or more of the following conditions:*

- *Unplanned out of service of one or more supply points;*
- *Unplanned out of service of high, medium or low pressure systems that is responsible of the interruption of gas supply to one or more customers;*
- *Gas leakages responsible for unplanned gas supply interruption to one or more final customers;*
- *Rupture caused by a pressure error in the network.”*

Natural gas accidents are, instead, defined as “*an event involving gas distributed through networks, which interests any part of the distribution system and / or installations of final customers .... which causes death or serious injury to people or damages to for a value not less than 5,000 euros in case of occurrence in the*

distribution network and not less than 1,000 euros in the case it occurs in the final part of the system of which customer is responsible that is caused by one of the following:

- A dispersion of gas (voluntary or not);
- An uncontrolled combustion in a gas appliance;
- A bad combustion in a gas appliance, including in the case of insufficient ventilation;
- An inadequate ventilation of the space inside the buildings;
- An inadequate evacuation of the combustion products from a device that make the use of gas.”

In these cases, DSOs have to report main data to CIG in defined formats [87,88]. With these data, CIG annually defines the performances of the sector in terms of number of deaths and accidents as reported in Table 32 where performance between 2007 and 2016 are shown.

**Table 32.** Number of accidents and fatalities that occurred in Italian NG distribution sector recorded by CIG.

Year	2007	2008	2009	2010	2011	2012	2013	2014	2015	2016
Number of accidents	160	175	201	195	144	177	159	126	120	123
Fatalities	18	16	19	15	15	14	9	14	15	11

As shown, a reduction trend is present both for accidents and for death, demonstrating the increase in safety performance. However, accidents (and so deaths) included do not distinguish between failures occurring in the distribution systems (that is in the responsibility of DSO) and downstream the meter (that is in the responsibility of the customer). In this way, very poor analysis can be performed. It should also be noted that no public database is at the moment available make very difficult to find and elaborate data.

Consequently, no scientific approach can be performed with the scope to understand and improve the performance of the Italian natural gas system with existing available information. In fact, the following three steps should be considered in the research for the scope: data analysis, development of mathematical models and experimentation/validation. The lack of a dedicated database in which data are systematically recorded represents an obstacle. Consequently, it is opinion of the Author that a dedicated approach should be defined to record both near misses, accidents and emergencies occurred in NG distribution systems.

To conclude the paragraph, it should be introduced the project developed in 2008 after the NG accident occurred at San Benedetto del Querceto in 2006 and called in Italian “*Progetto rischio gas*”. The project represented an operative proposal to improve the knowledge of civil protection activities in case of gas accident occurred in the area of Bologna. A group of experts was instituted consisting of experts from local DSOs, local Authorities, and safety emergency teams. During the project an exchange of information was ensured, identifying possible issues on the territory and providing technical documentations to be sent to all interested stakeholders. The project gives interesting results even if it was performed only at local level.

### **3.2 Methodologies for risk analysis: ISO 31000**

ISO 31000 [51] should be used by those people that create and protect value in a company or in an organization through risk management independently from the market. For this reason, risk management should be applied

also to NG distribution. Particularly, the best decisions have to be taken in order to reach objectives and improving performances executing an iterative procedure able to identify the optimum strategies. In order to correctly understand the philosophy proposed by the standard the following are highlighted:

- *Purpose*: risk management scope is the creation and the protection of existing value, improving performances, encouraging innovation and supporting the achievement of better results than existing ones. To reach the scope, the following key words should be included in the design of a risk management strategy (Figure 62):
  - *Integrated*. Risk management should be an integrated process within the organization ensuring its contribution to each activities present;
  - *Structure and comprehensive*. Steps identified in the procedure should be the more structured and comprehensive as possible in order to ensure comparable and effective results;
  - *Customized*. The risk management strategy should be designed for the specific scope and to the context in which will be used;
  - *Inclusive*. As reported, appropriate and timely involvement of stakeholders enables their knowledge, views and perception has to be considered. For this reason, efforts should be given within the company about the importance of the risk management philosophy in order to ensure that all will give support;
  - *Dynamic*. Risk management strategy have to react against risk development the fastest as possible. Therefore, steps to evaluate possible risks should be considered in the methodology and updated frequently in accordance to sector dynamics.
  - *Best available information*. To ensure good results the best available information should be used. For the scope, literature, reports or dedicated database should be considered by organizations;
  - *Human and cultural factors*.
  - *Continual improvement*. Risk management should be continuously performed though the use of the most update information. In this way, the state of the art condition is identified.

However, the success of its integration depends on the importance given by decision makers inside the Company. For this reason, several steps are required to ensure the best results such as defined in Figure 63. As shown in the figure, top management has a fundamental role ensuring the application in company's framework for example defining plan to approach risks, assigning the required resources for the application and the authority at appropriate levels within the organization. Oversight bodies are also identified to identify risks, to ensure their management inside the organizations as a function of the specific context. For example, in NG distribution main risks to be considered are those produced by a pipeline failure.

Therefore, top management and oversight bodies have to show their efforts in the promotion of a risk management strategy at all company levels, allocating the needed resources to reach the identified goals, and promoting communication and consultation procedure in order to share the obtained or expected results to the interested stakeholders. That is, an optimum strategy has to be identified to allocate strategy: in the case of NG distribution assets, intervention should be prioritized as a function of risks.

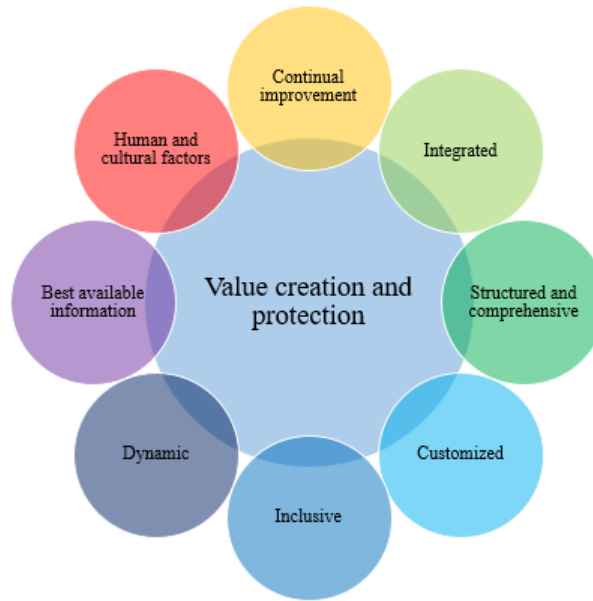


**Figure 62.** Purpose of risk management. Source [51].

A strategy to continuously improve risk management has also to be identified. Safety indexes from periodically reviews can be considered to evaluate the effectiveness of the plan (evaluation) and so to improve existing procedures. For the scope, data from the field have to be considered to improve performances (improvement).



**Figure 63.** Framework of risk management. Source [51].

Consequently, risk management can be summarized in main steps:

- *Identification of the scope, context and criteria.* While for context and criteria no particular evaluations seem to be done, some specifications should be considered about scope. In fact, different levels are available for risk management that have to be considered by top management:
  - Objectives and decisions. in the case of NG distribution, reducing the risk to people and environment to a tolerable value should be considered;

- Outcomes expected. In the analysed case a prioritization of interventions based on risk is expected. Furthermore, a continuously updated information about asset conditions through the year can be achieved;
- Appropriate risk assessment tools and techniques. The decision should be taken as a function of the available data and of the designed procedure;
- Resources required. Resources do not consider only economic ones but also human resources that should be inserted in the program;
- Relationship with other projects, process and activities.
- Risk criteria. A fundamental decision to be taken by the organization is about the amount and the type of risks that can be accepted. In the case of NG distribution, no standardized or commonly accepted value is present. However, tolerable values identified in chemical process or transportation is suggested for the scope as those reported in [89] as a function of the limit state type, the fluid transported and the location of the pipeline.
- *Risk assessment.* Risk identification, analysis and evaluation have to be performed in this phase using relevant, appropriate and up-to-date information (literature and databases are included). In Figure 64, main steps to be followed in case of NG distribution systems are proposed; it should be noted that the identification of sensitivity and confidence levels depends on the inputs used in the analysis.

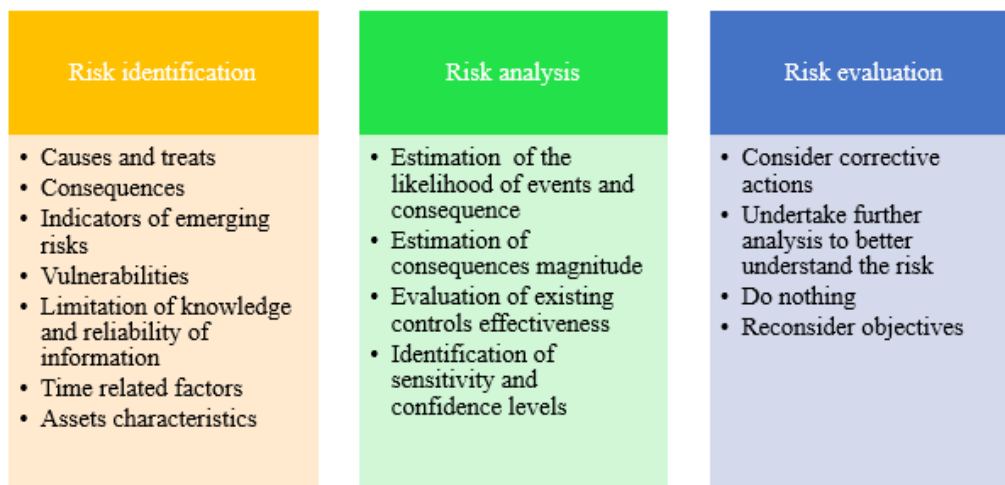


**Figure 64.** Main steps of risk assessment suggested in the case of NG distribution networks.

- *Risk treatment.* Risk treatment can be considered as an iterative process in which possible risk treatment options are evaluated in order to select the best solutions for the analysed case. Different solutions can be considered such as protective (reduction of the consequences), preventive (reduction of the probability) or both. When the solution is identified, an implementation plan has to be prepared containing the following information: description of the solution, the expected results, the resources allocated and a performance evaluation method.
- *Monitoring and review.* To ensure that the implemented method improve the overall quality of the company, a monitoring and review plan has to be identified and information reported to the top management.

- *Communication and consultation.* Obtained results and performances should be clearly and simply communicated to different stakeholders such as local Authorities but also to supplied customers.

Consequently, a risk management plan that follows the main requirements reported in this paragraphs can be considered for the application in NG distribution assets by utility companies in order to perform an integrity management plan. For the scope, in following paragraphs main causes of failures and possible consequences in NG distribution networks are analysed, while in next chapter the proposed method in accordance to paradigms of ISO 31000 is presented.

### ***3.3 Failure causes of NG distribution networks***

Risk analysis of buried pipelines starts from the identification of possible failure causes and consequences. Leaving the analysis of consequences to the following paragraph, failure causes are here identified. Before to begin the analysis, it should be noted that pipeline conditions can be evaluated considering the loads and the resistance offered by the system. As reported by [90], three different limit states for natural gas can be considered:

- *Ultimate limit states (ULS)* in which large leaks and ruptures are included;
- *Leakage limit states* characterized by a leak from a small hole that usually is not responsible for significant consequences;
- *Serviceability limit states (SLS)* in which damages such as local or global buckling, ovalization, denting and plastic deformation are present. In these case no leakage is present but a reduction of the resistance offered by the pipeline is estimated making necessary the repair intervention.

Limit states are usually identified with the following expression:

$$G(x, t) = R(x, t) - S(x, t) \quad (3-7)$$

Where  $G(x, t)$  is the limit state function as a function of a vector of  $x$  random variables and time  $t$ , while  $R$  and  $S$  are respectively the resistance offered by and the load exerted on the system. As shown, the following considerations have to be made:

- System failure cannot be generalized being strictly dependent on time and so on existing boundary conditions;
- Failure can be caused by resistance reduction but also by the increase of exerted loads;
- Time has to be taken into account for the evolution of risk of exerted systems. Therefore, risk assessments have to be periodically performed.

In accordance to [64] possible treats of NG distribution systems are divided in three main categories: time dependent, stable and time independent. Because of only metallic pipelines are included in the original documents, also possible hazards occurring in plastic pipes are inserted in the list:

- *Time dependent:*
  - External corrosion and graphitization;

- Stress corrosion cracking;
- Slow Crack Growth (SCG);
- Rapid Crack Growth (RCP);
- *Stable:*
  - Manufacturing-related defects;
  - Welding and fabrication related defects;
  - Equipment failures;
- *Time independent:*
  - Third party and mechanical damages;
  - Incorrect operational procedures;
  - Weather related and outside force.

That is, in the following paragraphs an analysis of possible treats occurring in NG distribution is proposed. It should also be noted that because of the size of gas distribution networks and differences in boundary conditions is very complex to evaluate with existing resources the limit states of each pipes in the networks. With the introduction of Industry 4.0 paradigm and so with the availability of more data (big data), however, it is opinion of the Author that this will be possible in next future.

### **3.3.1 Internal pressure, soil weight, traffic loads**

#### **3.3.1.1 Internal pressure load**

Internal pressure induces a tensile hoop stress that can induce excessive material yielding, ductile tearing or ultimate rupture and fracture.

For pressurized pipes, the maximum circumferential stress  $\sigma_p$  can be written as:

$$\sigma_{c,p} = \frac{p \times (D-t)}{2t} \quad (3-8)$$

Where p is the internal pressure [Pa], D is the external diameter [m] and t is the wall thickness [m]. This expression is usually known as the Barlow formula and it is derived by the Lamé's solution. In the case of plastic pipes where SDR is given the previous can be modified as:

$$\frac{2\sigma_{c,p}}{p} = SDR - 1 \quad (3-9)$$

#### **3.3.1.1 Earth loads and live loads**

Different approaches are present in the literature for the calculation of the total effectiveness stresses; however, in the following analysis modified Spangler stress equation with soil restraint is considered as the most accurate but at the same time simple to formulation be applied.

That is, soil weight and live loads have to be introduced. A difference exists between rigid (cast iron) and flexible pipes (steel and polyethylene); in the first case, in fact, the load is completely sustained by the pipe while in the second one part of the load is sustained by the soil as a function of the relative stiffness between the two.

Calling  $W_{soil}$  the soil load, the following can be written:

- *Rigid pipes:*

$$W_{soil} = C_d \gamma B_d^2 \quad (3-10)$$

Where  $\gamma$  is the soil unit weight [kg/m<sup>3</sup>],  $B_d$  is the trench width [m] and  $C_d$  is a coefficient calculated as follow:

$$C_d = \frac{1 - \exp\left(-2K\mu' \left(\frac{H}{B_d}\right)\right)}{2K\mu'} \quad (3-11)$$

Where  $K$  is the ratio of active lateral unit pressure to vertical unit pressure [#],  $\mu$  is the coefficient of friction between backfill and sides of ditch (= tan  $\phi$ ) and  $H$  is the height of fill above top of conduit.

**Table 33.** Values for  $\gamma$ ,  $K$  and  $\mu'$ . Source [91].

Soil type	Unit weight of soil, [kg/m <sup>3</sup> ]	Rankine's coefficient $K$	Coefficient of friction $\mu'$
Partially compacted damp topsoil	1440	0.33	0.50
Saturated topsoil	1760	0.37	0.40
Partially compacted damp clay	1600	0.33	0.40
Saturated clay	1920	0.37	0.30
Dry sand	1600	0.33	0.50
Wet sand	1920	0.33	0.50

- *Flexible pipe:*

$$W_{soil} = \gamma HD \quad (3-12)$$

Where the units of measure are the same of previous case.

As reported in the two correlations, a higher load is exerted on rigid pipes than in flexible pipe thanks to the support of the lateral soil.

In the case of surface loads two different situations verify: surface wheel load  $W_{c,l}$  and rectangular footprint load  $W_{d,l}$ . In this case the same formulation is proposed for rigid and flexible pipes.

- *Surface wheel load:*

$$W_{c,l} = \frac{C_t W I_c}{L} \quad (3-13)$$

Where  $C_t$  is the wheel load coefficient as a function of the trench,  $W$  is the concentrated wheel load [kg],  $I_c$  is the impact factor [#] and  $L$  is the section of the pipe considered (1 m or less).

- *Rectangular footprint load:*

$$W_{d,l} = \frac{C_r W_r D}{A} \quad (3-14)$$

Where  $C_r$  is the rectangular load coefficient as a function of the trench characteristics,  $W_r$  is the distributed load [kg] and  $A$  is the area in which the load is distributed [m<sup>2</sup>].

With the identified loads, it is possible to calculate the circumferentially bending stress  $\sigma_{c,b}$  exerted on the pipe:

$$\sigma_{c,b} = \frac{6K_b W_v E t r}{E t^3 + 24K_z p r^3 + 0.732E' r^3} \times \frac{g}{10^6} \quad (3-15)$$

Where  $K_b$  and  $K_z$  are the bending moment and deflection parameters,  $E$  is the Young's modulus of the material [MPa],  $r$  is the pipe radius [m],  $p$  is the fluid pressure [MPa],  $E'$  is the soil reaction modulus [MPa] and  $W_v$  takes into account of the vertical loads as proposed in the previous equation [kg/m] and  $g$  is the acceleration of gravity. Of particular importance was the analysis reported by [92] in which gas leakages occurred in the city of Genoa were analysed. In particular, it results that cast iron joints had the highest failure rates (17.5 and 8.6 failures/km for medium and low pressures) followed by steel systems (2.30 and 2.11 failures rates) in streets with high traffic loads. Values for the reported parameters are given in the following tables.

**Table 34.** Impact factor  $I_c$ . Source [91].

Height of cover, [m]	Highways	Railways	Runways
0 – 0.30	1.50	1.75	1.00
0.30 – 0.60	1.35	*	1.00
0.60 – 0.90	1.15	*	1.00
> 0.9	1.00	*	1.00

\* Refer to data available from American Railway Engineering

**Table 35.** Load coefficients  $C_l$  and  $C_r$ .  $M$  is the width on which the load is exerted. Source [91].

$D/(2H)$ or $B/(2H)$	$M/(2H)$ or $L/(2H)$														
	0.1	0.2	0.3	0.4	0.5	0.6	0.7	0.8	0.9	1	1.2	1.5	2	5.0	
0.100	0.019	0.037	0.053	0.067	0.079	0.089	0.097	0.103	0.108	0.112	0.117	0.121	0.124	0.128	
0.037		0.072	0.103	0.131	0.155	0.174	0.189	0.202	0.211	0.219	0.229	0.238	0.244	0.248	
0.053		0.103	0.149	0.190	0.224	0.252	0.274	0.292	0.306	0.318	0.333	0.345	0.355	0.360	
0.400	0.067	0.131	0.190	0.241	0.284	0.320	0.349	0.373	0.391	0.405	0.425	0.440	0.454	0.460	
0.500	0.079	0.155	0.224	0.284	0.336	0.379	0.414	0.441	0.463	0.481	0.505	0.525	0.540	0.548	
0.600	0.089	0.174	0.252	0.320	0.379	0.428	0.467	0.499	0.524	0.544	0.572	0.596	0.613	0.624	
0.700	0.097	0.189	0.274	0.349	0.414	0.467	0.511	0.546	0.584	0.597	0.628	0.650	0.674	0.688	
0.800	0.103	0.202	0.292	0.373	0.441	0.499	0.546	0.584	0.615	0.639	0.674	0.703	0.725	0.740	
0.900	0.108	0.211	0.306	0.391	0.463	0.524	0.574	0.615	0.647	0.673	0.711	0.742	0.766	0.784	
1.000	0.112	0.219	0.318	0.405	0.481	0.544	0.597	0.639	0.673	0.701	0.740	0.774	0.800	0.816	
1.200	0.117	0.229	0.333	0.425	0.505	0.572	0.628	0.674	0.711	0.740	0.783	0.820	0.849	0.868	
1.500	0.121	0.238	0.345	0.440	0.525	0.596	0.650	0.703	0.742	0.774	0.820	0.861	0.894	0.916	
2.000	0.124	0.244	0.355	0.454	0.540	0.613	0.674	0.725	0.766	0.800	0.849	0.894	0.930	0.956	

**Table 36.** Typical values for  $K_z$  and  $K_b$ . Source [91].

Bedding angle, [deg]	$K_z$	$K_b$
0	0.110	0.294
30	0.108	0.235
60	0.103	0.189
90	0.096	0.157

**Table 37.** Modulus of soil reaction E' [MPa]. Depth of cover between 0 and 1.5 m is considered. Source [91].

Type of soil	Relative compaction			
	85%	90%	95%	100%
Fine grained soils with less than 25% sand content	3.45	4.83	6.90	10.34
Coarse grained soils with fines	4.14	6.90	8.27	13.10
Coarse grained soils with little or no fines	4.83	6.90	11.03	17.24

As reported in [91] also ring compression stress has to be included in the calculation of total circumferential stress; the following correlation is proposed:

$$\sigma_{c,r} = \frac{W_v \cdot g}{2t \cdot 10^6} \quad (3-16)$$

Total circumferential stress is therefore calculated as:

$$\sigma_c = \sigma_{c,p} + \sigma_{c,b} + \sigma_{c,r} \quad (3-17)$$

### 3.3.1.3 Longitudinal stresses

In addition to circumferential loads, longitudinal loads have to be considered in the calculation of stresses. The following ones have to be considered:

- Poisson effect. It takes into account stress applied in one direction produces stress or strain in the perpendicular direction:

$$\sigma_{p,l} = \nu \sigma_c \quad (3-18)$$

Where  $\nu$  is the Poisson ratio for the material.

- Temperature increase or reduction. The expansion or contraction of the material is opposed by soil inducing a longitudinal stress in the material, calculated as follow:

$$\sigma_{T,l} = \alpha \Delta T \times E \quad (3-19)$$

Where  $\alpha$  is the linear coefficient of expansion [%/°C],  $\Delta T$  is the temperature change [°C] and E is the Young's modulus [MPa].

- Unevenness or settlement of the pipe bedding can cause bending longitudinal stress:

$$\sigma_{b,l} = E \times r \times X \quad (3-20)$$

Where X is the longitudinal curvature of the bent pipe [rad/mm].

Total longitudinal stress is calculated as:

$$\sigma_l = \sigma_{p,l} + \sigma_{T,l} + \sigma_{b,l} \quad (3-21)$$

### 3.3.1.4 Limit state condition

Different conditions are considered to evaluate pipeline status depending if the pipeline is rigid or flexible.

- *Steel flexible pipes.* Distortion energy theory is applied thanks to the good results for ductile materials. Failure occurs when:

$$\sigma_c^2 - \sigma_c \sigma_l + \sigma_l^2 > \sigma_y^2 \quad (3-22)$$

Where  $\sigma_c$  and  $\sigma_l$  are the total circumferential and longitudinal stresses [MPa] and  $\sigma_y$  is the yield strength of the material [MPa].

- *Polyethylene flexible pipes.* For polyethylene flexible pipes, ring deflection  $\Delta X/D$  [%] is the main issue and it should be calculated as:

$$\frac{\Delta X}{D} = \frac{12K_z W_b r^3}{Et^3 + 24K_z p r^3 + 0.732E'r^3} \times \frac{g}{D \times 10^6} < 5\% \quad (3-23)$$

About the apparent modulus, the short term should be used considering that deformation is a series of instantaneous deformations consisting of rearrangement and fracturing of grains while the bending stress decreases due to stress relaxation [93]. The value of 5% should be considered as a safety condition during operation. Also inside pressure should be compared to MRS:

$$\sigma_{c,p} = \frac{p \times (D - t)}{2t} \leq MRS \quad (3-24)$$

- *Rigid pipes.* Schlick's criterion is usually considered for rigid pipes; however, no considerations are made about axial stresses. For the scope, a modified failure criterion is suggested as proposed by [60]:

$$\min \left( \frac{\sigma_y}{\sigma_l}, \frac{\sigma_y}{\sigma_c} \right) < 1 \quad (3-25)$$

Where the following correlations are proposed for the calculation of the loads:

$$\sigma_l = \alpha E \Delta T + \frac{p}{2} \left( \frac{D-t}{t} - 1 \right) v + \frac{\left( (1 + f_f) \frac{6K_b C_d \gamma B_d^2 E t r}{Et^3 + 24K_z p r^3 + 0.732E'r^3} + \frac{6K_b C_r W_r D E t r}{A(Et^3 + 24K_z p r^3 + 0.732E'r^3)} \right) g}{10^6} v \quad (3-26)$$

$$\sigma_c = \frac{p(D-t)}{2t} + \frac{\left( (1 + f_f) \frac{6K_b C_d \gamma B_d^2 E t r}{Et^3 + 24K_z p r^3 + 0.732E'r^3} + \frac{6K_b C_r W_r D E t r}{A(Et^3 + 24K_z p r^3 + 0.732E'r^3)} \right) g}{10^6} \quad (3-27)$$

Where  $f_f$  is the frost factor considered between 0 and 1. A value of 0.5 can be considered.

Both for rigid and flexible pipes, no considerations have been made about loads due to soil movement or settlement. Therefore, it is suggested to make dedicated evaluations in their presence.

From the above equations considerations about relative importance of technical parameters can be made. For the scope a variation of +/- 15% has been considered respect to a defined nominal conditions in order to make a sensitivity analysis:

- *Steel flexible pipes:*
  - Gas pressure: 5 bar;
  - Trench depth: 0.9 m;
  - Pipeline diameter: 114.3 mm;
  - Wall thickness: 3.2 mm;

- Modulus of elasticity: 201,000 MPa;
- Thermal coefficient of expansion:  $11.7 \times 10^{-6} \text{ } \%/^{\circ}\text{C}$ ;
- Temperature difference:  $5 \text{ } ^{\circ}\text{C}$ ;
- Impact factor: 1.50;
- $K_z = 0.108$ ;
- $K_b = 0.235$ ;
- Wheel load (concentrated): 1500 kg;
- Poisson ratio: 0.3;
- Length of pipe: 1000 mm;
- Soil weight:  $1600 \text{ kg/m}^3$ ;
- $C_t = 0.230$ ;
- Modulus of soil reaction: 3.45 MPa
- No settlement.

As shown in Figure 65 it results:

- Total stresses are particularly sensitive to nominal wall thickness. The same variation is responsible for the highest variation of total stresses;
- External diameter is the second most important parameter;
- Also bedding angle influence the effective stress condition of the pipe such as impact factor and wheel load parameter. The reduction of trench depth is responsible for an increase of total stress experienced by the pipe:
- Also trench depth has a big influence as reported in the parameter  $C_t$ .

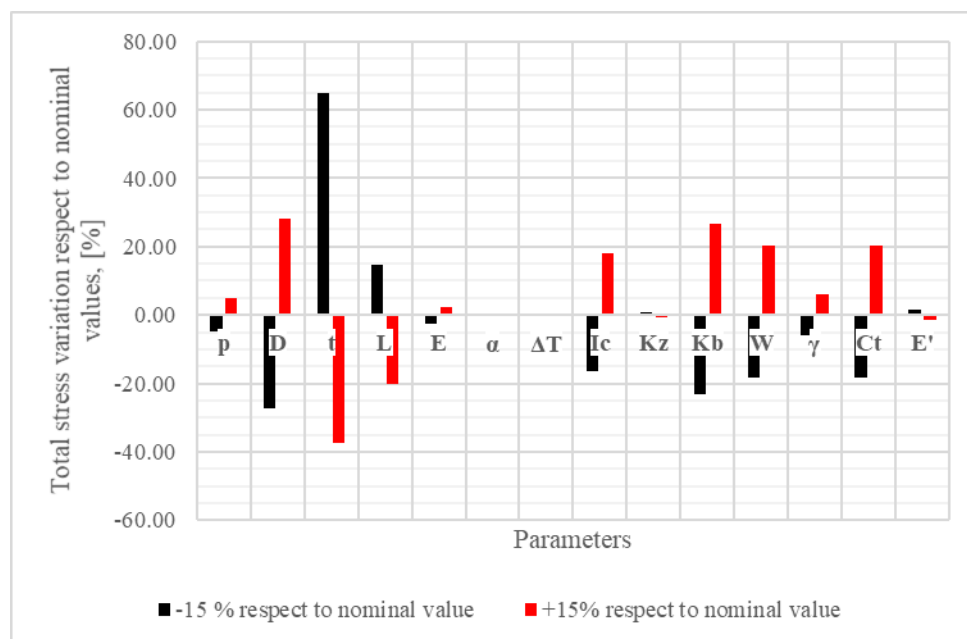


**Figure 65.** Sensitivity analysis of total stress respect to design parameters.

- *Polyethylene flexible pipes:*
  - Gas pressure: 5 bar;

- Trench depth: 0.9 m;
- Pipeline diameter: 114.3 mm;
- Wall thickness: 3.2 mm;
- Modulus of elasticity: 565 MPa;
- Thermal coefficient of expansion:  $20 \times 10^{-5} \text{ \%}/^{\circ}\text{C}$ ;
- Temperature difference: 5 °C;
- Impact factor: 1.50;
- $K_z = 0.108$ ;
- $K_b = 0.235$ ;
- Wheel load (concentrated): 1500 kg;
- Length of pipe: 1000 mm;
- Soil weight: 1600 kg/m<sup>3</sup>;
- $C_t = 0.230$ ;
- Modulus of soil reaction: 3.45 MPa

It results that:

- Installation condition, effective length of conduit, weight load and thickness influence the effective ring deflection;
- Loads over the pipe should be distributed or protective equipment should be considered to avoid overload conditions.

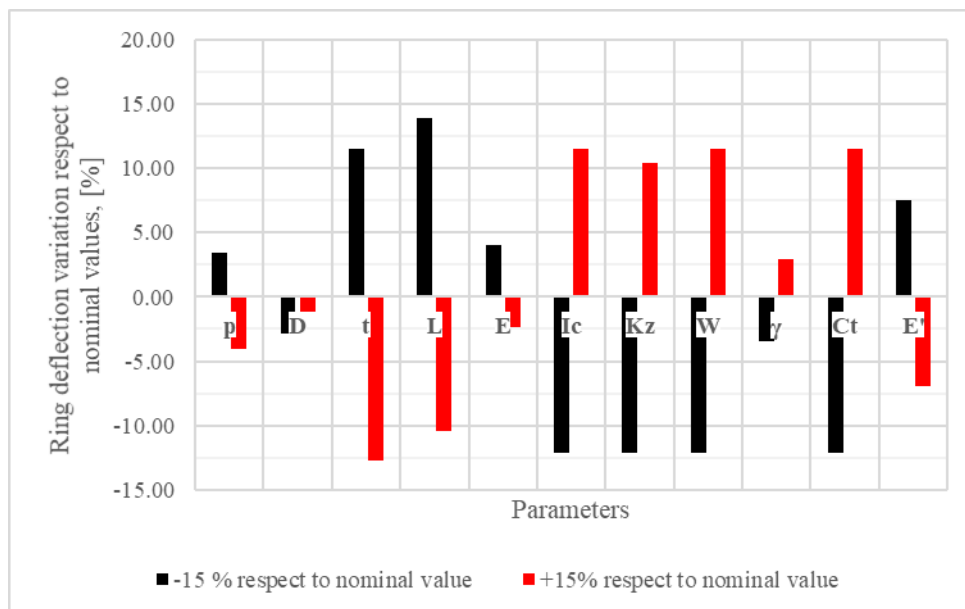


Figure 66. Sensitivity analysis of ring deflection respect to design parameters.

- *Cast iron pipes:*
  - Gas pressure: 5 bar;
  - Trench width: 0.6 m;
  - Trench depth: 0.90 m;
  - $C_d$ : 1.18;

- Frost coefficient: 0.5;
- Pipeline diameter: 118 mm;
- Wall thickness: 3.7 mm;
- Modulus of elasticity: 120,000 MPa;
- Thermal coefficient of expansion:  $1.07 \times 10^{-5} \text{ } \%/^{\circ}\text{C}$ ;
- Temperature difference: 5 °C;
- Impact factor: 1.50;
- $K_z = 0.108$ ;
- $K_b = 0.235$ ;
- Wheel load (concentrated): 1500 kg;
- Poisson ratio: 0.23;
- Length of pipe: 1000 mm;
- Soil weight: 1600 kg/m<sup>3</sup>;
- $C_t = 0.230$ ;
- Modulus of soil reaction: 3.45 MPa

For cast iron, circumferential stress has been considered; it results:

- Wall thickness is the most important parameter followed by trench width, bending coefficient, soil weight and coefficient  $C_d$ ;
- Gas pressure seems not to be a relevant parameter about the loads exerted on the pipe;
- Frost factor is responsible for a variation between  $\pm 5\%$ .

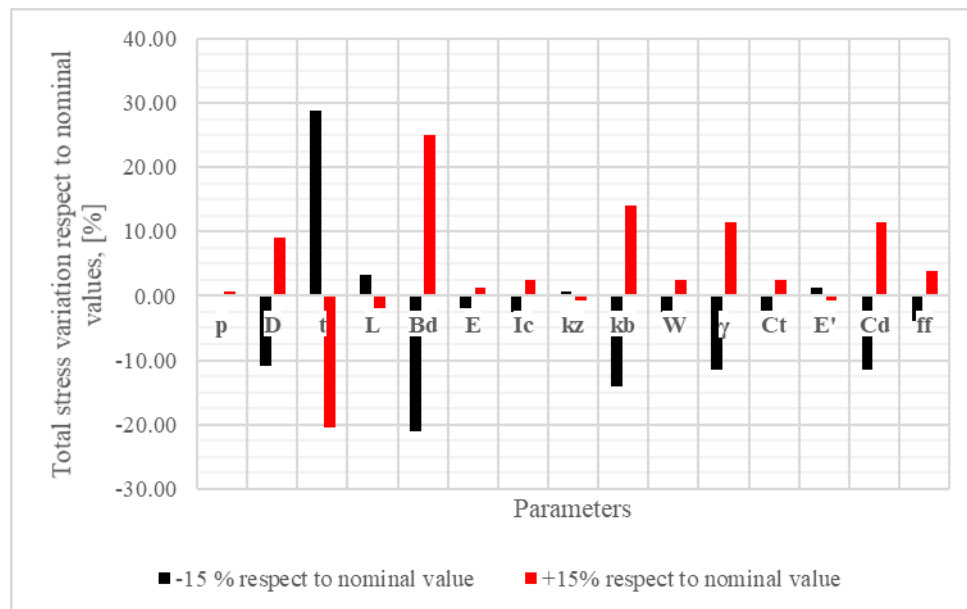


Figure 67. Sensitivity analysis of circumferential stress respect to design parameters.

### 3.3.2 External corrosion

As defined by the National American Corrosion Engineers (NACE), corrosion is an electrochemical process responsible for the deterioration of a material, usually a metal, which results from a reaction with its

environment, that in this case is usually moist soil that acts as electrolyte. From a chemical point of view, the following reactions occur:

- *Anode area reaction:*



- *Cathode area reactions:*



As shown, a deterioration occurs in the anodic area because of the iron ions move away from the pipe, while electrons move through the electrolyte to the cathode. It should be noted that the electrochemical reaction proposed in equation 44 verifies in the case of excessive current densities or in the absence of oxygen with the production of hydroxide ions that increase the pH values in the surround of the pipe. The produced atomic hydrogen can dissolve in steels being responsible in some cases for hydrogen embrittlement especially in the case of high strength material with a high martensitic content.

As defined by Romanoff, at the anode the most negative potential is present and material degradation occurs while cathode is usually protected from corrosion. Even if the chemical reactions are simple, it is very difficult to characterize the phenomenon in real applications because of the influence of several parameters.

That is, two main types of corrosion can verify:

- Uniform or near uniform corrosion characterized by the same degradation rate in all the exposed area;
- Localized or pitting corrosion characterized by localized attacks that induce wall perforation.

Several factors are responsible for corrosion development [94] and can be distinguished as:

- *Related to pipe:*
  - Grain structure. The orientation of steel grain structure is responsible for the behaviour as anode or cathode;
  - Chemical anisotropy, non-metallic inclusions, strained or unstrained areas, defects in the surface of the pipe
- *Installation location:*
  - Soil resistivity. Because of electrolyte is necessary to close electric circuit, higher soil resistivity [ $\Omega - \text{cm}$ ] is responsible for lower corrosion rate as reported in Table 38. High moisture soils are usually characterized by low resistivity;
  - Sulphate and chloride content;
  - Soil aeration. Because of the presence of oxygen stimulates corrosion, a high soil aeration is responsible for a high corrosion rate because the shield produced by corrosion products is removed;

- Clay, silt or sand. The nature and the amount of soluble salts in addition to the moisture content influence the capability of soil to conduct electric current. In particular, clay and silt type soils are usually considered responsible for higher corrosion rate than for sand soils;
- Soil pH. Extremely acid (below pH 4.5) and very alkaline soils (above pH 9.1) are characterized by the highest corrosion rate.

**Table 38.** Corrosion potential as a function of soil resistivity. Qualitative comparison. Source [94].

Resistance classification	Soil resistivity [ $\Omega - \text{cm}$ ]	Corrosion potential
Low	0 – 2.000	Severe
Medium	2.000 – 10.000	Moderate
High	10.000 – 30.000	Mild
Very high	> 30.000	Unlikely

The influence of several parameters makes very difficult the estimation of corrosion rate for specific cases. As reviewed by [95], several authors studied the phenomenon finding sometimes different results and very weak correlations to describe it. That is, many correlations are available in literature for the scope:

- [96]. The wall thickness loss  $l_w$  of steel pipes is modelled through the use of the following power law:

$$l_d = kt^n \quad (3-31)$$

Where  $k$  is a multiplying constant [mm/y],  $t$  is the exposure time [y] and  $n$  is an exponential constant [#]. The parameters introduced are estimated through the performance of a regression analysis respect to existing data of underground corrosion. Gaussian distributions with average values equal to 0.066 mm/y and 0.53 and standard deviations of 0.037 mm/y and 0.14 are identified respectively for  $k$  and  $n$ ;

- [97]. A different expression is proposed for wall thickness loss of steel pipelines after the statistical analysis of 257 coated and cathodically protected steel pipes buried for 17 years.

$$l_{d,max} = k(t - t_0)^n \quad (3-32)$$

Where  $t_0$  is the pit initiation time, while  $k$  and  $n$  are identified as a function of operative conditions. In the model the following values are suggested for clay, clay loam and sandy clay loam respectively:  $k$  equal to 0.178, 0.163 and 0.144 mm/y while  $n$  equal to 0.829, 0.793 and 0.734. In addition to the values that are different respect to previous model, it should be noted the presence of a pit initiation time that represents the time before which no pit creation is expected. Also in this case difference values are obtained as a function of soil type: 3.05, 3.06, 2.57. General values are also proposed for all type of soil:  $k = 0.164$  mm/y,  $n = 0.780$  and  $t_0 = 2.88$  y.

A comparison between the two have been done. For the scope a Monte Carlo simulation with 200 tests has been performed to evaluate depth distribution in accordance to the first. As shown in Figure 68 it results:

- A higher maximum corrosion depth results from [96];
- Even if more than 200 simulations should be performed, comparable results are obtained from the two models in terms of maximum corrosion depth;

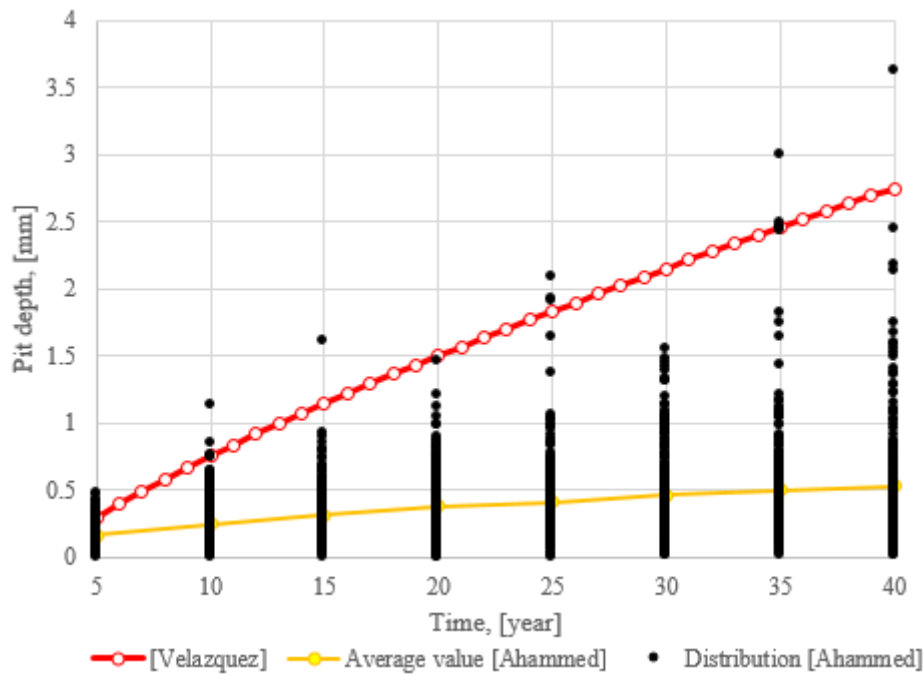


**Figure 68.** Comparison between the correlations proposed in the two references.

- [98] proposed a correlation for external corrosion in cast iron pipes in which a two parameters Weibull distribution is used to describe pit depth probability:

$$f(l_d) = \frac{k}{\lambda_t} \left( \frac{l_d}{\lambda_t} \right)^{k-1} \frac{\exp\left(-\left(\frac{l_d}{\lambda_t}\right)^k\right)}{1 - \exp\left(-\left(\frac{h}{\lambda_t}\right)^k\right)} \quad (3-33)$$

Where  $k$  is the shape factor and  $\lambda_t$  is the scale factor that depends on pipe age,  $g$ , and soil corrosivity as described by NSRI index. The National Soil Resource Institute (NSRI) divides soil depending on the content of clay, wetness class, sulphate content in different classes: (0-1) non aggressive, 2 (slightly aggressive), 3 moderately aggressive, (4) high aggressive, (5) very high aggressive. That is, scale factor is calculated as follow:

$$\lambda_t = \exp(\beta_1 \ln g + \xi NSRI) \quad (3-34)$$

Where  $\beta_1$  and  $\xi$  is reported in Table 39.

**Table 39.**  $\beta_1$  and  $\xi$  to evaluate corrosion in cast iron pipes. Source [98].

Parameter	Coefficient
Age constant, $\beta_1$	0.4774
Shape factor, $k$	1.1738
NSRI = 1, $\xi$	-0.0695
NSRI = 2, $\xi$	0.0775
NSRI = 3, $\xi$	0.214
NSRI = 4, $\xi$	0.3497

### 3.3.2.1 Protection against external corrosion

In order to reduce corrosion, cathodic protection is required for steel while for cast iron it is applied only in the case of very corrosive environment. For the scope, two different protection philosophies are generally used:

- *Cathodic protection.* In order to protect pipes from cathodic corrosion a pipe-to soil potential of 0.85V (respect to a  $\text{CuSO}_4$  reference electrode) has to be maintained in the system. For the scope, a certain amount of drainage current is forced to the pipe in accordance to [99] and discharged through a ground bed that works as earth in order to close the circuit. Typical values are in the range of  $10^{-5}$  A/cm<sup>2</sup>. Two different cathodic protection systems can be designed and operated:
  - Galvanic anode systems. These systems consist in the connection of more negative anodes (ground bed) to the pipe. In this way, during the corrosion of the anode the discharged current is used to protect the pipe. Because of size limitation, these systems can be used where a low discharged current is required and in low resistivity soil. Typical materials for the buried anodes are magnesium, zinc or aluminium;
  - Impressed current systems (Figure 69). For more severe conditions a rectifier is used to drive the required current into the system. Rectifiers, that convert alternating current electric power to low voltage direct current, are able supply the desired current and voltage as a function of the requirements defined in the design phase.
- *Coating solutions.* In order to reduce current requirements, coating is applied on pipe external surface to increase total electric resistance and so to reduce corrosion potential. In fact, a good coating is characterized by an insulation specific resistance of  $10^6$   $\Omega\text{-m}^2$  even if lower values are acceptable for this application ( $10^4$   $\Omega\text{-m}^2$ ). However, coatings can be damaged by several phenomena reducing the resistance to corrosion [100]:
  - Loss of adhesion respect to pipe surface and cathodic current shielding;
  - Presence of holidays in the coating due to handling or installation activities. To maintain the correct potential, a higher current is required to the cathodic protection systems;
  - Coating disbondment (i.e. adhesion degradation due to cathodic protection products, pH or defects);
  - Blisters formation due to water penetration;
  - Loss of adhesion and loss of cohesion;
  - Water penetration;
  - Air penetration increasing the probability of disbondment.

In [97] a preliminary score of coating types is reported as a function of their vulnerability; a comparison with bare pipe to which is associated the value 1 is made: asphalt enamel (0.9), wrap type (0.8), coal tar (0.7) Fusion Bonded Epoxy (FBE) (0.3).

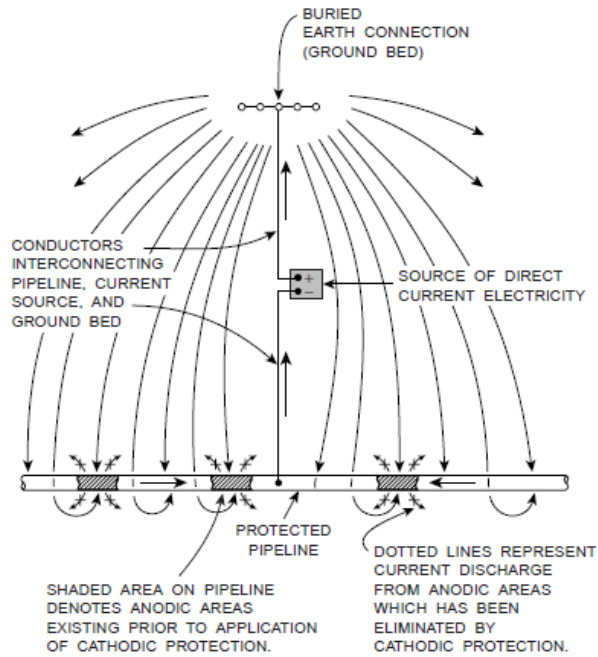


**Figure 69.** Impressed current system. Source [101].

In order to verify the efficacy of the cathodic protection, the Italian Association for the Protection against Electrolytic Corrosion (APCE) introduces an indicator defined as  $K_T$ :

$$K_T = \left( K_1 \times \sqrt{\frac{K_2}{70}} + K_2 \right) \geq 60 \text{ for effective protection} \quad (3-35)$$

Where  $K_1$  is related to the design (size of the protected system and number of monitoring point) and  $K_2$  depends on the management of the cathodic protection system (through monitoring). Thanks to its definition, the parameter  $K_T$  ensures the possibility to qualitatively rank pipelines as a function of the effectiveness of the corrosion protection.

For all the reported reasons the identification of corrosion in distribution networks is very difficult respect to transmission systems due to the impossibility to use Inline Inspection Tool (ILI) such as pigs that are moved inside the pipes and that measure wall thickness loss through Magnetic Fluxes Leakages (MFL) or simply through calipers that evaluate the inside geometry of the pipe. In fact, because of pipeline dimensions, at the moment no technologies are available in the market able to be inserted in gas pipes in order to evaluate wall thickness reduction.

### 3.3.2.2 Microbiologically influenced and stray current corrosion

Other phenomena can be responsible for pipeline external corrosion such as microbiologically influenced and stray current corrosion. The first one results from the presence and activities of microorganism in the soil such as sulphate reducing bacteria and acid producing bacteria that increase the probability to have localized corrosion. As reported by [102] the 27% of the corrosion deposits has to be correlated to such organisms. That is, in the most case the presence of microbiologically is responsible for coating disbondment with particular effects on new generation ones.

Stray current corrosion can be defined as corrosion induced by current produced by an external source as shown in Figure 70. The current enter in one side of the pipe (the cathode) and exits from another point (the anode) to close the electric circuit.

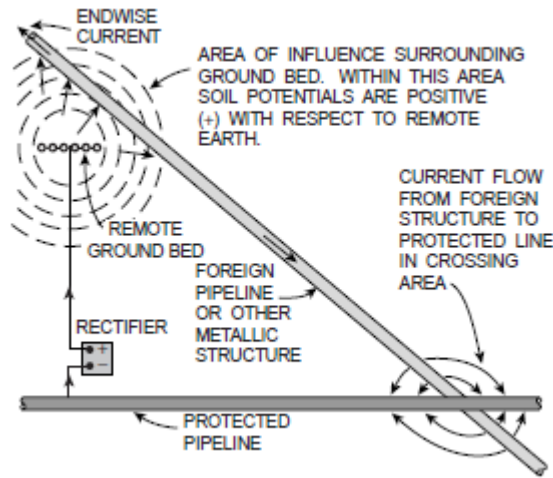


**Figure 70.** Type of stray current generated into a pipe from an external impressed current system. Source [101].

In the review proposed by [103], it is highlighted that anode current corresponds to cathode current; therefore, higher current density and so corrosion rate is present reducing anode area. From the review several systems are identified as possible sources of stray currents such as railway, cathodic protection systems, high voltage DC transmission systems, DC communication systems, AC traction systems. However, AC interferences are usually considered less dangerous respect to DC ones and a ratio of 1:4 is considered between AC and DC stray current to create similar damages. That is, no damages have been observed for AC current density lower than  $30 \text{ A/m}^2$ .

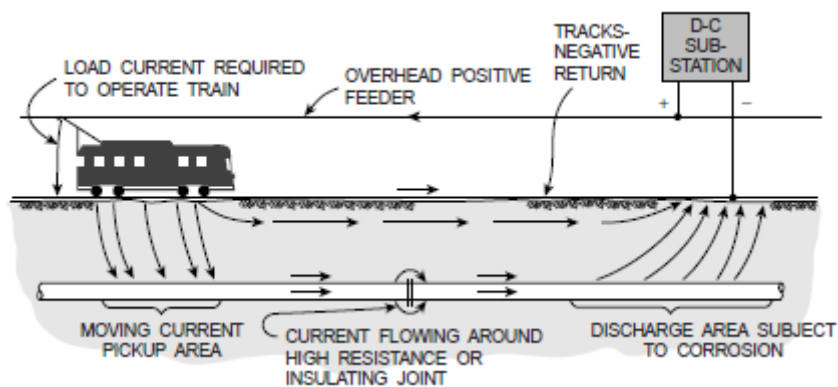


**Figure 71.** Stray current due to the presence of a railway near to the pipeline. Source [101].

In [104] the interference between two crossing pipelines (only one protected) is analysed considering the following parameters: crossing angle, crossing distance, distance of the two pipelines, anode output current, depth and soil resistivity. It results that a negligible effect is due to crossing angle, installation depth while corrosion is very sensitive to horizontal distance, soil resistivity and current density. In fact, at distance greater than 200 m very poor interference is observed. Furthermore, it is observed that an increasing interference with soil resistivity is present justified by the fact that current tends to close the circuit preferably into the affected pipeline rather than in the ground bed worsening the corrosion situation at the intersection point.

In [105], a reduction of the electrode potential is observed with the increase of exerted stresses in a X80 steel specimen. Considering different value of DC current density, it is observed an increase of the number of pit corrosion point in accordance to current density. In [106] it is reported that DC current density of 1 A/m<sup>2</sup> generated by a corrosion protection system is responsible for a corrosion rate of 1.2 mm/y. In [107], an experimental study on stray current corrosion of coated pipeline is proposed. In the paper corrosion rates are reported as a function of the value of AC and DC current density. Furthermore, considering a X70 steel pipe it is observed that the increase of AC current density changes corrosion degradation of the material from uniform to very localized pitting corrosion especially for current higher than 100 A/m<sup>2</sup>. Finally, in [108] corrosion morphology due to DC stray current is investigated finding that up to 100 A/m<sup>2</sup> there is an accumulation of corrosion products on the pipe surface in addition to general corrosion while an exfoliating surface is observed for higher current densities.

Protection solutions can be installed in the systems to reduce stray current corrosion such as electric drainage bonds, electrical shields, insulating couplings, intentional anodes and coatings; however, a detailed description to reduce the effects of DC and AC stray current is reported in [109] and [110] respectively.

### 3.3.2.3 Stress Corrosion Cracking (SCC)

Stress Corrosion Cracking (SCC) is a destructive cracking that occurs in steel pipelines in aggressive environment and in the case that a tensile stress acts on a susceptible microstructure. For this reason, three conditions have to be contemporary present in order to have SCC propagation. From a morphology point of view, SCC presents a group of cracks that are directed in axial directions and so perpendicular to the operative circumferential stresses. Cracks frequently coalesce to a bigger failure path that can be responsible for the rupture of the pipe. In some cases, cracks directed circumferentially have been identified in response to predominant axial stresses such as soil movement or residual welding strength at girth welds [111].

SCC is further divided into two categories:

- High pH SCC. Because of it is usually observed for temperature higher than 40 °C, a very low probability of occurrence in natural gas distribution networks is estimated.
- Near neutral SCC. It is responsible for a trasgranular cracking and usually verifies when CO<sub>2</sub> is dissolved in groundwater near to the pipelines at a pH between 5.5 and 7.5; also very poor corrosion protection increases the probability of occurrence. Since 1977, 22 failures have been identified due to near neutral SCC of which twelve were ruptures and 10 leakages; of these the main part occurred in polyurethane tape coated pipes installed between 1968 and 1973.

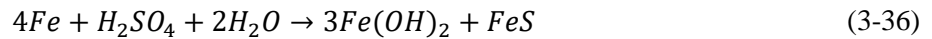
### 3.3.2.4 Graphitization

Graphitization is a degradation phenomenon that occurs in grey cast iron very similar to corrosion and usually identified as a different type of corrosion. During the process iron moves from the pipes leaving a matrix of graphite flakes characterized by a brittle behaviour.

Respect to corrosion, no structural damage is observable in graphitized cast iron pipes making very difficult the individuation of a damaged structure; only thermal and sound response is different in the case of a

deteriorated material. In [112] a review of the most important studies of the time was reported. The following results:

- Sulphate reduction play an important role in cast iron graphitization. In fact, great graphitization occurs in presence of hydrogen sulphide as justified by the presence of iron sulphide as corrosion product. The empirical equation proposed is:



- The formation of iron sulphide and hydrogen sulphide preferably occurs in soil in absence of air thanks to the activity of a microbe of strictly anaerobic life process called *Spirillum desulfuricans* that reduces the sulphate present in hydrogen sulphide into water. Four primary reaction stages occur even if they can be summarized with the following:



- The main soil parameters to evaluate aggressiveness are soil type (clay, sand, loam), organic content, pH, sulphate content, electric conductivity and organic matter content of the ground water.
- Clay and peat soils are the most likely environment in which graphitization could occur thanks to the absence of atmospheric oxygen and to the presence of sulphate reduction products. However, the presence of sand in the trench in order to evade the contact between pipeline and aggressive soil can be detrimental. In fact, sand can increase the contact between groundwater where sulphate reduction runs its course and the pipe: therefore, anaerobic process can still verify. Then, in presence of aggressive soils, cast iron pipes should be completely avoided.
- The most severe graphitization was found in soil with a pH not far from 7;
- In clay soil graphitization seems to be more rapidly because the absence of air reduces the formation of rust in the pipelines as a protective layer.

In the past several failures in NG distribution attributed to graphitization occur. One of these occurred the December 17, 2013. In the accident two flats were seriously damaged, one person died and one was seriously injured. NG distribution system consists of a 2 inches cast iron main enamel coated of the 1951 operated at 19.5 psig and a 1 ½” service lines of steel for the supply of gas in the buildings. During the investigations it was found that the cast iron pipe presents graphitization as shown by the typical dark grey area on the fracture face near to outer surface as shown in Figure 72 below due to the iron sulfide. As shown in the right, a very different morphology is present between inner and outer surface of the pipe where iron leaves the graphite matrix.

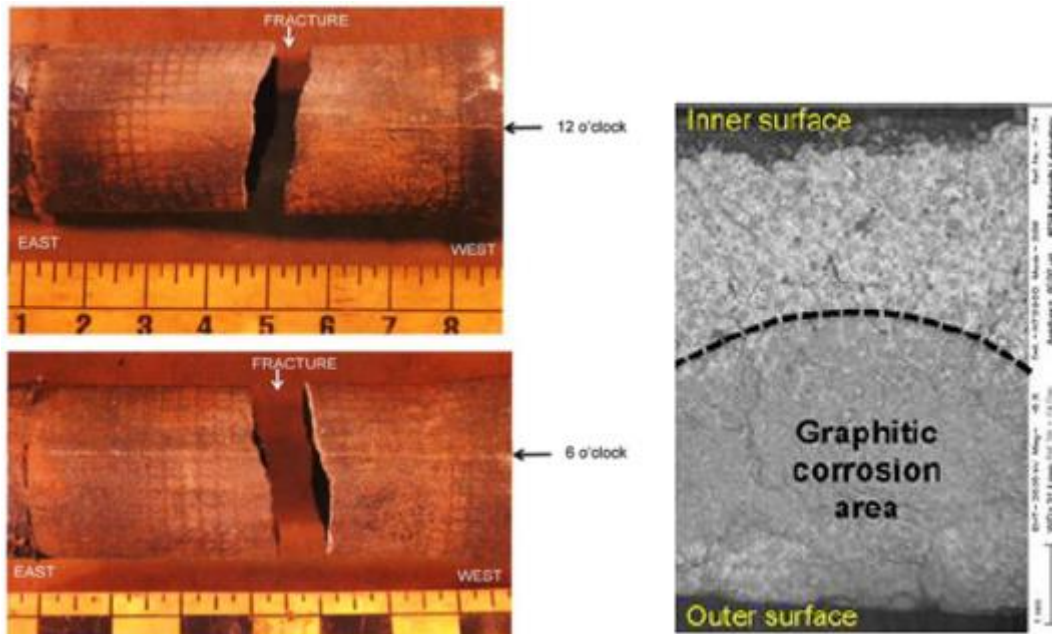


**Figure 72.** Failed pipe due to graphitization.

A circumferential rupture is shown (a crack at 5 o'clock position of approximately one quarter to one half inch long was found). The morphology of the rupture can be justified by the presence of axial stress as exerted by soil movement or directly by a root found near the pipelines.

### 3.3.2.5 Statistical analysis of past accident due to corrosion in NG distribution networks

Several accidents occurred in the past due to external corrosion, as those of the March 5, 2008 at Plum Borough (Pennsylvania) where a residence was completely destroyed, a man killed and a girl seriously injured. The gas system consists of a 2" and an 8" carbon steel carbon steel pipelines installed in 1961 and operated at 10 psig (0.69 barg). Coal tar enamel was used as coating. As shown in Figure 73, a circumferential rupture occurred leaving gas free to exit the pipe; rupture morphology indicates that the reduction of wall thickness in addition to axial forces were responsible for the failure. That is, NTSB identifies a dent present at the bottom of the pipe that was presumably made by an excavator that in the past have substituted a sewer line near to the gas system: hitting the pipe, the coating layer was removed leaving the pipeline without corrosion protection (a wall thickness loss of 0.05 mm / year was calculated).

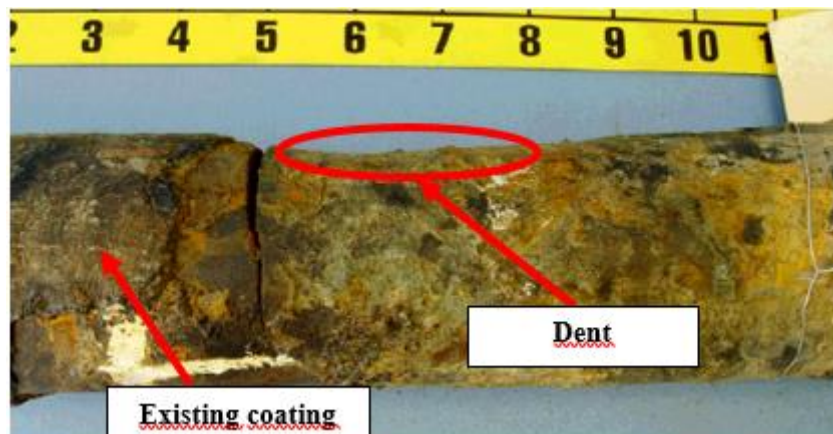


**Figure 73.** Damaged pipeline due to external corrosion.

Because of the importance of the phenomenon, a statistical analysis of accidents caused by corrosion in NG distribution system between 1984 and 2016 has been performed. The following results have been found:

- A decreasing failure rate is observed in the period between 1984 and 2016 (Figure 74). Considering the period after 2004 as representative for state of the art conditions, an average value of  $6.89 \times 10^{-7}$  [# / km year] and a standard deviation of  $5.13 \times 10^{-7}$  [# / km year] have been calculated.

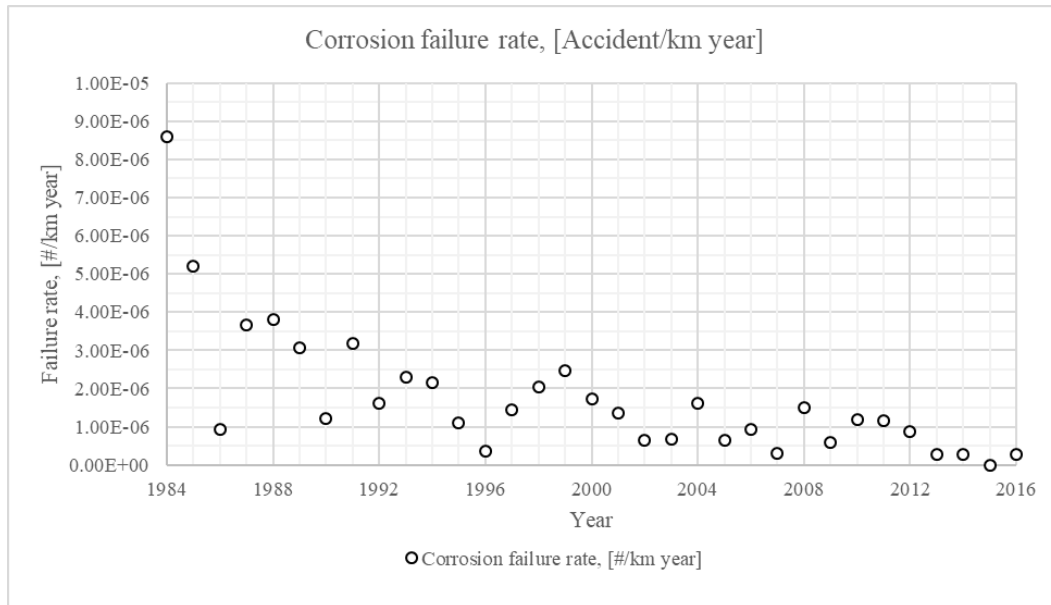


**Figure 74.** Corrosion failure rate [Accident / km year] in the American NG distribution network between 1984 and 2016.

That is considering steel and cast iron pipelines, an average frequency of occurrence has been calculated. For the scope system exposure has been introduced defined as the sum of system size as reported for each year. In the analysis only accidents occurred in mains have been considered because it is not clear how data about service lines are calculated in available database. With the available data cast iron pipes are characterized by higher failure rate than to steel ones. It should be noted that data about accidents are available in different formats for the following periods 1984 – 2004, 2004 – 2010 and 2010 – 2017.

**Table 40.** Corrosion failure frequency for American NG distribution networks for the period between 1984 and 2016.

Material	System exposure, [km-y]	Number of accident, Mains / total [#]	Failure frequency, [# / km year]
Steel	$3.01 \times 10^7$	67 / 105	$2.23 \times 10^{-6}$
Cast iron	$2.60 \times 10^6$	12 / 13	$4.62 \times 10^{-6}$

- Considering nominal diameter, a similar trend is observed in the three periods considered:
  - The highest number of failure occurred in small diameter pipes (Figure 75);
  - Considering the effective size as a function of diameter, the highest failure probability results for pipeline with a diameter greater than 12” (Table 41); this can be justified by the higher stresses exerted with the increase of nominal diameter. In the case of cast iron, a high failure frequency is also present in small diameter, but these failures are concentrated in the period 1984 – 2004 (Table 42);

- In the case of cast iron, a dedicated strategy of renovation should be promoted by operators to reduce the probability of failure.

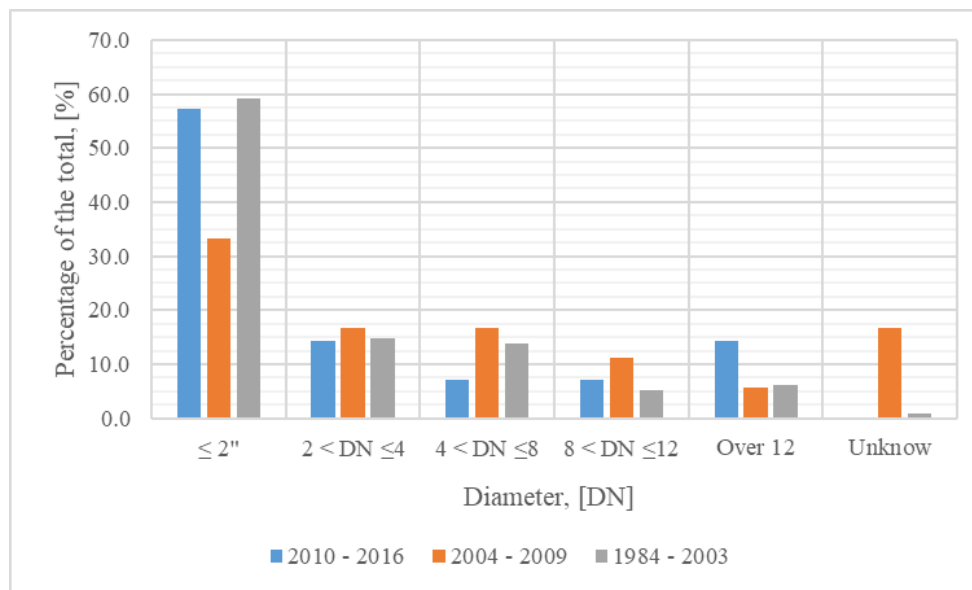


**Figure 75.** Percentage of the rupture occurred in American NG distribution system.

**Table 41.** Failure probability for steel mains as a function of nominal diameter considering the period between 1984 – 2016.

Steel mains (1984 – 2016)					
DN	≤ 2"	2 < DN ≤ 4	4 < DN ≤ 8	8 < DN ≤ 12	Over 12
Accident number	22	15	16	7	7
Frequency, [# / km year]	1.43E-06	1.75E-06	3.14E-06	7.35E-06	2.12E-05
Exposure [km - year]	1.54E+07	8.56E+06	5.10E+06	9.53E+05	3.31E+05
Derating factor	0.07	0.08	0.15	0.35	1.00

**Table 42.** Failure probability for cast iron mains as a function of nominal diameter considering the period between 1984 – 2016.

Cast iron mains (1984 – 2016)					
DN	≤ 2"	2 < DN ≤ 4	4 < DN ≤ 8	8 < DN ≤ 12	Over 12
Frequency, [# / km year]	2	2	3	2	3
Frequency	1.72E-05	1.63E-06	3.06E-06	9.21E-06	2.50E-05
Exposure [km - year]	1.16E+05	1.22E+06	9.81E+05	2.17E+05	1.20E+05
Derating factor	0.69	0.07	0.12	0.37	1.00

- Considering failure type, leaks or ruptures are possible. From data analysis the following result:
  - In steel pipes leaks have been identified in the 91.6% of cases;
  - In cast iron pipes ruptures occurred in the 80.0% of cases in accordance to the brittle nature of the material. Therefore, a high risk due to gas leakage verifies in the case of cast iron pipes.
- Considering steel pipelines, the presence of coating and cathodic protection have been considered. From the investigation it results:
  - In 1984, in 2004 and in 2010 the percentage of unprotected steel system was calculated respectively equal to 23.1%, 13.0 and 11.5% respectively;
  - The percentage of failure occurred in unprotected systems was 66.7%, 46.1% and 80% considering the following periods: 1984 – 2003, 2004 – 2009 and 2010 – 2016;

- As shown, corrosion protection reduces failure probability of almost an order of magnitude. Therefore, protective solutions have to be considered very important parameters in qualitative risk analysis (Table 43);
- Also the presence of coating is an important parameter that should be taken into account in qualitative analysis (Table 44);
- As expected the worst case is the absence of cathodic protection and coating (Table 45). Unprotected coated pipes and protected bare pipes have an almost similar failure probability. Coated and protected pipes have instead the best performance with a failure probability that is almost two order of magnitude lower than unprotected bare pipes.

**Table 43.** Analysis of cathodic protection effects on failure probability.

Parameter	Unprotected	Protected
Accident number	40	27
Frequency, [# / km year]	8.80E-06	1.06E-06
Exposure [km - year]	4.54E+06	2.54E+07

**Table 44.** Analysis of coating effects on failure probability.

Parameter	Coated	Bare
Accident number	26	31
Frequency, [# / km year]	1.01E-06	7.32E-06
Exposure [km - year]	2.57E+07	4.23E+06

**Table 45.** Analysis of the influence of the two parameters together.

Parameter	Unprotected bare	Unprotected coated	Protected bare	Protected coated
Accident number	37	4	5	22
Frequency, [# / km year]	1.15E-05	3.05E-06	4.99E-06	9.01E-07
Exposure [km - year]	3.23E+06	1.31E+06	1.00E+06	2.44E+07
Derating factor	1.00	0.27	0.44	0.08

- Finally, also pipeline age has been considered. Data used regards the period between 2004 and 2016 because no division for the installation year is present in the database dedicated to the period between 1984 and 2004. From the analysis it results that attention has to be given to pipelines installed from more than 50 years (Table 46).

For each parameter a derating factor can be calculated defined as the ratio between the frequency and the maximum frequency obtained for the analysed parameter as made for pipeline age.

**Table 46.** Pipeline age influence respect to corrosion failure.

Age	10 < t ≤ 20	20 < t ≤ 30	30 < t ≤ 40	40 < t ≤ 50	50 < t ≤ 60	60 < t
Accident number	0	0	1	7	4	6
Exposure, [km - year]	3016000	2004087	1702714	2556028	1413848	1248026
Frequency, [# / km year]	0	0	5.87E-07	2.74E-06	2.83E-06	4.81E-06
Derating factor	0.00	0.00	0.12	0.57	0.59	1.00

### 3.3.3 Material and equipment failure

Material and equipment failures were responsible for several failures in the past. To analyse the possible failure modes, the paragraphs is divided as follow. Failures occurred in pipes are considered with a preliminary distinction between materials. While for steel and cast a statistical analysis of failures occurred in the American NG distribution networks is performed, a brief examination of Slow Crack Growth (SCG) and Rapid Crack Growth (RCP) is also proposed for polyethylene. For the scope data from PHMSA database are considered. It should be noted that respect to corrosion, only the period after 2004 has been used. In fact, as shown in Figure 76, a possible mistake can verify using the previous period because of very poor identification is present for previous years.

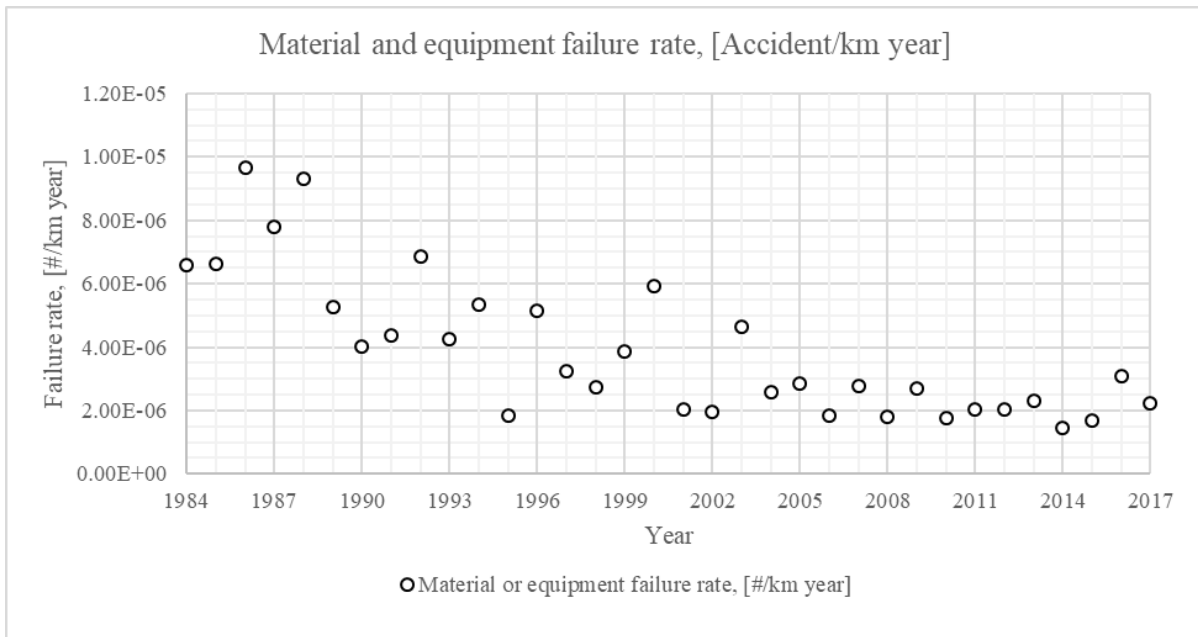


Figure 76. Material and equipment failure rate in NG distribution networks between 1984 and 2017.

#### 3.3.3.1 Statistical analysis of accidents occurred in steel, cast iron pipelines

As for corrosion, failure rates are calculated only for distribution mains even if the total number of accidents is reported; however, it has to be noted that more than 80% of failures occurred in mains. As shown, cast iron pipes present higher failure rate than steel ones. No failures were instead recorded for ductile iron systems that account for a total size of almost 850 km.

Table 47. Failure rate calculated for steel, cast iron and ductile iron in the period between 2004 and 2017 in American NG distribution networks.

Material	System exposure, [km-y]	Number of accident in mains / total, [#]	Failure frequency in mains, [Acc/km year]
Steel	$1.24 \times 10^7$	32 / 40	$2.58 \times 10^{-6}$
Cast wrought iron	$7.54 \times 10^5$	8 / 8	$1.06 \times 10^{-5}$

From the analysis no correlation with operative conditions of the pipe such as diameter and pressure results. Therefore, more attention is given to understand where the failure principally occurs. For the scope the following division have been considered: body of the pipe, component and joint/connections. Because no

frequency is calculated also service lines are considered. In the case of steel, the main part of failures has been identified in joints and connection while very few failures are identified in the body of the pipe. A different situation has been found for cast wrought iron where failures occurred principally in the body of pipe.

**Table 48.** Failure rate calculated for steel, cast iron and ductile iron in the period between 2004 and 2017 in American NG distribution networks.

Material	Number of failure in the body of the pipe, [#]	Number of failure in components, [#]	Number of failure in joints/connections, [#]
Steel	4 (10%)	12 (30%)	24 (60%)
Cast wrought iron	6 (75%)	1 (12.5%)	1 (12.5%)

In order to conclude the analysis, an evaluation of failure morphology is proposed distinguishing between leak and rupture. From the analysis it results that leaks are the most probable events even if small difference is identified in the body of the pipe.

**Table 49.** Failure rate calculated for steel, cast iron and ductile iron in the period between 2004 and 2017 in American NG distribution networks.

	Percentage of failure in the body of the pipe, [%]	Percentage of failure in components, [%]	Percentage of failure in joints/connections, [%]
<b>Total</b>			
Leak	60	92	88
Rupture	40	8	12
<b>Steel</b>			
Leak	50	100	87.5%
Rupture	50	0	12.5%
<b>Cast wrought iron</b>			
Leak	67 (*)	0	100 (*)
Rupture	33 (*)	100 (*)	0
Because of the small dataset, this data should not be used for risk calculation.			

### 3.3.3.2 Slow Crack Growth and Rapid Crack Propagation in polyethylene pipelines

Slow Crack Growth (SCG) is a typically failure mode for polyethylene pipelines, occurring at long times and relatively low stresses after a crack has been initiated from a material inhomogeneity. This condition can be caused by microvoids, crystalline defects, aggregation of fillers or from a macroscopic flaw caused by an accidental indentation such as rock impingement [113]. In addition to SCG, ductile failure due to internal pressure, incorrect installation and squeeze off procedures are responsible for PE failures.

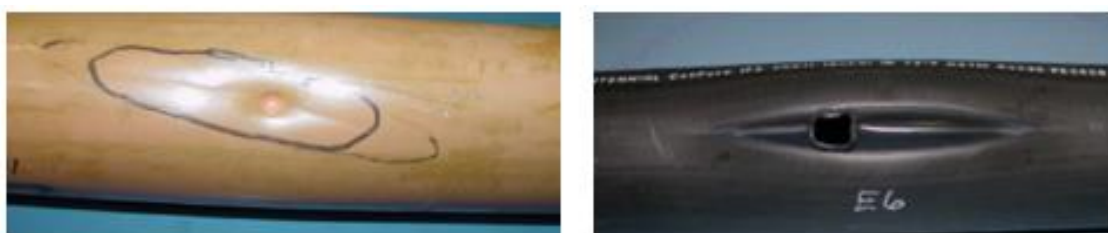


**Figure 77.** Slow Crack Growth (SCG) due to rock impingement (left) and ductile failure due to internal pressure (right). Source [114].

That is, a brittle failure occurs in the case of SCG in which the crack propagates in successive steps from the inner surface (the initiation point) where stresses are concentrated. Circumferential residual stresses are in fact originated during manufacturing cooling as reported in Figure 78. As shown, a compressive stress is present at the outer surface (almost 1000 psi) while a tensile stress is present at the inner one (almost 400 psi). About axial direction, a residual value of 350 psi is usually estimated.

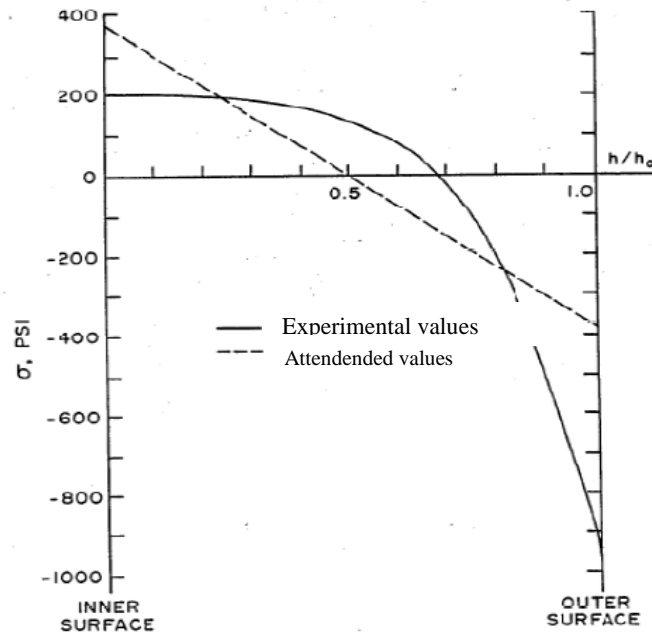


**Figure 78.** Circumferential stress distribution in a Aldyl-A polyethylene pipe. Source [114].

Macroscopic and microscopic aspects of SCG in polyethylene are analysed in order to evaluate the development of the failure. For the scope, a circumferentially notched high density polyethylene is tested in [113]. The following result:

- Three different stages are identified in SCG: incubation, propagation stage and termination stage;
- The stress intensity is the driving force of the process: particularly SCG at low stress intensity is more stable than at high intensity;
- Crack propagation can be described as a function of the number of stress cycles with Paris propagation law (Figure 79):

$$\frac{da}{dN} = A\Delta K^m \quad (3-38)$$

Where  $a$  represents crack propagation,  $N$  the number of cycle,  $\Delta K$  is the amplitude of stress intensity fatigue signal ( $K_{\max} - K_{\min}$ ) [ $\text{MPa m}^{0.5}$ ] while  $A$  [ $\text{mm/cycle}$ ] and  $m$  are constant depending on the material. From data analysis it results a correlation factor of 0.9855 with Paris propagation law. So, crack propagation does not depend on the stress history but on the instantaneous stress state at the crack position. For externally notched pressurized pipes, the following correlation is proposed for stress intensity factor:

$$K = \frac{[Y(\sigma_{c,p} + \sigma_{c,res})]}{\sqrt{\pi a}} \quad (3-39)$$

Where  $Y$  is a geometric factor that depends on the ratio of the notch depth and thickness of the pipe,  $\sigma_{c, res}$  is circumferential residual stress and  $a$  is the crack depth in radial direction. Crack speed is more or less constant in accordance to the applied stress intensity factor and in relation to microstructure features.

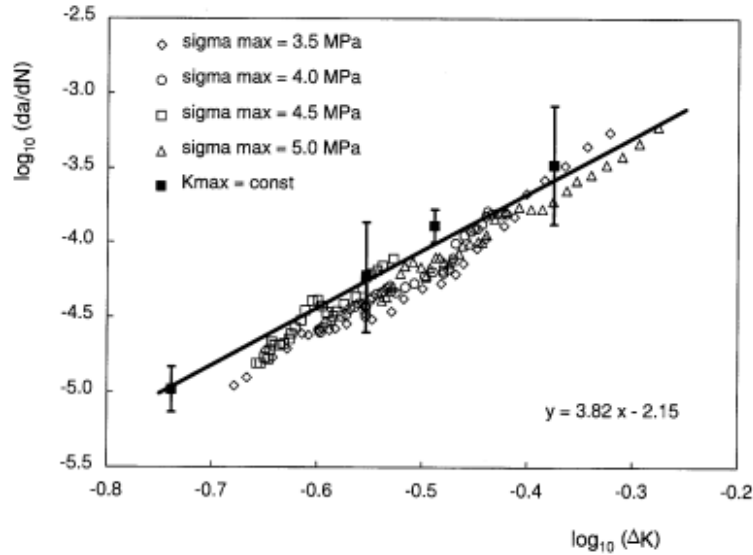


**Figure 79.** Paris plot of the stable crack propagation at constant stress and constant  $\Delta K$  (filled squares). Source [113].

That is, it is very difficult to estimate the remaining life of buried pipes subjected to SCG. Tests are therefore performed to compare performances of different materials. Among these, PENT test (in accordance to ASTM F1473) and the Accelerated Long Term Hydrostatic Stress Rupture tests (LTHS) are the most used. A brief description of these methods is proposed:

- **Bidirectional Shift Functions**, that ensures the prediction of time to failure on the base of laboratory test failure time  $t_{test}$  during tests performed at a defined temperature  $T_t$  [°C] and pressure  $p_t$  [psig].

$$F_1 = \exp(0.109 \times (T_t - T)) \quad (3-40)$$

$$F_2 = \exp(0.0116 \times (T - T_t)) \quad (3-41)$$

$$t = t_{test} \times F_1 \quad (3-42)$$

$$p = \frac{p_t}{F_2 TF} \quad (3-43)$$

Where  $t$ ,  $T$ ,  $p$  are respectively time to failure [h], operative temperature [°C] and accidental pressure [psig] expected in field.  $TF$  is a temperature factor equal to 2 in the case of values lower than 50 °C.

- **Three Coefficient Rate Process Method (RPM)**, that is based on Arrhenius equation:

$$\log_{10}(t) = A + \frac{B}{T} + C \frac{\log_{10}(p)}{T} \quad (3-44)$$

Where  $A$ ,  $B$  and  $C$  are constants that depends on the material, stresses and temperature  $T$  in [K];  $t$  is the time to failure at the pressure  $p$  (Pa) and temperature  $T$ . Because of three constants are present, three test are required for their identification;

- **PENT test.** A correlation is proposed for the estimation of time to failure based on PENT test time to failure:

$$t = t_{PENT} \times \left(\frac{0.468}{K}\right)^n \times \exp\left(\frac{Q}{R} \times \left(\frac{1}{T} - \frac{1}{353}\right)\right) \quad (3-43)$$

Where  $t_{PENT}$  is the time to failure derived by PENT test in [h],  $K$  is the intensity factor,  $Q$  is the activation energy estimated between 85 – 110 kJ/mol,  $R$  is gas constant (0.008314 kJ/molK),  $T$  is the operative temperature [K] and  $n$  is a constant that depend on the polyethylene type between 2 and 4 (a value of 3.82 is proposed for high density in [113]).

- On the base of the results from the application of the Paris propagation law to SCG crack, an exponential rate is proposed:

$$\frac{da}{dN} = A \times \exp\left(\frac{Q}{RT}\right) K^p \quad (3-45)$$

Where  $A$  and  $p$  are constants.

It should be noted the complexity related to the application of the proposed models to estimate the residual life for real application in NG distribution networks. In fact, several boundary conditions interact being responsible of different responses of the material. Consequently, at the moment, it seems that these methods should be used to compare the performance of different materials and evaluate the conditions of the pipe.

Rapid Crack Propagation (RCP) is another possible failure mode for polyethylene pipes (Figure 80). As for SCG a brittle development of the crack is observed even if higher velocity rates (usually greater than 100 m/s) are observed due to the presence of an axial flaw.



**Figure 80.** Rapid Crack Growth (RCP) in polyethylene pipes. Source [114].

As observed in several works, RCP is positively influenced by the increase of diameter, gas pressure, and SDR ratio and by the decrease of operative temperature. That is, RCP failures consist of two successive phases:

- First of all, a critical crack is created in the wall thickness (between the 50% and 90% of the nominal value) due to impingement or to an impact with an external body. During this phase elastic energy is stored in the material;
- The accumulated energy is released to sustain crack propagation.

In order to sustain the phenomenon a minimum gas pressure and temperature are required. ISO 13477 and ISO 13478 suggest to perform tests in order to know:

- The critical pressure beyond which RCP verify at the test temperature;
- The critical temperature below which RCP verify at the test pressure.

These data have to be supplied by the manufacturer of the pipe. DSOs can only compare the different performance of materials and so select the best appropriate for their scope of use.

### 3.3.3.3 Statistical analysis of accidents occurred in polyethylene pipelines

As made for steel and cast iron pipeline, also failure occurred in polyethylene pipes are analysed. A lower failure frequency has been calculated resulting safer than other materials from a statistical point of view. In Table 50, values are reported to make possible comparison.

**Table 50.** Failure rate calculated for steel, cast iron and ductile iron in the period between 2004 and 2017 in American NG distribution networks.

Material	System exposure, [km-y]	Number of accident in mains / total, [#]	Failure frequency in mains, [Acc/km year]
Polyethylene	$1.41 \times 10^7$	28 / 48	$1.99 \times 10^{-6}$
Steel	$1.24 \times 10^7$	32 / 40	$2.58 \times 10^{-6}$
Cast wrought iron	$7.54 \times 10^5$	8 / 8	$1.06 \times 10^{-5}$

From the reported data it was possible to analyse also the type of polyethylene. Nomenclature in accordance to ASTM specification has been considered; it should be however noted that an effective comparative analysis is not possible because of no data are present about the total length as a function of the characteristics of the material. However, a reduction of the number of accidents seems to be present with the increase of density. Considering the resistance to SCG, very poor difference is present even if only one accident occurs in the case of high resistance to SCG (rank number = 7).

**Table 51.** Number of failure as a function of polyethylene type.

Material	PE 2XXX	PE 3XXX	Unknown
Number of failure, [#]	20	10	18
Percentage of failure, [#]	41.6	20.8	37.6

Also in this case a distinction between body of the pipe, component and joint/connections has been made. Because of no frequency is calculated also service lines are considered resulting that the highest number of failures occurred in joints/connections: in particular, the most critical parts of the system are fusion joints.

**Table 52.** Failure rate calculated for steel, cast iron and ductile iron in the period between 2004 and 2017 in American NG distribution networks.

Material	Number of failure in the body of the pipe, [#]	Number of failure in components, [#]	Number of failure in joints/connections, [#]
Polyethylene	16 (33.3%)	4 (8.3%)	28 (58.3%)

As example for this, the accident occurred the August 21, 2004 at DuBois (Pennsylvania) is reported. In the accident a residence was completely destroyed and two residents were killed. The gas system consists of a 2" plastic pipe and the gas leakages through a butt fusion joint as identified by the NTSB investigators.

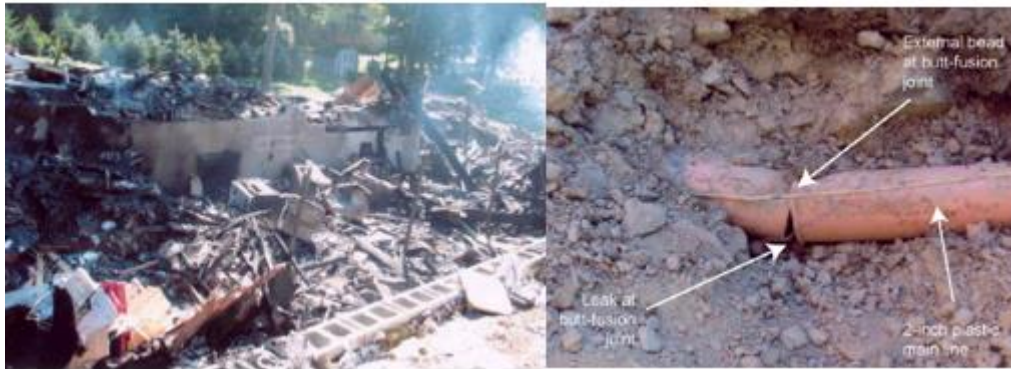


**Figure 81.** Gas accident consequences (left) and failed plastic NG pipeline.

In order to conclude the analysis, leaks and ruptures occurred were analysed. As shown, leak is the preferably consequence in the case of polyethylene failure. However, some ruptures are occurred in the case that the failure occurred in a component.

**Table 53.** Failure rate calculated for steel, cast iron and ductile iron in the period between 2004 and 2017 in American NG distribution networks.

	Percentage of failure in the body of the pipe, [%]	Percentage of failure in components, [%]	Percentage of failure in joints/connections, [%]
<b>Polyethylene</b>			
<b>Leak</b>	81.3	50	89.2
<b>Rupture</b>	18.7	50	10.7

### 3.3.5 Excavation damages

About excavation damages, several works are present in literature trying to describe the phenomenon as a function of the excavator characteristics. For example, an analysis of the effectiveness of prevention methods against these events is proposed in [115]. In the paper a fault tree model is present to identify the possible failure paths that can determine the event such as:

- The presence of excavation damage on pipeline alignment;
- The failure or preventive measures as excavation procedures, and alignment markers;
- The failure or protective measures;
- An excavation depth bigger than cover depth.

With the proposed fault tree (Figure 82) is therefore possible to evaluate existing procedures and identify possible deficiencies. Furthermore, probabilities for the basic events are proposed even if they are not specifically for gas distribution. From the work also the following conclusions result:

- Particular attention should be given about construction measures such as cover depth, permanent surface or buried markers that can reduce significantly the probability of failure;
- Site supervision is of particular importance in order to reduce the probability of damage the pipe. However, in the case of unreported excavation, buried warning tapes are effective in probability reduction;

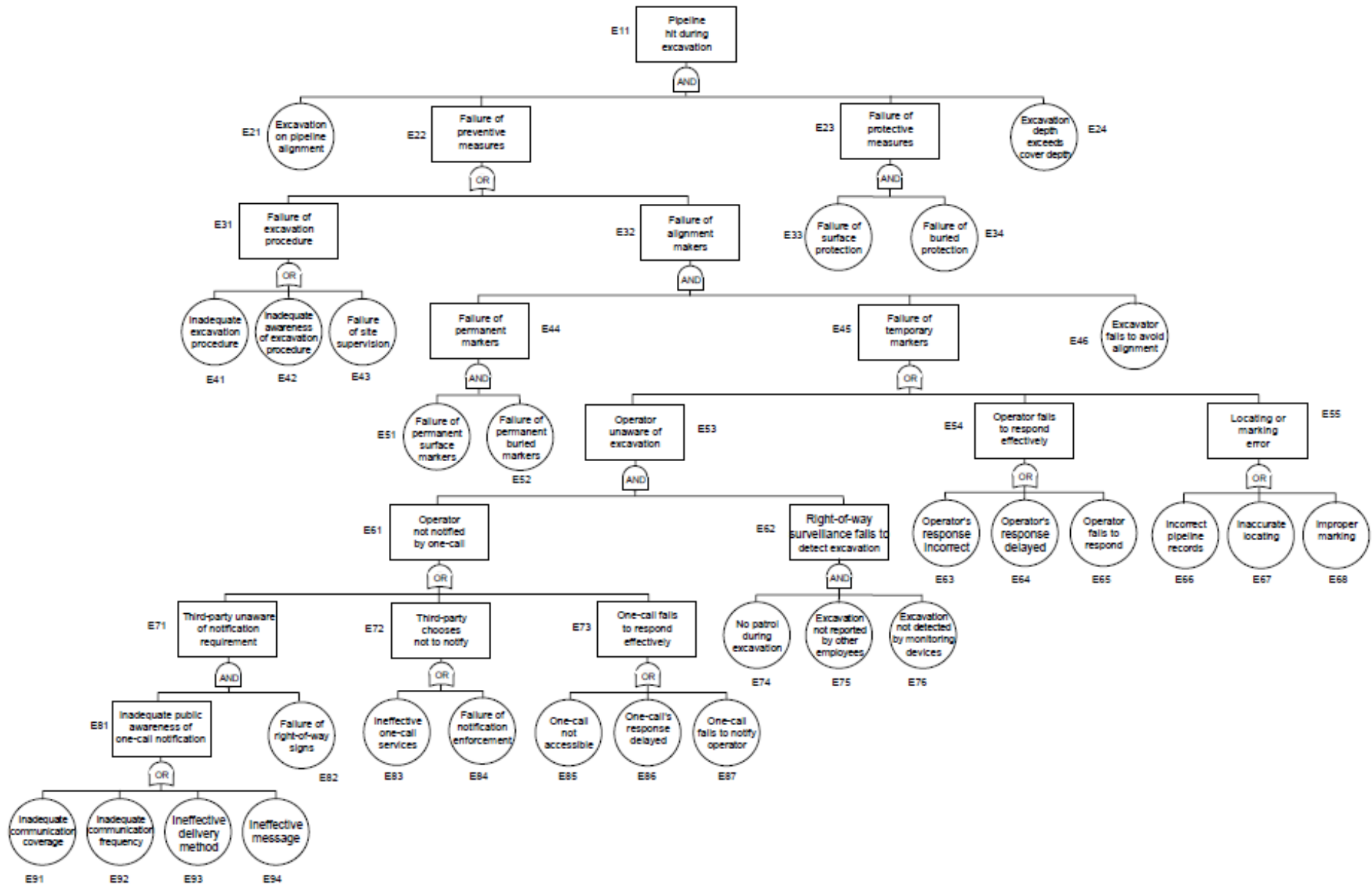


Figure 82. Fault Tree model for excavation damages. Source [115].

- Efforts should be given for the enforcement of notification and to improve public and contractor awareness and training.

That is, excavation damages do not be always responsible for pipe leaks or ruptures. In fact, other defects such as dents or gouges can be caused without gas escaping. A dent is a permanent plastic deformation of the circular cross section of the pipe which hazardousness is represented by its depth; therefore, the following division is usually reported in literature as a function of geometry and boundary conditions:

- Geometry:
  - Smooth dent: a smooth change in the wall curvature is present;
  - Kinked dent: an abrupt change in the wall curvature is present;
  - Plain dent: no wall thickness reduction or other defects are present.
- Surrounding conditions:
  - Unconstrained dent: a dent that is free to rebound elastically thanks to the effects of inside pressure;
  - Constrained dent: a dent that is not free to rebound because the indenter has not been removed.

The presence of a dent decreases dramatically the operative live of the pipe reducing the effective bursting pressure of the pipe. That is, gouges can be responsible for long effects pipe deterioration such as coating deterioration or stress concentration. Even if considerations about the calculation of strains and stresses in dented pipelines are made in [115], several issues appear in the application in NG distribution network because of the absence of monitoring devices in the market able to geometrically characterize dent size while it can be simpler in NG transmission pipe thanks to the use of ILI tools.

For this reason, statistical analysis about occurred accident due to excavation damages have been performed considering data from PHMSA database in the period 2004 – 2017. In fact, in the period 1984 – 2003 the voice “excavation damages” does not exist. For this reason, possible mistakes can arise during the analysis.

### *3.3.5.1 Statistical analysis of accidents due to excavation damage*

In order to highlight the importance of excavation damages, two accidents occurred in the past are reported. The first one occurred the December 13, 2005 at Bergenfield (New Jersey); an apartment was completely destroyed, three residents killed and five injured. The gas system consists of a 1” ¼ steel natural gas operated at 0.8 bar and was damaged during the excavation of a buried structure. From NTSB investigation the following results:

- No procedures for protect buried lifelines are present in the excavation company;
- No operators from the gas company assists during the excavation activity even if was considered as a possible risk.

The second one occurred the June 2, 2003 at Wilmington (Delaware) where two residences were completely destroyed and other two have severe damages. Furthermore, three contractor employers sustained severe

injuries and other eleven people minor injuries. Also in this case excavation activity was responsible for the failure of the 1" ¼ steel service line.

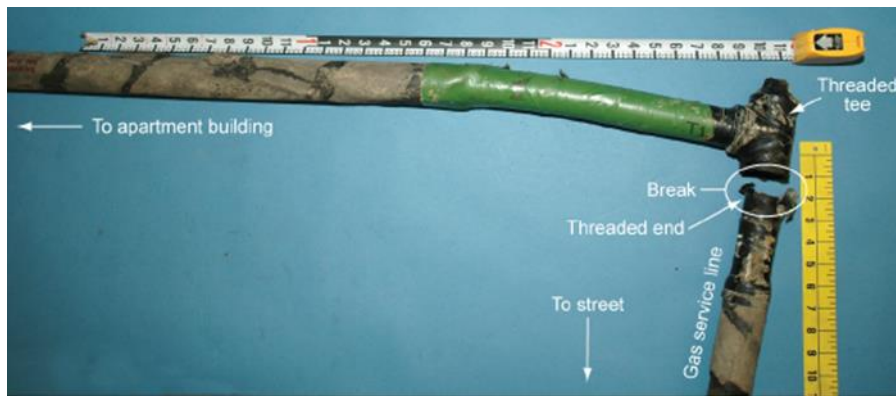


**Figure 83.** Damage on the pipe due to excavation damage at Bergenfield.

As investigated by NTSB, excavation was performed in a wrong position where no evaluations have been made about the presence of gas infrastructure. During the activities gas pipe was pulled producing a break in the basement of a residence. The following considerations result:

- Gas emergency teams are not immediately called because the risk was underestimated;
- No coordination between gas company and excavation teams (the two parties should be present contemporary during inspection activities).

It is therefore clear the importance of excavation damage that represents the main cause of accidents occurred in NG distribution systems. For the analysis no distinction is made about pipeline materials. Considering accident failure rate, a decreasing trend seems to be present even if, as anticipated, particular attention should be given to accidents occurred before 2004.

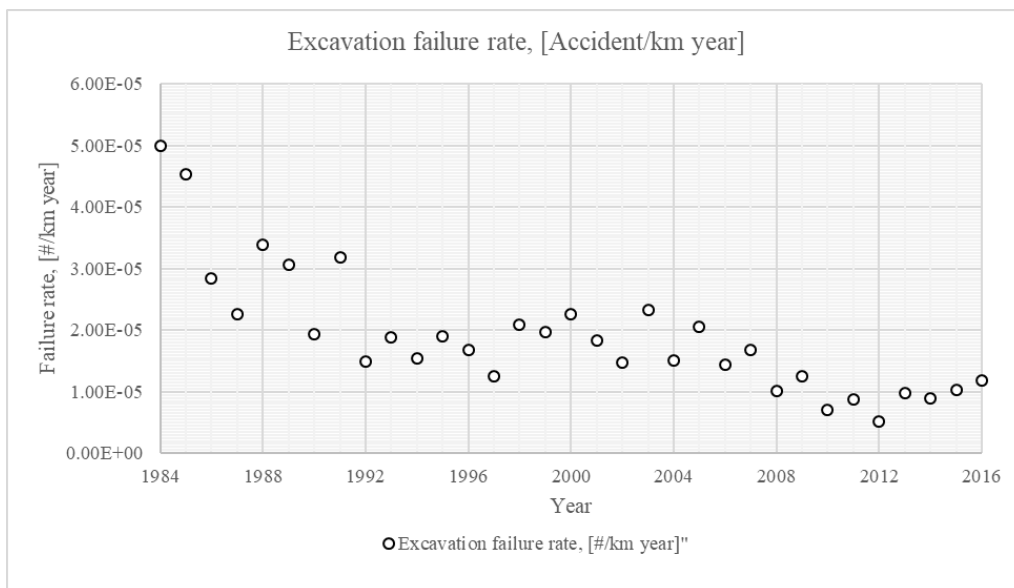


**Figure 84.** Excavation damage failure rate.

Considering the years after 2004 a failure rate of  $1.13 \times 10^{-6}$  [Acc / km y] have been calculated in NG distribution networks; of these the main percentage occurred in mains (71.3%) while lower values are present in service lines (28.7%).

**Table 54.** Failure rate calculated for excavation damages in the period between 2004 and 2017 in American NG distribution networks.

Part of the system	System exposure, [km-y]	Number of accident, [#]	Failure frequency, [Acc/km year]
Mains and service	$4.73 \times 10^7$	536	$1.13 \times 10^{-5}$

That is the influence of the following parameters are evaluated: pipeline location, population density, diameter, presence of markers, morphology of the failure (leaks or rupture).

About pipeline location, a different condition is present between mains and service lines. As shown in the tables, four different locations are identified: operator controlled property, private property, public property and utility right of way. The main percentage of main failure occurred in public property followed by utility right of way while in the case of service lines, private property is the primary locations where accidents occurred.

**Table 55.** Percentage of mains failures due to excavation damage as a function of pipeline location.

Year	Mains			
	Operator-controlled property	Private property	Public property	Utility right of way / easement
2010	0.0%	11.8%	58.8%	29.4%
2011	0.0%	9.5%	57.1%	33.3%
2012	0.0%	7.7%	69.2%	23.1%
2013	0.0%	12.5%	58.3%	29.2%
2014	0.0%	4.2%	58.3%	37.5%
2015	0.0%	11.5%	53.8%	34.6%
2016	0.0%	3.0%	60.6%	36.4%
2017	0.0%	11.5%	42.3%	46.2%

**Table 56.** Percentage of service lines failures due to excavation damage as a function of pipeline location.

Year	Service lines			
	Operator-controlled property	Private property	Public property	Utility right of way / easement
2010	0.0%	28.6%	71.4%	0.0%
2011	0.0%	66.7%	11.1%	22.2%
2012	0.0%	80.0%	20.0%	0.0%
2013	0.0%	90.0%	10.0%	0.0%
2014	14.3%	28.6%	28.6%	28.6%
2015	0.0%	70.0%	20.0%	10.0%
2016	0.0%	44.4%	22.2%	33.3%
2017	0.0%	80.0%	0.0%	20.0%

The following suggestions are therefore identified:

- The collaboration between public authorities and distributors has to be improved. For the scope, distributors should share the existing maps of gas networks and improvements should be made in the procedure required to start excavation activity;

- Public and contractor awareness has to be increased with specific programs in order to highlight the risk in case of damage. Also notification procedures with dedicated systems that could include a phone number, a web page or a dedicated mail to start activities in private property is necessary.

About location class, how expected, the highest percentage of accidents occurred in class 3 location. Even if no data is available about the total size in the different location class, it is evident that priority in the execution of the suggested informative programs should be given in such location. Furthermore, dedicated procedure and authorization should be required to excavator contractors for their activities in such locations (class 3 and 4 location).

**Table 57.** Percentage of mains failures due to excavation damage as a function of location class.

Year	Mains			
	Class 1	Class 2	Class 3	Class 4
2010	6.5%	9.7%	74.2%	9.7%
2011	12.1%	9.1%	72.7%	6.1%
2012	3.7%	3.7%	77.8%	14.8%
2013	5.9%	11.8%	79.4%	2.9%
2014	6.9%	6.9%	82.8%	3.4%
2015	2.9%	11.8%	82.4%	2.9%
2016	5.9%	23.5%	52.9%	17.6%
2017	4.8%	9.5%	66.7%	19.0%

**Table 58.** Percentage of service lines failures due to excavation damage as a function of location class.

Year	Service lines			
	Class 1	Class 2	Class 3	Class 4
2010	0.0%	18.8%	81.3%	0.0%
2011	0.0%	9.4%	90.6%	0.0%
2012	5.0%	0.0%	85.0%	10.0%
2013	4.8%	0.0%	85.7%	9.5%
2014	0.0%	0.0%	80.0%	20.0%
2015	12.5%	0.0%	87.5%	0.0%
2016	0.0%	0.0%	85.7%	14.3%
2017	0.0%	11.1%	88.9%	0.0%

About pipeline diameter, an increasing failure rate is observed with the increase of diameter. For this reason, dedicated solution should be implemented in the network to reduce the failure rate such as the increment of burial depth or the use of more visible markers.

**Table 59.** Excavation failure rate as a function of diameter calculated in mains for the period between 1984 and 2004.

Diameter	≤ 2"	2" < D ≤ 4"	4" < D ≤ 8"	8" < D ≤ 12"	D > 12"
Number of accident, [#]	87	117	100	35	16
Total exposure, [km year]	1.57E+07	6.87E+06	3.37E+06	5.20E+05	1.91E+05
Failure rate, [# / km year]	5.55E-06	1.70E-05	2.97E-05	6.74E-05	8.37E-05

In Table 60 the percentage of failure occurred in marked and not marked systems is reported. It should be noted that no data about the length of this system is available so comparative analysis are difficult to be

effectively performed. That is, because of the highest number of failure occurred in marked pipelines, NG distributors and Authorities should verify excavation procedures or introduce dedicated courses to improve existing conditions.

**Table 60.** Percentage of failures due to excavation damages as a function of the presence or absence of the markers.

Percentage of failure [%]					
	D ≤ 2"	2" < D ≤ 4"	4" < D ≤ 8"	8" < D ≤ 12"	D > 12"
<b>Marked</b>	48.5	66.9	68.3	71.4	50.0
<b>Not marked</b>	36.6	24.2	20.8	20.0	31.3
<b>Unknown</b>	14.9	8.9	10.9	8.6	18.8

In case of excavation damage, four possible conditions can verify: leak, rupture, mechanical puncture and other. Considering different diameters, it is evident that for small diameter the same probability for each failure morphology is present. Increasing the diameter, instead, rupture probability reduces while mechanical puncture and leak are more frequent. However, even if no gas leak is present in mechanical puncture, the formation of a dent can be responsible of a delayed gas accident with severe consequence. For this reason, gas distributors should stress the importance to notify mechanical puncture even if no gas immediately escapes from the pipe.

**Table 61.** Failure evolution as a function of the pipe diameter.

	Percentage, [%]			
	Leak	Rupture	Mechanical puncture	Other
<b>D ≤ 2"</b>	23.3	29.2	24.6	22.9
<b>2" &lt; D ≤ 4"</b>	29.3	16.3	41.5	13.0
<b>4" &lt; D ≤ 8"</b>	37.6	5.9	42.6	13.9
<b>8" &lt; D ≤ 12"</b>	34.3	2.9	57.1	5.7
<b>D &gt; 12"</b>	0.0	0.0	81.8	18.2

### 3.3.6 Incorrect operations

Incorrect operations are usually due to human errors, lacks of procedures or controls. For this reason, it is very difficult to forecast their occurrence.

In the past, several accidents occurred due to incorrect operations even if the most emblematic is that occurred the December 24, 2008 when a house was completely destroyed, a man died and other five people were severely injured. The failure occurred in a repaired connection of a 2" gas main operated at 3.8 barg. As reported by NTSB investigators, a wrong spool piece that does not respect dimensional requirements was used to replace a part of damaged main. For this reason, gas pressure pushed away the piece from the coupling leaving the gas free to escape.

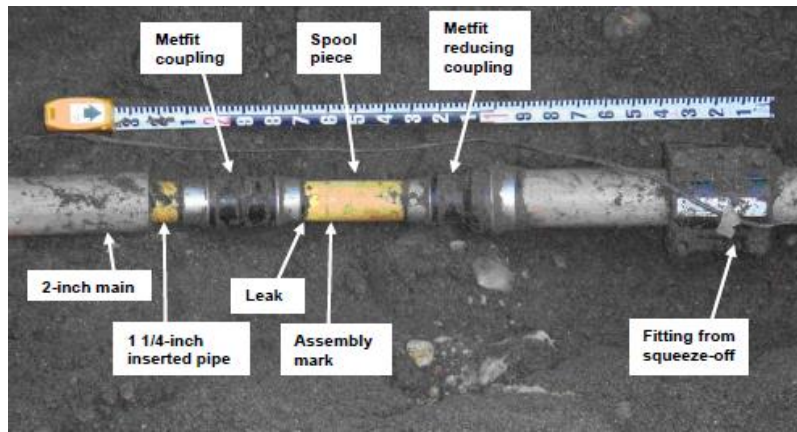


**Figure 85.** Failure occurred in a NG distribution main due to an incorrect operation.

Several errors were detected in the procedure such as:

- The use of a wrong pipe that is usually used to mark underground infrastructure as a stub marker;
- The definition of wrong procedures during the inspection activities and unavailability of the correct instruments to find the leak;
- The absence of communication between emergency team and coordinator in the case of delays. This information could help the management of the risk.
- The absence of procedures to inform people when they are outside of their property.

For this reason, a statistical analysis is performed to evaluate accident failure rate. As shown in Figure 86 **Errore. L'origine riferimento non è stata trovata.** a constant trend is present after 2004. This period is therefore considered as representative for state of the art conditions.

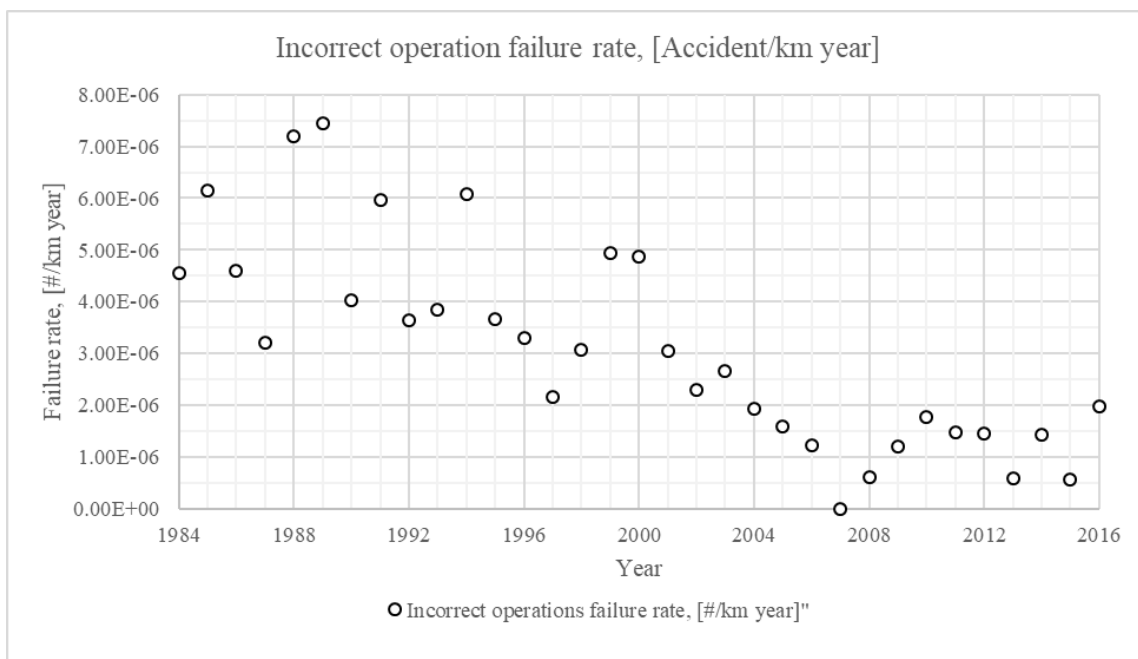


**Figure 86.** Accident failure rate due to incorrect operation in the period between 1984 and 2017 in American NG distribution network.

**Table 62.** Failure rate calculated for incorrect operation in the period between 2004 and 2017 in American NG distribution networks.

Part of the system	System exposure, [km-y]	Number of accident, [#]	Failure frequency, [Acc/km year]
Mains and service	$4.73 \times 10^7$	14	$2.96 \times 10^{-7}$

In order to evaluate where to intervene the following distinction was made: failure to follow procedures or human error, inadequate procedure and other. As shown, the first type was the most recurrent. However, it seems necessary to specify better the voice “other” that accounts for more than the 50% of accidents in future survey formats.

**Table 63.** Identified reasons for NG distribution networks failure.

Type of failure	Percentage, [%]		
	1984 - 2003	2003 - 2009	2010 - 2017
Failure to follow procedures / human errors	42.7	85.7	36.8
Inadequate procedures	4.0	9.5	0.0
Other	53.3	4.8	63.2

From the elaborated data, it is therefore suggested to improve existing courses for the operator in the field. Different courses should be defined as a function of responsibility and updated considering the state of the art and new achievement in safety performances.

### 3.3.8 Natural forces

“Natural forces” term contains several phenomena that can induce failure such as heavy rains, floods, lightning, temperature, high winds and earthquake and earth movement. Therefore, it is very difficult to analyse all possible events and also to forecast them because of the low predictability. However, because of earthquake and earth movement are the most hazardous phenomena for Italian NG distribution, an insight is proposed.

#### 3.3.8.1 Some outlooks on earthquake and earth movement

As reported in [116], during earthquakes a release of vibration energy due to the contact between moving tectonic plates in the lithosphere is present as proposed by Wegener in the so called plate tectonics theory. In fact, during the contact elastic energy is stored as elastic strain until soil stresses remain lower than material yield strength; exceeded this limit, plastic strain and failure occur. At this point, the energy is suddenly discharged through wave propagation as explained by the Rebound Theory that was firstly introduced by Reid to explain damages after San Francisco Earthquake in 1906. Three types of wave are present: the primary waves (p-waves), the secondary waves (s-waves) and the surface waves, that are responsible for soil transient motion.

Before wave propagation, local plate ruptures, defined as “faults”, occur. Three types can be identified depending on the principal directions of the faults as reported in Figure 87 causing Permanent Ground Deformation (PGD): strike slip, normal fault and reverse fault.

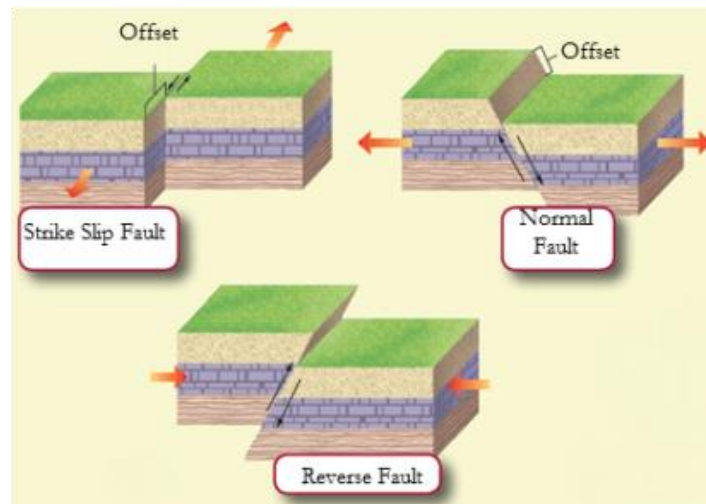


**Figure 87.** Type of different movement of faults causing earthquakes. Source [116].

PGD can be also induced by other events defined as preparatory, triggering or sustaining depending on the type of movement induced. The following are the principal ones to be considered [117]:

- Landslides, which are defined as a movement of a mass of rock, earth and debris down a slope, are the most hazardous for lifelines integrity. A further division can be made between:
  - Rotational slides that are “*more or less a rotational movement about an axis that is parallel to the slope contours*” [118];
  - Translational slides are a non-circular failure which involves translational movement.

Landslides can be induced by earthquake as secondary events and correlations are proposed in literature to estimate their magnitude as a function of earthquake characteristics.

- Lateral spreading presents the collapse of a sensitive soil layer at a certain depth followed by settlement of the above soil layer caused by the liquefaction of the below sustaining layer if particular soil conditions are present.

Different types of instrumentation have been proposed to monitor earth movement such as extensometric transmitters, automatic topographic systems, borehole wire extensometers, linear Synthetic Aperture Radar (SAR), a satellite Interferometric Synthetic Aperture Radar (InSAR), Global Positioning System (GPS), high resolution tiltmeters but also to evaluate the strain induced on buried lifelines as, for example, fiber optic technology [116].

In all these cases, however, the definition of the frequency with which record and elaborate data is essential. For the scope, the dynamics of the event has to be estimated. [119] proposes a class division as reported as a function of occurrence velocity: seven classes are defined ranging from extremely slow to extremely rapid (Table 64). Analysing past events, it results that fatalities and important damages to structures usually occur in the case of Class 6 and Class 7. For this reason, monitoring system should be designed in order to identify at least Class 5 events.

**Table 64.** Earth movement class division. [119]

Class	Description	Velocity, [mm/s]	Typical velocity
7	Extremely rapid	$5 \times 10^3$	5 m/s
6	Very rapid	$5 \times 10$	3 m/min
5	Rapid	$5 \times 10^{-1}$	1.8 m/h
4	Moderate	$5 \times 10^{-3}$	13 m/month
3	Slow	$5 \times 10^{-5}$	1.6 m/year
2	Very low	$5 \times 10^{-7}$	16 mm /year
1	Extremely slow	$< 5 \times 10^{-7}$	$< 16$ mm/year

### 3.3.8.2 Stresses induced to pipelines in the case of earth movement

Interaction between soil movement and pipelines has to be considered in the evaluation of stresses. For the scope a primary division between longitudinal and transverse PGD is made. The difference between longitudinal and transverse is that the first are characterized by a ground movement parallel to while the second by a movement perpendicular to the axis of the pipe (Figure 88).

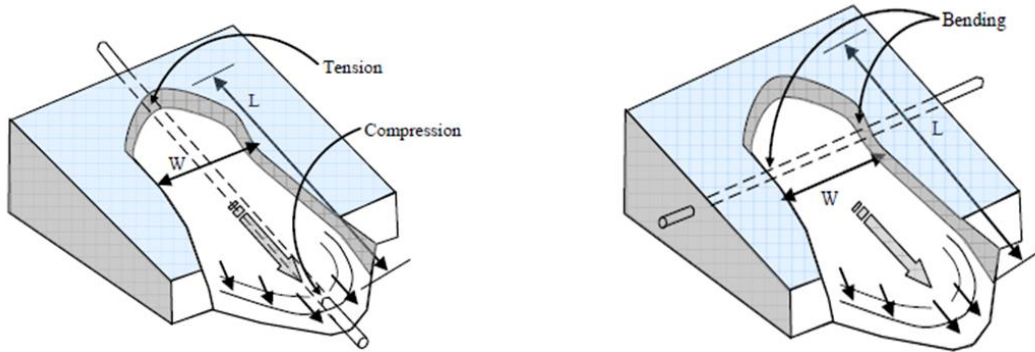


**Figure 88.** Longitudinal (left) and transverse (right) PGDs. Source [120].

- Longitudinal PGD

In the case of longitudinal PGD, compressive and tensile stresses arise respectively at the toe and the head of the moving slide. Ground strain and displacement can be calculated in accordance to [121]:

$$\varepsilon(x) = \frac{\beta_p x}{E} \left( 1 + \frac{n}{1+r} \times \left( \frac{\beta_p x}{\sigma_y} \right)^r \right) \quad (3-47)$$

$$\delta(x) = \frac{\beta_p x^2}{E} \left( 1 + \frac{2}{2+r} \times \frac{n}{1+r} \times \left( \frac{\beta_p x}{\sigma_y} \right)^r \right) \quad (3-48)$$

Where  $\varepsilon(x)$  and  $\delta(x)$  are respectively pipeline strain [%] and ground displacement [m] at a distance  $x$  [m] from the head of the slide.  $\beta_p$  is pipe burial parameter [N/m<sup>3</sup>],  $E$  is pipe young modulus [MPa],  $\sigma_y$  is material yield strength [MPa] and  $r$  and  $n$  are Ramberg-Osgood parameters that depend on the material.

From the analysis of past events, it results that compression wrinkling at compressive side is the primary cause of failure. However, soil displacement has to be greater than a minimum value, defined as critical length, that is function of material and pipe characteristics.

- Transverse PGD

In case of transverse PGD tensile stresses and bending conditions occur along the pipe. Also in this case, a critical ground displacement is present within which soil and pipeline deformations are exactly the same [122]. Therefore, it is possible calculate pipeline strain knowing ground displacement and vice versa. Also in this case the threshold value is defined by the characteristics of the slide and of the pipe. As for longitudinal slide, a correlation is present to calculate pipeline strain from ground deformation:

$$\varepsilon = \begin{cases} \frac{\pi\delta}{2} \sqrt{\frac{t_u}{AEW}} \pm \frac{\pi^2\delta D}{W^2} & \text{if } \delta \leq \delta_{crit} \\ \frac{\pi\delta_{crit}}{2} \sqrt{\frac{t_u}{AEW}} \pm \frac{\pi^2\delta_{crit}D}{W^2} & \text{if } \delta > \delta_{crit} \end{cases} \quad (3-49)$$

where  $\delta$  is ground displacement [m],  $t_u$  is longitudinal resistance [N/m], A is pipe cross sectional area [m<sup>2</sup>], D is external pipe diameter [m], W is slide width [m], E is Young modulus [Pa]. However, slide width and displacement have to be known in order to estimate strain.

- Faults

The analysis of faults is more complex even if several work are present about pipeline performance exposed to soil offsets. For example, different stresses arise on pipelines depending on the intersection angle between pipeline and soil direction in case of strike slip faults.

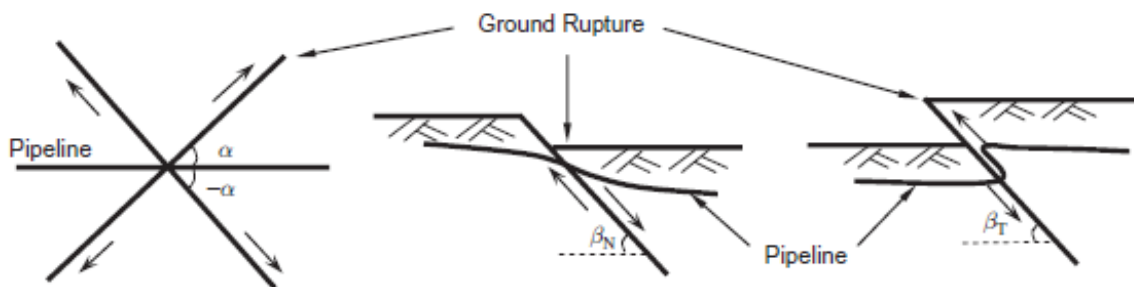


**Figure 89.** Different type of fault events. From the left to the right: strike slip, normal and reverse fault. Source [127].

[123] identified that axial and bending strains increases with buried depth while only axial strain reduces increasing the angle of intersection. Remediation techniques are proposed to improve buried pipeline performances against strike slips such as the substitution of soil with a more lightweight material around the pipe [124].

Also analytical models are available in order to estimate the maximum fault offset above which safety conditions are not assured [125] or to calculate the maximum strain present in the pipe as a function of the normalized offset, defined as the ratio between displacement and pipeline diameter [126]. Both models can be used to evaluate pipeline operative conditions in case strike slip faults are present: elaboration should be periodically performed in order to assess the hazardousness of pipeline operation and so to interrupt the service in the case of abnormal conditions.

In case of normal and reverse faults pipeline tensile and compressive stresses arise respectively while bending stress is present in both. In this case an axial strain lower than for strike slip fault is present [127]. Moreover,

bending strain reduces with the increase of pipeline stiffness and the reduction of buried depth, offset distance and soil internal angle of friction [128].

The following limit conditions have to be considered in order to ensure safety conditions:

- Steel pipelines. A strain threshold is defined for tensile and compression loads: a maximum value equal to 1-2% and 0.175 t/R is respectively allowed.
- Polyethylene pipelines. Ground deformation rates has to be considered for the calculation of the maximum stress. That is, bending stress and ovalization occur and have to be monitored during transverse slide. In order to monitor pipeline conditions, sensors should be installed at the top of the pipe (location A) where the highest stresses are present: for the scope, fiber optic cables can be used.

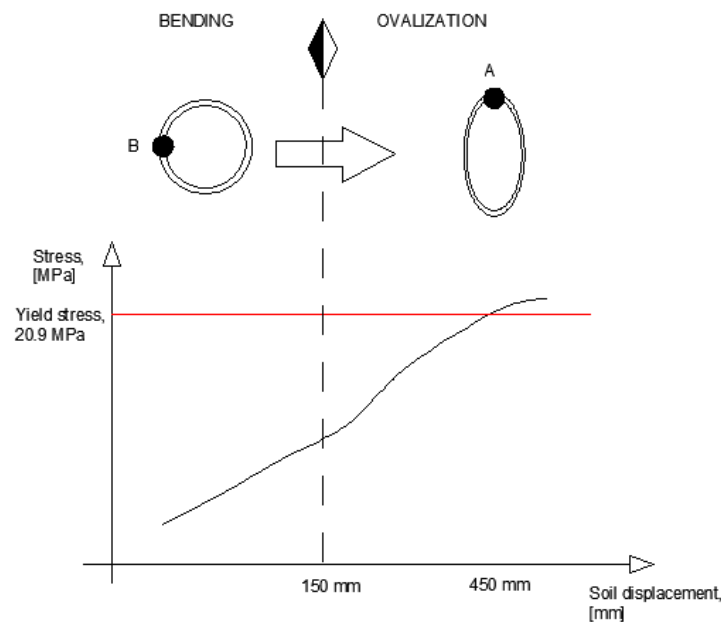


**Figure 7.** Stress imposed on polyethylene pipe for different soil displacement. Source [129].

### 3.3.8.3 Buried pipelines vulnerability respect to seismic and seismic induced loads

As shown in previous paragraphs, several correlations can be applied in order to evaluate stress conditions in buried pipelines subject to earth movement. At the same, because of a very strong interaction exists, soil movement can be evaluated from pipeline conditions.

The estimation of risk in case of earthquake and earth movement has to be performed considering the following parameters:

- *Seismic hazard (H)*. It depends on environment boundary conditions and so on the characteristics of the area in which the pipeline is installed. Furthermore, hazard is composed by two terms:
  - General hazard: being defined by seismic frequency and magnitude, it is usually valid for large areas on the territory;
  - Local hazard: it takes account of specific local conditions that could be responsible for an amplification of expected consequences. It is therefore of particular importance to identify where amplification occur in order to dedicate or implement dedicated protective solutions in those areas. For the scope seismic micro zonation maps should be considered.

- *Vulnerability (V)*. It represents the capacity of the pipeline to react against the stresses exerted during the event;
- *Exposition (E)*. It depends on the population distribution;
- *Resilience (R)*. It is the capacity of the community to react against the catastrophic event in terms of economic, commercial and social activities.

Therefore, a dedicated correlation has to be implemented in order to calculate the seismic risk for gas pipelines:

$$R = f(H, V, E, R) \quad (3-50)$$

Because of this formulation requires a dedicated analysis, simple correlations are available in literature in order to evaluate the risk to population. For the scope fragility curves are presented. Fragility curves relate the possibility to reach a damage state due to the presence of ground deformation and/or ground shaking.

For both events, fragility curves are generically identified in terms of the repair ratio (RR):

$$RR = K \times a \times IM^b \quad (3-51)$$

Where K is a corrective factor accounting for pipeline characteristics, a and b are two regression parameters that are calculated from existing data about failures while IM are the unit of measure for the event, i.e. Peak Ground horizontal Velocity (PGV) in [m/s] for ground shaking and Permanent Ground Deformation (PGD) in [m] for ground movement.

However, very few works are present in literature about gas distribution while the several contributions are present about water distribution. Among these, repair rates for NG distribution systems are evaluated. In [130] failures occurred in the gas distribution network during the earthquake occurred at L'Aquila in 2009 are analysed finding that the greatest number of interventions were made to pipelines (37%) of which the 72% in low pressure steel (particularly in gas welded joints) and the 16% in low pressure polyethylene ones. A lower number of interventions is identified for medium pressures even if no considerations were made considering the effective length of each parts. From the experimental activity it results that:

- The correlation proposed by [131] seems to be the best for buried NG distribution networks.

$$RR_{transitory} = k \times 0.0001658 \times PGV^{1.98} \quad (3-52)$$

Where k is equal to 1 in the case proposed and 0.5 for steel arc welded pipes.

- The estimated values are smaller than the real ones because a high number of gas welded steel pipes is present in L'Aquila networks while the correlation is precisely valid for arc welded joints;
- No repair to polyethylene systems have been identified in the localized area used for the analysis demonstrating the good performances of the material in accordance to the results reported in [132].

In order to estimate the expected PGV in a defined area the following can be used the following [133]:

$$PGV = 0.16 \times PGA \times S_s \times St \times T_c \quad (3-53)$$

Where PGA is the Peak Ground Acceleration that can be derived from the Software Spettri-NTCver.1.0.3.xls,  $S_s$  is the amplification coefficient for the existing stratigraphy,  $S_t$  is the topographic coefficient of amplification and  $T_c$  is the period considered and assumed equal to 0.5 s.

In the study proposed by O'Rourke about earthquake occurred the June 13, 2011 repair ratio curve respect to liquefaction is proposed. The following results:

- Repair ratios after large earthquakes are three to four times greater respect to the case of absence of previous event;
- Repair ratio is generally 10 to 30 times greater in areas subjected to liquefaction;
- No repair activities were done in MDPE and HDPE networks.

In the work of [134] seismic vulnerability of buried lifelines is studied identifying the following:

- Correlations to evaluate PGD are reviewed identifying the seismic parameters required for the estimation;
- Several leaks have been found in welds after earthquakes but this results from the poor quality of execution;
- Submerged arc welds present higher performance than oxyacetylene weld respect to earthquake events.

Because of in previous works no correlation is given between RR and PGD, the following is considered in accordance to [135]:

$$RR_{permanent} = K_2 \times 1.06 \times PGD^{0.319} \quad (3-54)$$

Where  $K_2$  is a function of the pipeline material and joint type while the estimation of PGD can be performed in accordance to [136].

The total repair rate  $R_{tot}$  is therefore defined as the sum of two contributions:

$$R_{tot} = RR_{permanent} + RR_{transitory} \quad (3-55)$$

Applying the introduced correlation, it is possible to calculate the expected repair ratio. The result can be subsequently used to assess damage probability. For the scope the Poisson probability distribution is considered:

$$P(N = n/PGA) = e^{-RR \times L} \times \frac{(RR \times L)^n}{n!} \quad (3-56)$$

Where  $P(N = n)$  is the probability to have  $n$  failures in a pipe of length  $L$  [m] conditioned by an event with a Peak Ground Acceleration equal to PGA. Therefore, the probability to have zero failure is equal to:

$$P(N = 0/PGA) = e^{-RR \times L} \times \frac{(RR \times L)^0}{0!} = e^{-RR \times L} \quad (3-57)$$

In order to take into account also the likely level of ground hazard, probabilistic earthquake curves should be used. These curves in fact gives the probability that the intensity of earthquake is greater than a defined value in a certain location. Therefore, the total annual probability to have n failures result:

$$P(N = n) = P(N = n/PGA) \times P(PGA) \tag{3-58}$$

Where P(PGA) is the annual probability to have an earthquake of peak ground acceleration equal to PGA. The probability to have more than zero failure is:

$$P(N > 0) = (1 - e^{-RR \times L}) \times P(PGA) \tag{3-59}$$

### 3.3.8.4 Statistical analysis of accidents due to natural forces

Only accidents due to earth movement and earthquake have been considered. As shown in Figure 90 a reduction of failure rate seems to be present during the years even if some doubts remain because of the change of the survey format during the years.

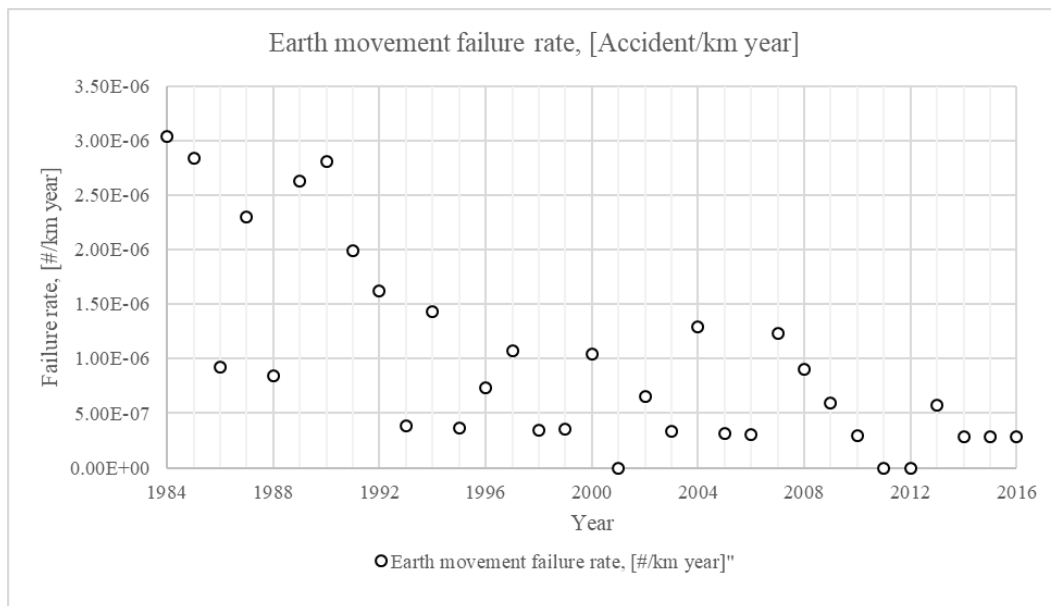


Figure 90. Earth movement failure rate for American NG distribution networks between 1984 and 2017.

Cast iron pipes are characterized by a higher failure rate than steel pipes and polyethylene; attention should be made in the use of the results especially for polyethylene where the data derives from the elaboration regarding only mains: in fact, six of the eight accidents occurred in polyethylene services lines so a very low database is available for evaluation.

Table 65. Failure rate calculated for earth movement in the period between 2004 and 2017 in American NG distribution networks.

Part of the system	System exposure, [km-y]	Number of accident, [#]	Failure frequency, [Acc/km year]
Steel mains	2.1 x 10 <sup>7</sup>	14	1.12 x 10 <sup>-6</sup>
Cast iron mains	7.5 x 10 <sup>5</sup>	11	1.45 x 10 <sup>-5</sup>
Polyethylene mains	1.4 x 10 <sup>7</sup>	2	1.42 x 10 <sup>-7</sup>

However, the reported data are in accordance to literature suggestions and particularly to the best performances of polyethylene pipes respect to other materials. For this reason, the renovation of old metallic pipes with polyethylene is suggested as soon as possible where operative conditions allowed it.

### ***3.3.9 Statistical analysis of repaired leaks in American NG distribution networks***

Even if for risk evaluation accident failure rate has to be used, an extremely higher number of leaks occurs in NG distribution networks. When a leakage is identified, a repair activity is performed to a gas accident. Furthermore, in case of leaks, hazardous leaks are usually identified representing *an existing or probable hazard to person or property* and requiring *an immediate repair or a continuous action until it is no longer hazardous* (Form PHMSA F-7100.1-2).

In order to perform a statistical analysis PHMSA database is used. Leaks occurred between 1984 and 2017 are considered even if distinction as a function of the specific cause is performed only for the period after 2004 because of a change in recording format is present in that year being responsible of possible errors.

#### ***3.3.9.1 Statistical analysis of repaired leaks in distribution networks***

From available records a reduction of the identified and repaired leaks occurred between 1984 and 2004 (-28.0%). As shown Figure 91, the highest number of leaks occurred in service lines (almost 400.000 leaks in 2017) while the highest reduction occurred in the main (-52.7%). A completely different trend is present for service lines where no clear trend is evident: in fact, after a slight reduction at the end of 20<sup>th</sup> century, an increasing number of leaks appear in following year with the maximum in 2016 that is slightly lower than that observed in 1984 (-11.4%).

However, it results necessary to make a comparative analysis in terms of leak rate defined as the ratio between the number of leakages and the length of the systems. Considering the total length of the system (mains and service lines), a decreasing trend is identified (Figure 92). As shown, an almost linear trend is present in the first part of the period up to 2009 (from 0.430 [leak / km y] to 0.170 [leak / km y]) after which a constant trend is present. In Figure 93 the leak rate in mains and service lines is shown. Particularly, respect to Figure 92, only repaired leaks during the year have been considered. As shown, leaks rate decreases both in mains and in service lines even if higher values are valid for service lines. Furthermore, a slightly reduction in decreasing trend of service lines is present in last years. In order to identify the reasons and so to take the best decisions in order to counteract the recorded behaviour, a preliminary analysis of failure causes is proposed.

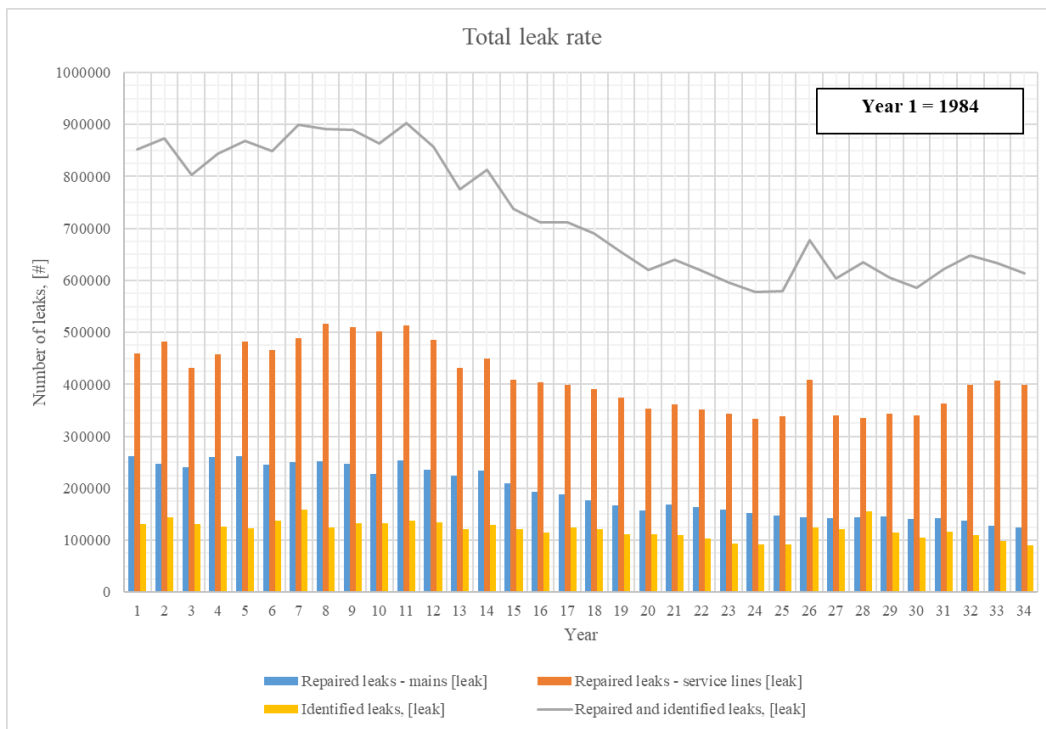


Figure 91. Number of leaks identified and repaired in the American NG distribution networks.

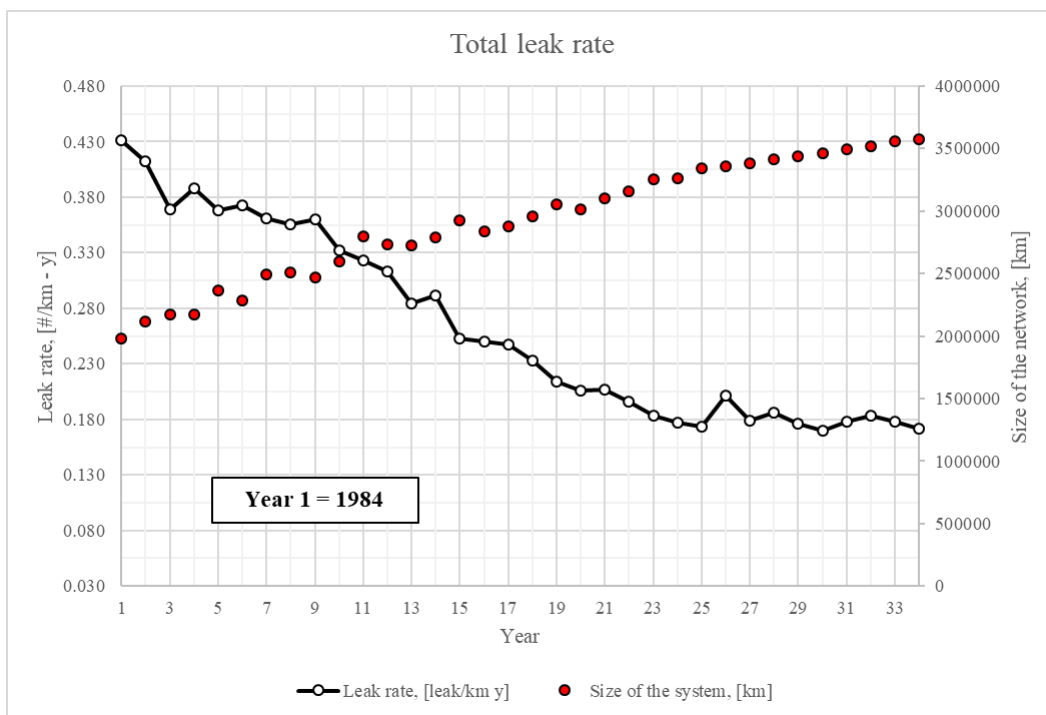
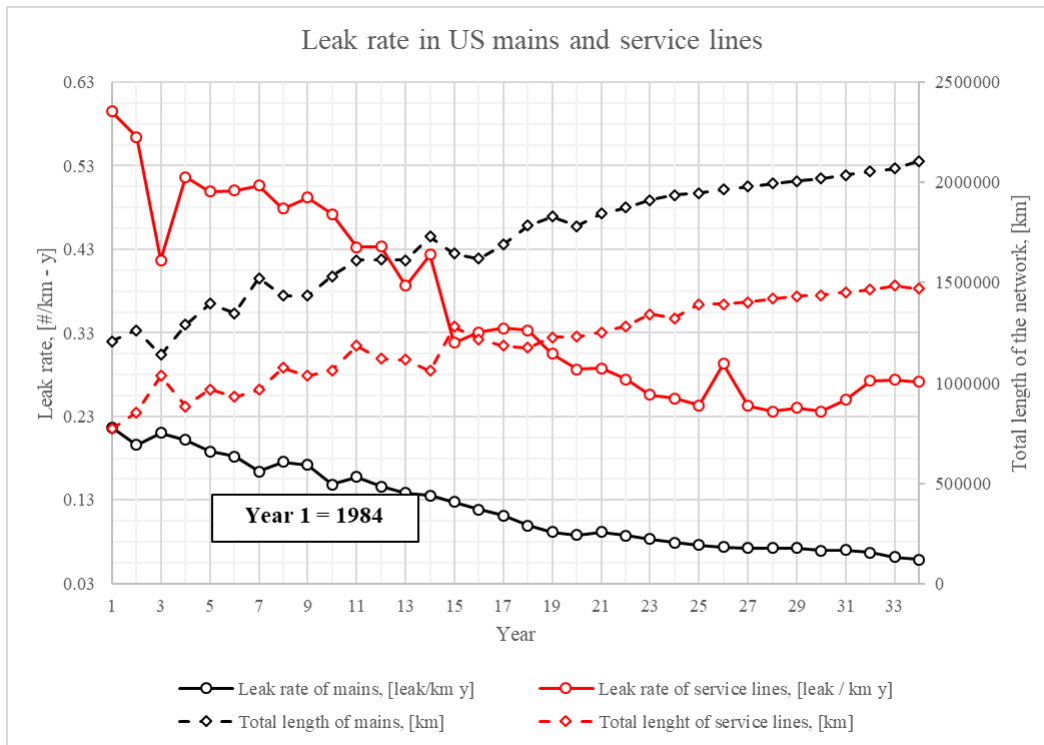


Figure 92. Leak rate [leak/km y] verified during the period between 1984 and 2004 in the American NG distribution networks.



**Figure 93.** Leak rate [leak/km y] verified during the period between 1984 and 2004 in mains and services lines. Only repaired leaks have been considered.

For the scope the following causes have been analysed: corrosion, natural forces, excavation damage, pipe weld or joint failure, equipment failure and incorrect operation. Causes defined as “Other” are not shown in the tables. The following considerations result:

- The first cause of failure in mains and in service lines are respectively corrosion and equipment failure.
- A reduction in the percentage of leaks caused by corrosion is present through the years thanks to the application of coating and cathodic protection systems as shown in Figure 94 where the percentage of unprotected pipes<sup>2</sup> are correlated to the leak rate.

**Table 66.** Percentages of leaks per different causes in American NG distribution network mains.

Year	Percentage [%] – mains					
	Corrosion failure	Natural force	Excavation damage	Pipe, weld or joint failure	Equipment failure	Incorrect operation
2004	36.0	8.1	16.2	7.8	4.1	1.0
2005	36.9	8.2	16.6	7.1	4.9	1.0
2006	36.5	7.5	16.5	6.9	5.0	2.5
2007	36.4	8.5	15.4	7.0	6.8	2.5
2008	38.4	8.1	13.2	7.5	6.6	2.9
2009	39.7	9.2	10.1	8.1	7.9	2.3
2010	36.9	8.1	11.4	9.0	8.8	1.6
2011	35.6	9.3	11.8	7.7	9.1	1.6
2012	37.0	7.9	12.2	7.6	10.3	1.3
2013	35.3	9.6	12.0	8.5	11.2	1.6
2014	34.4	11.2	10.4	8.1	11.4	1.6
2015	35.4	10.2	11.9	10.6	11.8	2.1
2016	35.1	8.2	13.8	11.5	12.4	2.4
2017	34.4	8.4	13.2	12.1	12.5	2.7

<sup>2</sup> Percentage of unprotected pipes = (Size of unprotected bare + unprotected coated steel pipes) / (Total size of steel pipes)

**Table 67.** Percentages of leaks per different causes in American NG distribution network service lines.

Year	Percentage [%] – service lines					
	Corrosion failure	Natural force	Excavation damage	Pipe, weld or joint failure	Equipment failure	Incorrect operation
2004	24.8	4.0	25.2	11.3	7.9	1.9
2005	22.3	3.9	26.0	11.8	9.6	1.7
2006	22.1	4.6	26.2	11.4	11.2	1.9
2007	21.6	3.4	24.9	11.2	12.7	2.6
2008	21.1	4.4	21.5	11.4	12.9	3.1
2009	22.0	3.4	15.0	15.0	19.3	2.7
2010	25.1	4.6	16.9	12.4	19.6	2.3
2011	23.6	4.6	16.4	10.8	23.3	2.4
2012	22.5	4.7	16.2	9.2	26.5	1.9
2013	20.8	4.8	15.7	9.5	30.3	2.0
2014	20.1	4.9	16.2	9.7	31.7	2.6
2015	18.5	4.7	15.5	9.8	34.1	2.9
2016	18.4	5.3	16.9	9.3	36.1	3.4
2017	18.0	4.9	15.8	9.7	39.1	3.6

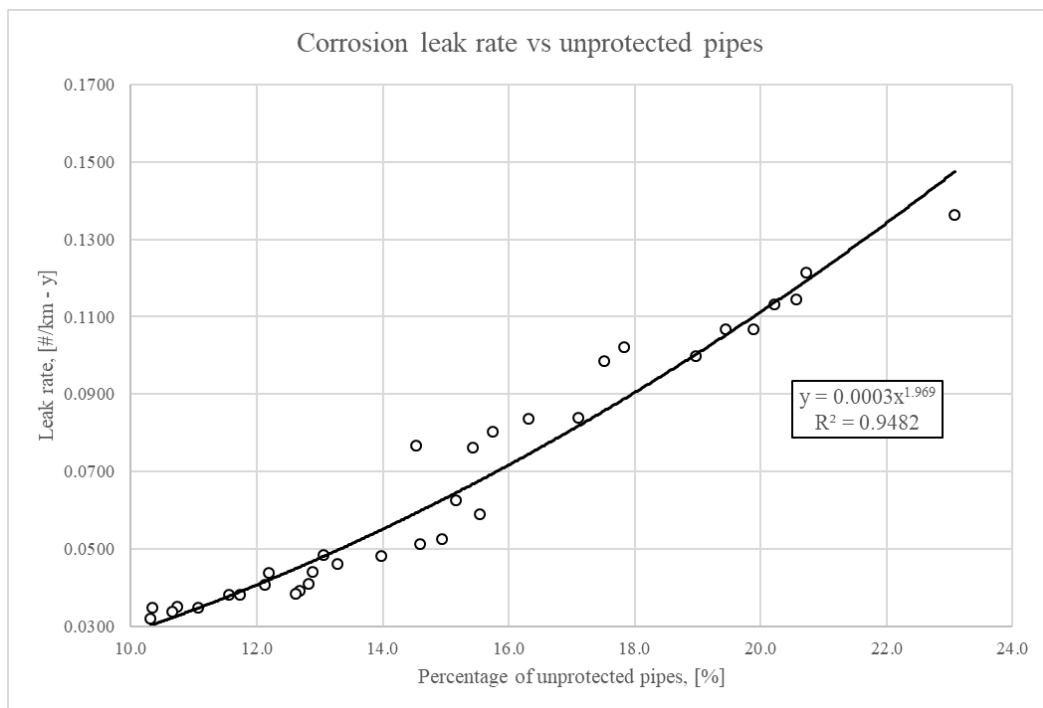


**Figure 94.** Corrosion leak rate as a function of the percentage of unprotected pipes.

- Improvements are present in excavation damage through the years thanks to the efforts given by distributors both in mains and service lines even if a slowdown occurs in recent years;
- A different trend is present about pipe, weld and joints were a reduction seems to be present in service lines while an increase is present in mains.
- Special attention should be given to equipment failure that present a warning trend especially in service lines where an increase of +31.2% occurs in last years. Consequently, a dedicated analysis is required in order to identify the reasons responsible for the failure of components such as the identification of trends or anomalies. For the scope, a dedicated database such as that proposed for fittings has to be created, populated and managed by a third party Authority responsible for data analysis.

- Incorrect operations have an always more important role increasing of more than 100% in 14 years. From the available data, however, it is not clear if this condition is due to company's or contractors' workers. In both cases solutions should be implemented by Authorities in order to reduce human factors. For the scope errors should be analysed and results shared among gas companies to improve sector performances. Furthermore, workers should be encouraged by companies to report errors or potential sources even if no gas leak immediately occurs.

Unfortunately, no information of the same type is present for Italian or European NG distribution systems even if they could be very useful to identify investment or research direction as shown. Therefore, this lack represents a very great obstacle respect to the improvement of safety performances in NG distribution and it should be removed as soon as possible by decision makers.

### 3.3.9.2 Statistical analysis of leaks in mechanical fittings

In accordance to Title 49 of the Code of Federal Regulations, gas distributors have to submit on annual basis all the hazardous leaks that involve a mechanical fitting. The following mechanical fittings are considered in the database: stab, compression fittings, bolted types and other compression fittings (such as electrofusion joint, electrofusion joint, gas service head, flange). The following result:

- An increasing trend of the number of leaks is present between 2011 and 2016 (Figure 94);
- The highest percentage of failed fittings is referred to nut follower, followed by other compression fittings type, stab and bolted (Figure 94). About other compression fittings, service head adapters are identified as the highest vulnerable part. It should be noted that the analysis of these data is very difficult and time consuming because many components has been defined in different ways in the database.

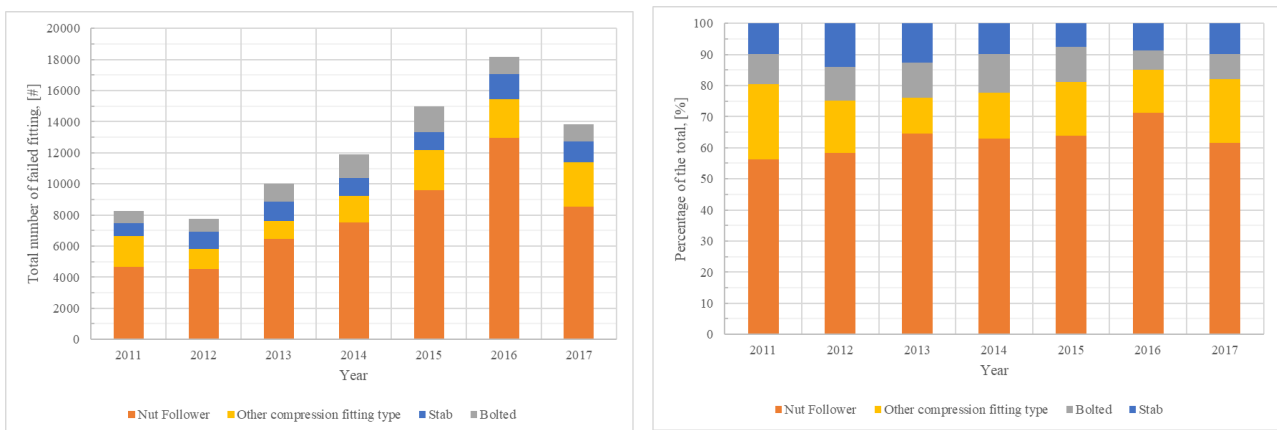


**Figure 95.** Failed mechanical fittings in American NG distribution system. Percentage (right) and total number (left).

From the available database is evident that the highest number of failure occurred in coupling followed by valves, adapters and risers (Figure 96).

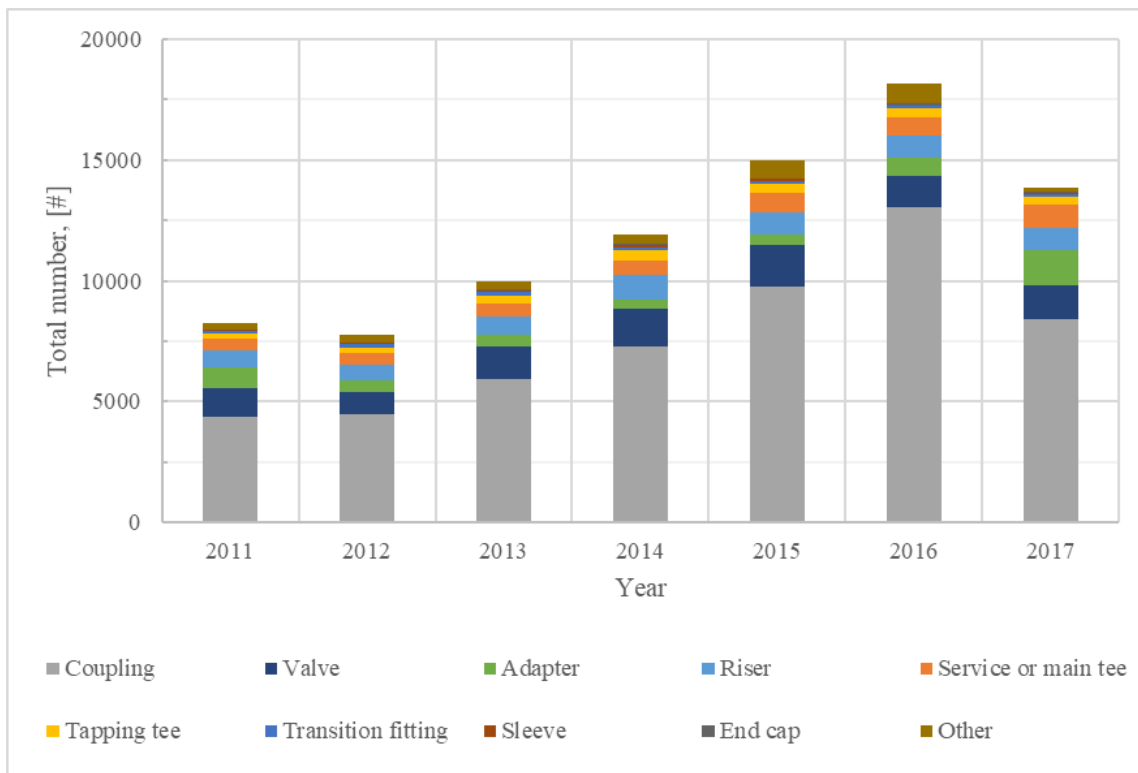


**Figure 96.** Total number of mechanical fittings failure per different parts of the system.

Considering the material, steels is characterized by the highest number of failed fittings. However, having no information about the total number of fittings present in the network it is difficult to identify the real performance of the material. Only in the case of stab a higher percentage is present for plastic.

**Table 68.** Percentage of failed fittings per different material in the American NG distribution system between 2011 and 2017.

Material	Percentage of failed fitting [%]				
	Steel	Plastic	Combination plastic and steel	Brass	Other
Nut follower	77.34	14.28	3.50	4.14	0.74
Bolted	68.43	19.51	3.76	0.94	7.36
Other compression type fitting	68.87	22.15	6.32	0.91	1.75
Stab	10.95	80.51	8.04	0.35	0.15

Because of nut followers are the elements with the highest number of failures, the influence of age is evaluated for steel and plastic systems. For the scope, fourteen intervals of five years have been considered. For each group, the number of failed fittings with a lower age has been considered (Figure 97). From the analysis it results that steel components seems to have a longer operative life respect to polyethylene ones even if the failed polyethylene fittings present lower performances respect to those available nowadays in the market. Therefore, continuous data updating should be performed year by year in order to monitor trends and to update existing ones.

Information about the number of fitting that are present in the distribution networks should be added in the existing database in order to evaluate trends and to compare different fittings. In fact, only absolute evaluations are possible with the current data.

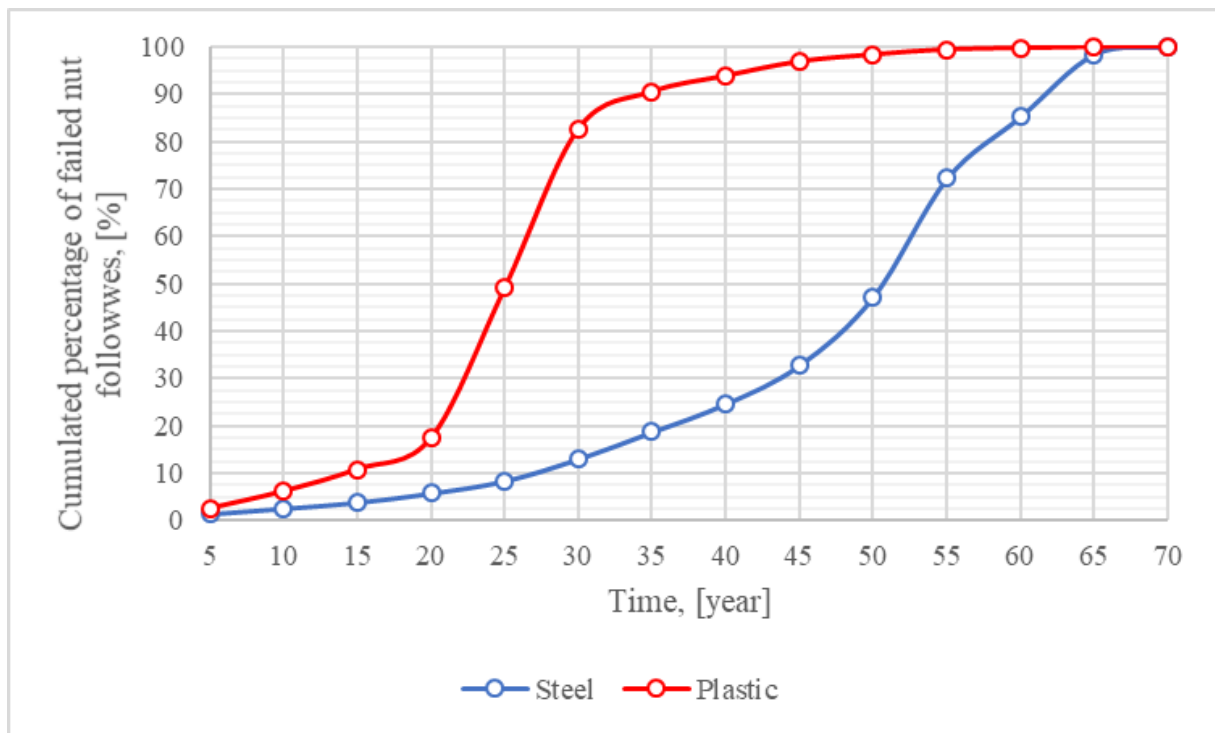


**Figure 97.** Percentage of failed nut follower as a function the operative life.

In order to evaluate possible solutions, the causes responsible for the failure of fittings have been analysed and results reported in Table 69. The following results:

- Nut fullower and other compression fitting type principally fail due to equipment deficiencies;
- Natural forces are responsible for a high percentage of failure in the case of bolted fittings and compression type fittings. Therefore, in the case of such events priorities should be given to verify the conditions of equipment in which these fittings are applied;
- Stab principally fails due to incorrect operation. Efforts should be given by DSOs to reduce this issue. A starting point should be the identification and the analysis of incorrect operations through the definition of database or similar recording format. Training activities and the enhancement of safety culture in the workers is also fundamental.

**Table 69.** Cause of failure, [%] for each mechanical fitting type.

Cause	Nut follower	Other compression type fitting	Stab	Bolted
Corrosion	4.3	7.0	2.7	9.1
Natural forces	13.9	19.1	6.3	28.2
Excavation damage	2.2	2.8	2.5	3.8
Other outside force damage	0.5	1.3	0.9	0.8
Material or welds/fusions	13.0	16.8	21.9	14.1
Equipment	55.2	36.3	21.4	27.7
Incorrect operation	4.2	8.2	34.4	8.4
Other	6.7	8.5	10.0	7.9

Also leakage type has been analysed and reported in Table 70. As shown, the seal of the fitting represents the most critical part for all the analysed fittings while a low number of leaks occur through the body. Therefore, in the case of failure a low gas flowrate is expected increasing the complexity to identify the source before gas can accumulate in available spaces.

**Table 70.** Leakage type [%] for each mechanical fitting type.

Leakage type	Nut follower	Other compression fitting type	Stab	Bolted
Leaked through seal	87.4	76.3	79.8	80.0
Leaked through body	6.6	15.3	12.2	13.9
Pulled out	6.0	8.5	8.0	6.1

### 3.4 Consequences of NG distribution accidents

Several works are present in literature in order to estimate consequences. In [137] thermal radiation from a sustained fire is considered as the main treat during a NG accident finding that the target distance and the hole size are the most important parameters to be identified. Several consequences such as jet fire, fire ball, detonation, deflagration, confined vapour cloud, flash fire are introduced in [138] while [77] distinguished between immediately ignition and delayed ignition. In [139] safety distances between target and flammable gas pipelines are estimated as a function of pipeline diameter and gas pressure.

In order to understand the severity of NG accidents real cases reported by NTSB can be considered. From the analysis of available reports, it results that jet fire and explosion are the most frequent events in case of NG leakages from distribution networks (Figure 98).



**Figure 98.** Explosion (left) and jet fire (right) occurred during the NG accident occurred in Birmingham the December 17, 2013.

A statistical method is implemented in consequence calculation such as the Dose – Response method linearized with the use of the Probit equation. The introduction of such formulation is required by the fact that a high degree of variation in response is present when a population is subjected to events of this type. Particularly, to calculate the probability of the outcome due to a certain dose, the following equation is used:

$$P = \frac{1}{2\pi} \int_{-\infty}^{Y-5} \exp\left(-\frac{u^2}{2}\right) du \quad (3-60)$$

Where P is the probability [%], Y is the Probit variable that is normally distributed with a mean value equal to 5 and a standard deviation of 1 and u is the integration variable. Also tables and graphs are available to estimate probability as a function of probit value as reported in Table 71. For example, for Y = 4.29 a probability equal to 24% is found.

**Table 71.** Conversion from Probit to percentages.

%	0	1	2	3	4	5	6	7	8	9
0	-	2.67	2.95	3.12	3.25	3.36	3.45	3.52	3.59	3.66
10	3.72	3.77	3.82	3.87	3.92	3.96	4.01	4.05	4.08	4.12
20	4.16	4.19	4.23	4.26	4.29	4.33	4.36	4.39	4.42	4.45
30	4.48	4.50	4.53	4.56	4.59	4.61	4.64	4.67	4.69	4.72
40	4.75	4.77	4.80	4.82	4.85	4.87	4.90	4.92	4.95	4.97
50	5.00	5.03	5.05	5.08	5.10	5.13	5.15	5.18	5.20	5.23
60	5.25	5.28	5.31	5.33	5.36	5.39	5.41	5.44	5.47	5.50
70	5.52	5.55	5.58	5.61	5.64	5.67	5.71	5.74	5.77	5.81
80	5.84	5.88	2.92	5.95	5.99	6.04	6.08	6.13	6.18	6.23
90	6.28	6.34	6.41	6.48	6.55	6.64	6.75	6.88	7.05	7.33
%	0.0	0.1	0.2	0.3	0.4	0.5	0.6	0.7	0.8	0.9
99	7.33	7.37	7.41	7.46	7.51	7.58	7.65	7.75	7.88	8.09

For each possible consequence Probit function is formulated in the following form:

$$Y = k_1 + k_2 \ln(V) \quad (3-61)$$

Where  $k_1$  and  $k_2$  are two constants depending on the phenomenon and  $V$  is representative of the dose absorbed by the target. Depending on the event, different type of energy is absorbed by the target such as thermal radiation in case of jet fire and pressure energy wave in case of explosion.

### 3.4.1 Jet fire consequence model

Jet fire results from the combustion of flammable gas and it is responsible for a high thermal radiation to surrounding people. As reported by [140], several works are present in literature about the modelling of jet fires even if the following one is suggested even if some simplifications are present. The method is based on the evaluation of thermal energy released by the jet fire. Particularly, the radiative heat flux received by a target can be written as:

$$E_{th,jet} = \tau_a Q_f F_p = \tau_a \eta G K_i F_p \quad (3-62)$$

Where  $E_{th,jet}$  is the radiative heat flux in [W/m<sup>2</sup>s],  $Q_f$  is the energy transported by the escaping gas [J/s],  $\tau_a$  is the atmospheric transmissivity [#],  $F_p$  is the point source view factor [m<sup>2</sup>],  $\eta$  is the fraction of energy converted to thermal radiation [%] (0.2 for methane),  $G$  is gas flowrate from the pipeline [kg/s] and  $K_i$  is the energy of combustion of the fuel [kJ/kg] equal to 54,512 kJ/kg for methane. In the proposed correlation geometric view factor and transmissivity have to be calculated. The following equations are considered:

$$F_p = \frac{1}{4\pi x^2} \quad (3-63)$$

Where  $x$  is the distance between the point source and the target in [m].

$$\tau_a = 2.02 \times (P_v x)^{-0.09} \quad (3-64)$$

Where  $P_v$  is the water partial pressure in [Pa] calculated in accordance to the following:

$$P_v = 1013.25 \times RH \times \exp\left(14.4114 - \frac{5328}{T_a}\right) \quad (3-65)$$

Where RH is the relative humidity [%] and  $T_a$  is ambient temperature in [K].

Probability of damages has calculated in accordance to Probit function. Even if different consequences are expected in the case of exposition depending on the heat power intensity and on the exposition as reported in Table 72 [141]. As expected, increasing the intensity of the heat flux less time is allowed to surrounding people to protect themselves.

**Table 72.** Time to pain as a function of the radiation intensity. Source [141].

Radiation intensity, [kW/m <sup>2</sup> ]	Time to pain, [s]
1.74	60
2.33	40
2.90	30
4.73	16
6.94	9
9.46	6
11.67	4
19.87	2

[142] suggests the following one to evaluate fatality in case of jet fire:

$$Y_{jet} = -14.9 + 2.56 \times \ln \left( \frac{t \times E_{th, jet}^{\frac{4}{3}}}{10^4} \right) \quad (3-66)$$

Where  $t$  is the time of exposure in [s]. A big uncertainty in the case of NG distribution systems is the presence of structures that can be considered as a possible shields respect to the radiative heat flux. In very few works, escaping time from the event is considered in the estimation of the received heat flux but it represents a critical point. To take into account of it, two times have to be considered: reaction time ( $t_r$ ) and escaping time ( $t_e$ ). The first term takes into account the time required to a person to identify the hazard, while the second one is the time required to reach a distance in which no hazard is present, i.e.  $E = 1 \text{ kW/m}^2$ :

$$t = t_r + t_e \quad (3-67)$$

A time equal to 5 sec. is usually considered for reaction, while a velocity of 5 m/s is used for the calculation of the escaping time. Considering the previous correlations and substituting  $E = 1 \text{ kW/m}^2$  the following is obtained:

$$t = 5 + \frac{1}{5} \sqrt{\frac{\tau_a \eta G K_i}{4\pi} - L^2} \quad (3-68)$$

Where  $L$  is the distance at which  $E = 1 \text{ kW/m}^2$ :

$$L = \sqrt{\frac{\tau_a \eta G K_i}{4\pi}} \quad (3-69)$$

In Figure 99 escaping times are reported as a function of gas flowrate. In accordance to the figure a value equal to 30 sec. has been considered for escaping time as the most representative for successive evaluations.

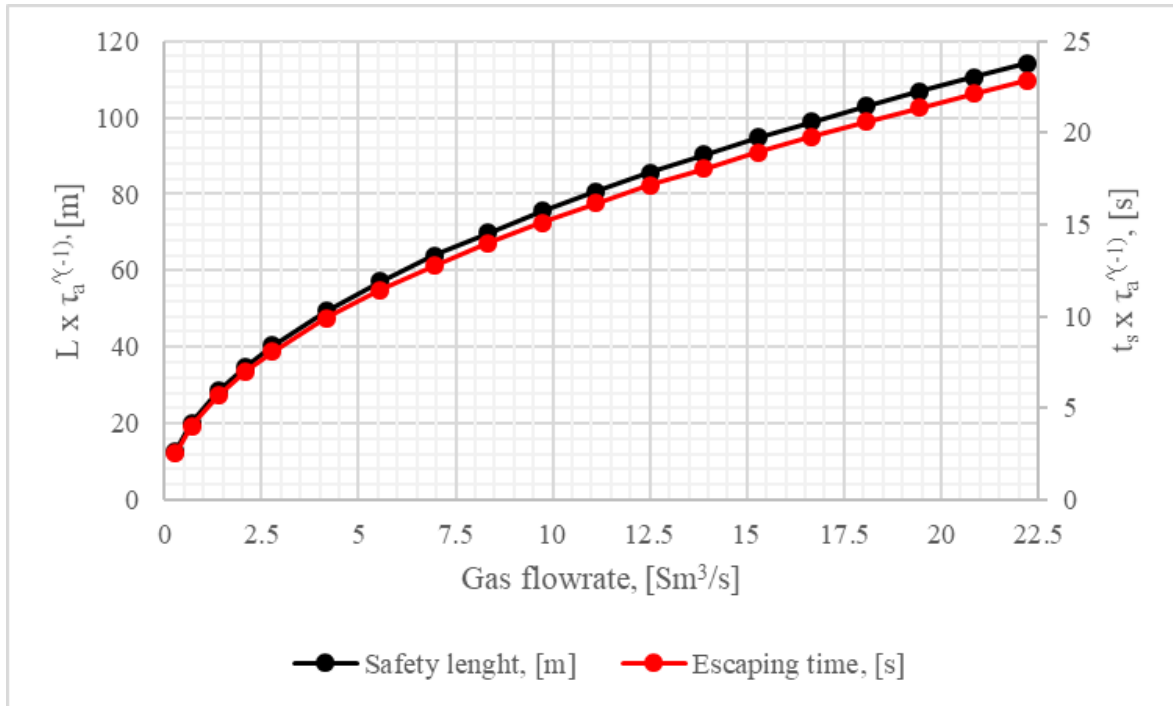


Figure 99. Safety length and escaping times as a function of NG leakages.

### 3.4.2 Confined and unconfined explosion models

The presence of escaping gas can be responsible of explosions that threat surrounding people and damage buildings. Several definitions are present in literature even if the main appropriate seems to be that proposed by [143] that defines an explosion as “a rapid expansion of gas resulting in a rapidly moving pressure or shock wave”.

Three methods are available to describe the effects of an explosion:

1. TNT equivalency model;
2. TNO multy energy model;
3. Modified Baker model.

Of the three proposed method, TNT equivalency model is the simplest considering a mass of TNT equivalent to the mass of leaked gas:

$$M_{TNT} = \frac{\eta_{exp} M_{gas} K_{i,gas}}{K_{i,TNT}} \quad (3-70)$$

Where  $M_{TNT}$  is the equivalent mass of TNT [kg],  $M_{gas}$  is the mass of gas [kg],  $K_{i,gas}$  and  $K_{i,TNT}$  are respectively the heat of combustion of natural gas [kJ/kg] and TNT (4437 – 4765 kJ/kg).  $\eta_{exp}$  is the explosion efficiency considered equal to 0.4 for asymmetric explosion.

From the TNT mass, overpressure effect ( $P_0$ ) can be calculated through the use of dedicated correlation as those proposed in [140] at different distance from the central point.

Because of the simplification required in the analysis, it is considered not useful to proceed in this phase with the use of most detailed correlation such as those reported in the second and third models. If believed of interest, those can be used in dedicated analysis to a small areas of interest.

Such as for jet fire, consequences due to explosion have to be carefully evaluated both for people and for buildings. In the case of human body, the formulation proposed by [144] is used:

$$Y_{exp,human} = -77.1 + 6.9 \ln(P_0) \quad (3-71)$$

If of interest, the following Probit function can be used to evaluate damages to buildings:

$$Y_{exp,structures} = -23.8 + 2.91 \ln(P_0) \quad (3-72)$$

Where  $P_0$  is overpressure due to produced pressure wave in case of explosion in [kPa]. To calculate the overpressure at a certain distance  $r$  [m] the following expression can be used:

$$P_0 = \frac{80800 \left(1 + \left(\frac{Z}{4.5}\right)^2\right)}{\left(1 + \left(\frac{Z}{0.048}\right)^2\right)^{0.5} \left(1 + \left(\frac{Z}{0.32}\right)^2\right)^{0.5} \left(1 + \left(\frac{Z}{1.35}\right)^2\right)^{0.5}} \quad (3-73)$$

Where  $Z$  [ $\text{m}/\text{kg}^{1/3}$ ] is defined as follow:

$$Z = \frac{r}{M_{TNT}^{1/3}} \quad (3-74)$$

### 3.4.3 Leakage gas flowrate calculation

As shown in previous correlations, gas leakage is required to estimate accident consequences. Several works and tool are present in literature.

Considering gas discharge from a hole, the integration of the mechanical balance energy assuming ideal gas behaviour, no heat transfers and no external work, gives:

$$G = C_D A p_1 \sqrt{\frac{2gM}{RT_1} \frac{k}{k-1} \left[ \left(\frac{p_2}{p_1}\right)^{\frac{2}{k}} - \left(\frac{p_2}{p_1}\right)^{\frac{k-1}{k}} \right]} \quad (3-75)$$

Where  $G$  is the mass flowrate in [ $\text{kg}/\text{s}$ ],  $A$  is the area of the hole [ $\text{m}^2$ ],  $C_D$  is discharge coefficient,  $g$  is the gravitational constant [ $\text{m}/\text{s}^2$ ],  $M$  is the molecular weight of the gas [ $\text{kg}/\text{mol}$ ],  $R$  is the ideal gas constant [ $(\text{Pa m}^3)/(\text{mol K})$ ],  $T_1$  is the temperature of the gas upstream of the hole [ $\text{K}$ ],  $k$  is the heat capacity ratio [ $C_p/C_v$ ],  $p_1$  is the upstream pressure and  $p_2$  is the downstream pressure both in [ $\text{Pa}$ ].

Increasing the upstream pressure, a maximum is found in the gas flowrate and no more dependence with the downstream conditions is present. Sonic conditions are therefore achieved and the following are valid:

$$\frac{P_2}{P_1} = \left(\frac{2}{k+1}\right)^{\frac{k}{k-1}} = 0.542 \text{ for methane} \quad (3-76)$$

$$G_{sonic} = C_D A p_1 \sqrt{\frac{2gM}{RT_1} \left[ \frac{2k}{k-1} \right]^{\frac{k+1}{k-1}}} \quad (3-75)$$

For the required scope, two main models can be considered.

The first one, described in [145], estimates gas flow rate considering all possible failure type as shown in Figure 100. Different possible flows such as subsonic or sonic flow in the pipe and subsonic and sonic flow through the hole are calculated thanks to iterative procedure.

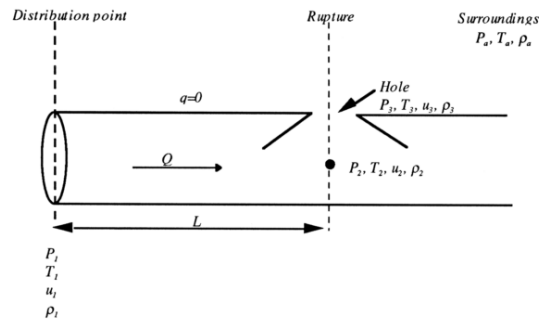


Figure 100. Accident scenario proposed. Source [145].

The second model is proposed by [146] and it identifies a new approach introducing dimensionless equations strictly valid in the pressure range between 0.4 MPa and 6.9 MPa. Therefore, not all distribution system can be modelled with it. In the model two possible consequences are modelled: hole model, for hole diameter smaller than  $0.15 \times D$ , and full rupture model. In the hole model dimensionless flowrate is almost independent from pressure, leakage position and friction term, while in the case of full bore rupture, flowrate depends on leakage position and friction term.

In order to estimate gas leakages, the model proposed by [145] has been implemented in Matlab workspace. The choice is due to the restriction required for the application of model proposed in [146]. This would have created a bit of confusion not useful in the successive steps. In Figure 101 gas flowrate has been calculated as function of hole size ( $d_{or}$ ) considering a DN 100 pipe and a pressure between 3 and 6 bar.

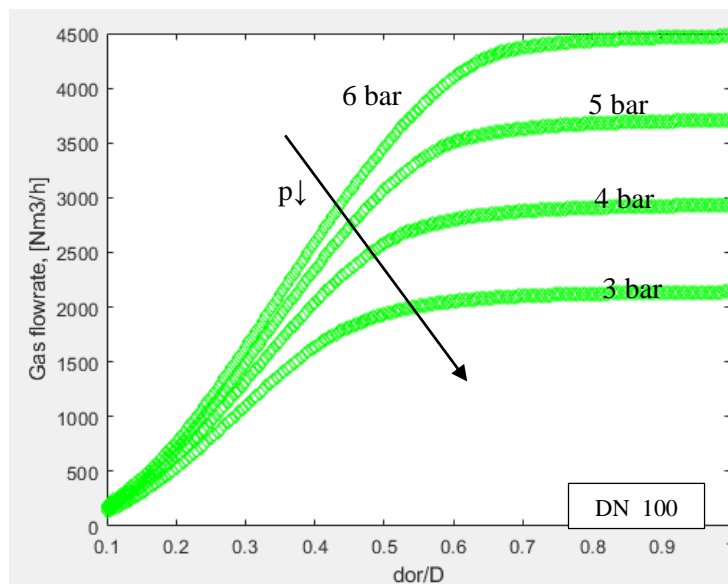


Figure 101. Gas flowrate as function of pressure and ratio between hole area and pipeline diameter.

### 3.4.5 Statistical analysis of verified consequences

In order to statistically evaluate consequences data from PHMSA database have been analysed. The period between 2004 and 2017 has been considered for the scope and only accidents occurred in mains and service lines have been used. In fact, no information about the presence of explosion or ignition is present in previous period.

From the analysis it results that the percentage of ignition and explosion almost constant in the two periods in the case of gas accident (Table 73).

**Table 73.** Number of accidents, explosion and ignition in the analysed periods.

Period	Number of accidents	Number of explosion	Number of ignition
2004 – 2009	532	164 (=30.8%)	300 (=56.4%)
2010 – 2017	566	150 (=26.6%)	326 (=57.6%)
<b>Total</b>	1098	314 (=28.6%)	626 (=57.0%)

An event tree is designed as shown in Figure 102 considering four possible scenarios in case of NG accident: jet fire (A), jet fire and explosion (B), explosion (C) and no treating phenomena (D). The selection of these paths derived from the analysis of databases and reports of NG accidents reported by responsible Authorities. From the analysis of data, it results that the most probable outcome is the scenario D where no explosion and ignition occur, followed by scenario A and B where both ignition and explosion are present. Therefore, only in 40% of events no hazardous phenomenon occurs.

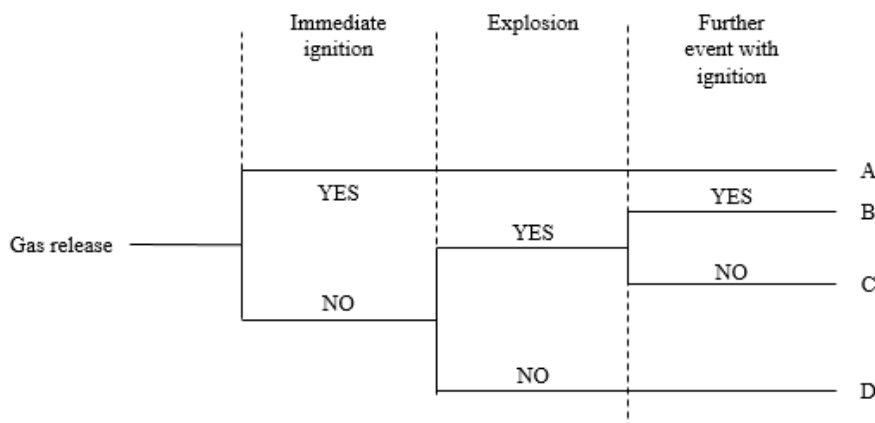


**Figure 102.** Event tree analysis of possible consequences in case of gas release.

**Table 74.** Possible scenarios and percentage of occurrence.

Period	Scenario			
	A	B	C	D
2004 – 2009	149 (=28.0%)	151 (=28.3%)	13 (=2.4%)	219 (=41.17%)
2010 – 2017	188 (=33.2%)	138 (=24.4%)	12 (=2.1%)	226 (=40.5%)
<b>Total</b>	337 (=30.7%)	289 (=26.3%)	25 (=2.3%)	445 (=40.8%)

Another fundamental parameter to be evaluated is Location class which is connected to the presence of possible ignition sources. In fact, the mixture of air and gas has to be in the flammability limits and a certain amount of

energy is required (activation energy  $\geq 0.2$  mJ) in order to start a combustion. Those events for which no information is available about location class are not included in the analysis which results are reported in Table 75. As reported, a higher percentage of ignition and explosion occur in high density populated areas with the highest value calculated in Location class 4.

**Table 75.** Number of ignition as a function of location class.

Period	Location class – Number of ignition			
	Location class 1	Location class 2	Location class 3	Location class 4
2004 – 2009	11 (=40.7%)	25 (=53.2%)	237 (=56.4%)	23 (=67.6%)
2010 – 2017	12 (=36.3%)	23 (=53.5%)	248 (=60.8%)	44 (=53.7%)
<b>Total</b>	23 (=38.3)	48 (=53.3%)	485 (=58.5%)	67 (=57.8%)

**Table 76.** Number of explosion as a function of location class.

Period	Location class – Number of explosion			
	Location class 1	Location class 2	Location class 3	Location class 4
2004 – 2009	4 (=14.8%)	12 (=25.5%)	128 (=30.5%)	18 (=52.9%)
2010 – 2017	4 (=12.1%)	7 (=16.3%)	120 (=29.4%)	20 (=24.4%)
<b>Total</b>	8 (=13.3%)	19 (=21.1%)	248 (=30.0%)	38 (=32.8%)

Also the scenarios reported in the event tree are evaluated considering Location class.

**Table 77.** Possible scenarios and percentage of occurrence: location class 1.

Period	Scenario			
	A	B	C	D
2004 – 2009	7 (=25.9%)	4 (=14.8%)	0 (=0.0%)	16 (=59.26%)
2010 – 2017	8 (=24.2%)	4 (=12.1%)	0 (=0.0%)	21 (=63.6%)
<b>Total</b>	15 (=25.0%)	8 (=13.3%)	0 (=0.0%)	37 (=61.7%)

**Table 78.** Possible scenarios and percentage of occurrence: location class 2.

Period	Scenario			
	A	B	C	D
2004 – 2009	13 (=27.7%)	12 (=25.5%)	1 (=2.13%)	21 (=44.7%)
2010 – 2017	16 (=37.2%)	7 (=16.3%)	0 (=0.0%)	20 (=46.5%)
<b>Total</b>	29 (=32.2%)	19 (=21.1%)	1 (=1.1%)	41 (=45.6%)

**Table 79.** Possible scenarios and percentage of occurrence: location class 3.

Period	Scenario			
	A	B	C	D
2004 – 2009	119 (=28.3%)	118 (=28.1%)	22 (=5.2%)	161 (=38.3%)
2010 – 2017	138 (=33.8%)	109 (=26.7%)	10 (=2.5%)	151 (=37.0%)
<b>Total</b>	257 (=31.0%)	227 (=27.4%)	32 (=3.8%)	312 (=37.8%)

**Table 80.** Possible scenarios and percentage of occurrence: location class 4.

Period	Scenario			
	A	B	C	D
2004 – 2009	8 (=23.5%)	16 (=47.1%)	2 (=5.9%)	8 (=23.5%)
2010 – 2017	26 (=31.7%)	18 (=22.0%)	2 (=2.4%)	36 (=43.9%)
<b>Total</b>	34 (=29.3%)	34 (=29.3%)	4 (=3.5%)	44 (=37.9%)

As shown in Figure 103, in Location class 1 a lower probability of ignition and explosion is present as expected thanks to the reduced number of people and so of possible ignition sources. Increasing the location class, a consequent rise of the severity of outcomes is identified.

However, considering the values reported in Table 74 a negligible error seems to be present thanks to the fact that a conservative estimation results for Location classes 1 and 2.

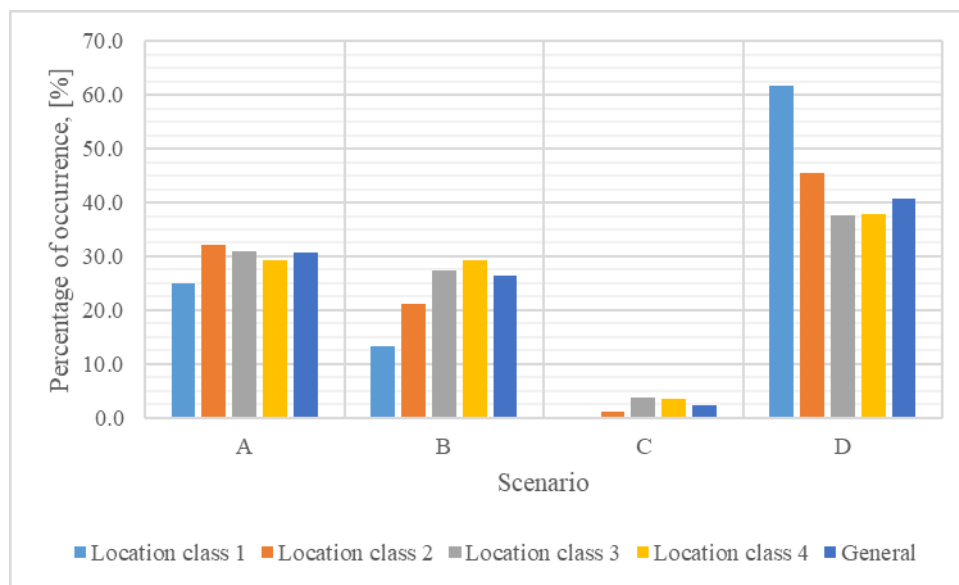


**Figure 103.** Probability of occurrence of the difference scenario as a function of the location class.

**About hazardousness, an analysis of injuries and fatalities have been performed. Before to proceed in a more detailed analysis, a general overview is introduced. As shown in Table 81 and**

Table 82, the most hazardous scenario are those characterized by jet flame and explosion.

As shown, fatalities and injuries are observed also in scenario D where no ignition or explosion occur due to secondary events.

**Table 81.** Number of accidents with at least one or more injuries. The percentages are referred to the total number.

Number and percentage of injuries				
Period	Scenario			
	A	B	C	D
2004 – 2009	38 (=25.5%)	57 (=37.7%)	4 (=30.8%)	8 (=3.7%)
2010 – 2017	56 (=29.8%)	63 (=45.7%)	4 (=33.3%)	18 (=7.9%)
<b>Total</b>	94 (=27.9%)	120 (=41.5%)	8 (=32.0%)	26 (=5.8%)

**Table 82.** Number of accidents with at least one or more fatalities. The percentages are referred to the total number.

Number and percentage of fatalities				
	Scenario			
Period	A	B	C	D
2004 – 2009	3 (=2.0%)	23 (=15.2%)	1 (=7.7%)	2 (=0.9%)
2010 – 2017	10 (=5.3%)	22 (=15.9%)	0 (0.0%)	4 (=1.7%)
<b>Total</b>	13 (=3.9%)	45 (=15.6%)	1 (4.0%)	6 (=1.3%)

From Figure 104 and Figure 105, it results that scenario A and B have more severe consequences in densely populated areas because of the effect of thermal radiation due to ignition and to possible domino effects in case of explosion.

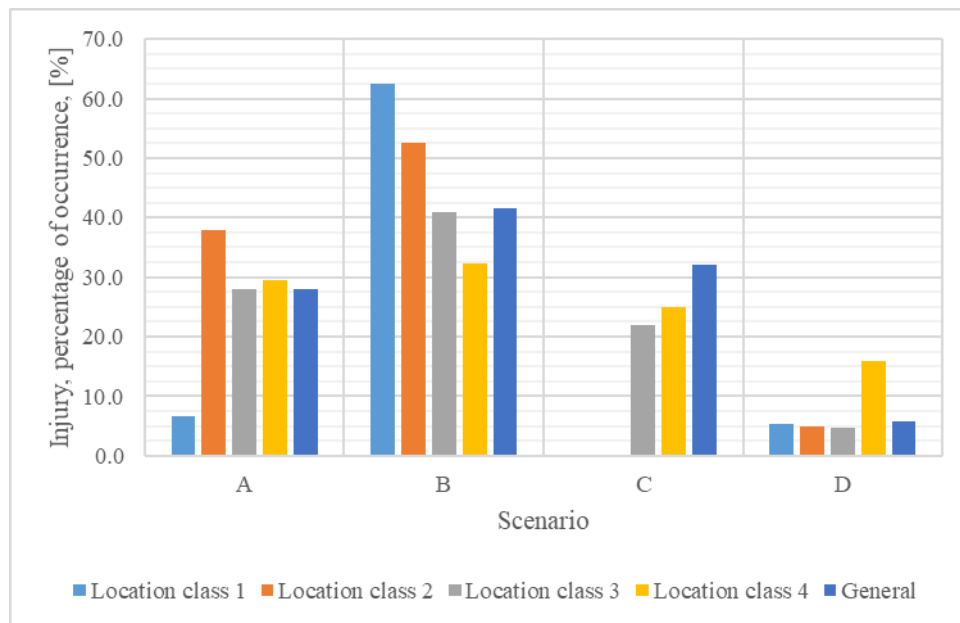


**Figure 104.** Percentage of occurrence of one or more injury per accident as a function of the scenario.

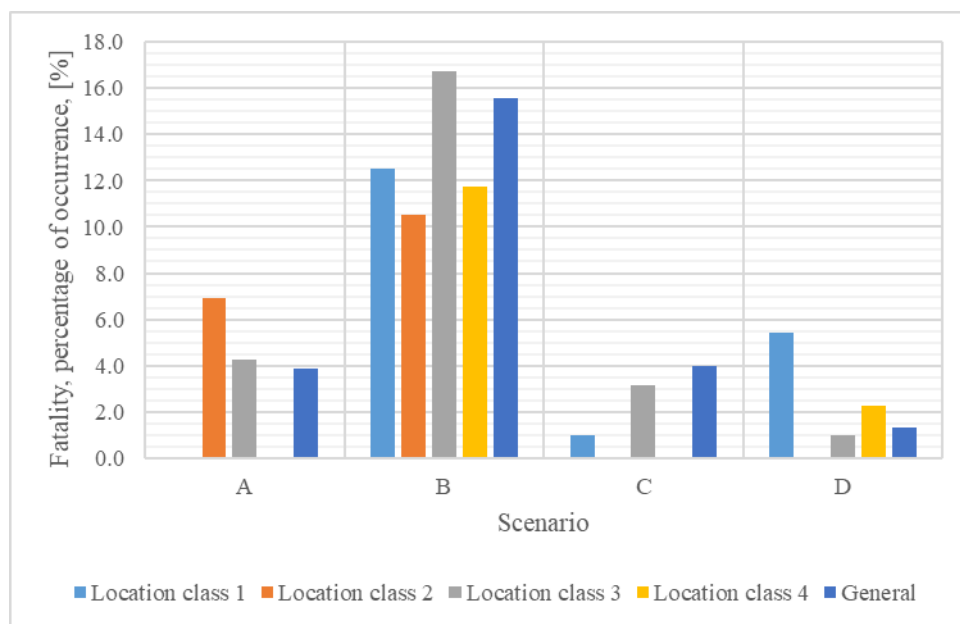


**Figure 105.** Percentage of occurrence of one or more fatality per accident as a function of the scenario.

In order to conclude the analysis, some considerations are made about the possible presence of correlations between ignition and explosion and operative data of NG distribution system. For the analysis operative pressure during the accident in [psi] and pipeline internal diameter (NPS) have been considered as recorded in PHMSA database. Twenty-four classes have been considered identifying for each one the total number of accident, number of ignition and explosion has been calculated. Percentage of ignition and explosion are simply calculated as the ration between the number of ignition and explosion and the total number of accident.

A decreasing trend with nominal diameter and pressure results for probability of ignition as reported in Figure 106. This can be justified by the higher presence of small pressure and diameter pipelines in high populated areas where a very high number of ignition sources is present. For explosion a similar trend is observed in Figure 105.

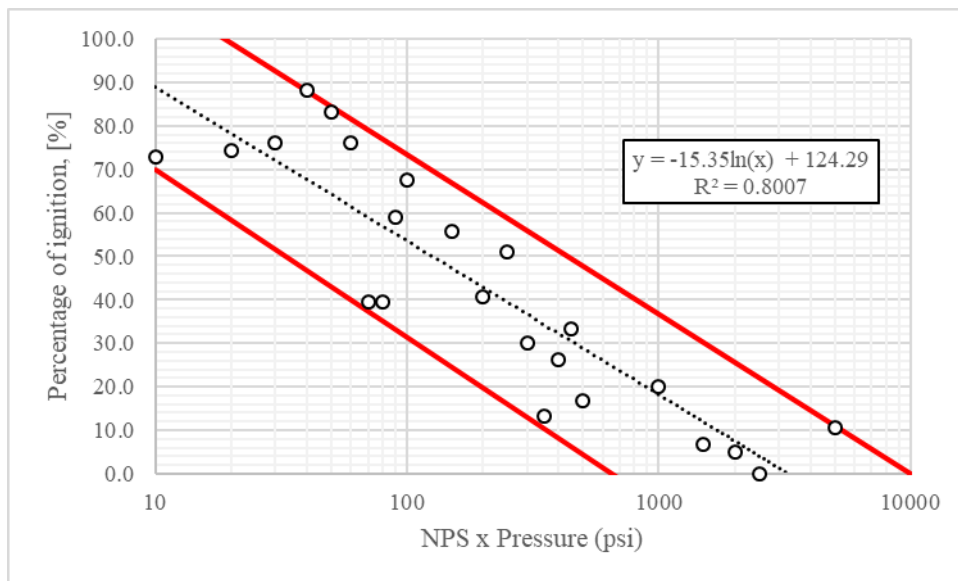


**Figure 106.** Probability of ignition as a function of pressure (psi) and diameter (NPS).

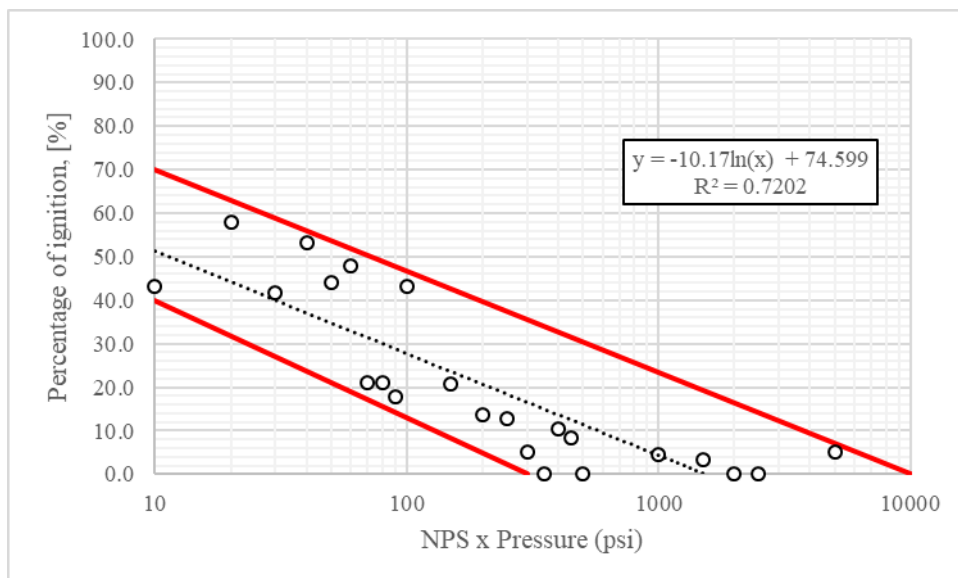


**Figure 107.** Probability of explosion as a function of pressure (psi) and diameter (NPS).

Considering that identified values distribution for the probability of ignition and explosion, it is possible to estimate the probability of ignition for example using a Monte Carlo simulation where average value is calculated in accordance to identified correlation and standard deviation is calculated in order that the 99.9% of the values obtained are between the two red lines for each abscissa.

The calculated values can be used in the definition of risk management plan by rescue team and so in order to evaluate ignition or explosion probability of a defined system and so to defined rescue emergency plans.

## **Chapter 4**

### **An innovative method to perform integrity management in NG distribution networks**

Natural gas distribution networks are, as anticipated, very complex systems that are designed, operated and maintained in order to minimize risks. Because of no continuous inspection is possible, decisions should be taken in order to prioritize the interventions even if no standardized method is available in literature.

For this reasons, a risk assessment method is proposed based on paradigms identified in ISO 31000. The following main objectives are identified:

- Definition of priorities and of the optimum strategies to allocate the budget;
- Identification of failure causes in order to take correct existing performances;

The aim of the analysis it to give suggestions in order to improve NG distribution where decisions are often based on experience or very complex algorithms with very poor connection to real conditions.

Moreover, the presence of an international accepted method to evaluate risks in gas distribution will ensure the possibility to compare companies, to recognize criticalities and to improve sector concurrency without reducing safety performances. In fact, those DSOs with poor safety performances or that operate high risk assets can be identified and obliged to intervene as soon as possible in order to continue their business activity.

In the following paragraphs, the proposed method is introduced with particular attention to the steps to be followed for risk assessment.

#### ***4.1 Introduction to the method***

In order to identify the required steps to perform risk assessment in NG distribution networks, several considerations have to be made in order to ensure that all the possible aspects have been considered:

- *Context and expected objectives.* The method has to be applied by DSOs in NG distribution networks while the main scope is risk assessment;
- *Type of tolerable risks and possible solutions.* The identification of a threshold for tolerable risk is a very difficult challenge. For the scope, typical values considered in Oil & Gas and chemical industry are considered.
- *Method and techniques to perform the analysis.* The method and the techniques applied in the proposed model have to be in accordance to [51].
- *Available resources in terms of time and money.* In order to minimize the complexity of the method, simplification and computer based procedures have to been implemented in accordance to the paradigms of Industry 4.0.

- *How does risk assessment integrate into organizational processes?* The results of risk assessment should be used by decision makers to improve the allocation of budgets and to plan inspections or renovation programs. Furthermore, company's technicians have to use the results in order to identify the best solutions for the specific cases.
- *How will the results and documentation be presented?* Results should be presented in dedicated reports to the decision makers, but also in a synthetized way to authority and public society. Result clearness is in fact of great importance in order to share the obtained results and the culture of safety thanks to specific examples.

From these considerations, a general procedure is identified and reported in Figure 108.

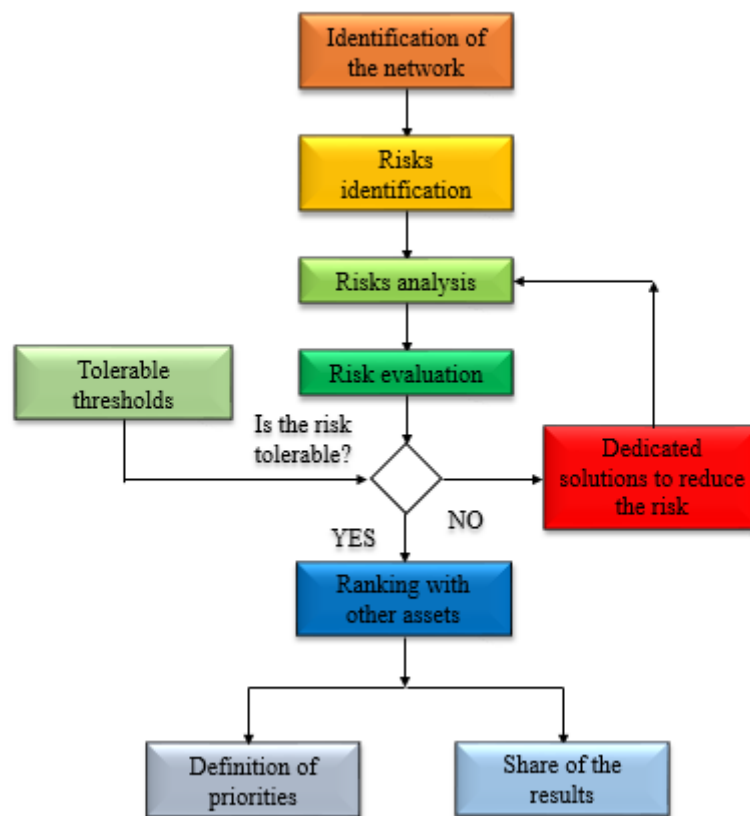


**Figure 108.** Main steps of the proposed method for NG distribution networks integrity management.

As shown in the figure, the first step is the identification of the networks.

In this phase main technical parameters such as operative and boundary conditions have to be identified. The successive step is the recognition of possible treats that can induce a loss of containment and so risks to surrounding people, buildings and environment as a function of the severity of the event. In order to avoid very time consuming analysis, a small number of different conditions have been considered in accordance of decision makers' decision. During the second phase, also possible consequences have to be identified: in the case of flammable substances, several events can verify such as toxic gas dispersion, jet flame, confined or unconfined explosion, fire ball but also economic consequences like the supply interruption. However, in the

method only jet flame and explosion are considered being the most probable events in accordance to historical trends. Nevertheless, other consequences can be easily evaluated.

When possible events have been identified, risk analysis is performed in accordance to one of the method proposed in [51] and results compared with accepted thresholds. In the case that an unacceptable risk is identified, corrective solutions have to be introduced. In order to compare the effectiveness and the improvement, risk analysis has to be performed again. Instead, pipelines are ranked as a function of the calculated risk if this is acceptable. For the scope, risk indexes have to be introduced in order to make simpler the analysis of the obtained results.

It should be noted that ranking can be performed in several ways even if the multi criteria analysis is considered the best appropriate for natural gas distribution where more than one risks indexes can be present.

Finally, results are used by the Top Management in order to:

- *Identify priorities*: the identification of priorities is necessary because of the low available budget;
- *Share and compare results*: low detail information has to be shared with social communities, other stakeholders and Authorities. In this way safety improvements in all gas distribution sector is expected.

In following sections each step of the method is analysed with higher detail.

#### ***4.2 Step I: Identification of the gas distribution network***

The identification of the distribution network is necessary in order to perform a complete risk analysis. Particularly, information about pipeline system and environment are required in order to estimate failure probability and consequences.

Therefore, a distinction between data about pipeline system and environment is proposed as follow:

- *Pipeline system*:
  - ID number;
  - Length;
  - Material;
  - Diameter;
  - Thickness;
  - Burial depth;
  - Operative pressure;
  - Corrosion protection;
  - Presence of other lifelines or railway near to the pipelines;
  - Main accessories such as fittings, joints and valves;
  - Failure frequency (if available in company's database).
- *Environment*:
  - Laying conditions;
  - Type of soil: pH and identification as clay, sand or loam;

- External loads expected to the pipeline;
- Population distribution near to the analysed network.

As it results, data have to be collected from different sources. About pipelines systems main information should be collected from company's database even if very poor information is usually recorded and often less information than the required is available.

About environment, different sources should be considered. About laying conditions and type of soil, data should be taken from local authorities or during interventions by workers. The same could be considered for external loads to be identified in accordance to the position of the pipeline and to the collaboration with other interested parts as for example in case of ground movement, soil settlement or other events that are not usually monitored by the DSOs.

About population density in the area, agreements should be made by public Authority and DSOs in order to constantly update information about the number of people surround the pipelines. In this way overestimation or underestimation of the consequences will result not possible.

#### ***4.2 Step II: Risk identification***

The identification of possible threats due to gas accidents has to be performed in this phase. Particularly, both causes and consequences have to be included being risk defined as the product of the two.

For the scope, several methods can be used even if a different complexity is present (Figure 109). To clarify this point, differences in terms of resources and results are presented:

- *Check list*: one or more recognized expert in the field has to define possible events responsible for system failure. Therefore, based on experience, some limitations should be considered especially in the case of rare events or for those events that are not common to experts. Therefore, in order to correctly perform the check list, a statistical and historic analysis should be made. For the scope, technical reports and literatures have to be analysed in order to not forget any possible events.
- *Preliminary Hazard Analysis (PHA)*: PHA is used in the case of a project characterized by few technical information. Being an inductive methodology, PHA gives oversimplified results when applied to very complex systems such as gas distribution networks. Furthermore, a great amount of resources is required in the case of big assets even if the obtained results do not differ so much respect to a simple check list.
- *HAZard and OPerability study (HAZOP)*: HAZOP identifies possible failure modes of a system, a process or a procedure. However, because of it starts from unwanted outcomes and deviation from intended ones, an oversimplification seems to be achieved in the case of NG distribution networks. In fact, as outlined in previous chapter, thousands of components are present in the asset so it will result very difficult to perform the HAZOP. Furthermore, very few information is available about the boundary conditions in which the devices are operated. For these reasons, HAZOP analysis seems to

be more useful if applied to a part of the system such as, for example, a specific plant installed in the distribution network in detailed analysis.

- *Failure Modes and Effects Analysis (FMEA) and Failure Modes and Effects and Criticality Analysis (FMECA)*: both techniques are used to evaluate failure modes of a components, system or process and to rank the failures as a function of their criticality. Furthermore, information about the mechanism and effects of failures can be obtained. However, it should be noted that these methods require a high level of detail in the input data in order to perform a meaningful analysis; consequently, it is not suggested their use in this step of the method but only in detailed analysis.

For the scope of risk assessment in NG distribution networks, check list seems to be the most appropriate technique because of no detailed information and quantitative outputs are required. Furthermore, check lists can be simple performed company’s workers and easily updated during the time thanks to experience.

### Risk identification

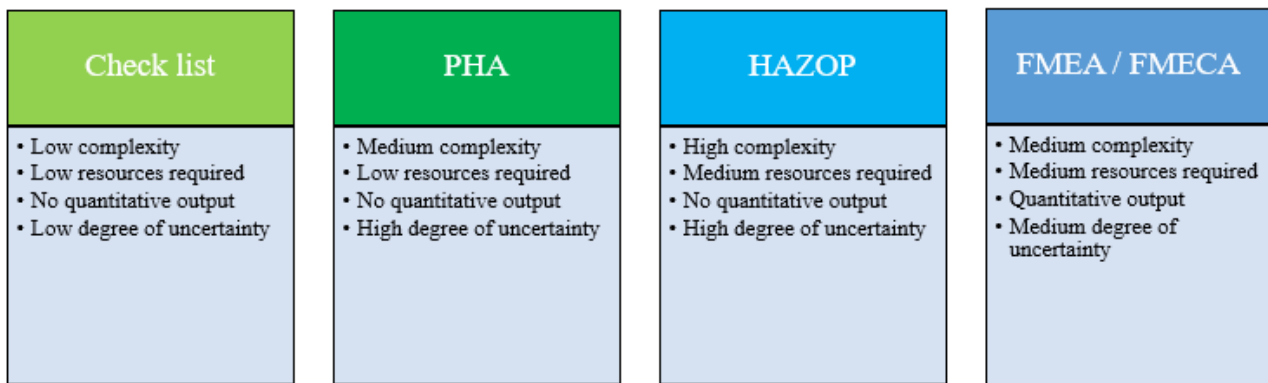


Figure 109. Techniques considered for risk evaluation.

That is, the definition of possible failure causes is proposed in accordance to those presented in previous chapter. A preliminary division is proposed as a function of material and time factors as proposed in [64], where only steel pipelines are however considered (Figure 110).

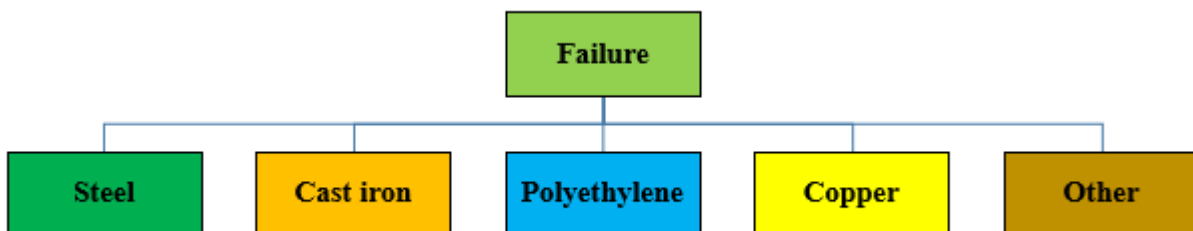


Figure 110. Proposed division as a function of pipeline’s material.

For each material, possible failure causes are analysed and reported in a dedicated check list that should be controlled by experts (Figure 111). In the case of copper, no time dependent phenomena have been considered. In fact, time degradation phenomena (such as the chemical interaction with odorant) because of no accidents have been found in literature.

The scope of this preliminary check list is to identify all possible causes of failures in order to take better decisions in the case that corrective actions are required or to calculate probability of failure.

Steel	Cast iron	Polyethylene	Copper
<ul style="list-style-type: none"> <li>• <b>Time dependent:</b></li> <li>• Corrosion</li> <li>• <b>Stable:</b></li> <li>• Manufacturing defects</li> <li>• Welding or installation defects</li> <li>• Equipment failure</li> <li>• <b>Time – Independent:</b></li> <li>• Third party / mechanical damage</li> <li>• Incorrect procedure</li> <li>• Weather related</li> <li>• External forces</li> <li>• Earth movement</li> </ul>	<ul style="list-style-type: none"> <li>• <b>Time dependent:</b></li> <li>• Corrosion</li> <li>• <b>Stable:</b></li> <li>• Manufacturing defects</li> <li>• Welding or installation defects</li> <li>• Equipment failure</li> <li>• <b>Time – Independent:</b></li> <li>• Third party / mechanical damage</li> <li>• Incorrect procedure</li> <li>• Weather related</li> <li>• External forces</li> <li>• Earth movement</li> </ul>	<ul style="list-style-type: none"> <li>• <b>Time dependent:</b></li> <li>• Slow Crack Growth (SCG)</li> <li>• Rapid Crack Growth</li> <li>• <b>Stable:</b></li> <li>• Manufacturing defects</li> <li>• Welding or installation defects</li> <li>• Equipment failure</li> <li>• <b>Time – Independent:</b></li> <li>• Third party / mechanical damage</li> <li>• Incorrect procedure</li> <li>• Weather related</li> <li>• External forces</li> <li>• Earth movement</li> </ul>	<ul style="list-style-type: none"> <li>• <b>Stable:</b></li> <li>• Manufacturing defects</li> <li>• Welding or installation defects</li> <li>• Equipment failure</li> <li>• <b>Time – Independent:</b></li> <li>• Third party / mechanical damage</li> <li>• Incorrect procedure</li> <li>• Weather related</li> <li>• External forces</li> <li>• Earth movement</li> </ul>

Figure 111. Main failure cause as function of the material.

Regarding consequences several methods are available in literature as reported in previous chapter even if the use of Probit function is suggested. That is, they have to be clearly defined at the beginning of the process. As reported in several works gas release can be responsible of jet fire, explosion, toxic gas dispersion, fire ball and flash fire as shown in Figure 112 even if only jet fire and explosion should be considered for the application in NG distribution networks.

### Proposed check list

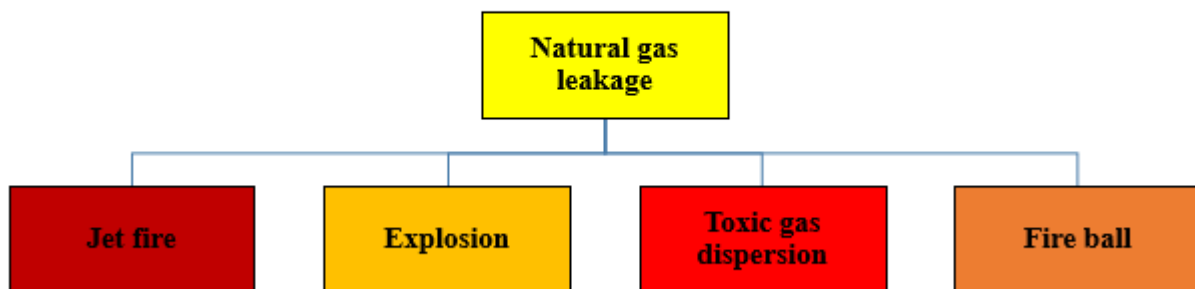


Figure 112. Possible consequences in the case of NG leakage from a distribution network.

When possible causes and consequences have been identified, a simple way to schematically represent them should be considered in order to make easier the verification of possible errors before to proceed in the risk analysis.

For the scope, Bow Tie analysis can be used displaying a range of possible causes and consequences. In fact, respect Event Tree that considers a top event and failure paths, in bow tie analysis both causes and

consequences are contemporary displayed. Furthermore, escalation factors such as controls, recovery solutions can be immediately applied to improve the information about the network.

Therefore risk identification can be summarized as made in Figure 113.

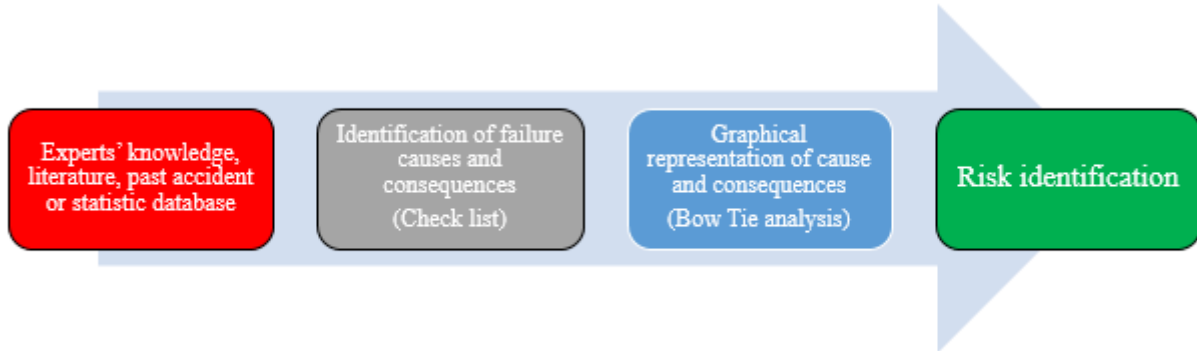


**Figure 113.** Flowchart for risk evaluation step.

### 4.3 Step III: Risk analysis

Risk analysis is the most important phase of the model because of the calculated results depend on the assumptions and the hypothesis considered.

Risk R is defined as the product between the probability P and the consequences C due to an accident:

$$R = P \times C \quad (4-1)$$

In case of pipeline failure, different consequences are possible as a function of the distance from the release point. Individual risk (IR) at the position (x,y) for NG distribution is calculated in accordance to [73,147] with the following:

$$IR = \sum_i \sum_{scenario} \int_{-l}^{+l} \varphi_i P_i(x, y) dl \quad (4-2)$$

Where  $\varphi_i$  is the failure rate associated [Acc/km y] for the identified treat i-th,  $P_i$  is the probability associated to the scenario and  $l_+$  and  $l_-$  are the ends of the pipeline in which an accident pose hazard to the specified location (x,y). In the case of NG distribution accidents jet fire and explosion can occur.

Assuming a constant failure rate along the pipeline, the following simplification is made:

$$IR = \sum_i \varphi_i \sum_{scenario} \int_{-l}^{+l} P_i(x, y) dl \quad (4-3)$$

Where the integral of equation (4-2) can be written as:

$$IR = \sum_i \varphi_i \sum_{scenario} \left( l_{i,100-99} \times \frac{\int_0^{r_{i,100-99}} P_i(x,y) dr}{\int_0^{r_{i,100-99}} dr} + l_{i,99-50} \times \frac{\int_{r_{i,100-99}}^{r_{i,99-50}} P_i(x,y) dr}{\int_{r_{i,100-99}}^{r_{i,99-50}} dr} + l_{i,50-1} \times \frac{\int_{r_{i,99-50}}^{r_{i,50-1}} P_i(x,y) dr}{\int_{r_{i,99-50}}^{r_{i,50-1}} dr} \right) \quad (4-4)$$

The following equations have been used:

$$l_{i,100-99} = Re \left( 2(r_{i,99}^2 - h^2)^{0.5} \right) \quad (4-5)$$

$$l_{i,99-50} = Re \left( 2(r_{i,50}^2 - h^2)^{0.5} \right) \quad (4-6)$$

$$l_{i,50-1} = Re \left( 2(r_{i,1}^2 - h^2)^{0.5} \right) \quad (4-7)$$

Where  $h$  is the distance between the source point and the target, [m]. The radius  $r_{i,j}$  [m] represents the area around the source point in which the fatality probability is higher than  $j$ . For its calculation, the probability  $P_i$  is calculated through the Probit function, reported in previous chapter for jet fire (Eq. 3-64) and explosion (Eq. 3-69).

- Jet fire (a value equal to 1 have been considered for transmissivity for conservative approach, while the total exposure time  $t$  is assumed equal to 30 sec. Also in this case conservative results are assured).

$$P_{jet,99\%} = -14.9 + 2.56 \times \ln \left( \frac{t \times E_{th,jet}^{\frac{3}{4}}}{10^4} \right) = 7.33 \rightarrow r_{jet,99} = 3.891\sqrt{G} \quad (4-8)$$

$$P_{jet,50\%} = -14.9 + 2.56 \times \ln \left( \frac{t \times E_{th,jet}^{\frac{3}{4}}}{10^4} \right) = 5.00 \rightarrow r_{jet,50} = 5.498\sqrt{G} \quad (4-9)$$

$$Y_{jet,1\%} = -14.9 + 2.56 \times \ln \left( \frac{t \times E_{th,jet}^{\frac{3}{4}}}{10^4} \right) = 2.67 \rightarrow r_{jet,50-1} = 7.767\sqrt{G} \quad (4-10)$$

Where  $G$  is the gas flowrate in [kg/s].

- Explosion (an explosion efficiency equal to 0.4 is assumed and a  $K_{TNT}$  equal to 4437 kJ/kg).

$$P_{exp,99\%} = -77.1 + 6.9 \times \ln(P_0) = 7.33 \rightarrow r_{exp,99} = 3.795(G \times t_{acc})^{\frac{1}{3}} \quad (4-11)$$

$$P_{exp,50\%} = -77.1 + 6.9 \times \ln(P_0) = 5.00 \rightarrow r_{exp,50} = 4.422(G \times t_{acc})^{\frac{1}{3}} \quad (4-12)$$

$$P_{exp,1\%} = -77.1 + 6.9 \times \ln(P_0) = 2.67 \rightarrow r_{exp,1} = 5.189(G \times t_{acc})^{\frac{1}{3}} \quad (4-13)$$

Where  $G$  is the gas flowrate [kg/s] and  $t_{acc}$  is the accumulation time in [s].

It should be noted that a time during gas accumulates is required: for the scope the average time required to the rescue teams to arrive in site after an emergency call is considered as reported by ARERA.

As shown, gas leakage has to be calculated. For the scope, the method implemented in Matlab and shown in previous chapter has been used.

The average fatality probability can be calculated representing the fatality probability as a function of  $r \times G^{-0.5}$  and  $r \times M^{-1/3}$  respectively for jet fire and explosion:

- Jet fire:

$$\frac{\int_0^{r_{i,100-99}} P_{jet}(x, y) dr}{\int_0^{r_{i,100-99}} dr} = 1 \quad (4-14)$$

$$\frac{\int_{r_{i,100-99}}^{r_{i,99-50}} P_{jet}(x, y) dr}{\int_{r_{i,100-99}}^{r_{i,99-50}} dr} = 0.805 \quad (4-15)$$

$$\frac{\int_{r_{i,99-50}}^{r_{i,50-1}} P_{jet}(x, y) dr}{\int_{r_{i,99-50}}^{r_{i,50-1}} dr} = 0.172 \quad (4-16)$$

- Explosion:

$$\frac{\int_0^{r_{i,100-99}} P_{exp}(x, y) dr}{\int_0^{r_{i,100-99}} dr} = 1 \quad (4-17)$$

$$\frac{\int_{r_{i,100-99}}^{r_{i,99-50}} P_{exp}(x, y) dr}{\int_{r_{i,100-99}}^{r_{i,99-50}} dr} = 0.83 \quad (4-18)$$

$$\frac{\int_{r_{i,99-50}}^{r_{i,50-1}} P_{exp}(x, y) dr}{\int_{r_{i,99-50}}^{r_{i,50-1}} dr} = 0.17 \quad (4-19)$$

Therefore, the individual risk for jet fire and explosion result:

$$IR_{jet\ flame} = \sum_i \varphi_i (l_{jet,100-99} + l_{jet,99-50} \times 0.805 + l_{jet,50-1} \times 0.172) \quad (4-20)$$

$$IR_{explosion} = \sum_i \varphi_i (l_{exp,100-99} + l_{exp,99-50} \times 0.83 + l_{exp,50-1} \times 0.17) \quad (4-21)$$

Considering the event tree proposed in Figure 102, four different scenarios (A, B, C and D) are possible in the case of gas leakage. Therefore, the total individual risk has to be calculated considering all the four. In order to weight them, percentages of occurrence are considered:

$$IR_{TOT} = \sum_i \varphi_i (w_A IR_A + w_B IR_B + w_C IR_C) \quad (4-22)$$

Where the following applies:

$$IR_A = IR_{jet\ flame} \quad (4-23)$$

$$IR_B = IR_{jet\ flame} + IR_{explosion} \quad (4-24)$$

$$IR_C = IR_{explosion} \quad (4-25)$$

The scenario D has not been considered because of no consequences in terms of jet fire and explosion are present.

For each pipelines it is possible to calculate the IR at the distance h from the pipeline with the reported equation and report it easily in a risk map easily designed in digital systems as GIS ones. In order to evaluate societal risk (SR) is necessary to know the existing population density around the pipeline:

$$SR = \int \rho_p P_i dA \quad (4-26)$$

Where  $A_i$  is the area [ $\text{km}^2$ ] associated to the hazard of the incident scenario  $i$  and  $\rho_p$  is the population density [people /  $\text{km}^2$ ].

In Figure 114 a schematic of the described risk analysis is reported.

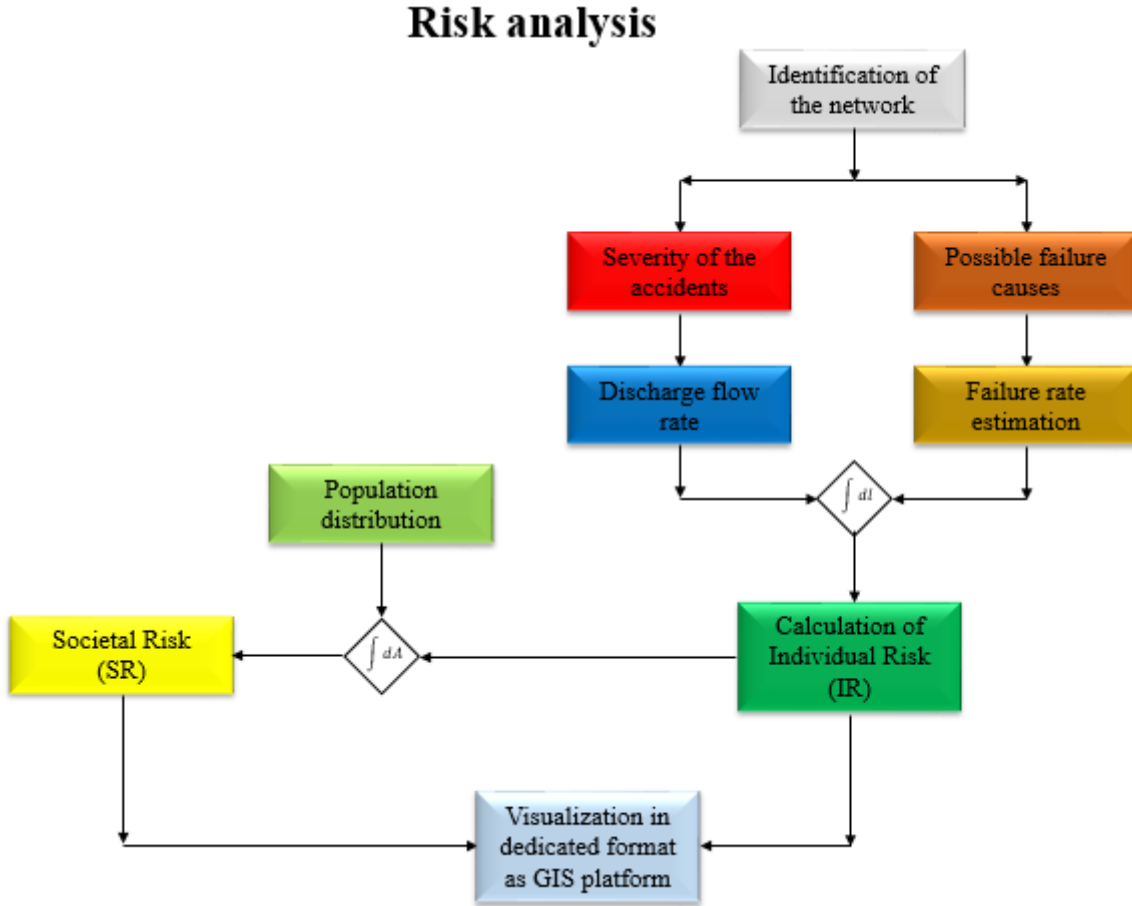


**Figure 114.** Risk analysis flowchart.

The same analysis can be performed also to evaluate damages to buildings and structures. In this case the distance within a damage occurs is defined. Overpressure values are taken by [140]:

- *Partial collapse of walls:*

$$P_0 = 13.8 \text{ kPa} \rightarrow r_{collapse} = 1.32(G \times t_{acc})^{\frac{1}{3}} \quad (4-27)$$

- *Minor structural damages:*

$$P_0 = 2.76 \text{ kPa} \rightarrow r_{minor \text{ damages}} = 3.3(G \times t_{acc})^{\frac{1}{3}} \quad (4-28)$$

- *Safe distance, 10% of the wall broken:*

$$P_0 = 2.07 \text{ kPa} \rightarrow r_{safe} = 2.97(G \times t_{acc})^{\frac{1}{3}} \quad (4-29)$$

Introducing building distribution economic damages in case of NG leakage can be estimated through the reported equations.

No evaluations are still made about failure rate estimation. Different ways can be followed for the scope:

- *Application of physical models for the estimate failure probability.* As reported several works are present in literature that propose models to estimate pipeline failure probability. For the scope, Monte Carlo method or First Order Reliability Method (FORM) are suggested in order to take into account the uncertainty and statistical distribution of input parameters. Nevertheless, many issues seem to reduce their applicability to NG distribution networks such as:
  - Only few of the events that can occur in NG distribution networks are described by mathematical models. For example, no description of failure occurring in fittings or joints are present while a lot of research about external corrosion is present;
  - A high grade of uncertainty of the obtained results is present because of the specific boundary conditions in which the system is installed that usually differ from that used to validate models;
- *Use of data from open database:* input failure data from open database can be used to improve the analysis, even if the following have to be taken in mind:
  - The systems from which data are taken should be a NG distribution network. Several studies in fact use data from other type of systems resulting in misleading results;
  - Boundary conditions can be slightly different from the specific conditions such as technical requirements. Therefore, attention in the analysis of the results has to be given by decision makers.
- *Use of data from a dedicated database created within the company.* The creation of a dedicated database is the best option ensuring a high value added to risk assessment. Furthermore, a continuous update of risk quantification is possible (Figure 115).

### Risk analysis with updated information

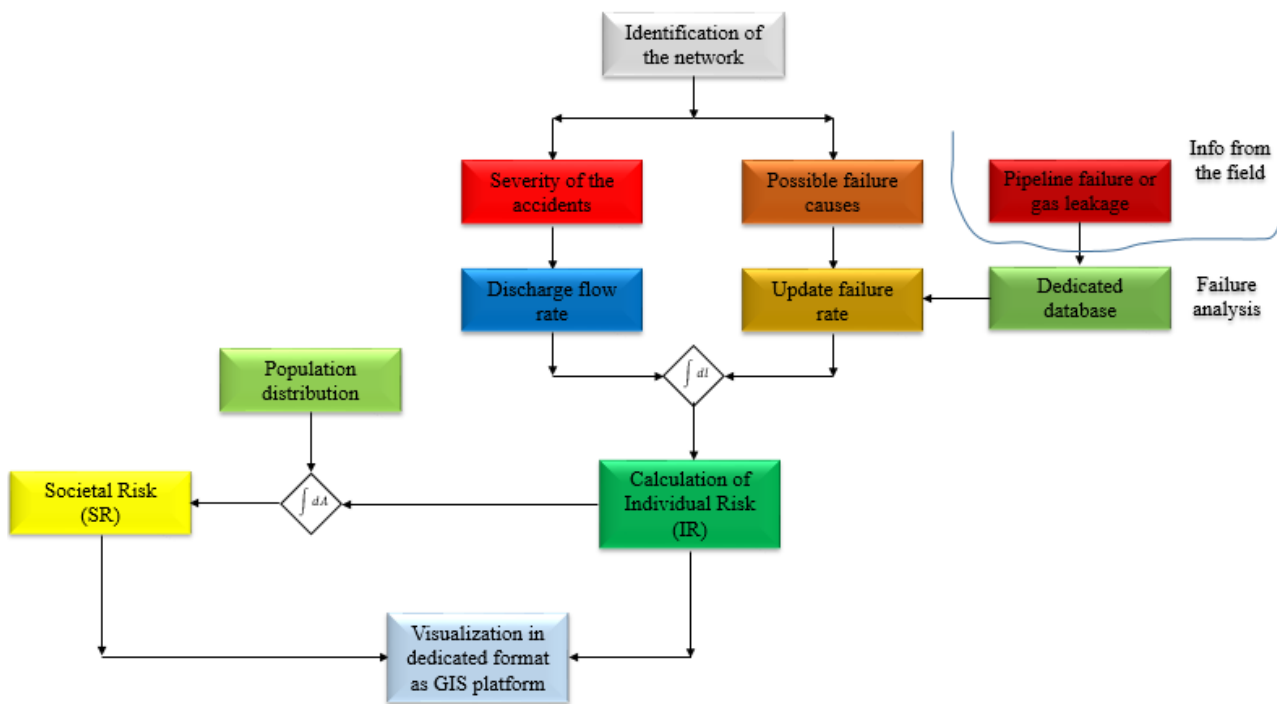


**Figure 115.** Flowchart of risk analysis in the case of continuous improvements thanks to the presence of a dedicated database.

In fact, even if a greater amount of resources is required respect to other two options, better information will be available. However, it should be noted that, failure probability of rare events like due to soil movement should be calculated through dedicated mathematical models as reported in previous paragraph. Also information about gas leakage should be recorded. In fact, these events should be considered by DSOs as an opportunity to improve know-how and to have more reliable information in order to identify abnormal trends. “Root Cause” analysis seems to be the best method for failure analysis because of it “attempts to identify the root or original causes instead of dealing only with immediately obvious symptoms”. However, also other methods can be considered for the scope.

#### ***4.4 Step IV: Risk evaluation***

Risk evaluation is necessary to understand risks, and to provide an input to decisions makers about where and how risks have to be treated. For the scope qualitative, semi-quantitative or quantitative method can be applied with the attention to identify thresholds.

It should be noted that no standardized and international accepted rules exist about the acceptability of a risk even if different philosophies exist for population living in the vicinity of hazardous facilities as reported by [148]:

- A risk based criteria where safety goal is specified and not the means of achieving it (UK);
- Risk based criteria where a prescribed maximum level of risk is used for risk control (the Netherland, Hungary, Czech Republic) and some form of risk reduction may be specified but not necessarily implemented;
- Consequence based criteria where the prescribed level of impact is used for control (France) or no risk is allowed outside the boundary of the facility (Germany)

Being gas distribution different respect to a hazardous facility, some considerations should be made defining acceptable limits. For the scope, the following limits have been considered:

- $R > 10^{-4}$  fatality/year. Not acceptable risk. DSO has to immediately intervene to reduce the risk to public safety;
- $R$  between  $[10^{-4}; 10^{-6}]$  fatality/year. As Low As Reasonable Practicable (ALARP) condition. Interventions or modification should be performed by the DSO to reduce the risk to population only if the complexity and the cost of the corrective measure are extremely greater than the obtained improvements;
- $R > 10^{-6}$  fatality/year. Acceptable conditions. The risk induced to surrounding people is acceptable and so no improvements are required.

Because of the complexity of the topic, however, it is suggested that NG DSOs and Authorities evaluate together the proposed levels of risk. In fact, for the success of safety culture that all interested stakeholders agree about limits of acceptability and so strategies to reach them.

## 4.5 Step V: Risk ranking, identification of the priorities and share of the results

### 4.5.1 Risk ranking and identification of the priorities

At the conclusion of the procedure a risk ranking is required in order to evaluate issues that are present in the network. For each j-th pipeline of the network the following results have to be obtained in previous steps:

- Pipeline accident failure rate,  $F_j$  [failure/year].
- Individual risk maps,  $IR$  [fatality / year];
- Societal risk,  $SR$  [fatality / year].

In order to prepare a list of priorities the following indexes have to be calculated:

- Normalized accident failure rate for the pipeline j-th,  $N_{1,j}$ :

$$N_{1,j} = \frac{F_j - \min_j F_j}{\max_j F_j - \min_j F_j} \quad (4-30)$$

- Normalized individual risk for the pipeline j-th at a certain distance from the pipeline,  $N_{2,j}$ :

$$N_{2,j} = \frac{IR_j - \min_j IR_j}{\max_j IR_j - \min_j IR_j} \quad (4-31)$$

- Normalized societal risk for the pipeline j-th at a certain distance from the pipeline,  $N_{3,j}$ :

$$N_{2,j} = \frac{SR_j - \min_j SR_j}{\max_j SR_j - \min_j SR_j} \quad (4-32)$$

Each normalized factor assumes a value between 0 and 1. Results can be divided in the following five classes if a matrix representation is proposed: [0, 0.2[, [0.2, 0.4[, [0.4, 0.6[, [0.6, 0.8[, [0.8, 1].

### 4.5.2 Share of the results

A consequence – failure rate matrix can be used to share the results to Authority and to customers. That is, the design of the risk matrix has to be the clearest as possible in order to be unambiguously. For the scope a risk matrix has been designed considering normalized value as reported in Figure 116. In the figure for each cell identified, a rating is defined to give priorities.

Consequences	5	II	III	IV	V	V
	4	II	III	III	IV	V
	3	I	II	III	IV	V
	2	I	II	III	III	V
	1	I	I	II	III	IV
		1	2	3	4	5
		Total failure rate				

**Figure 116.** Risk matrix considering probability and consequences calculated for each pipeline of the network.

For the scope also dedicated F-n curve for each section of pipeline can be constructed reporting the number of fatalities and the probability of occurrence. For NG distribution networks, the calculation can be graphically made superimposing the impact zone onto the population density and evaluating the number of fatality. F-n curves can be finally constructed considering cumulative frequency and plotted in dedicated diagrams that can be shown to Authority or other interested stakeholders.

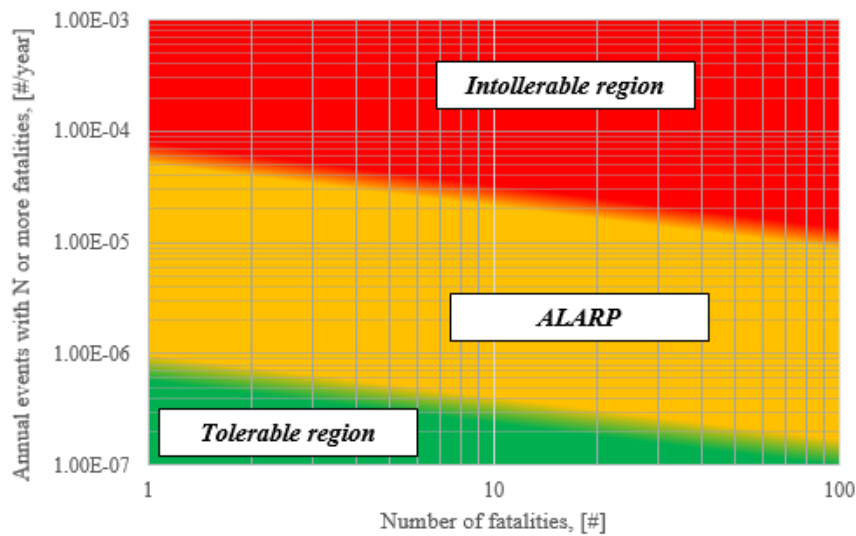


**Figure 117.** Proposed F-n curve to report specific risk for each pipeline of the network.

Furthermore, the following parameters are proposed to give a synthetized information about the network:

- Network average failure rate,  $\bar{R}$  [leak/km]:

$$\bar{R} = \frac{\sum_{j=1}^N R_j}{N} \quad (4-33)$$

Where  $R_j$  is the failure rate [leak/km] for the j-th pipeline, while N is the total number of pipeline in the analysed network.

- Failure rate standard deviation,  $\sigma_R$  [leak/km]:

$$\sigma_R = \sqrt{\frac{\sum_{j=1}^M (R_j - \bar{R})^2}{N}} \quad (4-34)$$

- *Network average societal risk,  $\overline{SR}$  [fatality/year]:*

$$\overline{SR} = \frac{\sum_{j=1}^N SR_j}{N} \quad (4-35)$$

- *Societal risk standard deviation,  $\sigma_{SR}$  [fatality/year]:*

$$\sigma_{SR} = \sqrt{\frac{\sum_{j=1}^N (SR_j - \overline{SR})^2}{N}} \quad (4-36)$$

The lowest are the parameters the safest is the operated network.

As introduced, a case study is proposed to show the potentiality of the method in next paragraph.

## ***4.6 Application of the proposed risk assessment method to a real case study***

In order to demonstrate the potentiality of the proposed method, a real case study has been considered; therefore, the risk assessment methodology has been introduced distinguishing the different steps proposed.

### ***4.6.1 Analysis of the NG distribution network***

A NG distribution network located in an area of 1 km x 1 km in Central Italy has been considered for the application of the model as shown in Figure 118. The network consists of almost 27 km of pipelines: of these 3.2 km are operated at a MOP equal to 5 barg while the other are operated at a MOP equal to 0.4 barg.



**Figure 118.** NG distribution network considered for the application of the method.

About materials the 66.3% of the total is made of cast iron, followed by steel (14.0%) and polyethylene (7.9%), while the remaining part is constituted by old materials especially present in low pressure service lines and not allowed in the case of new installation (Figure 119). Steel is the only material implemented in the systems characterized by a MOP equal to 5 barg (= 3.2 km), while other materials are present in the connection to final

customers. Furthermore, a low percentage of polyethylene is present in the analysed network even if higher performances have been usually identified for the latest generations.

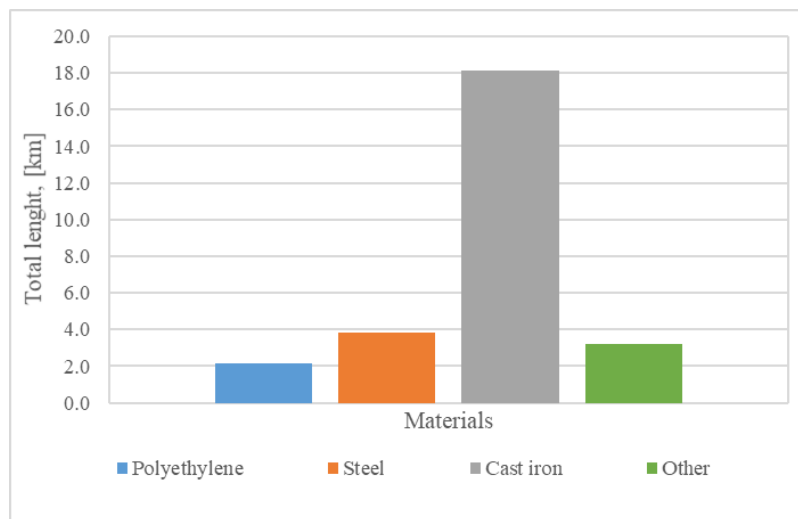


**Figure 119.** Materials installed in the analysed network.

A very poor characterization of the material is however present at the moment in the existing database because of no more detailed data are available such as manufacturer and type in accordance to those presented in chapter 2. Furthermore, no information about thickness and burial depth is present in available database. Consequently, it has been assumed that these are in accordance with the minimum requirements defined in technical standards. It is therefore suggested to NG company to improve the identification of their system in accordance to available standards; for the scope QR codes with required information should be applied to the system. These records can also be used in addition to possible surface loads in order to rank pipelines in accordance to expected loads and offered resistance.

About corrosion, the 78.9% of steel pipes is cathodically protected while 19.6% is not protected. For the remaining part no confirmed information is present in the database. It is interesting to note that no data are present about the presence of coating so further analysis is not possible. Because of the high percentage of cast iron, particular attention has to be given to graphitization phenomenon; so, maintenance engineers have to be carefully evaluate failure trend in cast iron in order to identify the degradation of the system in specific areas of the network. As shown previously, in fact, graphitization is a localized phenomenon that depends on the specific conditions in which the pipeline is installed. For the scope, environmental data have to be taken from local database such as those available from the ARPAE where information about the presence of groundwater, the presence of ground movement or subsidence can be found. In the analysed case, no groundwater is present at the typical burial depth, such as ground movement. A sinking rate equal to 5 mm/y has been used to characterize subsidence in the area.

About stray current generator, GIS has to be used. For the scope, only railway has been considered. As reported in the figure, a railway line is present in the right corner at a distance lower than 150 m respect to some of the pipelines installed in the network.

About failure probability, some preliminary data are present in proprietary documents even if no information about service lines is present. As reported in Figure 120 failure rate can be evaluated for the specific network. From the analysis of the figure, it is interesting to note that the north-east area is characterized by a higher failure rate.

For the scope, the age and the material of the network have been analysed in order to identify possible trends or correlation in Figure 121 and in Figure 122. Even if in some cases older networks are responsible of higher leakage rate, however, it seems that more detailed considerations have to be made such as existing loads, installation procedures and so on that can be made only thanks to a dedicated database. For example, it seems that cast iron pipelines installed outside the street are characterized by higher failure rate. This can be explained by the higher probability to present graphitization: however, because of the number of pipelines it is not possible to proceed to a manually investigation that it would instead possible in the case that database have contained this information.



**Figure 120.** Leakage rate recorded in the existing database. Only qualitative information is given in order to protect DSOs' privacy.



**Figure 121.** Characterization of the network as a function of the age.



**Figure 122.** Characterization of the network as a function of the material.

#### **4.6.2 Risk identification**

Even if possible causes of failure are the same as described chapter 3, failure rates reported in Company's database do not distinguish between different causes identifying a total value representative for all possible phenomena responsible for failure. In the risk analysis, this value is considered because of it is more representative of existing conditions. However, these data have to be corrected in order to evaluate the probability that a gas accident occurs following a leakage. For the scope, a mean value equal to  $1.9 \times 10^{-4}$  accident/leak with a standard deviation equal to  $4.5 \times 10^{-9}$  accident/leak from 2010 has been estimated considering the data recorded in the American database. It should be noted that the available data are not update from 5 years. Therefore, risk analysis should be carefully performed. Nevertheless, the importance of a continuously updated analysis of failure rate is evident from Figure 120 where failure rate is reported with different colours. In order to protect the privacy of gas company no values are reported even if yellow colour represents pipeline characterized by a low number of leakage in the year while red is used for pipelines characterized by a high number of leakage point. Because of no efforts is made at the moment to identify the probable cause of failure it is very difficult to implement dedicated measures such as instrumentation in order to ensure a preventive maintenance.

In some cases, it is also possible that DSOs have no data about failure rate. In this case, the accident failure rate proposed in previous chapters should be considered. If different values are used explanations should be given.

- Corrosion: different values have been considered for steel and cast iron pipelines. No corrosion is assumed for polyethylene. Values in accordance to Table 41 and Table 42 have been used;
- Equipment and material failure: values in accordance to Table 51 have been used;
- Excavation damage: values in accordance to Table 59 have been used;
- Incorrect operation: values in accordance to Table 62 have been used;
- Natural forces: values in accordance to Table 65 have been used.

Different considerations, instead, have to be made for consequences where jet fire and explosion are considered as possible outcomes. As shown in previous paragraphs, gas leak flowrate has to be carefully calculated in order to quantify possible consequences for each pipeline of the network. For the scope, the model proposed by [145] has been implemented in Matlab in order to calculate gas flowrate in the case of total rupture, small hole (assumed equal to 30% of the external diameter) and very small hole (5% of the external diameter). Results are reported in Figure 123, Figure 124 and Figure 125 respectively. In the three cases analysed, gas leakage increases as expected with internal diameter and pressure. The results obtained can be used for different scopes such as the identification of hazardous distances within which very severe consequences can occur. For example, considering a DN 100 pipe operated at a pressure of 5 barg, 1 Nm<sup>3</sup>/s of escaping gas occurs in the case of total rupture.

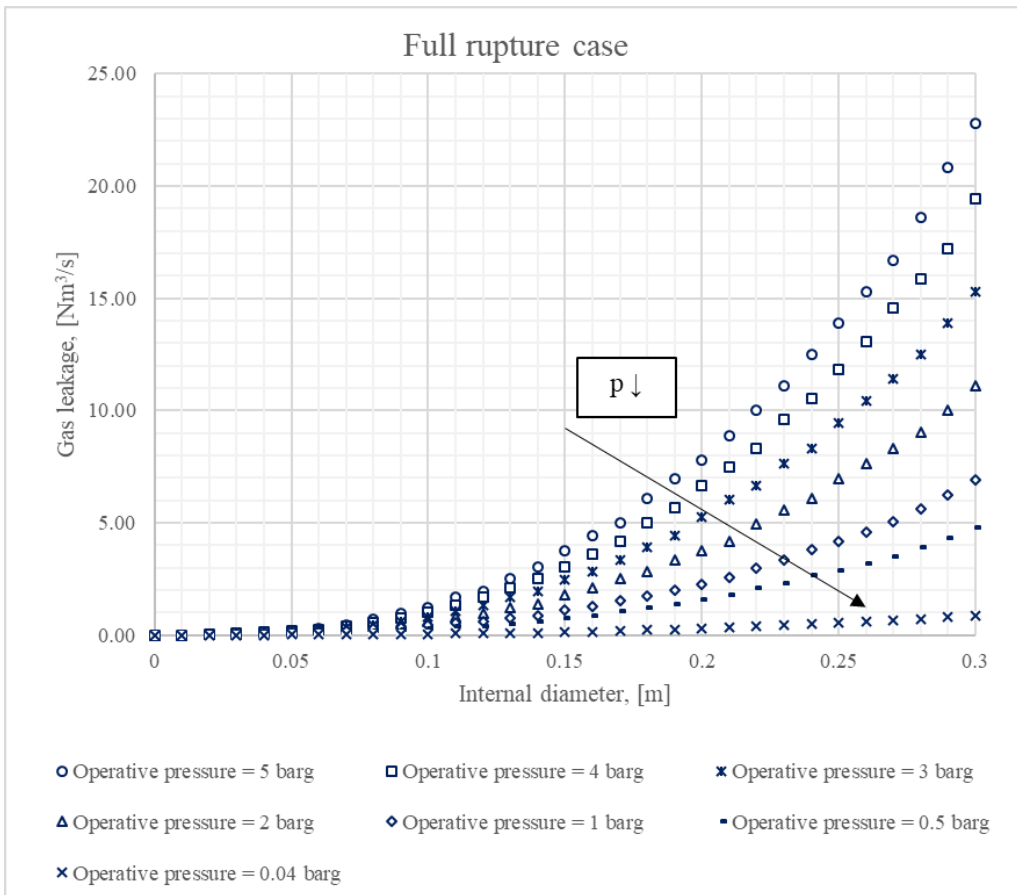


**Figure 123.** NG leaks in case of pipeline rupture as a function of pressure and internal diameter.

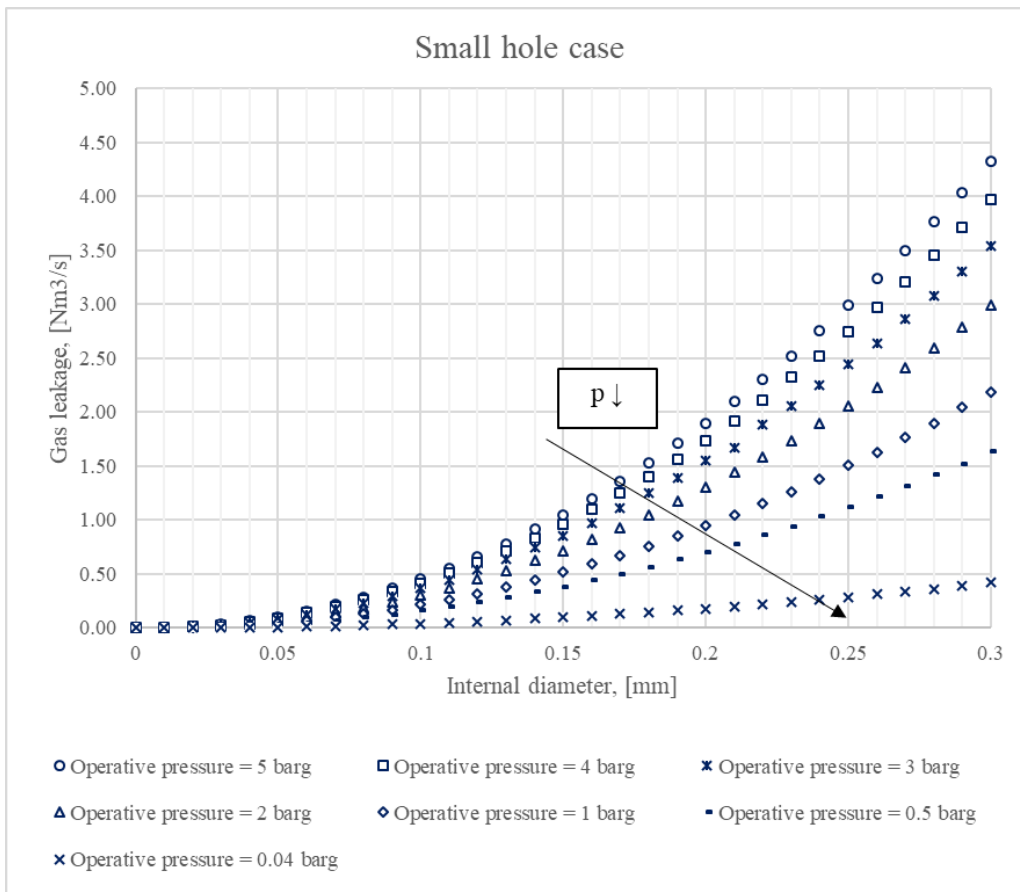


**Figure 124.** NG leaks in case of small hole as a function of the diameter of the pipe and of operative pressure.

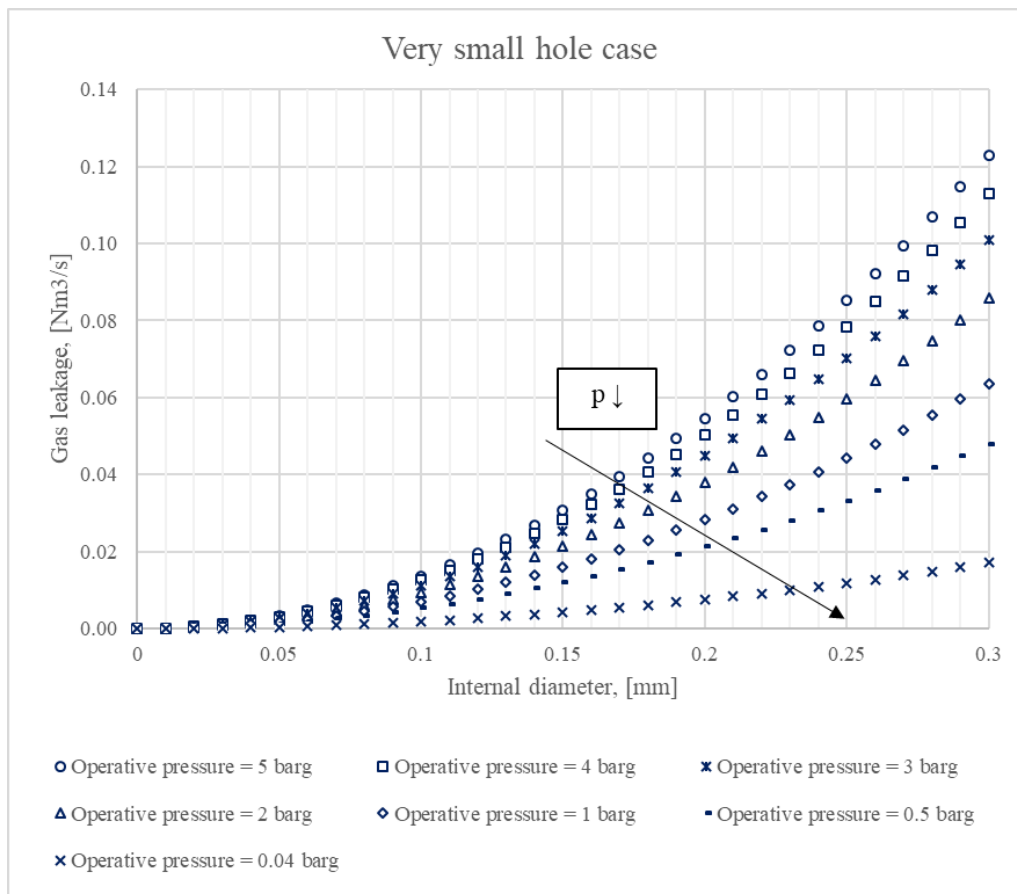


**Figure 125.** NG leaks in case of very small hole as a function of the diameter of the pipe and of operative pressure.

Considering that 40 minutes are usually required to rescue team to reach the area, a total mass of 2880 kg of methane escaped from the gas system that are equivalent to 7230 kg of TNT (from equation 3-70). A safe area of radius 80 m has to be identified in order to avoid treat to people. Therefore, the tool can be used to identify the development of the hazardous area as a function of time as reported in Figure 126.

For all the analysed case, operative pressure does not influence the quantity of escaping gas for diameter lower than DN50. Therefore, a negligible error is committed not considering the influence of pressure for smaller diameters.

Respect to that reported in Figure 126 where only explosion is considered, several accidental scenarios can occur as described in Table 79. As a function of the population density different probability can be considered for the identified scenario: however, for the proposed case, Class 3 location has been considered.

That is, applying equation from 3-62 to 3-72, it is possible to calculate the consequences in case of failure for different leakage rates both in case of jet fire and explosion.

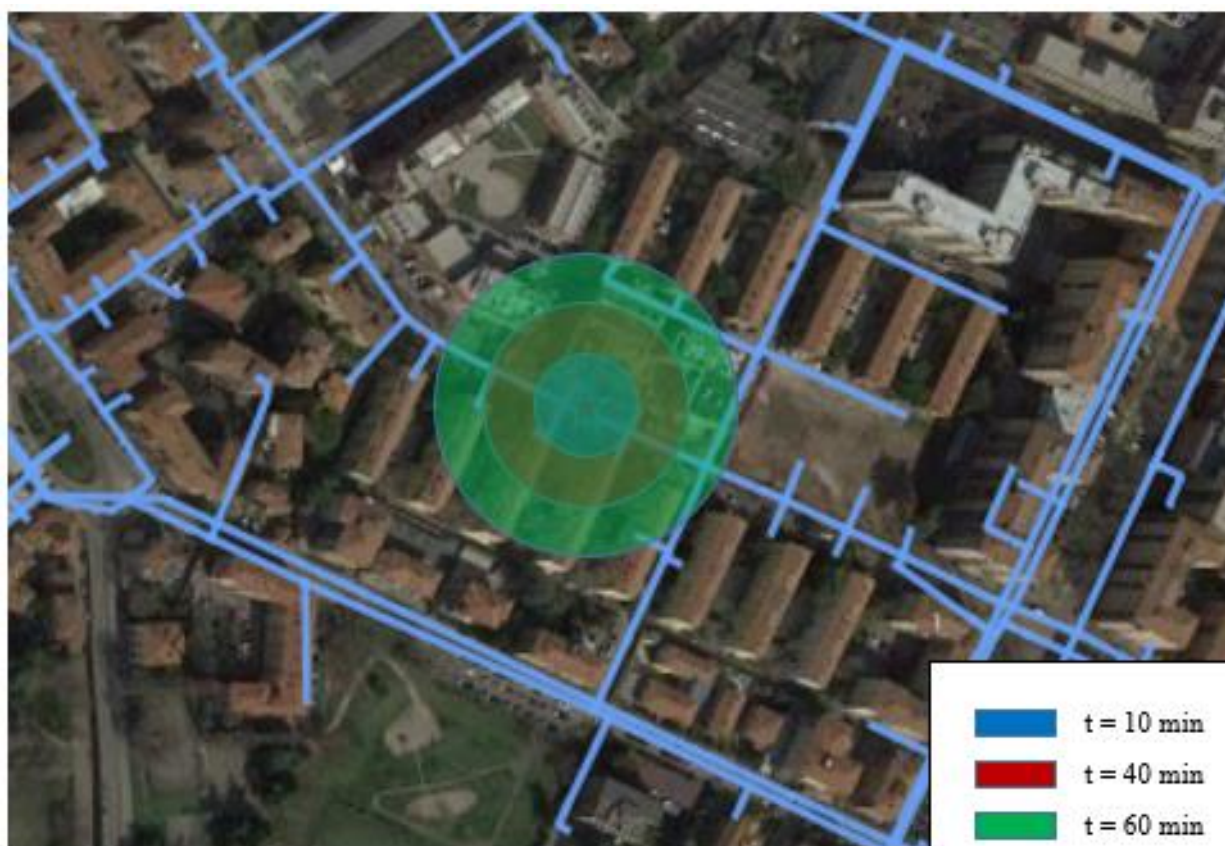


**Figure 126.** Development of the hazardous area as a function of the time from the beginning of gas release. A case for a DN 100 gas pipe is reported.

#### **4.6.3 Risk analysis**

The introduced equations have been applied for the analysed gas network considering three different possible conditions: full rupture, small hole and very small hole. In order to show the potential of the method only full rupture case is shown. Equation from 4-2 to 4-26 have to be used in order to calculate for each pipeline the individual risk (IR) at different distance from the pipeline as reported in Figure 127 for the distance of 20 m. It should immediately be noted that the proposed method ensures the identification of a quantitative value for the IR in different scenario. However, because of it is difficult to correctly evaluate so low percentage, a comparative and not absolutely analysis is suggested.

Furthermore, in order to have a more detailed result, societal risk (SR) has to be calculated. This is due to the fact that, while IR does not take into account of population density in the area, SR does. Two different pipelines with the same IR have been considered (circled in red in Figure 127).

The two sections of the gas network are reported in Figure 127 and in Figure 128. In the left case, the SR has been calculated equal to 0.0321 fatality/year results while in the second case a value equal to 0.0578 fatality/year has been calculated. From the analysis therefore the pipeline in the right side is more hazardous than that in the left side. It should be noted that the other considerations can be made in order to prioritize interventions such as those considering economic damages, environmental impact and so on. In this case, different objectives are identified by the Top Management resulting therefore necessary to use a multi-criteria approach.

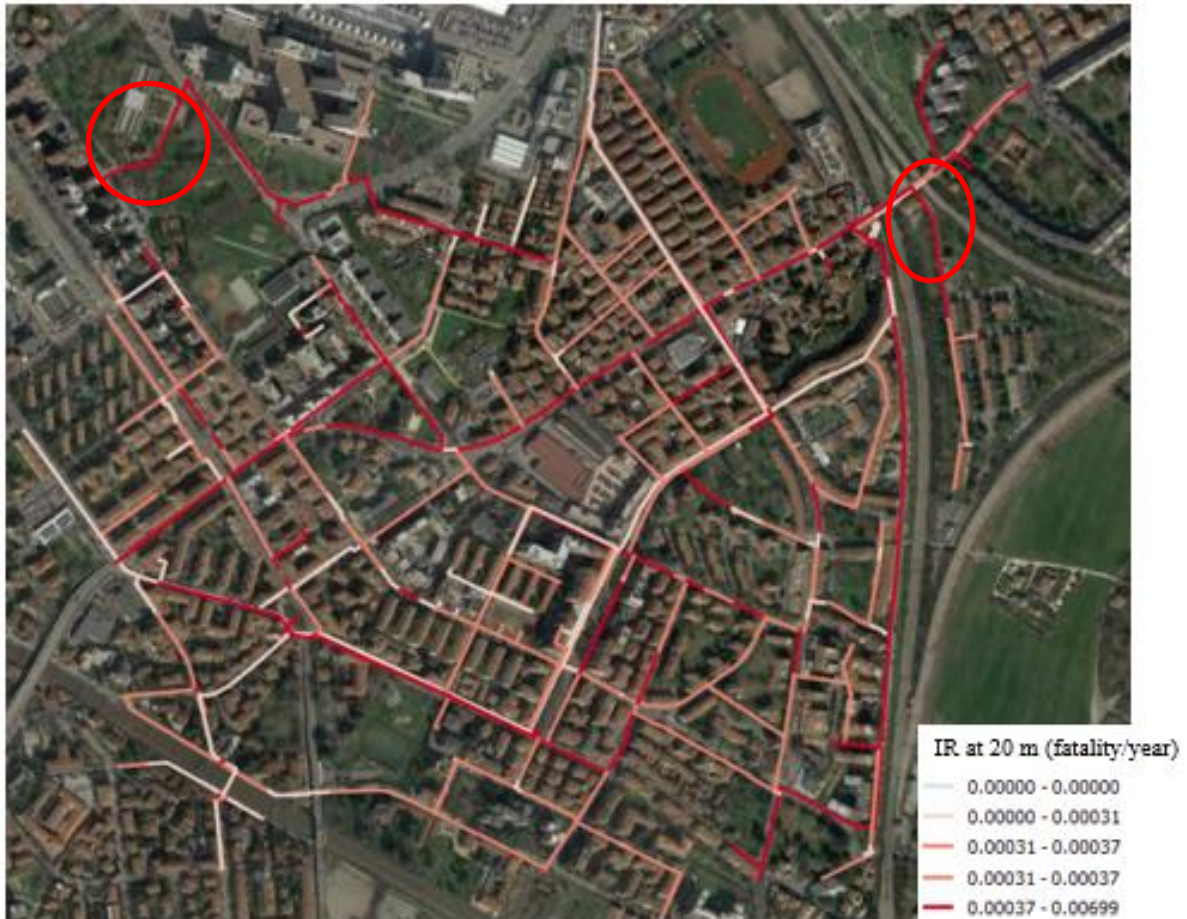


**Figure 127.** Individual risk IR at 20 m from the pipeline. Different distances can be considered applying equation from 4-1 to 4-26.

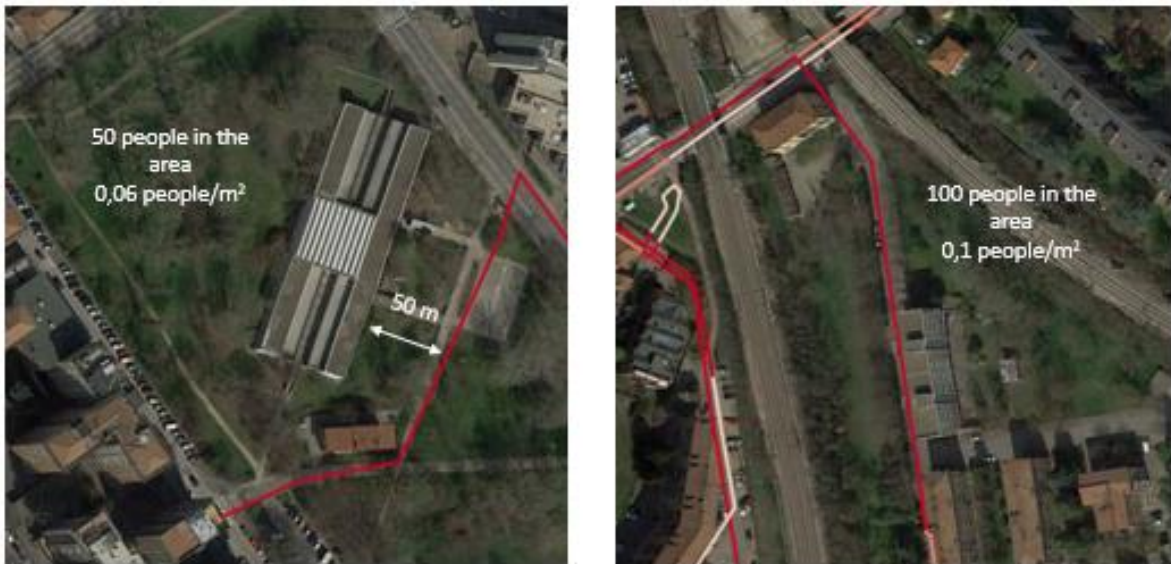


**Figure 128.** Focus on the identified pipelines. Population density values are estimation and used only to demonstrate the potential of the method. More accurate estimation is suggested.

#### **4.6.4 Risk evaluation and ranking of priorities**

The last step of risk analysis consists in the critical evaluation of obtained results. For the scope, skilled person should be employed. As reported in previous chapter a  $10^{-4}$  can be considered as a possible threshold between acceptable and not acceptable risk. In the proposed case study, some parts of the network are characterized by an individual risk higher than acceptable. For these cases, however, a more detailed analysis is required before to take a decision for the following reasons:

1. Simplifications are present in the procedure especially in the calculation of probability and so a more detailed analysis is suggested of the specific section of pipeline;
2. Attentions should be given in order to identify if the high risk is due to accident probability or to consequences. For each cases different actions can be performed:
  - a. The high risk is due to failure probability and the cause of failure is known. For example, if a high failure probability is caused by earth movement, a dedicated monitoring system can be applied in the specific location. In this case technical parameters and safety working thresholds have to be clearly identified before the implementation;
  - b. The high risk is due to failure probability but the cause of failure is not clearly known. In this case, the identification of the best solution appears to be more difficult. System renovation can be considered in order to achieve higher performances;
  - c. The high risk is due to consequences. In this case, protective solutions should be identified in order to reduce the outcomes in the case of gas escaping. For example, the following interventions can be considered: the reduction of the time required to rescue team to reach the location, the installation of remote controlled valves in order to stop gas supply in the case of abnormal situations and of instrumentation in order to control networks conditions from remote.

Consequently, different actions can be performed but only a more careful evaluation in order to use the available budget in the most effective way.

In order to rank pipelines, three index have been proposed in equation 4-31, 4-32 and 4-33 and called respectively  $N_{1,j}$ ,  $N_{2,j}$  and  $N_{3,j}$ . In the following figure  $N_{1,j}$  and  $N_{2,j}$  are reported. In fact,  $N_{3,j}$  requires detailed information and so its calculation is suggested only for those pipes characterized by the highest risk in order to reduce the requirements in terms of resources.

The two indexes are reported in Figure 129 and Figure 130. As shown different priorities and so ranking results considering failure probability or risk. In accordance to available standards in Oil & Gas sector (such as the [149]) a risk based inspection is however suggested. Furthermore, as shown in the figure,  $N_{1,j}$  index does not make possible a clear prioritization between pipelines due to its definition.

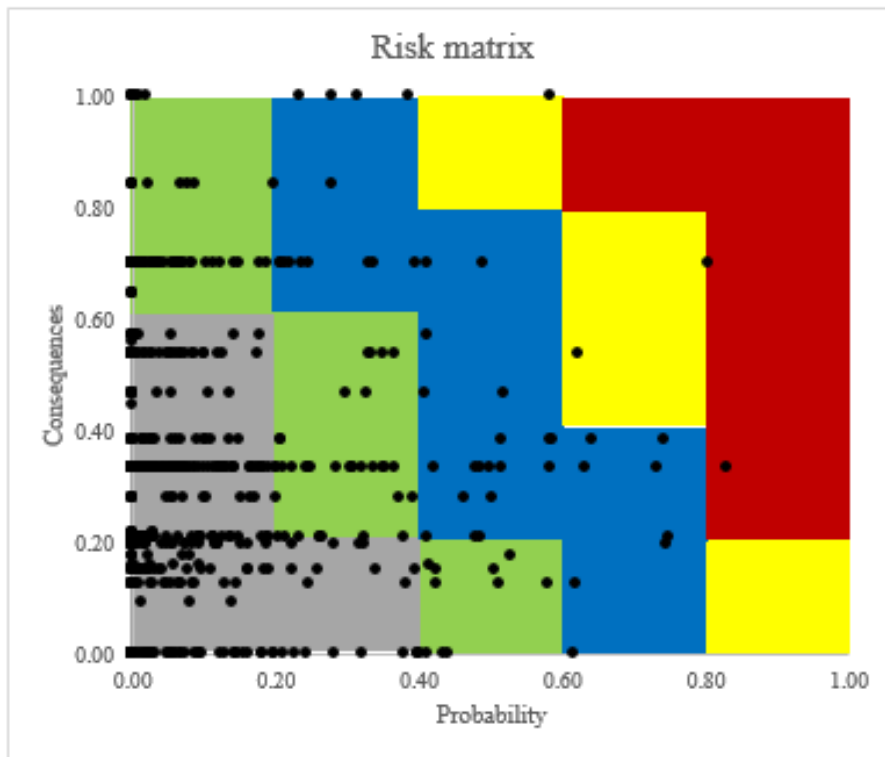


Figure 129.  $N_{1,j}$  index for the analysed network.



Figure 130.  $N_{2,j}$  index for the analysed network.

In Figure 131 the risk matrix for the analysed network is proposed. As shown, this representation makes possible to operator to evaluate to what is due the main contribution to the risk. As shown, only few pipelines are characterized by relative high probability of failure while the situation is different for consequence where more one pipelines are characterized by not negligible values.



**Figure 131.** Risk matrix for the analysed network.

## Chapter 5

# Proposal of a database for NG distribution network failures

### 5.1 Reasons for the creation of a failure database

As reported in previous chapter, a database is suggested in order to characterize accidents and near missing occurred in NG networks. In this way more information able to improve company's performance will be available; particularly, the possibility to have more information will help DSOs to take more conscious decision as required in the Plan – Do – Check – Act (PDCA) model (Figure 132) [150].

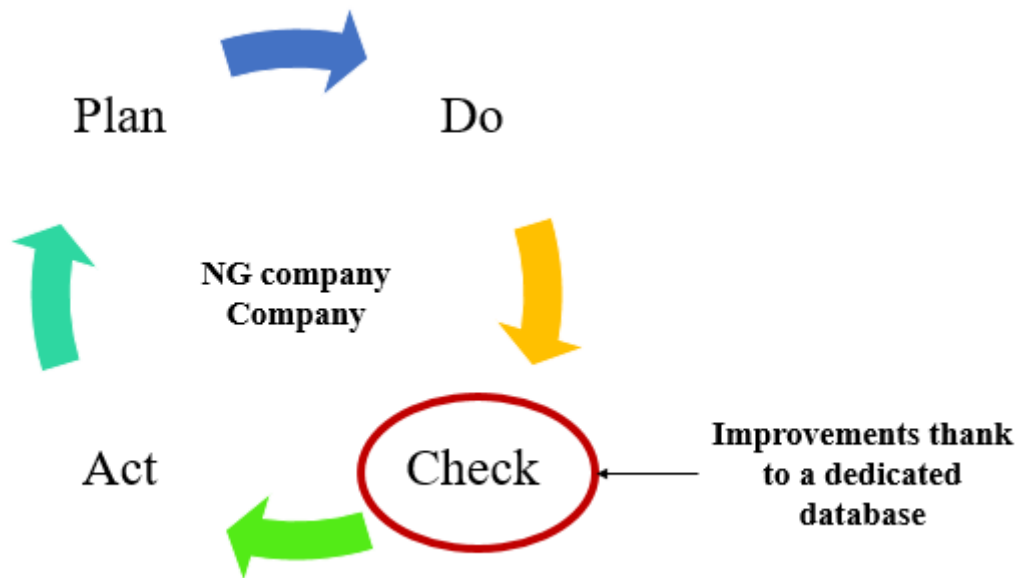


**Figure 132.** Plan – Do – Check – Act model. The presence of a dedicated database will help decision maker to check performance and take the best decision.

In fact, even if the identification of the exact cause results difficult in some cases, the outcome identification will be other ways very important for statistical analysis. A simple schematization of the proposed method to characterize pipeline failures is consequently proposed in Figure 133 where three main steps are identified.

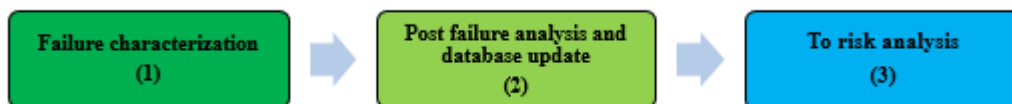


**Figure 133.** Summary of the proposed method for the characterization of failure in NG distribution networks.

A brief description of the proposed sequence is reported as follow:

1. **Failure characterization.** In this step data are recorded during the interventions in field. For the scope, formats should be prepared in order to be simply and quickly compiled by workers that are not

necessary experts in failure analysis. A dedicated app can be designed by gas utilities in order to ensure the immediate transmission of records to a central server;

2. **Post failure analysis and database update.** In this step, a team of experts examines the data received by the field in order to identify the possible causes of failure and the presence of trends. Considering a total number of almost 10.000 leaks in the Italian distribution network and a number of working days equal to 200 days/year, an average value of 50 leaks are identified daily in the national territory; this quantity can be managed by a number of 20 – 25 workers considering a 2 – 3 leaks/(man day). Even if it could be considered a high investment cost for DSOs, it should be noted that know-how and so improvements in terms of safety and quality will result.
3. **Data to risk analysis.** With the information identified in previous steps, failure rates can be continuously updated and high value information can be transferred to risk assessment. Therefore, decision makers will be driven in their decision by real data from the field that are constantly updated.

In the following paragraphs an insight into each step is proposed in order to show the applicability and the potentialities of the proposed model in NG distribution networks.

### ***5.1.1 Failure characterization***

A dedicated survey has to be prepared to collect all the required information from the field. Different reasons should be considered in the design of the questionnaire as schematically reported:

- **Information required should be the clearest as possible.** The questions should be simple to avoid errors during the compilation. Particularly precompiled answers should be prepared in the format in order to avoid free answers by the operators in accordance to the technical information available in the relevant technical standards;
- **Information should not be redundant.** The minimum number of information should be required to characterize the system and external phenomena that could be responsible of the failure. In fact, increasing the number of information, two effects can verify such as the presence of errors during the compilation or the absence of records;

Having these considerations in mind, different sections are suggested for the database. These can be schematically identified as successive steps one after the other in accordance to the sequences of activities such as the identification of the leakage location, the excavation of the trench (in the case of buried systems), and the repair of the failure. In Figure 134 a preliminary schematization is reported:

1. **General indications.** Several information has to be recorded in the first sheet such as the operator responsible for the activity, the date, and the position of the failed system that could be geo-referenced with coordinates and introduced in GIS (Geographic Information System) systems in order to identify immediately the concentration of failures in the same area or in those areas with similar operative conditions;

2. **Characterization of the location.** In this part, general information about the surrounding environment should be identified. In some cases, confirmations should be made in the post failure analysis by the use of other source of data if some of the required information are not know by the operator in the field;
3. **Characterization of the trench.** The characterization of the trench gives information about the possible loads exercised on the buried system. Being not possible to realize chemical analysis of the material in the trench, only qualitative questions should be considered for the scope in order to suppose if laying conditions had an impact on the failure;
4. **Characterization of the failed system/device.** A preliminary characterization of the failed system or device is present in this step. The information reported in this section can also be used to assess and to verify the information reported in company's database. In fact, after the identification of the system (SAP number or other specific identification) by the worker in the field, some data should be directly imported from the central database and rapidly verified by the operator during the intervention. For the scope, QR codes with all the information should be applied during the installation. Furthermore, general description of the system surrounding the failed part has to be made helping the identification of possible issues.
5. **Failure characterization.** In this section questions about the status of the failure in order to make a failure analysis are required.

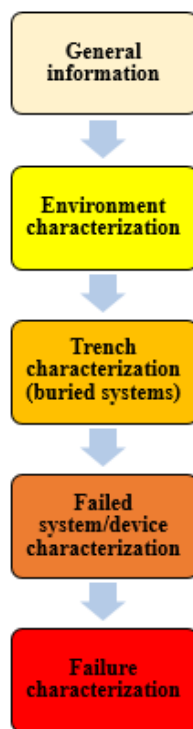


**Figure 134.** Schematization of the information required to characterize the failure.

In order to complete the survey attention should be given to all the possible scenario that affects NG distribution networks conditions. Information should be required only if they can be considered of concern for the following analysis. For example, in the case of polyethylene systems no information has to be required about the presence of corrosion or about coatings.

### ***5.1.2 Post failure analysis and database update***

In this step, data from the field should be directly saved in the database as a “To do activity” for dedicated skilled experts. Two main activities are considered in this phase:

1. Confirmation of the data received from the field and of the presence of anomalies in the records and database updating;
2. Identification of the possible causes responsible for the failure. A brief description of the reasons that justify the result should be given in order to maintain traceability of the analysis for future investigations.

In the database automated operations should be present in order to simplify the elaboration and to give immediate results. Furthermore, threshold should be considered in order to give an alarm in the case of specific values are overtaken but also in the case that an irregular trend occurs. The main information to be automatically updated should be:

- *Global information:*
  - Total number of failure occurred in the network specifying at least component, material, pressure, diameter;
  - Total size of the network specifying at least length, material, pressure, diameter
- *Area information:*
  - Because of the analysis of a single pipeline could be ambiguously, especially in the case that no failures have been already occurred, failure rates of the pipelines included in a defined area of a size for example equal to 100 m x 100 m can be considered. Such as for global information also in this case a division per component, material and pressure should be performed in order to evaluate eventual correlations with the surrounding environment.

## ***5.2 Main information required for failure database***

In this section preliminary suggestions for the creation of a failure database are given. Only preliminary questions are considered even if other can be introduced based on the experience of the DSOs. In fact, the main scope of the chapter is to show the potentiality that could be achieved if implemented.

### ***5.2.1 General information***

Information is required to make a high level characterization of the failure. Between the suggested the following are considered:

- *Name of the worker.* Only for procedural purpose, the name of the responsible worker in the field has to be registered.
- *Date.* This information is important to evaluate trend during time.
- *Type of failed system:* main, service lines, meter or other.
- *Geographical position of the failure.* The geographical position of the failure point has to be made recording the name of the place and the GPS coordinates that at the moment can be easily identified with

an electronic device. In case of mains or service, the failure density in a defined area  $A_{km^2}$  should be calculated:

$$\rho_A = \frac{\sum_i N_i}{A_{km^2} \times \sum_j L_j} \quad (5-1)$$

Where  $N_i$  is the total number of leakages occurred in the area of defined dimensions  $A_{km^2}$  [m<sup>2</sup>] and  $L_j$  is the length of the j-th pipeline; without normalization respect to system length an evaluation error could occur because of the high number of failures could be justified by the high density of pipeline and not by an effective fragility of the same. In order to evaluate the trend, a rate for the area density leakage can be evaluated as:

$$v_{\rho_A} = \frac{\rho_{A,t_2} - \rho_{A,t_1}}{t_2 - t_1} \quad (5-2)$$

Where  $t_2$  and  $t_1$  are time at the instant 2 and 1.

- *Identification of the failed system.* After geographical and type of failed system identification, the software should automatically propose the system located in the identified position. At this point the worker in the field should only to confirm the information. In case of main or service, it can also be automatically calculated the failure linear density:

$$\rho_{L,j} = \frac{\sum_i N_{i,j}}{L_j} \quad (5-3)$$

Where  $N_{i,j}$  is the total number of failure occurred in the pipeline j and  $L_j$  is its length [m]. In this way it is possible to evaluate the presence of more vulnerable pipeline. As made for the previous parameters, also in this case a rete can be introduced:

$$v_{\rho_{L,j}} = \frac{\rho_{L,j,t_2} - \rho_{L,j,t_1}}{t_2 - t_1} \quad (5-4)$$

All the identified parameters, can be automatically update in real time by the software and so a continuously monitoring of system performance can be possible.

Another important potentiality is the identification of other lifelines near to failed system through the connection with other available database. In fact, lifelines can be preferable paths for the escaping gas and so an immediate information about possible hazard is given to worker operator that as a function of its experience and of field examination can perform the activities the safest as possible. Preventive measures can be for example immediately taken for those buildings supplied by the identified lifelines.

### **5.2.2 Environment characterization**

After general information, some other data are suggested in order to help in the successive analysis. That information regards the environment surrounding the pipeline. In fact, some of them can increase the failure probability due to a defined cause. The main suggested are the following:

- *Failure location*: buried or unburied. The information is necessary to evaluate what type of loads can have been exerted in the system. In case of buried system, the final use of the area should be specified: street, sidewalk, off-road or other have to be selected in order to qualitative evaluate the possible magnitude of loads;
- *Evidences near to failure*. To be compiled only in the case of buried system. In the parenthesis it has been indicated for which materials the parameter is responsible to increase the probability of failure:
  - Presence of settlement near to the pipeline (for all material, loss of support and overload). The worker in the field should evaluate the presence of settlement or street adjustment neat to the pipeline with a qualitative judgment: no, low (if settlement is lower than 10 mm), yes. This would help in the qualification of trench support and of the superficial loads over the pipeline;
  - Presence of tree near to the pipeline (for all material, responsible for a concentrated loads and loss of support). Because of roots have been often responsible for system failure it is suggested to record the information. A qualitative answer is proposed: yes, no.
  - Presence of groundwater at pipeline level or of other water source (only for metallic pipes, responsible for corrosion and graphitization). The presence of water and groundwater is in important factor increasing corrosion or graphitization probability in steel and cast iron pipes. Because of this information could be not easy to be answered by operator it could be compiled during data analysis through the use of other data sources. A qualitative answer is proposed: yes, no.
  - Presence of other current sources in the proximity of the pipe (only for metallic pipes, responsible for stray current corrosion). As shown, stray current could increase corrosion phenomenon. Between them the following sources can be considered: railway, tramway, electric transmission sources, radio sources. Operator should identify the presence of one of these if visible from his position. Therefore, the possible answer should be: visible and not visible. In the case that the voice “visible” is selected operator should specify the current source. If not visible, more dedicated analysis has to be made during data analysis if failure path makes credible a corrosion failure.

From the obtained results is possible to proceed in the following step that should be made only for buried system: trench characterization.

### **5.2.3 Trench characterization**

The correct execution of trench is of fundamental importance because of different stress conditions can be verified by the buried system. As shown, as a function of soil type different phenomena can be advantaged such as corrosion, graphitization or SCG in presence of concentrated loads. For this reason, the following should be compiled:

- *Presence of the marker*: worker in the field should define if the marker above the pipeline has been found easily of it has been deteriorated in the time. This could give important information in order to evaluate safety performance against excavation damages.

- *Soil type inside and surround the trench (for metallic pipes, the information could be correlated with corrosion and graphitization)*: clay, loam, sand. Only a qualitative high level characterization is required. For this reason, indications should be given to worker in field to help him in the identification;
- *Presence of extraneous bodies within the trench (for PE and metallic material, the information could be correlated with SCG or with corrosion)*: in the case that a positive answer is given by the operator in the field, specification about the type and dimensions of the found body should be given: high quantity of rocks and pebbles, low quantity of rocks and pebbles, ferrous materials, tree roots, other.
- *Presence of groundwater inside the trench (for metallic pipes, the information is correlated to corrosion and graphitization)*. A qualitative answer is suggested: yes, no.
- Presence of protection elements over the pipes (*for all the pipes, the information is correlated to the resistance against superficial loads*). A qualitative answer should be given by operator: yes, no.

#### **5.2.4 Failed system characterization**

To complete failure analysis the characterization of the failed system or device has to be completed in order to evaluate if some operative conditions are responsible for a high percentage of failure or other observable trend. A preliminary division is proposed as a function of the failure location in the system:

- *Body of the pipe*. The following should be compiled or confirmed:
  - Nominal diameter. Immediately compiled by the software after pipeline identification and confirmed by the worker in field;
  - Operative pressure. Immediately compiled by the software after pipeline identification;
  - Material. Immediately compiled by the software after pipeline identification and confirmed by the worker in field. The following additional information should be considered:
    - Steel: pipeline grade and presence of welds;
    - Iron: pipeline class designation;
    - Polyethylene: standard dimension ratio (SDR), designation in accordance to ASTM F-412.
  - Manufacturer. Compiled automatically by the software after pipeline identification. This information would be useful to qualify the manufacturer of the pipeline.
  - Presence of cathodic protection. Compiled automatically by the software after pipeline identification only for metallic pipes.
  - Presence, type and status of the coating. Compiled only for metallic pipes in field. For the scope, photos should be realized in order to help analysis in successive steps.
    - Presence of coating: “yes” or “no”;
    - Type of the coating: asphalt enamel, wrap type, coal tar, fusion bonded epoxy, polyethylene tape, other. This information is considered important to evaluate possible shielding or disbondment;
    - Status: “good” or “not good”;
  - Installation year. Compiled automatically by the software after pipeline identification.
  - Responsible for the installation. Compiled automatically by the software after pipeline identification;

- *Fittings and joints.* The following should be compiled or confirmed:
  - Fittings and joint type. In accordance to DSO, a list of available fittings and joints should be realized as a function of operative conditions. In this way low probability of error will be present during compilation in field;
  - Material of the fitting and of the pipe or pipes to which is connected. Immediately compiled by the software after pipeline identification and confirmed by the worker in field;
  - Size of the fitting and of pipe to which is connected. Immediately compiled by the software after fitting identification and confirmed by the worker in field.
  - Operative pressure. Immediately compiled by the software after fitting identification;
  - Connection type. As a function of the identified material, only some configurations should be showed to operator:
    - Steel: “welded”, “flanged”, “threaded”, “compression fittings”;
    - Cast iron: “flanged”, “spigot or socket”;
    - Polyethylene: “butt fusion”, “electrofusion”, “compression fitting”;
    - Copper: “brazing”.
 Other connection type can be considered and added as a function of DSOs experience.
  - Fittings manufacturer. If available, it should be compiled directly by the software after have identified the failed component;
  - Installation year. Compiled automatically by the software after identification;
  - Responsible for the installation. Compiled automatically by the software after identification.
- *Component.* In the case the failure is identified in a component of the NG distribution network:
  - Component type. DSOs should identify a list of possible components present in the network such as valves, pressure reduction station and other;
  - Material of the component. Immediately compiled by the software after pipeline identification and confirmed by the worker in field;
  - Size of the component. Immediately compiled by the software after pipeline identification and confirmed by the worker in field;
  - Operative pressure. Immediately compiled by the software after identification;
  - Component manufacturer. If available, it should be compiled directly by the software after identification;
  - Installation year. Compiled automatically by the software after identification;
  - Responsible for the installation. Compiled automatically by the software after identification;
- *Other.* This section should be compiled by operator if the failure is present in an element different respect those reported. A brief description and photo should be recorded in the report to help successive analysis.

In case of evident cause of failure such as excavation damage or incorrect operation, the operator in the field should immediately record it in this section; before to conclude the report, however, photos of the failed part have to be made.

Possible trends can be evaluated with the recorded information as made in the simplified analysis of leaks occurred in American NG distribution in chapter 3. However, in this case, trends can be evaluated locally verifying the presence of critical conditions. In this way very precise and interesting statistics for the selection of the best practice can be ensured.

### 5.2.5 Failure characterization

The last step of the analysis is the most important one in order to help failure analysis performed by experts. In fact, different causes are responsible for failure modes as reported in Figure 135 and in Figure 136.

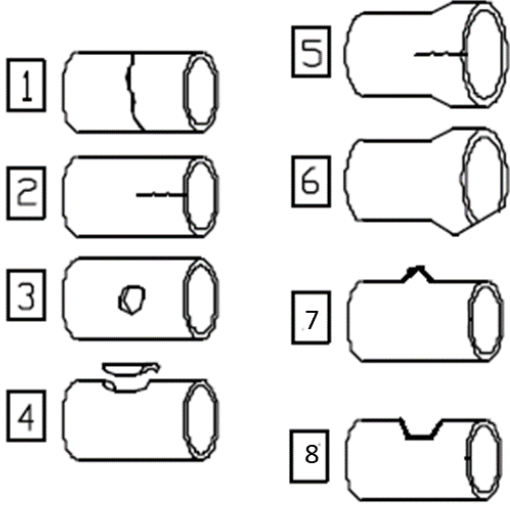
Failure modes	Description
	<ol style="list-style-type: none"> <li>1. Circumferential crack: possible causes are soil thermal expansion, soil settlement or other axially induced stresses.</li> <li>2. Longitudinal crack: possible causes are internal pressure or external loads such as traffic loads;</li> <li>3. Uniform thickness reduction or localized hole: corrosion or other deteriorating phenomena can be responsible;</li> <li>4. Distributed crack: thickness reduction due to deteriorating phenomena have to be considered;</li> <li>5. Bell splitting or flange fracture: in cast iron is principally due to the different thermal expansion coefficient of the material;</li> <li>6. Bell or flange rupture: bending stresses or axial stresses between the connected pipelines have to be considered.;</li> <li>7. Superficial deformation due to concentrated load: usually due to axial compression stress on the pipeline;</li> <li>8. Dent or gouges: usually due to excavation damages or due to the presence of extraneous bodies.</li> </ol>

Figure 135. Failure modes in steel and iron pipes. Source [151].

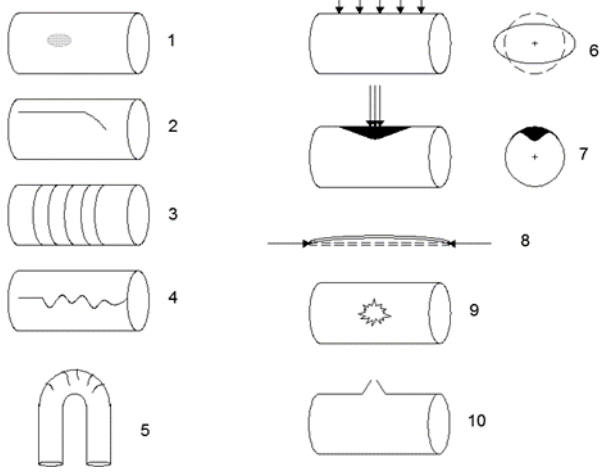
	<ol style="list-style-type: none"> <li>1. Superficial cracks: usually due to internal pressure or concentrated loads on the pipe;</li> <li>2. Longitudinal crack: due to internal pressure;</li> <li>3. Circumferential crack: due to excessive bending or thermal deformations;</li> <li>4. Axial rupture: rapid crack propagation;</li> <li>5. Circumferential crack near to a 90°-degree elbow: minimum curvature radius not respected;</li> <li>6. Ovalization: due to excessive vertical load or earth movement;</li> <li>7. Dent: due to an excessive concentrated load;</li> <li>8. Compression instability: due to thermal expansion.</li> <li>9. Presence of hole: due to the contact with an external object;</li> <li>10. Ductile rupture: due to internal pressure.</li> </ol>
---	--

Figure 136. Failure modes in polyethylene pipes. Source [42].

In this step is therefore very important to make a correct description and make photos of the failed part.

To complete the analysis, so, the following questions have to be answered as a function of the failed element:

- *Body of the pipe:*

- As a function of the material, operator should identify the failure path with one of the proposed in the two figures. In the case that the failure mode cannot be associated with one of the proposed one, a brief description of the failure should be made. Also photos of the failed part have to be made.
- Position of the failure in the body of the pipe. An hourly classification can be used, considering the top of the pie such as twelve o'clock, and the bottom as six o'clock.
- Size of the leak: leak or rupture;
- *Fittings*. In the case of fittings failure, the following information seems to be sufficient:
  - Failure characteristics: escaping gas through body, connection, seal or fitting pulled out;
  - Size of the leak: leak or rupture;
  - Presence of deteriorating phenomena such:
    - Presence of corrosion: “yes”, “no”;
    - Presence of cracks: “yes” “no”;
- *Components*. As for fittings the same information seems to be sufficient:
  - Failure characteristics: escaping gas through body, connection or seal;
  - Size of the leak: leak or rupture;
  - Presence of deteriorating phenomena such:
    - Presence of corrosion: “yes”, “no”;
    - Presence of cracks: “yes” “no”;

In the case of fittings or components it results more difficult to evaluate the cause of failure. Nevertheless, the database proposed will ensure the identification of similar failure modes. Considering the other data recorded in previous section will be possible to evaluate fittings performance as a function of material, manufacturers, installation year. If common trends are identified it will be easier to intervene immediately for example reviewing procedures, evaluating other manufacturers or materials in specific conditions.

### ***5.3 Future development suggested***

The creation of a database ensures many improvements in the exercise of NG distribution networks. For this reason, it is in opinion of the Author that the proposed steps have to be introduced in a dedicated format for example thanks to the creation of an application connected to a central datacentre.

Several advantages can be obtained respect to the philosophy adopted at the moment:

- The identification and characterization of failure at local level will ensure:
  - Evaluation of abnormal trends respect to the recorded parameters;
  - Immediate interventions in order to mitigate the identified issue;
  - Better allocation of resources respect to the effective problems identified in the field;
- Effective application of the philosophy reported in the ISO 14001 called “Plan – Do – Check – Act”.

Therefore, the preliminary step suggested by the Author is the creation of a database in order to demonstrate its applicability and potentiality. However, some considerations should be made by DSOs during the realization such as:

- Collaboration between DSOs and other local Authorities to ensure the compilation of some of the fields reported directly by the software, reducing the possibility to make mistakes and reducing the time required for the survey;
- Collaboration between DSOs in order to share results. In this way trends or obtained results can be compared identifying immediately the presence of criticalities at national levels where to intervene. A beneficial outcome to safety performances will be obtained.

For the reported reasons a national legislative leader should be identified in order to coordinate the possible efforts from each DSOs. Also suggestions based on experience should be collected in order to improve the preliminary format proposed for the database. For this role the Comitato Italiano Gas seems to be the best option even if ARERA should be considered in order to make effective the project as preliminary proposed in Figure 137.

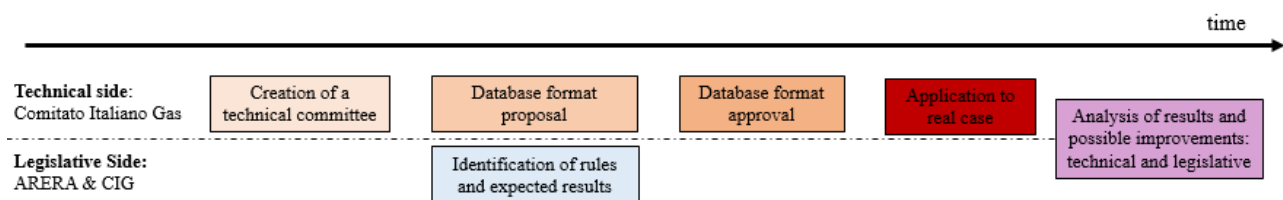


**Figure 137.** Time scheduling for the creation of the database.

In fact, thanks to the database the following should be expected:

- Improvement of safety and quality performances of the Italian distribution networks with dedicated solution or actions;
- Identification of the real performance of the Italian distribution networks in terms of operative conditions such as material, operative pressure, and other parameters;
- Comparative analysis between DSOs not only in terms of number but also for type of leaks in order to evaluate abnormal trends.

As observed several improvements to safety is ensured and for this reason economic incentives for the creation and implementation of the database seems necessary. Dedicated incentives can be considered and defined by the Authority; for the definition the following should be considered:

- The total performances of the system in the period;
- Reduction of leakages identified in the period.

Considering only the reduction rate of leakages occurred in the period, in fact, DSOs characterized by high performances would receive small incentives and consequently would not be effectively helped in the implementation of the system in their procedure. At the contrary, considering only total performances, DSOs characterized by low performances would not receive incentives for the effective improvements realized in the operated networks.

The obtained results from different Distributors should be collected by the Authority and made them available for the compilation of reports to interested stakeholders such as Universities or other research centres in order to find common behaviours and to define suggestions to CIG and Authority.

## **PART 2: Quality and safety performance of smart meters implemented in NG distribution networks**

In order to improve NG distribution performances, a new measuring philosophy has been introduced by the Authority in 2008. The new method is called NG smart metering and introduces new concepts for energy fiscal measurement. In fact, respect to the past, the smart metering consists of remote located devices (the smart meters) that automatically communicate with the central unit, defined as the Central Acquisition System without the need of lecturers. Therefore, a very close link between final customers and NG Distributors is present.

The need to implement the new technology was introduced by the Directive 2006/32/CE of the European Community, in which the necessity to implement intelligent measuring systems if economically justified by a Cost – Benefit Analysis (CBA) is reported [152]; particularly, a percentage of new meters equal to 80% is suggested at 2020, and an annual reduction of consumption equal to 3% is estimated thanks to their use.

That is, different results were calculated by European countries from CBA analysis. In Germany a negative CBA resulted leaving therefore the decision about the implementation to single operators; in France, Gazpar started in 2015 a big development project consisting of 150 thousand smart meters deciding to proceed with the substitution of other 11 million of devices before 2022. In the United Kingdom, the government started the promotion of smart meters in 2009 to substitute all the existing devices before 2020 even if a substitution rate lower than expected is reached because no all the final customers decided to substitute the device. In the Netherlands the rollout started in 2012 in order to substitute the 90% of existing devices (almost 7 million of devices) before 2020; thanks to the low percentage of refuse, the four most important Distributors of the country started the supply of 3 million of devices in 2016 with a total investment of almost 470 million of euro. In this case a specific price equal to 150 €/smart meter is estimated that is lower respect to the preliminary estimation corresponding to 200 – 250 €/smart meter of the European Community.

Therefore, 23 million new devices have to be installed in the Italian market with almost the 50% since 2018. From the reported numbers several considerations immediately arise:

- A very great effort has to be done by NG distribution sector in order to make it possible, comprising Distributors, meters manufacturers and other ones that contribute in the supply chain;
- Quality and safety performances of the new technologies has to be assured for the success of the technology. In particular attention has to be given in order to ensure the operative life;
- Very few experimental activities have been made before the implementation. For this reason, corrective actions have to be identified in the case that technical issues are identified.

In the second part of the thesis, attention is given to smart meters that represent the physical boundary between DSO and final customer. In particular, some considerations and practical implications about the effective life of supply battery are reported in order to ensure the success of the technology.

## Chapter 6

### *Natural Gas smart metering: the new philosophy to measure natural gas consumptions*

In order to introduce the investigated issue, a brief introduction about the reasons for the implementation of the new measuring system is required. Because of a great effort is asked to the supply chain in order to effectively implement the devices in the networks in terms of economic and human resources. For this reason, a simple but effective analysis about installation resources required to respect identified objective is proposed. At the conclusion of the chapter, a brief description of the new meters, i.e. the smart meters, installed in the distribution networks is given in order to highlight the principal technical issues that could arise during the activities. In this part, the main scope of the activity performed is anticipated.

#### ***6.1 Reasons for the introduction of NG smart metering***

As reported in the brief introduction to the second part, Authority required in 2008 the necessity to implement smart metering for fiscal measurement of gas consumed in accordance to European directives. That is, the reasons for the introduction are reported in the document [152]:

- The calculation of daily gas balance able identify the national energy commercial balance;
- The reduction of operative costs due to remote reading;
- The possibility to identify abnormal consumptions or device malfunctions;
- The possibility to introduce a ranking to classify Operators as a function of distribution efficiency;
- The possibility to promote concurrence between NG operators;
- The definition of bills on effective and not on estimated consumptions;
- The possibility for the end users to identify their actual consumption and so to be aware of them.

Advantages are expected both for final customers and for Distributors. In particular, the identification of abnormal consumption thanks to the continuous measurement of gas consumption assures the possibility to immediately intervene and eventually stop the gas flow from remote reducing the mass of gas accumulated in the buildings since the arrival of emergency teams. As shown, in fact, the accumulation time defines the hazardousness of the failure increasing the hazard area in case of explosion.

The big amount of data produced by the new smart meters has therefore correctly managed in order to improve the planning of maintenance and inspection activities to find leaks as for example proposed in [153] with the introduction of other device. At the moment, the data sent by the meter to the Central Acquisition System consists of:

- Data about customer consumption such as the hourly flowrate, the total consumed volume and the supply pressure;

- Data about the status of the device such as the occurred events and a diagnostic report.

Nevertheless, more other data are produced in the smart meters but are not transmitted in order to reduce the electrical consumptions and so to preserve supply battery.

Furthermore, the daily comparison between the gas introduced in the network and the final consumption ensures the quantification of network losses. In this way it is possible to estimate the integrity of the networks and so the efficacy of the interventions defined by the Distributors during a temporal period, for example a year. A high level ranking factor can be introduced to compare the performance of each DSOs, even if, no more detail about the nature of the identified leak is possible.

Consequently, possible improvements in NG distribution are possible thanks to the introduction of the new measuring philosophy. For this reason, the success of the technology is fundamental.

## 6.2 Implementation of the NG smart metering in the Italian market

As reported in the introduction to the second part of the thesis, 23 million of devices have to be implemented before 2020 in the NG distribution networks representing therefore a big challenge to the supply chain. This issue is evident considering the percentage of the new meters installed respect to the total as reported by the Authority and shown in Figure 138 for the period between 2011 and 2016.

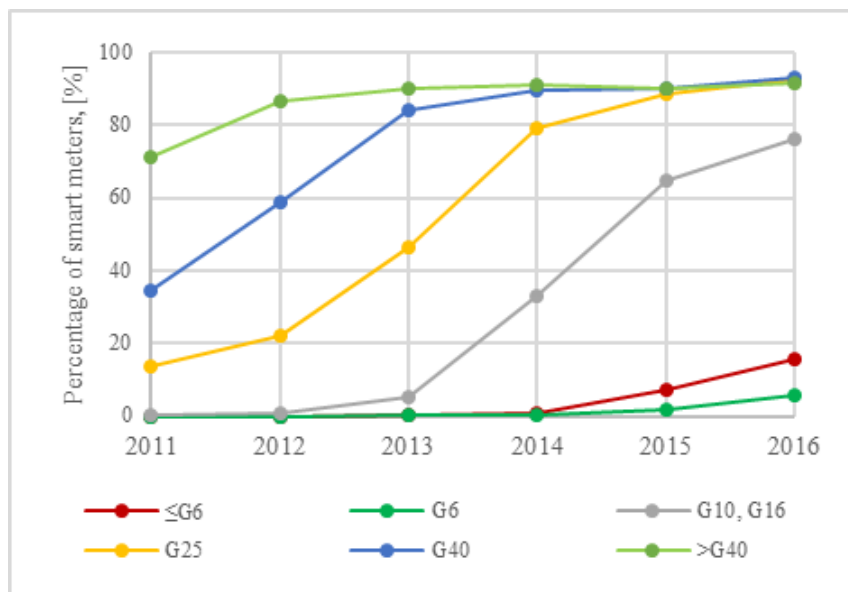


Figure 138. Percentage of smart meter installed respect to the total. Data from ARERA.

As shown, the roll out started from the industrial size meters ( $G > 10 \text{ Sm}^3/\text{h}$ ) which number in the distribution sector is lower than domestic ones. The delay respect to Authority decision is justified by the total absence of the smart metering markets and consequently of the devices that had to be installed in the networks. However, the decision to start from industrial size meters was motivated by the lower number to be installed respect to the domestic ones, by the possibility to easily change the existing meter in order to respect the new requirements and by the opportunity to evaluate their effective performances before to install a higher number of devices in the domestic sector.

For these reasons the roll out of domestic applications started in 2013 in order to respect the first objective required by the Authority [154]. It was immediately clear the difficulty to reach this objective and therefore a second installation plan was proposed in 2015 in order to give more reasonable objectives [155]. The updated objective for the domestic meters are reported in Table 83. As shown, different percentages were required as a function of the number of customers supplied by the gas company.

**Table 83.** Updated objectives in [155].

Meter size	Nominal flow, [Sm <sup>3</sup> /h]	Percentage 2016, [%]	Percentage 2017, [%]	Percentage 2018, [%]
< G6	< 6	15% (*)	33% (*)	50(*)
		3% (**)	15% (**)	33% (**)
		0% (***)	0% (***)	8% (***)
(*) = distributors with more than 200.000 end users. (**) = distributors with [100.000; 200.000] customers. (***) = distributors with [50.000; 100.000] customers.				

Considering the data reported by each DSO, it was possible to apply the defined percentage in the previous table and so to identify the number of meters to be installed in NG distribution network. Dividing the gas Distributors into three groups A, B and C in accordance to the supplied final end users, the total number of meters to be installed was calculated in Table 84.

**Table 84.** Number of smart meters to be installed in accordance to (AEEGSI, 2015).

Operators	Customers, [k#]	Installed, 2016, [k#]	Installed, 2017, [k#]	Installed 2018, [k#]
A	16.457	2.469	5.431	8.229
B	1.023	31	154	338
C	5.520	0	0	442
Total	23.000	2.500	5.585	9.009

As shown in the table almost nine million of device have to be produced, installed and operated before 2018. Considering only the final part of the supply chain and particularly that referred to the DSO, an estimation of costs and human resources required is proposed. For the scope, the total number of meters to be installed before the end of the i-th year simply results:

$$N_{SM\ i} = N_{SM\ required} - N_{SM\ i-1} \quad (6-1)$$

Where  $N_{SM\ i}$  is the number of smart meter to be installed at i-th year [meter/year] and the  $N_{SM\ required}$  is the number of smart meter installed as required by the Authority at the i-th year [meter/year]. The total number of men  $N_{men,i}$  required for the installation in the i-th is consequently:

$$N_{men,i} = \frac{N_{SM\ i}}{(N_{meter} \times N_{day})} \quad (6-2)$$

Where  $N_{\text{meter}}$  is the number of meters that can be installed by a dedicated worker in a day [meter/(man x day)] and  $N_{\text{day}}$  is the number of day available in a year [day/year].

From statistic interviews to local DSO, the following values have been supposed:

- $N_{\text{meter}} = 12$  meter/(man x day). Therefore, almost 40 minutes have been estimated for each installation. It should be noted that this assumption is optimistic because in some cases more time is required in order to ensure the respect of the safety requirements reported in installation standards;
- $N_{\text{day}} = 250$  day/year. The value has been taken considering typical values in the sector.

From these assumptions and the number of installed smart meters at 2016, it results a total number of men to be employed equal to 672 and 1.143 respectively in 2017 and 2018 (Table 85). It should be noted that in the calculation it was assumed the effective respect of the scheduled date but different plans are possible in order to optimize the budget and resources allocation. However, it should be noted that only the voice of cost regarding installation is considered even if other voices are required for the implementation of the smart metering. In fact, it is not in the interest of the thesis made a dedicated CBA analysis but only to highlight the necessity to ensure the expected performances.

**Table 85.** Number of men that should be employed to respect scheduled dates.

Operators	Meter installed at 2016, [k#]	Men employed, 2017, [#]	Men employed 2018, [k#]
A	3.542	630	933
B	31	42	62
C	0	0	148
<hr/>			
Total	3.573	672	1.143

The economic investment was calculated as the sum of cost due to the installation phase and the smart meter device:

$$C_{tot} = (C_{sm} \times N_{SM\ i} + C_{inst} \times N_{men,i}) \times (1 + f) \quad (6-3)$$

Where  $C_{\text{tot},i}$  is the total investment cost for the i-th year (€/year),  $C_{\text{sm}}$  is the specific cost for each smart meter [€/meter],  $C_{\text{inst}}$  is the installation cost that takes into account of the human resources required for the implementation in the network [€/man] and  $f$  is a safety factor that takes into account of all the surrounding activities required to the implementation such as the purchase activity, the coordination activity and the decision activity; for these a value equal to 0.1 is considered. For the scope it has been assumed a specific cost for smart meter equal to 60 €/meter and a daily cost of 160 €/(man x day) resulting in a specific cost for intervention near to 80 €/meter.

Considering the assumed value, the following value results only for installation. As shown in Table 86, more than 200 million of euros are required only for the installation activity.

For this reason, the analysis of the effective performance of the technology in the field is of primary importance in order to reduce field activities and so the unexpected operative costs (as for example in case of failure) that make more difficult the return of the investment.

**Table 86.** Estimation of the total costs for the installation of new smart meters.

Operators	Voice of cost	Total cost 2017, [M€]	Total cost 2018, [M€]
A	Device	195	185
	Installation	26	39.4
B	Device	8.1	12.1
	Installation	1.8	2.6
C	Device	0	7.4
	Installation	0	6.3
<b>Total</b>		231	253

### 6.3 The NG smart meters

The NG smart meter is the main components introduced in the smart metering. It is characterized by several new functionalities that make it possible to achieve several scopes. Particularly, different parts can be recognized (Figure 139):

- *The measuring elements.* Respect to traditional meters in which a diaphragm meter with moving parts is present, the new smart meters preferably present a measuring element completely electronic. In fact, reducing the moving parts lower friction and pressure drop are present; about the first, this ensure a higher operative life while the second gives the possibility to reduce pressure drops. That is, two main types of flowmeter are usually installed: the ultrasonic and the mass thermal flow meters. In both cases electric energy has to be supply to the instrument while in the mechanical case the required energy is directly absorbed from the gas stream. That is, a pressure and a temperature transmitters are installed inside the meter in order to measure mass flowrate. No elements with this function is present in traditional meter where a corrective coefficient is defined as a function of the geographical location. All the measured variables are communicated to the Central Processor Unit (CPU) through a 4 – 20 mA signal;
- *The Central Processor Unit (CPU).* While in the traditional meter only a totalizer and a visual display are present, an electronic processor is present in new smart meters. In the CPU data are elaborated, recorded and prepared to be sent to the Central Acquisition System through a dedicated communication protocol;
- *A communication device.* A communication device is required to transmit the measured parameters to the Central Acquisition System through GSM – GPRS communication or radiofrequency;
- *Remote controlled valve.* Only for domestic applications, a remote controlled valve is required in the installation in order to interrupt gas supply from remote [156]. Two different types of valves are available in the market: motorized bi – stable and solenoid normally opened valves. The first ones are usually installed in area subjected to earthquakes in order to reduce the possibility that the valve closed without the signal from remote such as could happen in the case of solenoid configuration. That is a higher cost, complexity and so possible failure events can happen during the life of the valve;

- Power supply.* Because electronic components are implemented, an electric power supply has to be considered necessary for the operation of the meter. Even if ATEX certification is not mandatory for domestic smart meters in accordance to [157], the possible presence of flammable atmospheres inside the casing requires to evaluate the possible risk of ignition in presence of escaping gas. For this reason, no connection is made to the low voltage electric national grid while electric batteries are installed for the scope. In the case of domestic meters usually two batteries are present supplying electric power respectively to the part dedicated to metrology and to the part dedicated to communication; of these only the second can be substituted during the life of the meter without the necessity to restore the metrological seals. In the case of industrial size meters, usually a single battery is present supplying power both to the metrological and communication parts.

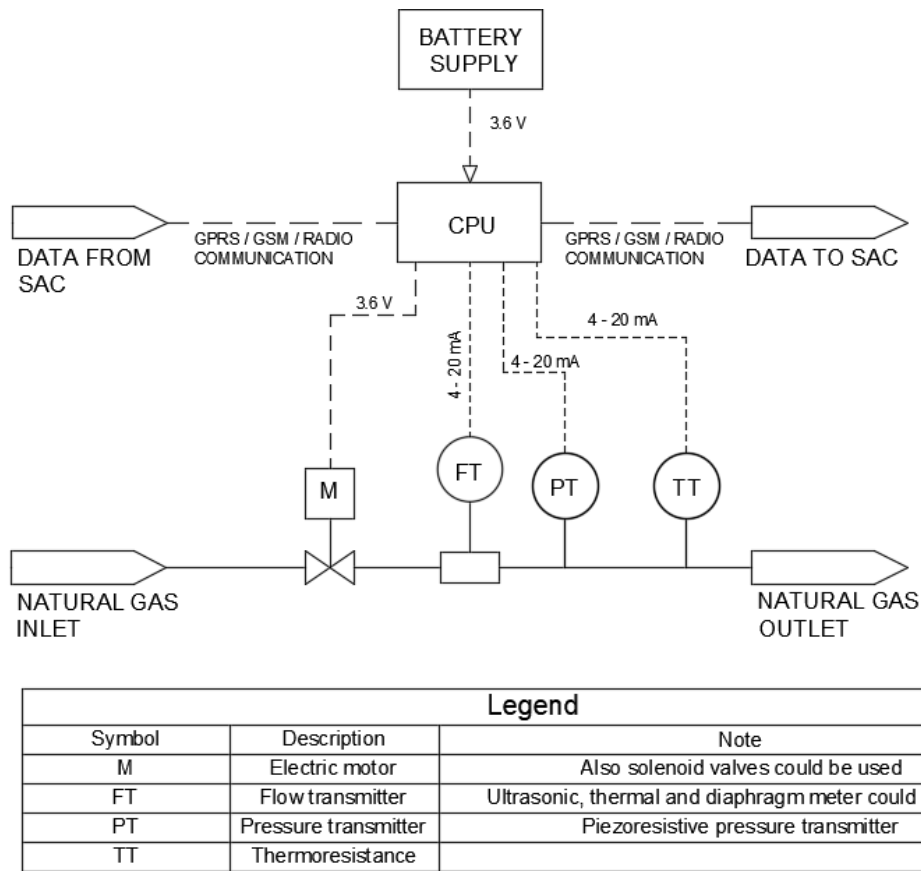


**Figure 139.** Schematic of NG meter with main components.

As reported power supply battery and remote controlled valves appears to be the most critical components in new smart meters. In both cases, in fact, a field intervention is required in case of malfunction. For example, in the case of valve, the presence of solid particle or contaminants in the gas and temperature variation can deteriorate the internal components of the valve, reducing the effective tightness and so the effective operative life, but also damages to the internal components could prevent the closure or the opening of the internal passage. Instead, in the case of electric battery, the effective consumption of the meter could require a capacity higher than that allowed.

For this reason, experimental activities are required to characterize the effective performance of these components and so to take the best actions and decisions to mitigate the possible outcomes during the operative

life. In the next parts of the thesis, the results obtained by experimental activity performed to evaluate the effective operative life of battery installed in industrial smart meters are reported.

## Chapter 7

### Experimental research about NG smart meters' battery pack performance

#### *7.1 Reasons and aims of the research activity*

The roll out of new meters was started some years ago in accordance to national objectives. Because of the scheduled objectives, no experimental phase was dedicated to the identification and the characterization of the possible issues in the new devices. That is, a high percentage of battery packs installed in industrial size converters discharged after 2.5 - 3 years from installation respect to the 4 years required: in fact, the replacement of the battery should be completed during the metrological control activities [158] in order to minimize the number of interventions in the field and so the operative costs. It should also be noted that the battery pack supplies power to all the function without division between metrological and communication devices as usually present in domestic devices.

In order to propose a solution to contrast the identified issue, a research activity began. During the analysis, the performance of the battery pack and the electric consumption of the converter were characterized. For the scope, different communication configurations have been investigated in order to evaluate the influence of:

- *Communication frequency between the smart meter and the Central Acquisition System;*
- *Quantity of data communicated between the smart meter and the Central Acquisition System.*

Thanks to the experimental activity it was possible to identify the impact of each parameter and so to evaluate the probability to reach an operative life of 4 years.

#### *7.2 NG Smart metering communication system description*

A brief description of communication system is proposed in the paragraph with particular attention to the communication architecture and to the available protocols for data communication in NG smart metering. That is, an insight to the communication protocols used in the specific application is given.

As reported in the technical standard [159] several configurations can be implemented for data communication between smart meters and Central Acquisition System as reported in Figure 140 where several components are present:

- *Datacentres:* they are responsible for the configuration of the smart meters' parameters and for the elaboration, recording and editing of the data received from Central Acquisition System that can be integrated in the datacentre;
- *Central Acquisition Systems:* they are the interface between smart meters and the datacentre. The following protocol profile can be implemented for the communication with other systems:
  - Point to Point protocol PP4 to remote smart meters;

- Point to Point protocol PP3 to remote concentrators;
- Point to Point protocol PP5 to datacentre.
- *Smart meters*: they are responsible for the measurement of customers' supply and for the transmission of data. As for Central Acquisition System, different protocol profile can be implemented:
  - Point to Point protocol PP4 to Central Acquisition systems;
  - Point to Multipoint protocol PM1 to data concentrator or translation devices.
- *Data concentrator devices*: they are responsible for the aggregation of the data transmitted by several smart meters and for the communication to Central Acquisition Systems. As for the above devices, different profile protocols can be implemented for data transmission:
  - Point to Point protocol PP3 to Central Acquisition systems;
  - Point to Multipoint protocol PM1 to smart meters.
- *Data translation devices and repeater*: they are auxiliary elements of the communication network that improve the communication capacity between the smart meters and the concentrator. Repeaters are installed in order to increase transmission distance while data translation devices are used to change protocol profile.

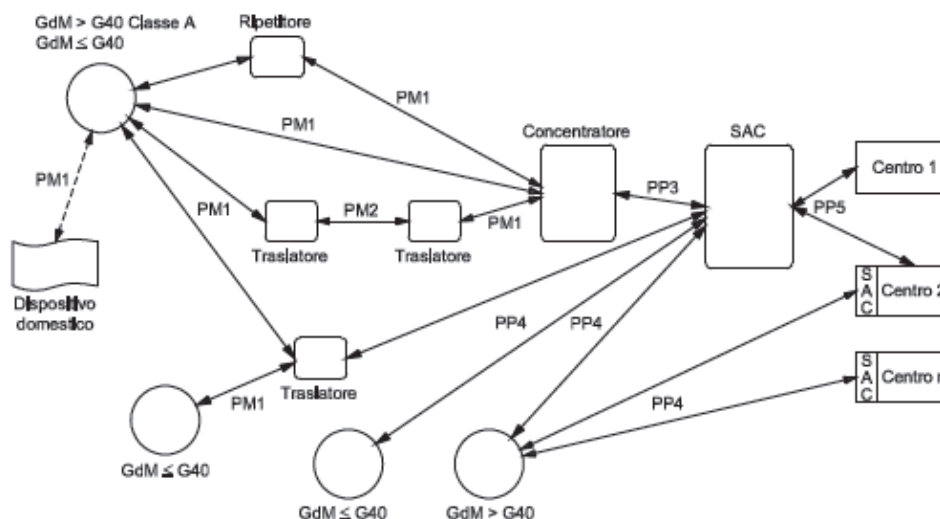


Figure 140. Available communication architecture. Source [159].

As shown, data communication can be divided between point to point protocols and point to multipoint protocols. Different characteristics and performances can be achieved even if the following have to be highlighted:

- The Point to Point (PP) profile is used for the communication between single communication devices. GSM or GPRS communication standards are implemented because of the high communication distances;
- The Point to Multipoint (PM) profile is used for the communication between the concentrator and several meters installed in the territory. Respect to point to point profile, radiofrequency (RF) communication is used.

That is, in the analysed case the Point to Point profile PP4 is implemented for data communication between meters and Central Acquisition System and messages are structured in accordance to the CTR protocol

(“*Comunicazione a Trame Ridotte*” in Italian) [160]. Particularly, data transmission is structured in message of fixed length that is equal to 142 Byte<sup>3</sup> or 140 Byte respectively in the case of GSM/GPRS communication or SMS transmission. Furthermore, messages are sequentially structured. So each byte or groups of bytes represent a specific information depending on the position that occupies in the message; for this reason, bytes are arbitrary identified as zero also in the case that they are not effectively used to ensure the correct interpretation of the message.

Because of the available length of each message, a Master – Slave communication is achieved with the CTR protocol. In this case, the Central Acquisition System represents the master that asks questions to the smart meters that become the Slaves of the network answering to each question of the master. Therefore, no communication is present between the two until a specific request of the master: a typical configuration composed by several questions and successive answers can be identified for the data communication.

As shown in Figure 141, a total number of six messages (6 x 142 byte = 852 byte) are transmitted by the meter to the Central Acquisition System during the communication. Furthermore, the presence of SMS in the memory is verified by the Central Processor Unit (CPU) at the beginning and at the end of the communication phase. That is, the connection to the network represents a high consumption voice especially in those cases characterized by low signal coverage: during the operation in the field it has been verified the presence of communications characterized by a duration higher than 2 minutes when a duration of 30 second was expected as defined by the manufacturer in the case of good signal. In the case that no connection is realized at the end of first tentative, the device is programmed to try consecutively for other two times the connection; if no connection is possible, data are transmitted to Central Acquisition System through SMS; this is responsible for a higher operative cost respect to the use of GSM / GPRS communication due to the contracts stipulated by the telephone operator and the DSOs. In order to summarize, the communicated data are reported:

- *Identification*: number of events occurred in the meter, state of the device, diagnostic and other data that are necessary to identify the device;
- *Gas flowrate*: the measured and the compensated consumption are transmitted. Hourly based values are considered;
- *Gas pressure*: the average hourly gas pressure is recorded and transmitted to Central Acquisition System.
- *Data and time*: the synchronization between the meter and the Central Acquisition System has to be verified;
- *Power supply status*: an estimation of the residual life of the battery pack is transmitted to the Central Acquisition System once a week.

---

<sup>3</sup> 1 Byte = 8 bit

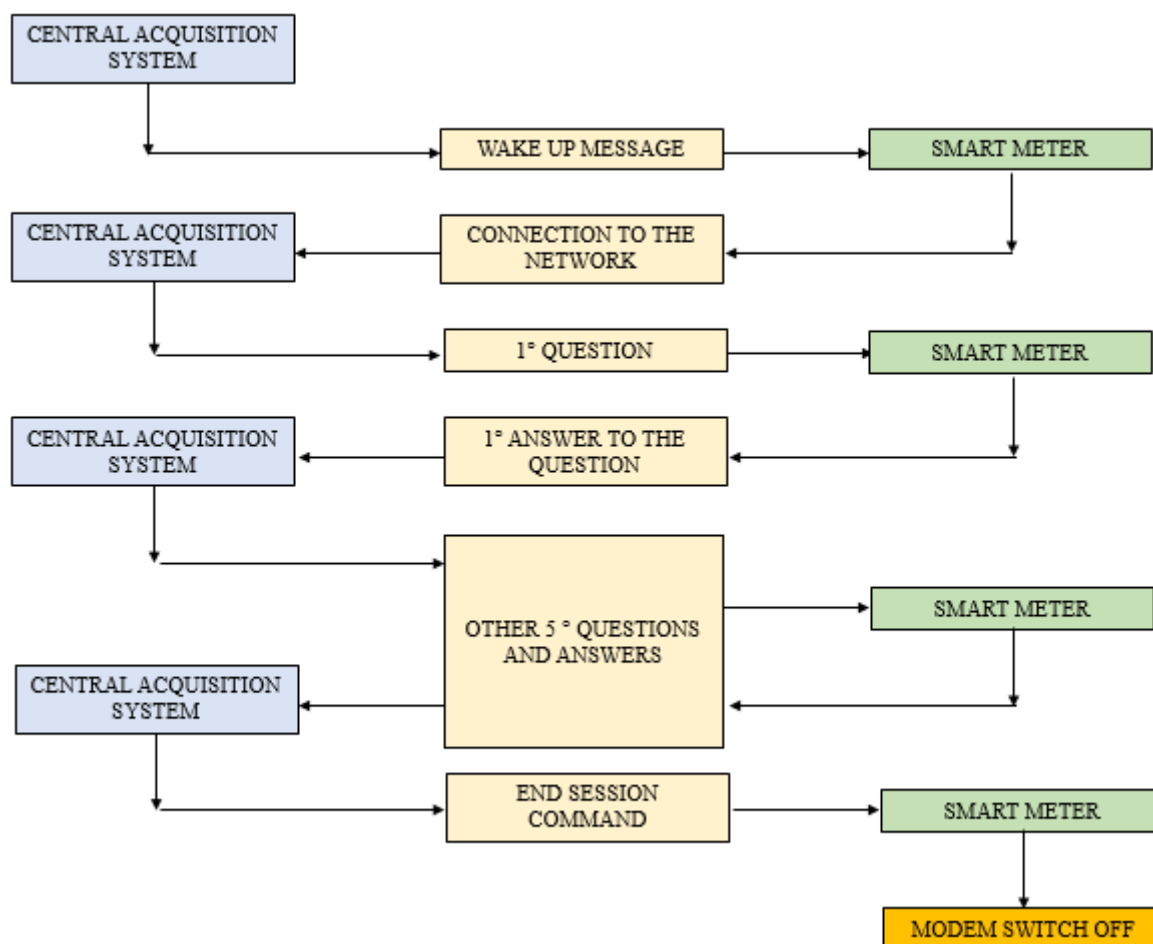


**Figure 141.** Communication structure between Central Acquisition System and remote meters in accordance to CTR protocol.

### 7.3 Main technical characteristics of the analysed device

The analysed device is implemented in the industrial size NG smart meters and it performs the conversion of natural gas volume from the operating conditions to the reference conditions, acquiring data from the volumetric flow transmitter inside the primary meter and from the pressure and temperature sensors installed in the gas supply line (Figure 142). Within the converter, the CPU, the data communication components and power battery pack are also present. In Table 87, the main technical data of the device are reported.

**Table 87.** Main technical data of the analysed device.

<b>Size (LxHxP), [mm]</b>	230 x 150 x 54
<b>Weight, [kg]</b>	2.0
<b>Protection class</b>	IP 66
<b>Operative temperature, [C]</b>	Da -25 °C fino a + 70 °C
<b>Power supply</b>	2 batterie al litio size D di tensione 3.6 V e capacità 13 Ah/cad.
<b>Operative pressure range, [bar A]</b>	0.8/2 bar A 0.7/15 bar A 2/10 bar A
<b>Precision, [%]</b>	< 0.5% del valore misurato < 0.25% del valore misurato
<b>Temperature sensor</b>	PT – 1000 sensor, Class 4 4 wire connection.
<b>Pressure transducer</b>	High impedance (4kΩ) piezoresistive pressure transducer.



**Figure 142.** The volume converter implemented in the industrial size gas meter.

The following components are implemented in the device (Figure 143):

- Modem for data communication;
- GSM/GPRS antenna;
- Terminal block for input / output of power supply cables and sensor communication;
- Terminal block for RS 232 communication;
- Processor card for the elaboration of metrological data;
- Six – key keyboard;
- Front casing;
- Input and output cards;
- Supply power battery pack;
- Back up battery.

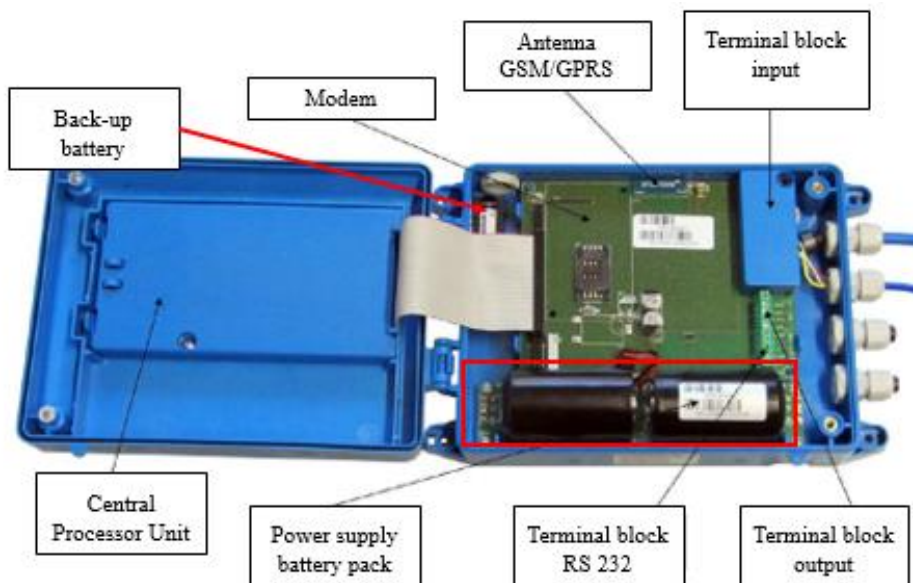


**Figure 143.** Main components visible in the internal side of the examined device.

As reported, a backup battery is present in the device in order to ensure power supply in case of complete discharge of the main battery pack (Figure 144). However, a limited electric capacity is guaranteed to ensure the minimum time waiting the substitution of the main pack.



**Figure 144.** Main power supply battery pack installed in the examined device.

A LCD display composed by three rows of sixteen characters each is present in the device. In this eight indicators that gives information about its status are present. Particularly, a defined sequence is completed during the communication as reported in the following figures derived from the experimental activity.

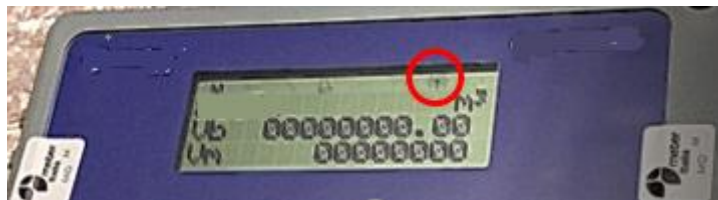


**Figure 145.** GSM indicator is switched on when the registration in the network is completed.



**Figure 146.** Telephone indicator (left) and GSM indicator (right) during the data transmission.



**Figure 147.** SMS indicator (left) and GSM indicator (right) at the end of the communication.

That is, no information about absorbed current during each phase was present and so the batteries' operative life cannot be calculated with the available information. In fact, only the following data about the electrical status of the device are available:

- *The temperature inside the casing of the device.* Even if this temperature is not the operative temperature of the battery it can be assumed a negligible difference between the two;
- *Power supply voltage.* The voltage measured is shown with a resolution of 0.1V and it can be used to understand if the power is supplied by the main battery pack or by the backup battery (Figure 138);

- *Percentage of remaining life.* An estimation of the residual life of the battery is given, even if it is not clear how it is calculated and no indication has been given by the manufacturer.



**Figure 148.** Power supply voltage indication. As shown the main battery pack is supplying power to the meter.

## 7.4 Main technical characteristics of the power supply battery pack

The smart meter converter is power supplied by a battery pack constituted by two thionyl chloride lithium batteries (LiSOCl<sub>2</sub>), which supply energy both to the metrology part and to the modem for data transmission. The main characteristics of each battery are shown in Table 88.

**Table 88.** Main technical characteristics of converter power supply batteries.

Parameter	Value
<b>Nominal capacity</b> (calculated with a discharged current of 15 mA and a cut-off voltage equal to 2.0 V), [Ah]	13.0
<b>Open circuit voltage</b> , [V]	3.67
<b>Nominal voltage</b> , [V]	3.60
<b>Maximum continuous discharged current</b> , [mA]	1800
<b>Maximum pulsed discharged current</b> , [mA]	4000
<b>Operative temperature range</b> , [°C]	-60 / +85

In the reported case, a minimum operative life of at least 5 years is guaranteed by the manufacturer in the following standard operating conditions:

- Data storage interval: 1 value representative for each hour;
- Data communication: 2 min/day;
- Display activity: 2 min/day;
- Input pulse frequency: ≤ 5 Hz;
- Measuring range: 15 seconds;
- Ambient temperature: 25 °C;
- GSM / GPRS field strength: excellent.

However, the real operating conditions in the field may differ from the defined conditions resulting in a lower life. Therefore, to better understand how the installed batteries work, an insight in their characteristics is proposed.

### 7.4.1 Electrochemical characteristics of the LiSOCl<sub>2</sub> batteries

In the installed batteries the oxidation of the lithium verifies at the anode in accordance to the following chemical reaction:



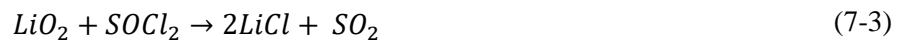
As shown, lithium ions ( $\text{Li}^+$ ) and electrons ( $e^-$ ) are produced. The ions go to the cathode where react with the thionyl chloride ( $\text{SOCl}_2$ ) producing lithium chloride ( $\text{LiCl}$ ), sulfur ( $\text{S}$ ) and sulfur dioxide ( $\text{SO}_2$ ). The electrons, instead, move in the external circuit reaching the cathode reducing the thionyl chloride.

The complete reaction is therefore:



The solid products, i.e. the lithium chloride and the sulfur, are deposited on the cathode where porous carbon is present; therefore, the quantity of carbon has to be sufficient in order to guarantee enough free space for the deposition which rate depends on the discharged current. Instead the sulfur dioxide ( $\text{SO}_2$ ), that is in a gaseous phase, dissolves in the electrolyte avoiding the increase of pressure inside the casing.

Another chemical reaction occurs during battery storage before the operation. Particularly, the formation of a lithium chloride passivation film ( $\text{LiCl}$ ) is present on the anode produced by the reaction of lithium with thionyl chloride according to the following reaction:



The created film has insulating properties reducing further reactions between lithium and electrolyte, and so preserving the electrical energy the battery.

That is, the thionyl chloride batteries include several components (Figure 149). The anode usually consists of a thin lithium plate separated from a generally non-aqueous mixture of thionyl chloride and lithium tetrachloroaluminate ( $\text{LiAlCl}_4$ ); the first acts as cathode while the second increases the electrical conductivity of the mixture. All the components are contained within a metallic casing that shield against the possible impact with external bodies and resist against the internal pressure produced during the discharge [161]



**Figure 149.** Main components within the battery (source [161]) and some available lithium thionyl battery available in the market.

### 7.4.2 Main phenomena occurring in the lithium thionyl batteries

Several phenomena have to be taken into account during the operation of the lithium thionyl batteries such as:

- *Voltage delay.* When the load is for the first time closed on the battery, a voltage reduction higher than that expected verify because of the presence of the passivation layer that acts as an additional resistance [162]. From a performance point of view, voltage delay is a transitory phenomenon and therefore it has not to be considered critical for the application.
- *Influence of the operative temperature.* Operating temperature is responsible for battery performance variations because of the influences on the internal resistance; in particular, as the outdoor temperature decreases, the available capacity is reduced due to the increase of the internal resistance. Therefore, attention should be given to the working temperature of the battery in order to estimate remaining life.
- *Self-discharge.* Battery self-discharge determines a reduction of the available capacity and it can be present both during storage and power supply operations. In the literature few jobs and correlations are able to identify a correlation between the intensity of the phenomenon and battery operating conditions, even if it is believed that a reduction of the self-discharge rate occurs over time and that peaks are present in the case of pulsed discharge [161].

However, there are three methods to quantify self-discharge. The first one is based on the direct measurement of the residual capacity after a defined time; the second is based on the implementation of an accelerated aging process, while the third is based on the measurement of the dissipated heat associated with the phenomenon and converted by means of complex thermodynamic models in self-discharge currents.

As said a preliminary distinction can be made between the phenomena that occurs during storage and those that verify during battery discharge. In the first case, several impurities such as  $\text{Li}_2\text{O}$  or  $\text{LiOH}$  are present in the lithium at the anode. After the contact, a reaction between  $\text{Li}$  and  $\text{SOCl}_2$  occurs with the formation of a thin and compact  $\text{LiCl}$  layer. This layer, that is usually called Solid Electrolyte Interphase (SEI), is principally constituted of lithium ions and present a high electrical resistivity. After the SEI formation, a second porous layer constituted of pure  $\text{LiCl}$  is formed creating the so called Passivation Layer. [163] suggested the following expression to calculate the capacity loss during the storage phase as a function of the storage temperature:

$$\text{Loss} = A \times e^{\left(\frac{-k}{RT}\right)t} \quad (7-5)$$

Where  $A$  [%] and  $k$  [ $\text{J}/(\text{mol} \times \text{day})$ ] are parameters that depend on the battery chemistry,  $R$  is the gas constant equal to  $8.314$  [ $\text{J}/(\text{mol} \times \text{K})$ ],  $T$  is the storage temperature [ $\text{K}$ ] and  $t$  is the storage time [ $\text{day}$ ]. As shown the capacity loss increase with the storage temperature and with the storage time. Another correlation to calculate the self-discharge current during storage is proposed by [164].

During power supply, the reduction of the passivation layer thickness is balanced by the production of  $\text{LiCl}$  at the anode. In order to estimate the importance of the phenomenon the faradaic efficiency  $\varepsilon$  is introduced:

$$\varepsilon = 1 - \frac{Q_{\text{discharge}}}{Q_{\text{tot}}} \quad (7-6)$$

Where  $Q_{\text{discharge}}$  is the heat emitted by the battery due to self-discharge [W] while  $Q_{\text{tot}}$  is the total heat emitted [W]. As shown,  $\varepsilon$  ranges between 0 and 1 where the value 1 is obtained in absence of self-discharge. As reported by [165], self-discharge increases with the discharged current and particularly in the case of pulse discharge; for the scope, a Duty Cycle (DC) is introduced in order to characterize the pulse discharge:

$$\text{Duty Cycle} = \frac{\Delta t_{\text{on}}}{\Delta t_{\text{off}} + \Delta t_{\text{on}}} \quad (7-7)$$

Where  $\Delta t_{\text{on}}$  is the time for which current is supplied [s] while  $\Delta t_{\text{off}}$  is the period in which no power supply is present [s]. As reported in Figure 150 self-discharge does not depend on the average current density up to  $1 \mu\text{A}/\text{cm}^2$ , while self-discharge decreases with the duty cycle for higher values.

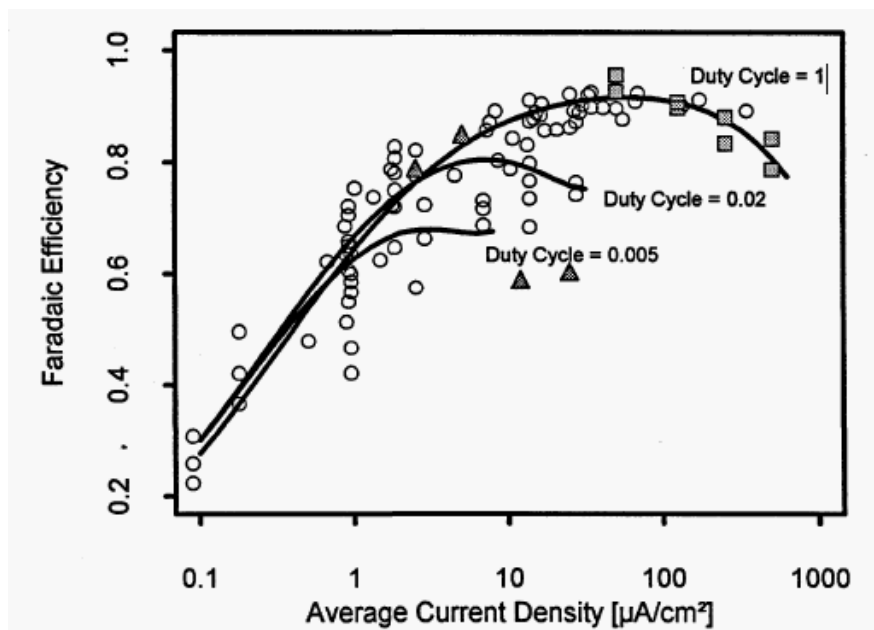


**Figure 150.** Faradaic efficiency as a function of the Duty Cycle and of the average supplied current. Source [165].

A correlation between self-discharge current density and average current density is proposed in [161] for a lithium thionyl battery. A size D battery with an anodic area of  $45 \text{ cm}^2$  with a duty cycle equal to 0.005 has been assumed:

$$j_d = 0.2817j + 0.2 \quad (7-8)$$

Where  $j_d$  and  $j$  are respectively the self-discharge current density and the supplied current density [ $\text{mA}/\text{cm}^2$ ]. Because of similar conditions are present in the specific application, the following discharge current has been calculated:

$$I_d = A \times j_d = 45 \times (0.2817j + 0.2) = 45 \times (0.2817 \times 28.7 + 0.2) = 0.37 \text{ mA} \quad (7-9)$$

- *Relaxation.* During data transmission a relatively high power is supplied for very short times. These conditions can be responsible for the deterioration of the battery due to the lack of relaxation as proposed in [166,167]. As reported in these works, battery performances depend on:
  - *Standby time:* it is the time delay between each impulse. An improvement occurs with its increase;

- *Pulse duration*: it is the interval for which power is supplied. In order to optimize battery performances, standby time is proportional to the square of the pulse duration.
- *Standby current*. The standby current has to be considered for the calculation of the battery operative life however it can be considered negligible respect to the relaxation phenomenon.

That is, no simple correlation exists in literature about the calculation of the optimum discharge time. However, because of the standby current has not to be considered for the phenomenon it is assumed that no issues are present to reach battery relaxation. In fact, 86,400 seconds (1 day) are present between two successive pulses due to data communication.

### 7.4.3 Available electrical capacity

LiSOCl<sub>2</sub> battery capacity depends on operative temperature and discharged current as reported by several manufacturers and reported by commercial datasheet. In Figure 151 the capacity curves are reported as a function of current and operative temperature. As shown in the figure, above 50 mA the available capacity increases with the operative temperature and decreases with the supplied current.

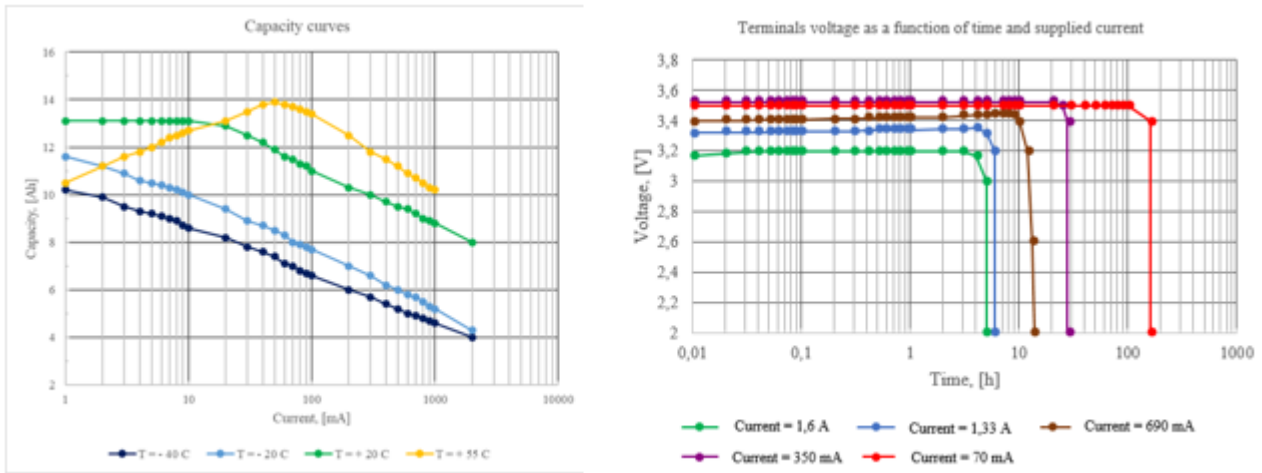


**Figure 151.** Capacity curves as a function of the operative temperature and supplied current (left) and voltage curves as a function of supplied current and time (continuous discharge is considered) (right).

The identified behaviour is explained as follow. A Thevenin equivalent circuit can be considered to schematize the battery. The voltage at the terminals  $V_L$  [V] can be written as:

$$V_L = V_0 - R_i \times I \quad (7-9)$$

Where  $I$  the discharged current [A] on the load,  $V_0$  is the open circuit voltage [V] and  $R_i$  is the internal resistance [ $\Omega$ ] that can be assumed function of the operative temperature in accordance to the following:

$$R_{INT} = A \times e^{-\frac{b}{R}T} \quad (7-10)$$

Where  $A$  [ $\Omega$ ] and  $b$  [J/mol] are parameters that depends on the specific battery. Considering a pure resistive load  $R_L$ , the supplied current current can be calculated as:

$$I = \frac{V_L}{R_L} \quad (7-11)$$

Consequently, introducing equation (7-11) in (7-9) it results:

$$V_L = V_0 - R_i \times \frac{V_L}{R_L} \rightarrow V_L = \frac{V_0}{\left(1 + \frac{R_i}{R_L}\right)} \quad (7-12)$$

That is, battery capacity is calculated as:

$$C = \int_0^{t(V_L=2.0V)} I \times dt \quad (7-13)$$

Considering equation (7-10), (7-12) and (7-13) a lower capacity is therefore available in the case of low temperature and high current because of it is required less time to reach the cut-off voltage, i.e. the voltage under which the battery is considered as completely discharged.

## Chapter 8

### Method and materials

In the present chapter the method and the materials considered for the development and the performance of the experimental activity are reported.

#### **8.1 Data transmission configurations analysed**

In order to reach the desired operative life four possible configuration have been considered for data transmission. Different quantity of data and frequency of transmission are present:

1. The first configuration is defined in order to have a baseline respect which compare the other ones. For the scope, existing configuration is considered;
2. A second configuration with a lower quantity of communicated data is introduced. Because of pressure data is not used at the moment it has been decided to avoid its transmission;
3. A third configuration with the same amount of data but a lower frequency of communication than the first one is evaluated. That is, data transmission is performed every two days instead every day;
4. A fourth configuration characterized by a lower amount of data and a reduced transmission frequency is analysed. In accordance to the second and the third configuration, pressure information is not sent and data are transmitted to the Central Acquisition System every two days.

Four converters have been supplied by the DSO for the analysis (Figure 152).



**Figure 152.** One of the four converters analysed in the experimental activity.

Furthermore, in order to speed up the test, it was initially evaluated the possibility to make a communication every hour in order to have the equivalent of 24 days for each day. However, because of the impossibility to implement this condition in existing Central Acquisition System, a daily communication has been performed increasing the time required to obtain significant statistical results.

## 8.2 Instrumentation used during the experimental activity

Because of no information is available about the supplied electrical loads, it has been decided to measure the supplied electrical current; for the scope an ammeter has been inserted in series with the load (Figure 153). For the scope, the ammeter has to be characterized by the lowest electrical resistance as possible in order to reduce the error.

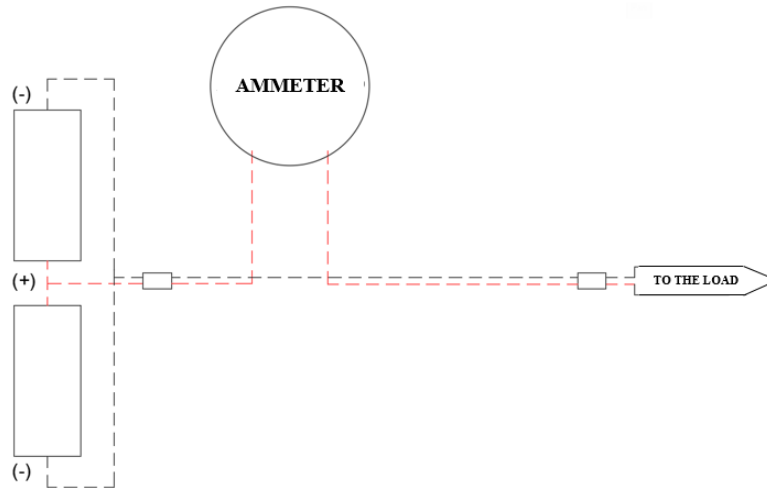


**Figure 153.** Schematic electrical wiring implemented to measure the discharge current by the battery pack.

During the experimental activity different instrumentations have been used as reported in following sections.

### 8.2.1 The tester ISOTECH IDM 305

The ISOTECH IDM 305 tester (Figure 154) is a high-precision measuring instrument that allows the measurement of many electric variables such as the electric current and the DC voltage. Many features are implemented in it including the automatic calibration, the check of eventual damages and the automatic selection of the optimum measurement range.



**Figure 154.** The tester ISOTECH IDM 305. In the images the front view (left) and the its application for the measurement of the battery pack voltage (right) are reported.

The main technical parameters of the meter are reported in Table 89.

**Table 89.** Main technical parameters of the ISOTECH IDM 305 reported in available datasheet.

Main characteristics	Value
Sampling rate, [times/sec.]	2
Operative temperature, [°C]	[0; 30[ °C with a maximum humidity of 80%; [30; 40[ °C with a maximum humidity of 75%; [40; 50] °C with a maximum humidity of 45 %
<b>Voltage measurement performance</b>	
Accuracy, [%]	±0.06% of the full scale up to 4.0 V
Electrical impedance, [ $\Omega$ ]	10 M $\Omega$ , < 100 pF
Overload protection, [V]	1000 V <sub>DC</sub>
Resolution, [V]	10 <sup>-6</sup> up to 40 mV
<b>Current measurement performance</b>	
Maximum input current, [A]	10
Accuracy, [%]	±0.2% of the full scale in the following ranges: < 40 mA; [40; 400[ mA, [400, 4A]
Resolution, [A]	10 <sup>-6</sup> up to 40 mA
<b>Other characteristics</b>	
Protection Class IP	IP 64
Safety	IEC 61010 – 1: CAT III 600 V / CAT II 1000 V
Power supply	9 V <sub>DC</sub>
Size, [mm]	100 (W) x 212 (L) x 55 (H)
Weight, [g]	650

The electrical wiring is ensured by the connection of the cables with battery connectors. In the first phase some tests have been performed in order to measure the battery voltage and so verify the relaxation phenomenon. In this case, the tester was connected in parallel with the load. In order to measure supplied current, instead, a connection in series to the load is made (Figure 155).

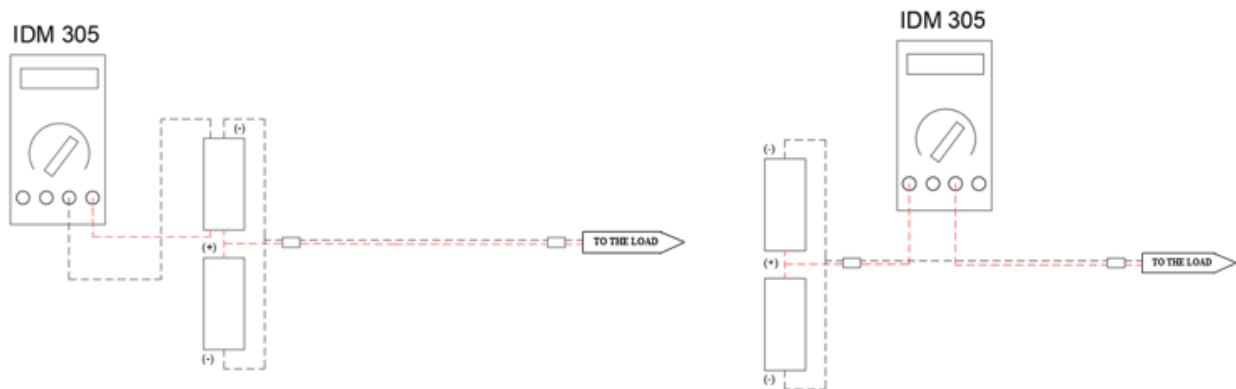


**Figure 155.** Voltage measurement (left) and current measurement (right) with the ISOTECH IDM 305.

The tester was used only in the first phase of the experimental activity, with the aim of calibrating and verifying the applicability of other measurement equipment. In fact, despite of the high accuracy, a long time would have been required in order to record and to manually transfer the data to a PC platform.

### 8.2.2 The multimeter AGILENT 34401A

In order to measure the supplied current, also the multimeter AGILENT 34401 A was used (Figure 156). The same wiring configuration of tester ISOTECH IDM 305 was used so it is not repeated in the text. This

instrument was used only in the first phases of the experimental activity in order to compare the measurement of the tester IDM 305 and so to ensure an automatic recording and data processing.



**Figure 156.** The multimeter Agilent 34401 A connected to one of the four analysed converters.

The main technical characteristics of the instrument are reported in Table 90.

**Table 90.** Main technical performance of the AGILENT 34401A available in technical datasheet.

Main characteristics	Value
Sampling rate, [#/sec.]	0.15, 1, 20, 50
Operative temperature, [°C]	[0; 55[ °C [0; 40[ °C with a maximum humidity of 80%;
<b>Voltage measurement performance</b>	
Overload protection, [V]	1000
Accuracy, [%]	$\pm 0.005\%$ of reading + 0.0001% of the range
Input resistance, [M $\Omega$ ]	10 M $\Omega$ up to 10 V
<b>Current measurement performance</b>	
Maximum measured current, [A]	3
Accuracy, [%]	$\pm 0.002\%$ of reading + 0.0020 of the range up to a 10 mA, $\pm 0.002\%$ of reading + 0.00050 of range up to 100 mA, $\pm 0.0050\%$ of reading + 0.0010 of range up to 1 A
Shunt resistor, [ $\Omega$ ]	0.1 $\Omega$ for 1 A and 3 A range. 0.5 $\Omega$ for 10 mA and 100 mA range.
<b>Other characteristics</b>	
Safety	In accordance to CSA, UL – 1244, IEC – 348
Voltage power supply, [V]	100 V / 120 V / 220 V / 240 V $\pm 10\%$
Average electrical consumption, [W]	10
Size, [mm]	245.4 x 374.0 x 103.6
Weight, [kg]	3.6

That is, it was not possible to use this instrument during the activity due to the difficulty to modify the sampling rate set up. Furthermore, another issue occurs regarding the location where the multimeter is installed; in fact, a very low signal coverage is present. Therefore, when the converter attempted to connect to the network a negative exit results and so no useful information was available for following analysis. Because it was not possible to move to another place the multimeter, it was decided to not continue to use the AGILENT 34401.

### 8.2.3 The Arduino INA 219 module

The INA 219 module allows the contemporary measurement of the current and of the battery voltage, through the implementation of the Arduino software (Figure 157). The module is produced by Texas Instruments and

programmed by Adafruit for the implementation in Arduino. Three separate components are provided by the manufacturer. These components have to be carefully assembled in order to avoid overheating and so damages to the sensors.



**Figure 157.** Components of the Arduino INA 219 (left) and assembling phase (right).

An electric wiring diagram for the connection and a code is supplied by Adafruit for the implementation in Arduino (Figure 158).

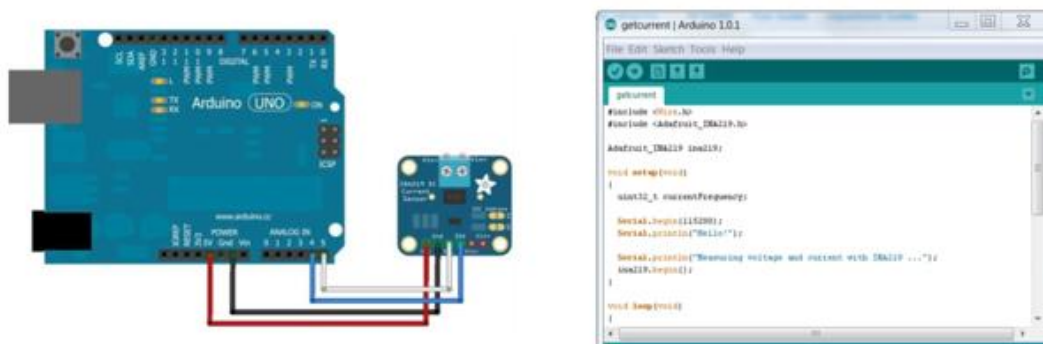


**Figure 158.** Electrical wiring diagram for the connection with the Arduino card (left) and software code (right).

Following the identified procedure, a INA 219 module has been installed in the Arduino board; after that the module has been connected to the converter Figure 159 in order to measure the required parameters. An unused plug has been implemented for the connection with the power supply socket present in the converter.



**Figure 159.** The INA 219 module (red) installed in the Arduino board (left) and connection with the analysed converter (right).

The main technical characteristics of the instrument are reported in Table 91.

**Table 91.** Main technical performances of the INA 219 module available in technical datasheet.

Main characteristics	Value
Operative temperature, [°C]	[- 40; 125]
<b>Voltage measurement performance</b>	
Full scale voltage range, [V]	32
Bus voltage measurement error, [%]	±0.2% (average), ±0.5% (max)
<b>Current measurement performance</b>	
Upper range limit, [A]	32
Shunt resistance, [Ω]	0.1
Resolution, [A]	0.1 mA in the range [0; 400[ mA 0.8 mA in the range [0.4; 3.2] A
Current measurement error, [%]	±0.2% (average), ±0.5% (max)
<b>Other characteristics</b>	
Voltage power supply, [V]	6
Average electrical consumption, [mW]	6
Size, [mm]	3.91 x 4.90
Weight, [g]	3.4

### 8.3 Method

In the following paragraphs the method used in order to estimate battery's operative life is shown. Thanks to the methods the identified procedure can be applied to all smart meters regardless their size.

#### 8.3.1 Electric loads characterization

Two steps have been identified in order to characterize the power consumption of smart meter's converter. In the first one existing power consumption loads have been identified. Scope of this phase is to qualitative recognized how many loads are electrically supplied by the battery. For the scope, literature review of similar application and calls with converter's manufacturer have been done.

In the second step, power consumption has been measured in order to qualitatively and quantitatively characterize the supplied loads. In fact, for each j-th load the daily discharged capacity  $C_{day,j}$  [mAh/day] has been calculated as follow:

$$C_{day,j} = \int_0^t I_j(t) dt = \sum_{i=1}^N I_{i,j} \Delta t_i + \varepsilon \quad (8-1)$$

Where  $I_j$  is the supplied current to the j-th load [mA],  $t$  is the time [h]. A sampling interval of 50 ms in order to minimize the error  $\varepsilon$  has been considered. For this reason, it has been supposed that equation (8-1) is equivalent to:

$$C_{day} = \int_0^t I_j(t) dt \sim \sum_{i=1}^N I_{i,j} \Delta t_i \quad (8-2)$$

Respect to other loads, for communication also a distinction between good and bad signal coverage has been made in order to evaluate battery's performances in the best and worst cases. In fact, reducing signal coverage an increase of duration and so discharge capacity is verified. For this reason, experimental activity was divided in two parts. In the first one converters were maintained in a place characterized by good signal in order to

characterize communication and to compare different configurations in the best possible conditions. For the scope, only the duration of the transmission phase registered in CPL Concordia's Central Acquisition System was available. However, the recorded information was statistically analyzed for each configuration in order to calculate the average value  $\mu_t$  [s] and the standard deviation  $\sigma_t$  [s]

$$\mu_t = \frac{\sum_{i=1}^N x_i}{N} \quad (8-3)$$

$$\sigma_c^2 = \left( \frac{N}{N-1} \right) \times \frac{\sum_{i=1}^N (x_i - \mu_t)^2}{N} \quad (8-4)$$

Where N is the number of available samples  $x_i$ .

With the defined data it is possible to define a confidence interval within which the true value of the mean  $\mu_t$  is present with a confidence level equal to "1 -  $\alpha$ " where  $\alpha$  represents the Gaussian area outside the defined extremes through the use of equation (8-5).

$$\mu_t \in \left[ \mu_t - t_{N-1, \frac{\alpha}{2}} \sqrt{\frac{\sigma_c^2}{N}}; \mu_t + t_{N-1, \frac{\alpha}{2}} \sqrt{\frac{\sigma_c^2}{N}} \right] \quad (8-5)$$

Where the term  $t_{N-1, \alpha/2}$  is found in dedicated tables. Because of some anomalous values (outliers) were verified, the Chauvenet method has been applied in order to reject them; in fact, this criterion defines that all the points evaluated in the experimental tests should be found in a centered band around the mean value corresponding to a probability equal to  $1 - \frac{1}{2N}$  in the case that a Gaussian distribution and constant boundary conditions are present.

To conclude the first phase, statistical distributions for transmission duration have been introduced for the four configurations. Thanks to this assumption, it is possible to calculate the time duration within which the 99.5% of communications are present in case of good signal coverage. The obtained values for the different configurations can be considered as a threshold between good and bad signal coverage.

In the second phase, converters are moved to the University of Bologna where daily discharge current has been measured and capacity calculated in accordance to previous equations.

The total daily capacity  $C_{tot}$  [mAh/day] is finally calculated as:

$$C_{tot} = \sum_{j=1}^n C_{day,j} \quad (8-6)$$

Where n is the total number of loads power supplied by the battery's pack.

### ***8.3.2 Estimation of battery's capacity***

The estimation of available capacity is of fundamental importance in order to calculate the operative life. However, since it is a function of temperature and current, a value of current and temperature should be carefully evaluated. For the scope, Thevenin equivalent electrical circuit has been considered. Because of the battery is considered discharged when a voltage lower than 2.0 V is measured and because terminals voltage depends on supplied current as previously reported, communication has been considered the most critical load

in terms of discharged current. Particularly, a value representative of possible measured cases has been considered and calculated as follow:

$$I_{com} = \mu_{I,comm} + 2\sigma_{I,comm} \quad (8-7)$$

Where  $\mu_{I,comm}$  is the mean value in [mA] while  $\sigma_{I,comm}$  is the standard deviation in [mA]. In fact, it seems that a too much conservative estimation could result considering the maximum value; furthermore, this value is representative of the 97.75% measured current.

Once the reference current value has been identified, capacity has been described in accordance to the Arrhenius model [168]:

$$C(T) = a \times \exp\left(-\frac{b}{T}\right) \quad (8-8)$$

Where T is the operating temperature in [K], while a [mAh] and b [K] are characteristic quantities of the specific type of battery that have been interpolated from the available datasheet. It should be noted that different values have been found during the year as a function of the operative temperature in accordance to equation (8-8). However, because it can be assumed that the temperature difference between the internal side of the battery and the external side of the meter is negligible, external air temperature has been considered for the calculation. Particularly, two reference locations in the Emilia Romagna have been considered. For the scope, values of the external hourly air temperature at 1 m above the ground have been downloaded from Dext3r platform: in order to make a statistical evaluation three years have been considered.

Having assumed a Gaussian distribution for external temperature, the normalized value Z for each temperature has been calculated:

$$Z(T) = \frac{C(T) - \mu_C}{\sigma_C} \quad (8-9)$$

Where Z is the normal variable [#],  $\mu_C$  is the average capacity during the year [mAh] and  $\sigma_C$  is the capacity standard deviation [mAh]. It is therefore possible to associate the probability of occurrence to each temperature and so to the capacity.

### ***8.3.3 Estimation of battery's operative life***

Battery's residual life  $t_p$  [day] is simply calculated as the ratio between available capacity and daily discharged capacity

$$t_p(T) = \frac{C(T)}{C_{tot}} \quad (8-10)$$

Where C(T) and  $C_{tot}$  have been calculated in accordance to previous equations.

The total number of years  $y_p$  is calculated:

$$y_p(T) = \frac{t_p(T)}{365} \quad (8-11)$$

Thanks to the calculation of C(T), battery's residual life can be statistically evaluated. Therefore, for each analysed configuration the probability to reach a defined operative life is estimated.

A simple schematization of the proposed procedure is reported in Figure 160.

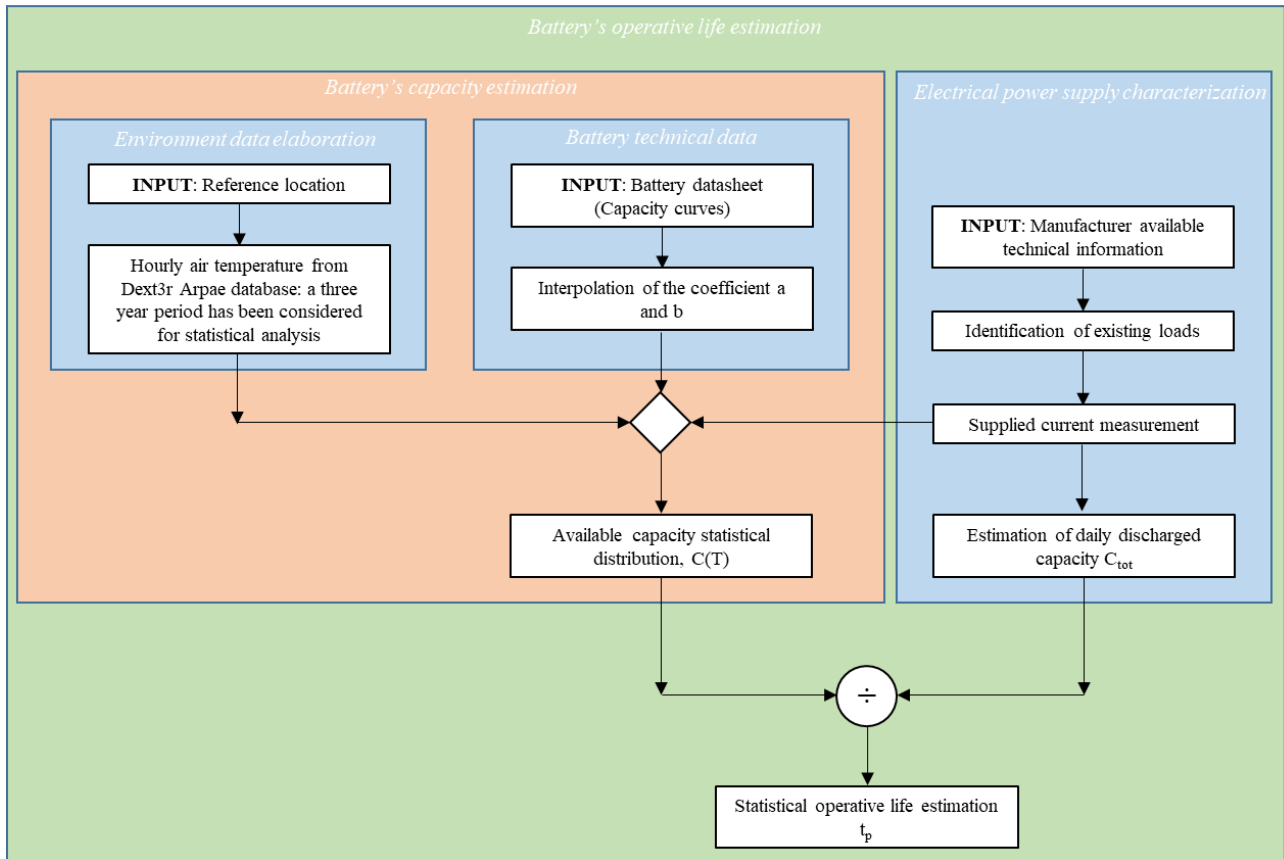


**Figure 160.** Flowchart of the proposed procedure to estimate battery's operative life.

## Chapter 9

### Results and discussion

#### 9.1 Available database

Even if the experimental activity started on 30/09/2017, no data was available until 15/10/2017 because a malfunction occurs in the dedicated Central Acquisition System.

The experimental activity was divided in two parts. In the first one the converters were kept at the DSO headquarters. Regarding this phase, data was available from 16/10/2017 to 14/12/2017 for the configurations 1 and 2, while for the configurations 3 and 4 it was decided to extend this phase until 7/02/2018 in order to have sufficient number of data to make statistical elaboration. For the purpose the following data was given by the operator of the Central Acquisition System:

- Date and time of converter's arrival on the remote server;
- Date and time of the first frame from the SAC to the converter: it represents the instant in which the SAC sends the identification request to the converter;
- Date and time of the first frame from the converter towards the SAC: it represents the instant in which the converter answers to the first question;
- Date and time of socket opening, required to receive and to transmit data;
- Date and time of socket end session.

As shown the data doesn't include information about the preliminary phase of connection to the network performed by the converter. This phase can be however considered independent from the configuration. A qualitative information about the influence of data quantity and of the transmission frequency can be obtained.

In the second phase, instead, electrical supplied current was measured at the University of Bologna. The measure was started on 20/01/2018 for configurations 1 and 2, while for configurations 3 and 4 the measure began on 9/02/2018. Even if the analysed data are until 20/05/2018 it was decided to continue the measurement in order to improve the confidence on statistical results. In both cases, environment temperature was controlled in order to reduce the possible influence of this parameter in the obtained results. A summary of the available data is reported in Table 92.

**Table 92.** Available database for the analysis.

Configuration	Total days (Modena)	Effective days (Modena)	Total days (Bologna)	Effective days (Bologna)
Configuration 1	60	53	121	92
Configuration 2	60	59	121	91
Configuration 3	59	57	51	23
Configuration 4	59	57	51	41

As shown, not all available days have been used. Particularly, the following days have been discarded:

- The days when the device was not able to connect to the SAC (first phase);

- The days when the device didn't start the communication procedure or it has not been possible to make the measurement.

During the experimental procedure some issues started with the configuration 3. It should be noted that this configuration start communication procedure 5 times on a total of 18 available after 9/04/2018. Several days were therefore lost even if no evident reasons justify it; in fact, device's manufacturer was contacted several times in order to solve the issues without getting any solution. However, the days following a lack of communication of the configuration 1 were considered for the configuration 3 in order to increase the available dataset. The same was done for the configurations 2 and 4.

## 9.2 Electrical loads' characterization

In accordance to manufacturer's experience, four main electrical loads have been identified in the analysed device. Following this step, current was measured firstly with high precision instrumentation (Tester ISOTECH IDM 305 and AGILENT 34401A) and after with the sensor INA 219 implemented in an Arduino board. A good comparison between the three instruments have been observed. From data analysis the following results (Figure 161):

- *Base load.* A current between 0.25 and 0.30 mA is continuously present. However, it wasn't possible to identify what functions are responsible for the discharge. In fact, no electrical wiring diagrams and detailed information about CPU were available during the research activity. Furthermore, the calculated self-discharge current has been estimated to have a similar amplitude. Consequently, more detailed analysis should be performed to investigate this voice.
- *Sensors.* Installed sensors are power supplied every 20 seconds with an average current of 5 mA for a duration of about 0.5 s;
- *Display.* When switched on, the display is electrical supplied by an average current equal to 0.75 mA. The display automatically switches off if no actions is performed for more than 30 s;

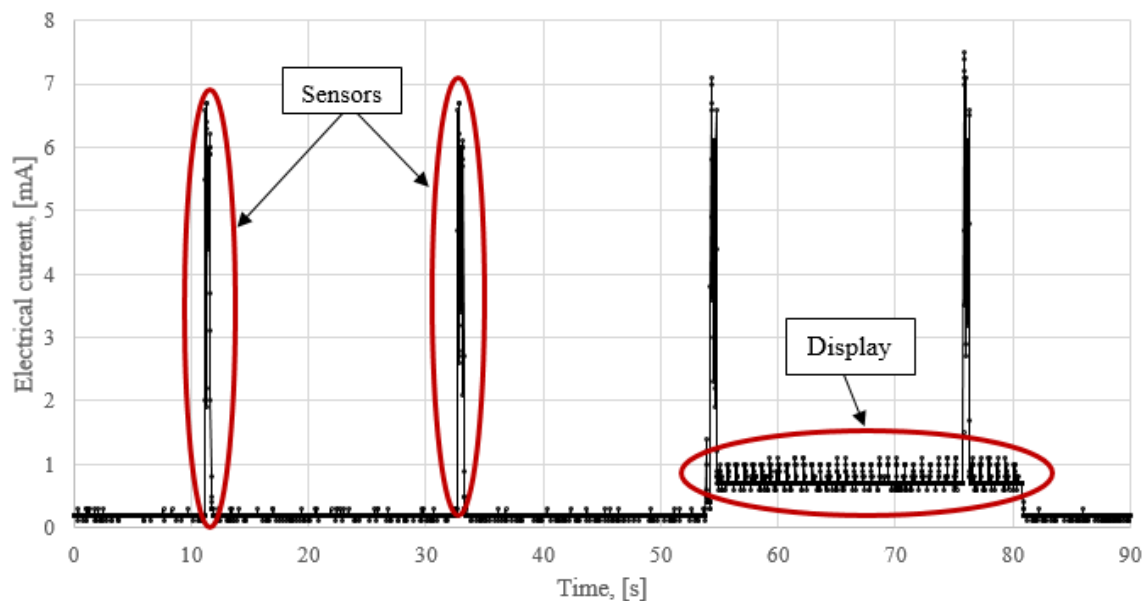


Figure 161. Battery's supplied current to base load, sensors and display.

- *Communication.* Supplied current and so capacity consumption depends on several factors including the quality of the signal during data transmission and the amount of transmitted data. Respect to other loads, a more in-depth analysis is preferred for its characterization.

Considering the first three voice and assuming that the display switches on for 2 min / day, the total daily discharged capacity for the three functions results:

$$C = \sum_{i=1}^3 I_i \times \Delta t_i = 0.25 \times 24 + 0.75 \times 2 \times \frac{60}{3600} + 5 \times 0.5 \times 3 \times \frac{60}{3600} \times 24 = 6 + 0.025 + 3 = 9.025 \frac{mAh}{day} \quad (9-1)$$

Therefore, 3.30 Ah/year is annually discharged, while a total value equal to 13.2 Ah has been estimated to be discharged after 4 years. Particularly, the base loads accounts for 66.5% while sensors for 33.2%. Without taking into account data transmission, a capacity higher than the nominal available in each battery is required for base load, sensors and display. Consequently, these loads should not be underestimated in following analysis.

### 9.3 Communication characterization

#### 9.3.1 Communication duration in the case of good signal strength

The following results have been obtained considering the data during the phase 1 of the experimental activity. In Figure 162, the number of days with a defined duration has been shown for each configuration; for the scope time steps equal to 0.25 s have been considered sufficient.

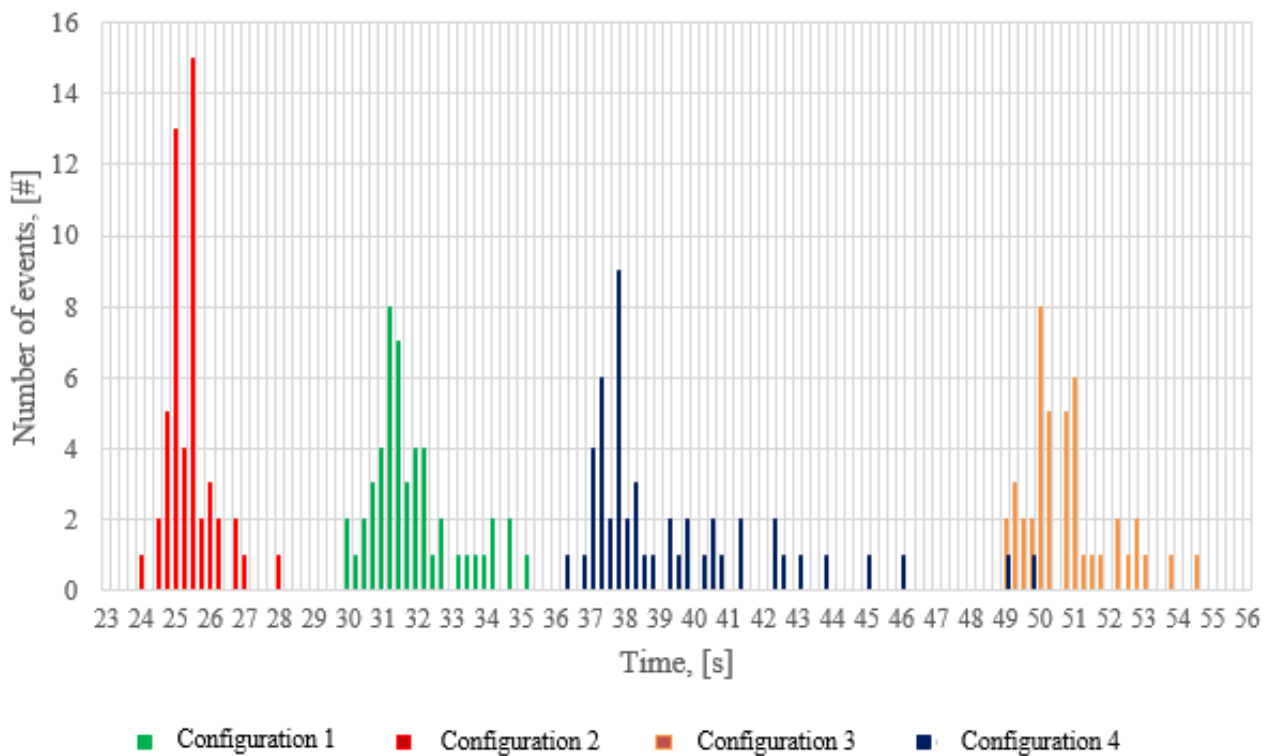


Figure 162. Number of days with a defined duration has been shown for each configuration.

From Table 93 it results that configuration 2 is characterized by the lowest mean value for each communication, followed by configurations 1, 4 and 3 in accordance to the increase of transmitted data for each communication. However, multiplying the obtained values for the transmission frequency, a different result is obtained. The minimum time duration for the data transmission is obtained for the configuration 4. A value almost lower than 40% respect the value is obtained for configuration 1. A reduction of 21.1% respect to configuration 1 is obtained also for the configurations 3 and 2. In fact, reducing the number of connection per day, some operations such as, for example, identification are made once every two days instead of every day.

As shown in Table 93, a greater standard deviation is obtained for configurations 3 and 4 respect to daily configuration. Furthermore, configuration 2 is characterized by the minimum value (-12.6% respect to the existing one). This can be justified by the fact that communication protocol is based on a typical master-slave configuration with successive questions and answer. Consequently, increasing the quantity of data to be transmitted in the single communication, any worsening of the network coverage during data transmission extends the total duration respect to nominal value.

**Table 93.** Summary of single communication time duration.

Configuration	Communicated data	Communication frequency	Mean value, [s]	Standard deviation, [s]	Mean confidence intervals, 99%
1	Same as the existing	Same as the existing (1 per day)	32.2	1.27	[31.7; 32.7]
2	No pressure	Same as the existing (1 per day)	25.4	1.11	[25.0; 25.8]
3	Same as the existing	1 every 2 days	51.1	2.58	[50.1; 52.1]
4	No pressure	1 every 2 days	39.1	2.03	[38.3; 38.9]

Assuming a Gaussian distribution, the probability density function can be identified. Elaborating mean values and standard deviation it can be also calculated the time duration of data transmission in the 99.5% of communications occurring in the case of good signal strength. Results are reported in Table 94.

**Table 94.** Probability density functions and time duration of data transmission in the 99.5% of cases.

Configuration	Probability density function	Time duration of data transmission in the 99.5% of cases*, [s]
1	$f_1(x) = \frac{1}{1.27 \times \sqrt{2\pi}} e^{-\frac{(x-32.2)^2}{2 \times 1.27^2}}$	35.5
2	$f_2(x) = \frac{1}{1.11 \times \sqrt{2\pi}} e^{-\frac{(x-25.4)^2}{2 \times 1.11^2}}$	28.3
3	$f_3(x) = \frac{1}{3.59 \times \sqrt{2\pi}} e^{-\frac{(x-51.1)^2}{2 \times 2.58^2}}$	60.0
4	$f_4(x) = \frac{1}{3.39 \times \sqrt{2\pi}} e^{-\frac{(x-39.1)^2}{2 \times 2.03^2}}$	44.3

\* Calculated as  $x = \mu + 2.58\sigma$

In the second phase of the experimental activity it has been possible to analyse all the communication starting from modem switching on until the end of communication in which the modem is switched off. A summary of the obtained results is reported in Table 95. Multiplying the obtained values for the transmission frequency, it is observed that configurations 2, 3 and 4 respectively show a reduction with respect to the current

configuration of 6.8%, 39.1% and 45.3%. Furthermore, it results that almost a great amount of time is spent to connect the converter to the network and to end the session. In fact, more than 40 sec. are required for these operations for all the analysed configurations.

**Table 95.** Duration of the overall communication phase in the case of a good signal strength.

Configuration	Communicated data	Communication frequency	Number of bytes, [bytes]	Mean value, [s]	Standard deviation, [s]
1	Same as the existing	Same as the existing (1 per day)	852	76.7	2.3
2	No pressure	Same as the existing (1 per day)	710	71.5	1.8
3	Same as the existing	1 every 2 days	1136	93.4	3.1
4	No pressure	1 every 2 days	994	83.1	3.6

Considering a statistical distribution, it is possible to calculate the total duration in which are included the 99.5% of communications as made the phase of data transmission in the case of good signal coverage. From the analysis of Table 96, a very important result appears: multiplying the obtained values for the transmission frequency it is possible to evaluate the effective time savings for each configuration to communicate data representative of the same number of days. As shown, it results a very important saving in the case of configurations 3 and 4 because of half of connections are required respect to daily configuration in order to communicate data regarding the same number of days. Consequently, communication frequency has a very great impact respect to time communication savings.

**Table 96.** Time duration of data transmission and of total communication phase in the 99.5% of cases.

Configuration	Time duration of data transmission in the 99.5% of cases*, [s]	Time duration of communication in the 99.5% of cases*, [s]	Minimum time saving respect to existing configuration**, [%]
1	35.5	82.6	0
2	28.3	76.1	-7.9
3	60.0	101.4	-38.6
4	47.8	92.4	-44.1

\* Calculated as  $x = \mu + 2.58\sigma$   
 \*\* Communication frequency has been considered in the calculation to normalize respect to the number of days communicated

No conclusions at this point can be identified about capacity savings. In fact, data about supplied current and so capacity has to be firstly analysed in order to evaluate the effective supplied current in each communication phase.

### 9.3.2 Analysis of supplied current in the case of good signal strength

During communication different operations are performed. Figure 163 shows the supplied current for configuration 1 in the case of good signal strength while Figure 164 reports also battery's voltage. Three main phases can be identified from the figure:

- *Phase 1: Modem switch on and GPRS registration on the network.* In this phase, the modem has to be connected to the network in order to start data communication. As shown, several peaks which

amplitude appear depending on the signal strength. Particularly, reducing signal coverage an increase of peaks amplitude and so of mean current is observed;

- *Phase 2: Data transmission and connection switch off.* In this phase, data are communicated to Central Acquisition System. In the figure is evident the structure of the protocol characterized by question from the SAC and successive answers by the converter. In the figure, because of the configuration 1 is reported, six peaks can be identified during the phase 2. Finally, at the end of the phase, transmission is finished.
- *Phase 3: Final checks and modem switch off.* In the last part of communication, final checks and modem switch off is observed. Respect to the other two phases, very few peaks are present and current is nearly constant to a mean value equal to 60 mA. This condition results by the fact that signal coverage has no influence during this phase.

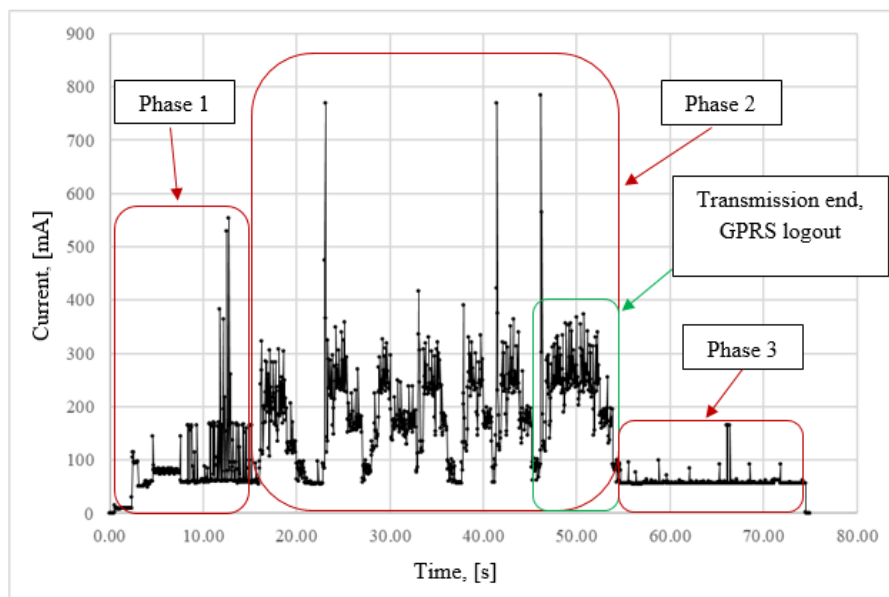


**Figure 163.** Supplied current by the battery for configuration 1. A good signal strength was present.

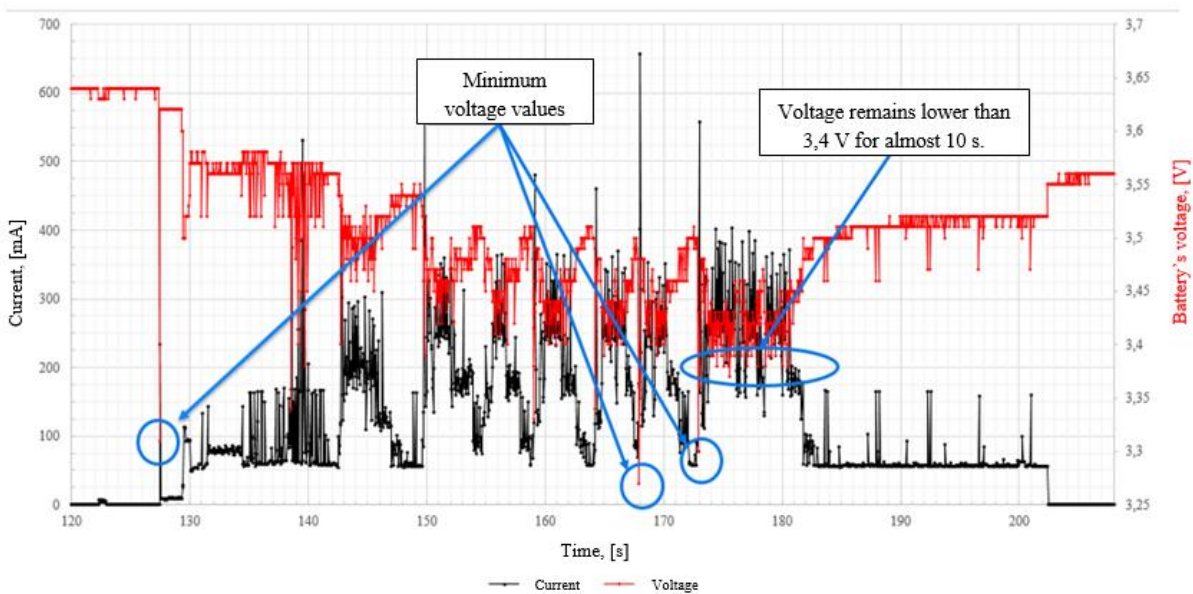


**Figure 164.** Current and voltage trends during communication for good coverage conditions in the case of new battery.

Respect to configuration 1, other configurations present almost the same first and last phases while in the phase 2 more or less peaks are present as a function of the number of transmitted data. In the following figures, five recorded cases for each configuration are reported. It should be noted that the analysed cases do not necessarily are referred to the same day. In fact, because of the communications do not verify in the same instant different signal coverage conditions can be present.

As shown from Figure 165 to Figure 168, the reported phases are present in all the configurations. However, considering the same configuration, some differences in the supplied current can verify due to the variation of signal strength during the communication.

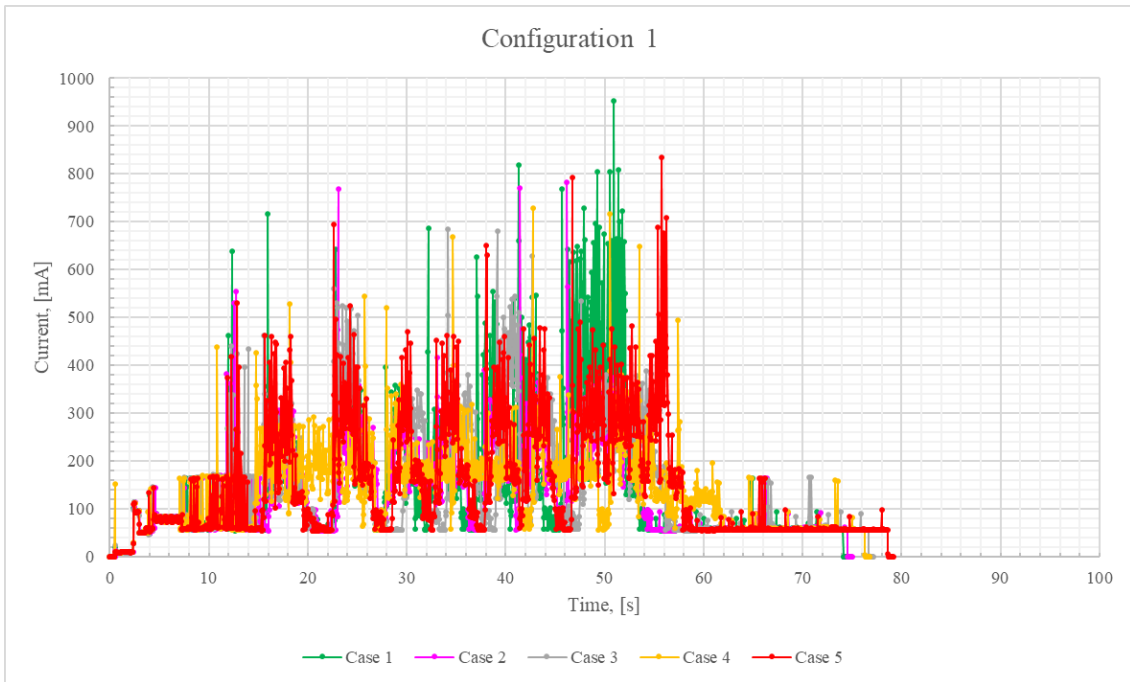


**Figure 165.** Measured current during communication for the configuration 1. Five samples have been reported.

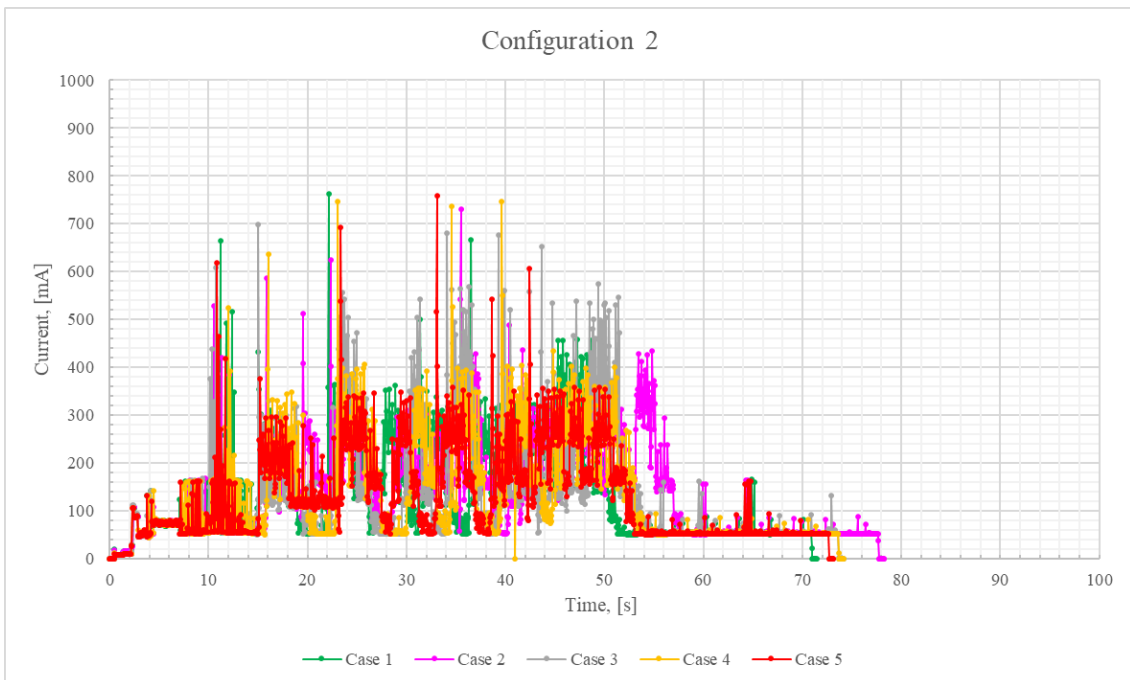


**Figure 166.** Measured current during communication for the configuration 2. Five samples have been reported.

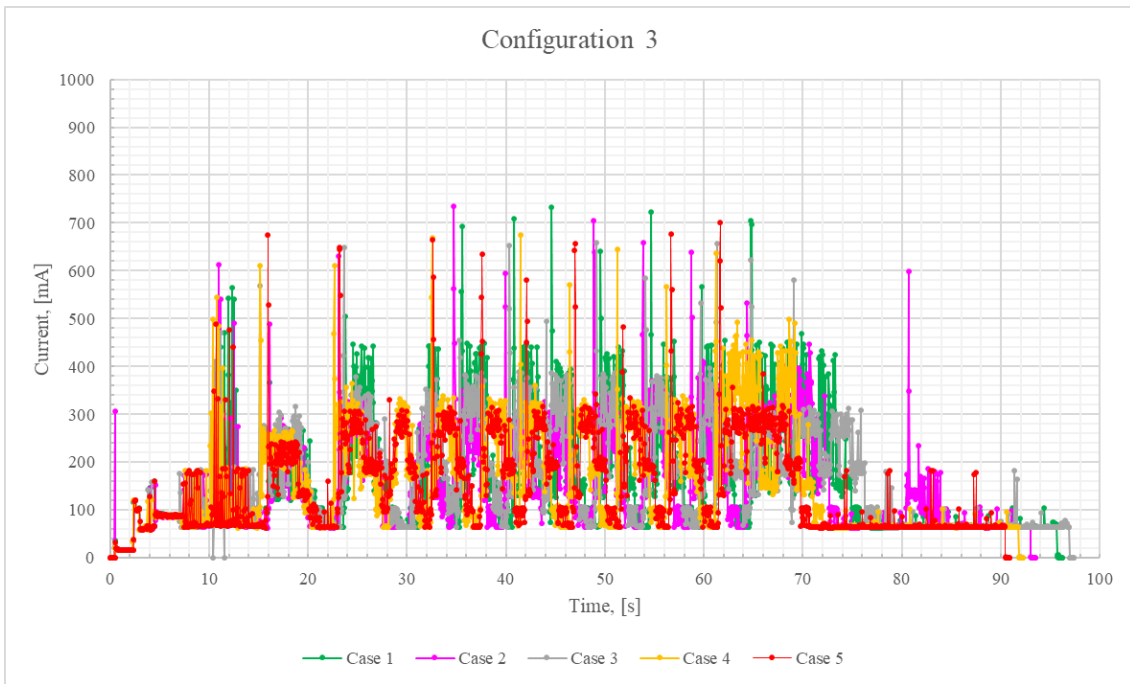


**Figure 167.** Measured current during communication for the configuration 3. Five samples have been reported.

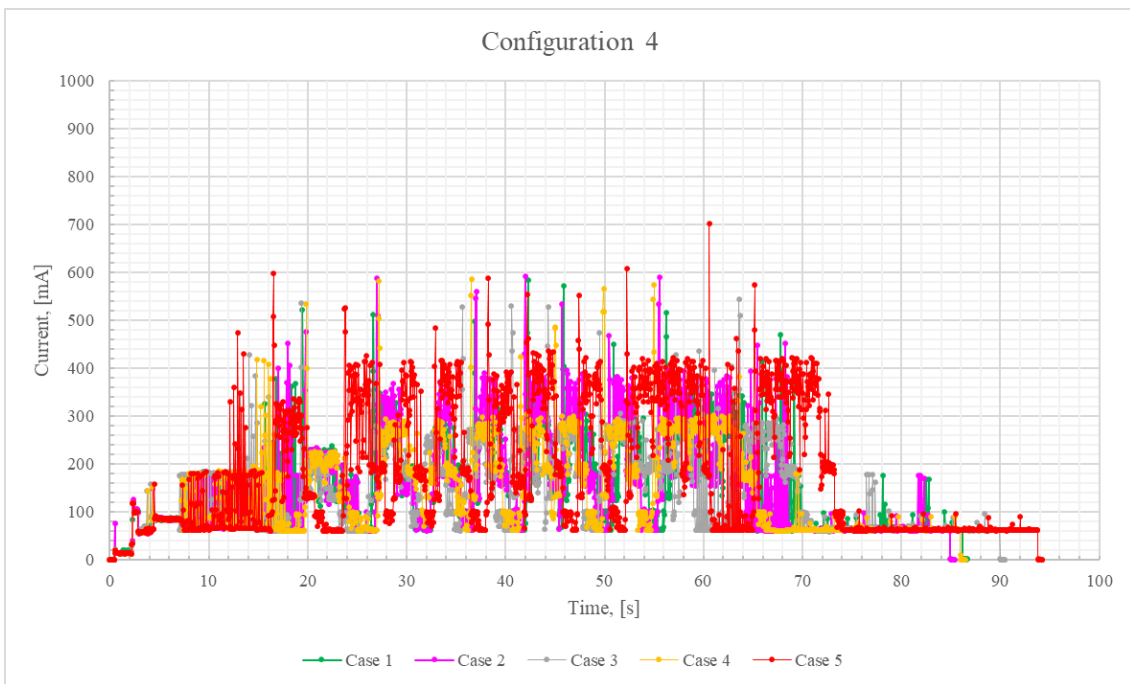


**Figure 168.** Measured current during communication for the configuration 4. Five samples have been reported.

Two considerations about the implemented communication protocol can be made considering the reported figures:

- Considering the total number of transmitted bytes and the mean value of transmission duration, it is possible to calculate the number of byte transmitted per second for each configuration. This quantity is not exactly the bit rate, that is the transmission velocity, because of waiting times between two messages and other operation performed by the converter are considered. As expected the lowest value is calculated for the configuration 3 (22.3 byte/sec.), followed by configuration 4 (25.4

byte/sec.), configuration 1 (26.5 byte/sec.) and configuration 2 (27.8 byte/sec.). Therefore, increasing the number of messages, more time is spent for secondary operations required to complete the communication with the existing protocol;

- The master – slave configuration result detrimental in the case of poor signal strength. In fact, because of signal strength conditions can change very quickly during communication, it results very difficult to estimate the discharged capacity. This issue becomes more severe as the number of messages sent by converter increases.

Therefore, as introduced, the signal strength greatly influences battery’s operative life. For this reason, an analysis of the identified three communication phases is reported as a function of time duration in the next sections.

### 9.3.3 Calculation of the discharged capacity during communication

The calculation of the discharged capacity is performed considering the three different phases that have been identified in the previous section during the communication.

In Figure 169, supplied capacity in phase 1 is shown as a function of the duration of the phase of all the four configurations. Analysing the behaviour, it seems that no precise protocol is set in order to interrupt converter connections. In fact, interruptions’ attempts (red points) have occurred in a very large interval between 60 seconds up to 900 sec. This condition is responsible for an increase of supplied current and so of discharged capacity. However, a linear trend between capacity and time duration is evaluated, making therefore possible a preliminary estimation of discharged capacity in real application.

Consequently, a timer which automatically interrupts the connection is suggested.

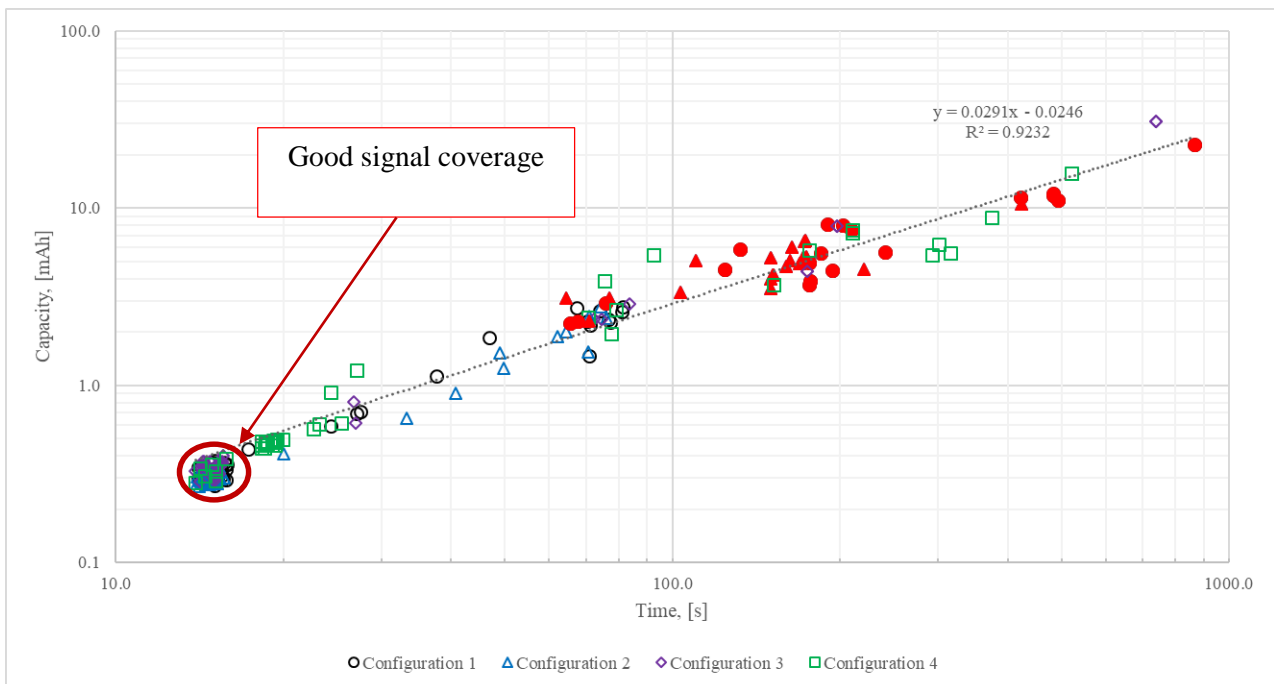


**Figure 169.** Capacity [mA] during the phase 1 for the four configurations. The points circled in red represent those events in which the converter tries to connect to the network without success.

Other data about the phase 1 are reported in Table 97. As shown, a mean capacity equal to 0.3 mAh is discharged in the case of good signal coverage. Furthermore, no great difference is also present in standard deviations for the four configurations because of the same connection procedure is performed.

**Table 97.** Consumption analysis of phase 1 for the four configurations.

Configuration	Mean time duration good signal strength, [s]	Mean capacity for good signal strength, [mAh]	Standard deviation for good signal strength, [mAh]
1	14.9	0.32	0.02
2	14.7	0.30	0.02
3	14.9	0.33	0.03
4	14.8	0.33	0.04

Regarding phase 2, capacity supplied during communications has been calculated and reported in Figure 170 where the specific capacity per byte is reported as a function of time. Detailed data are reported in Table 98.

As shown, configuration 2 is responsible for the lowest mean capacity in the case of good signal strength, followed by configurations 1, 3 and 4. An increase of standard deviation occurs with time duration with the exclusion of configuration 4 which is characterized by the lowest standard deviation. Because of this result is in contrast with what expected, detailed analysis will be made in future activities to find possible explanation.

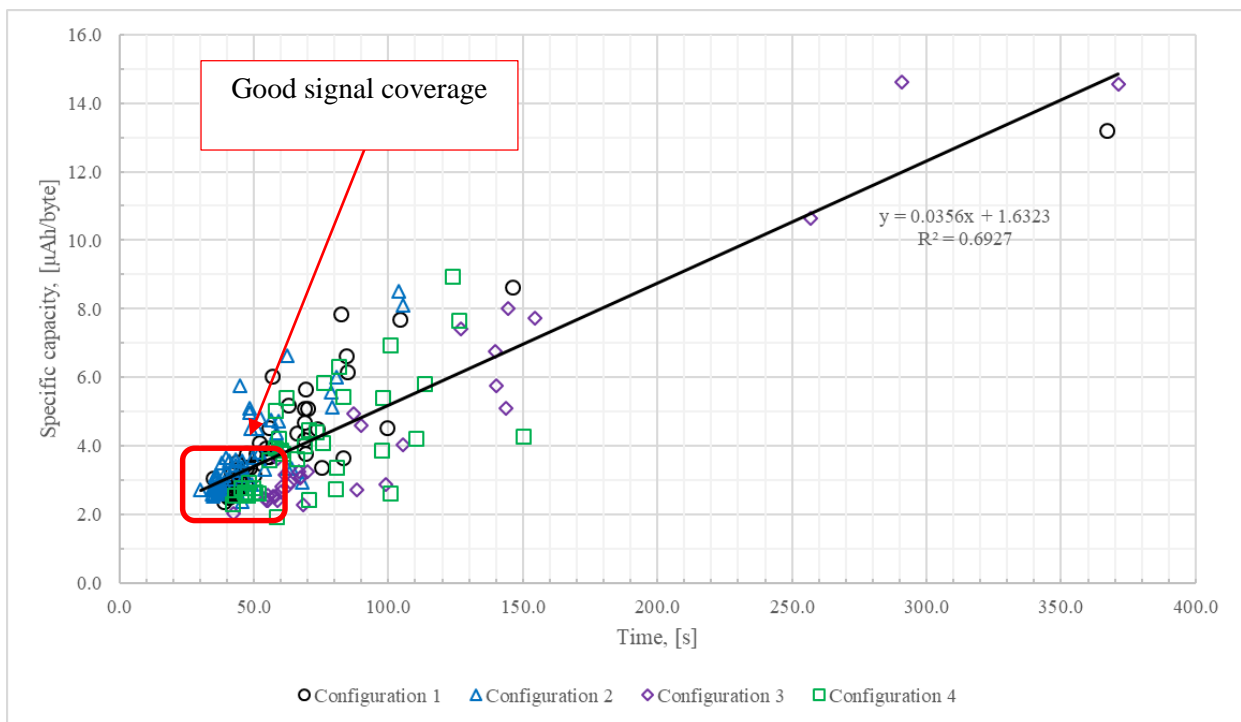


**Figure 170.** Capacity per second [µAh / byte] during phase 2 for the four configurations.

**Table 98.** Data about phase 2 for the four configurations.

Configuration	Mean time duration good signal strength, [s] *	Mean capacity for good signal coverage, [mAh]	Standard deviation for good signal coverage, [mAh]
1	41.5	2.40	0.23
2	35.8	1.98	0.19
3	59.1	3.38	0.34
4	47.0	2.64	0.16

\* Respect to Table 96, higher values are present because of modem switch off is considered.

From Figure 170, a poor correlation between specific capacity and time results. However, it can be justified by the fact that the transmission time is not an absolute parameter in the phase 2 as it is in the phase 1. In fact, if time  $t$  is taken equal to 100 sec., it signifies that data transmission lasted more than three times for configuration 1 and less than two times for the configuration 3. Therefore, to have a meaningful result the reported time has to be referred to the nominal time duration that can be considered equal to that reported in Table 98 for good signal coverage. From Figure 171 a good correlation appears. Also in this case, recording the effective duration of phase 2, it is possible to estimate with a good approximation the supplied capacity.

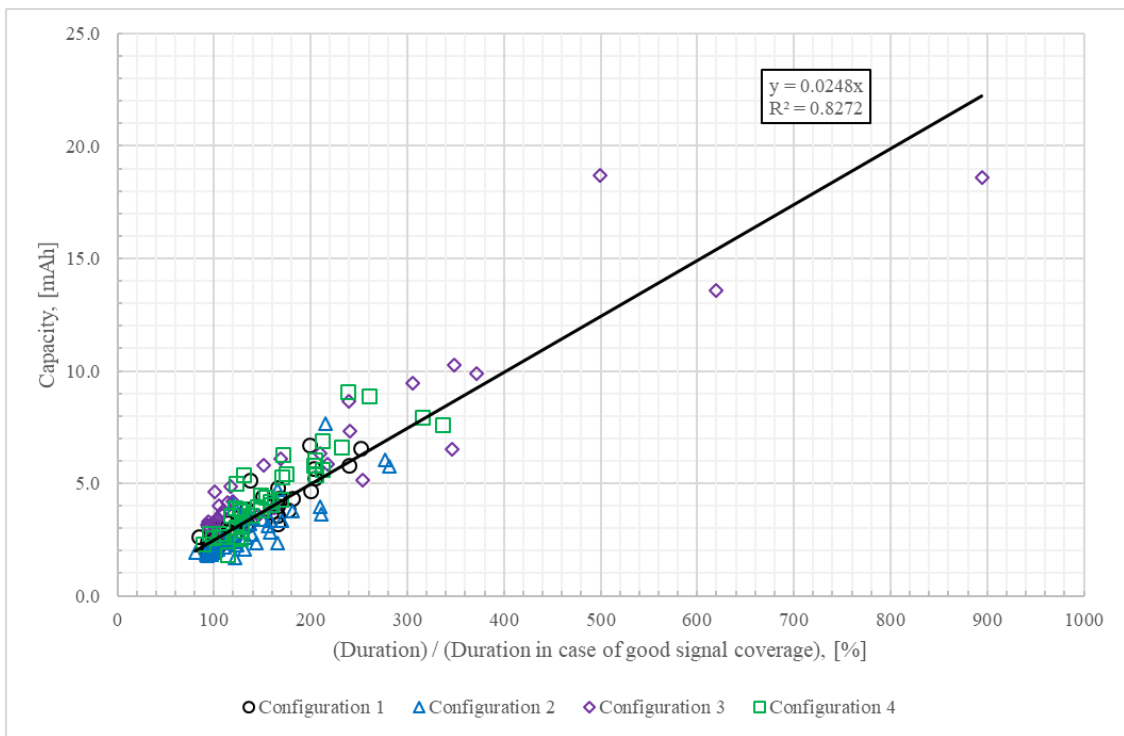


**Figure 171.** Capacity for the four configuration as a function of the ratio between effective and nominal duration of phase 2.

Regarding the last phase of the communication, it has been analysed that the mean duration is between 18.0 and 21.0 seconds and, as anticipated, is not influenced by signal coverage (Figure 172). However, during experimental activity some shorter values have been recorded but they represent very few events with poor statistical meaning.

About capacity, a value between 0.42 mAh and 0.20 mA has been calculated with a mean value of 0.34 mAh per communication (Table 99). It is noted a small difference between configurations but is practically negligible; however, this can be justified by the fact that, even if very small, differences are present between the four devices.

**Table 99.** Data about phase 3 for the four configurations.

Configuration	Mean time duration phase 3, [s]	Mean capacity, [mAh]	Standard deviation, [mAh]
1	20.1	0.32	0.03
2	20.1	0.35	0.02
3	19.9	0.35	0.05
4	19.3	0.33	0.03

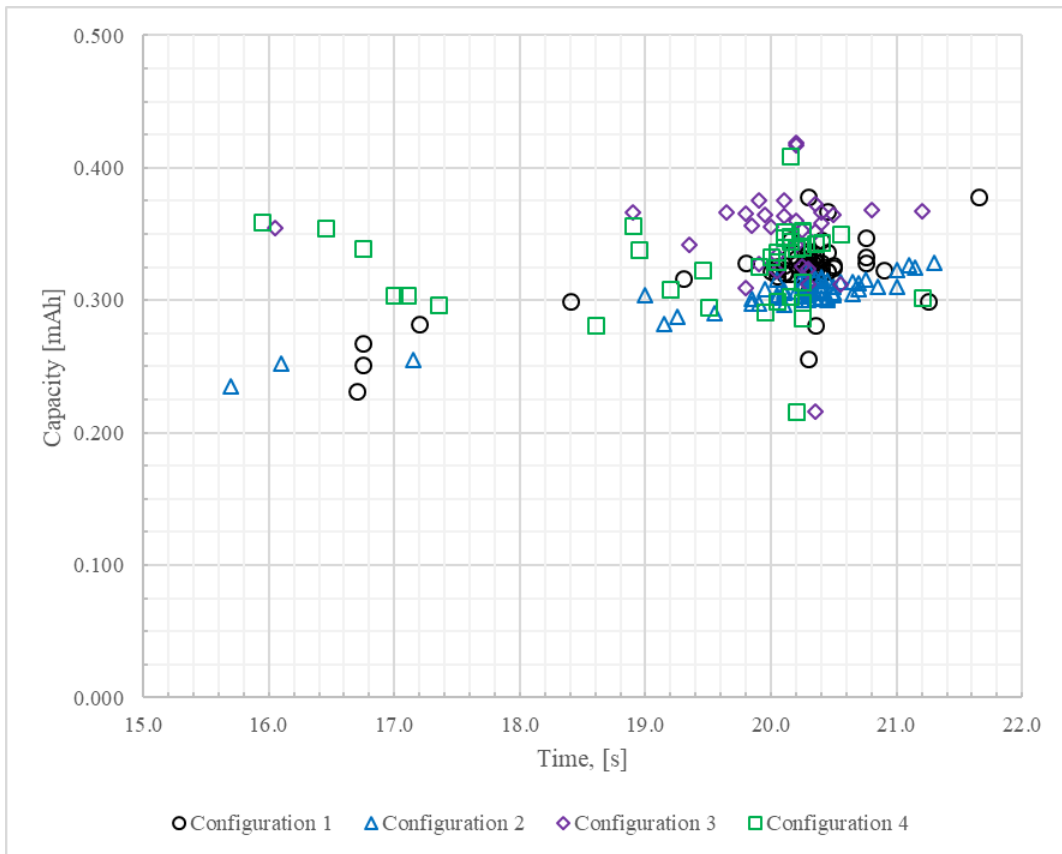


**Figure 172.** Capacity calculated for phase 3 for the four configurations.

As described, phases 2 and 3 are the most critical for communication being influenced by signal coverage strength. Considering the three phases together, measured capacity during experimental activity is reported in Figure 173 while discharged capacity in case of good signal strength is reported in Table 100. An increasing dispersion of the values with the total duration of the communication is observed. However, up to 120 sec. a good approximation of the discharged capacity can be done.

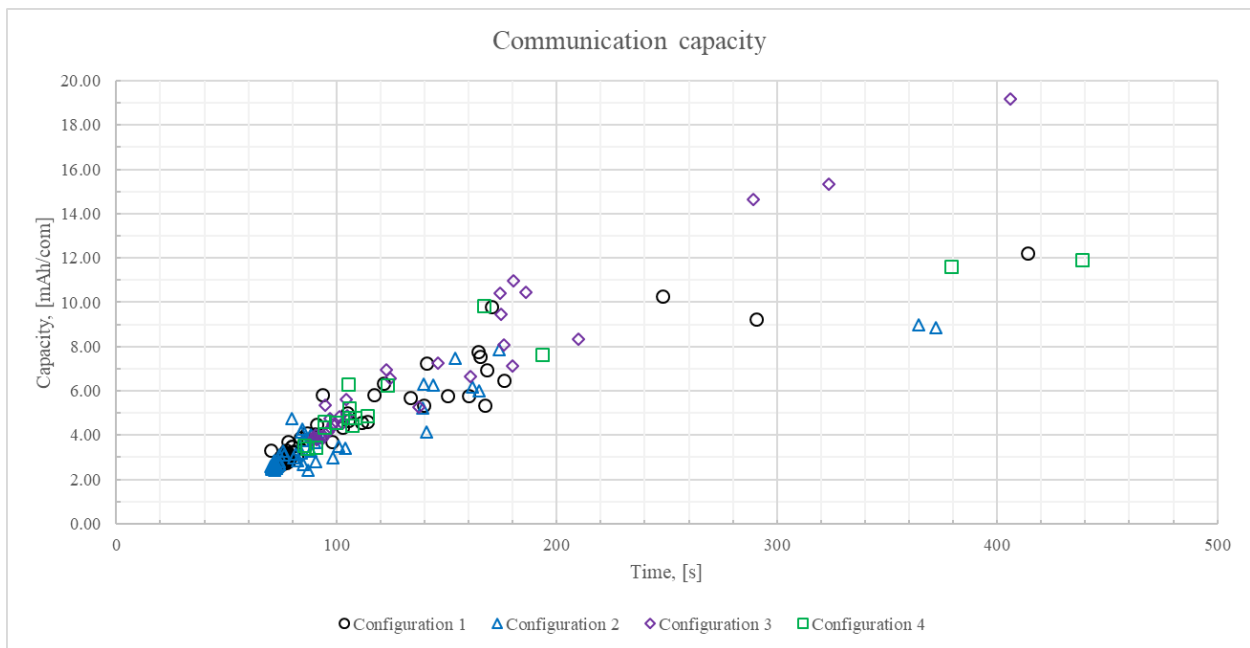


**Figure 173.** Measured capacity for the four configurations during the experimental activity.

**Table 100.** Data about communication for the four configurations in the case of good signal coverage.

Configuration	Mean capacity, [mAh]	Standard deviation, [mAh]
1	3.04	0.28
2	2.63	0.23
3	4.06	0.42
4	3.30	0.23

An estimation of supplied capacity in the case of poor signal coverage can be simply performed considering Figure 169 and Figure 171 as a function of the effective duration of the two phases. Nomograms can be designed in order to preliminary estimate the total discharged capacity as reported in Figure 174. It should be noted that total discharged capacity is influenced more by the phase 2 as it results from the sensitivity analysis (Figure 175). Therefore, efforts should be performed in order to minimize the possibility to communicate in the case of poor signal strength.

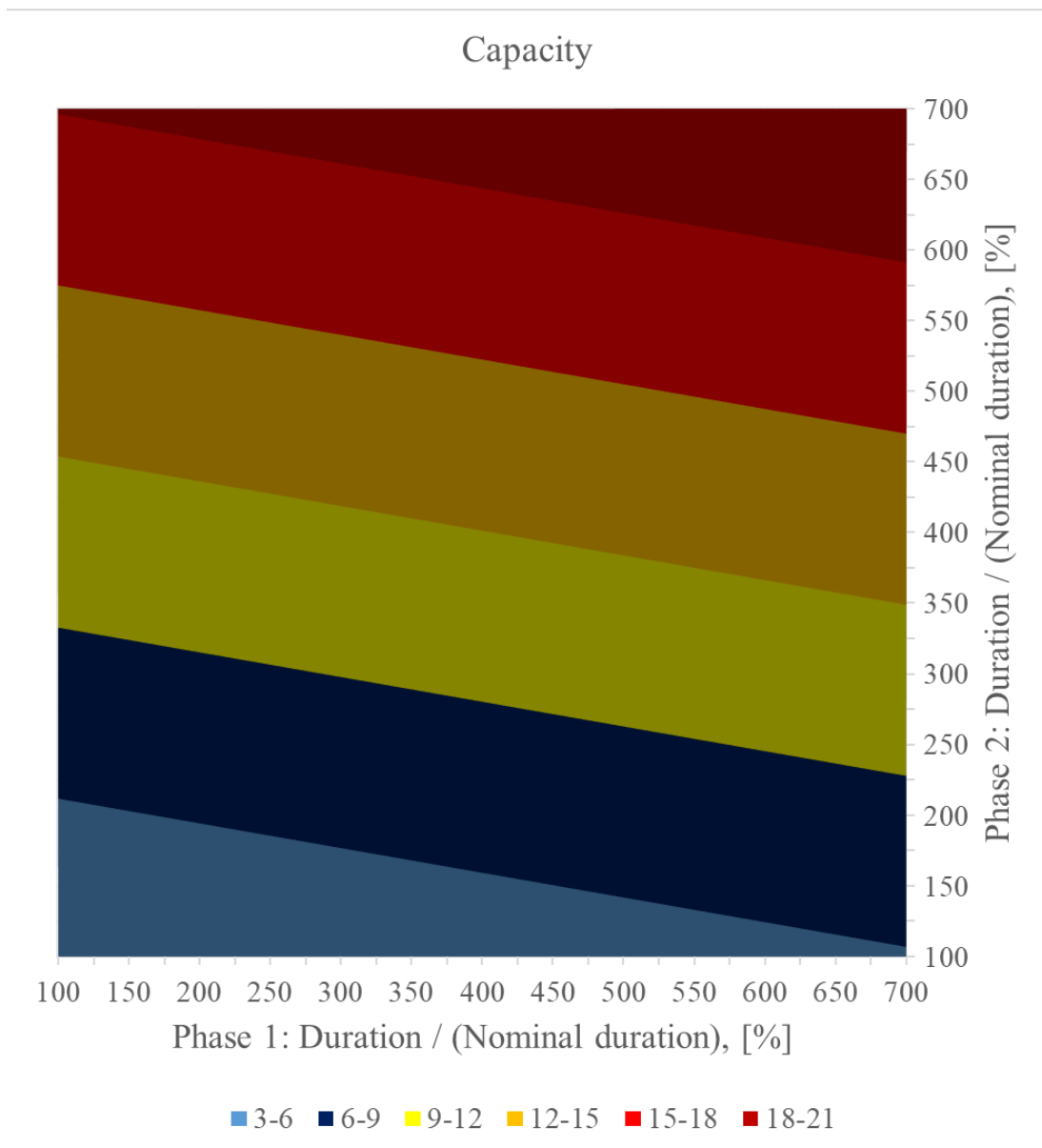


**Figure 174.** Nomogram for the preliminary estimation of discharged capacity as a function of the duration of phases 1 and 2.

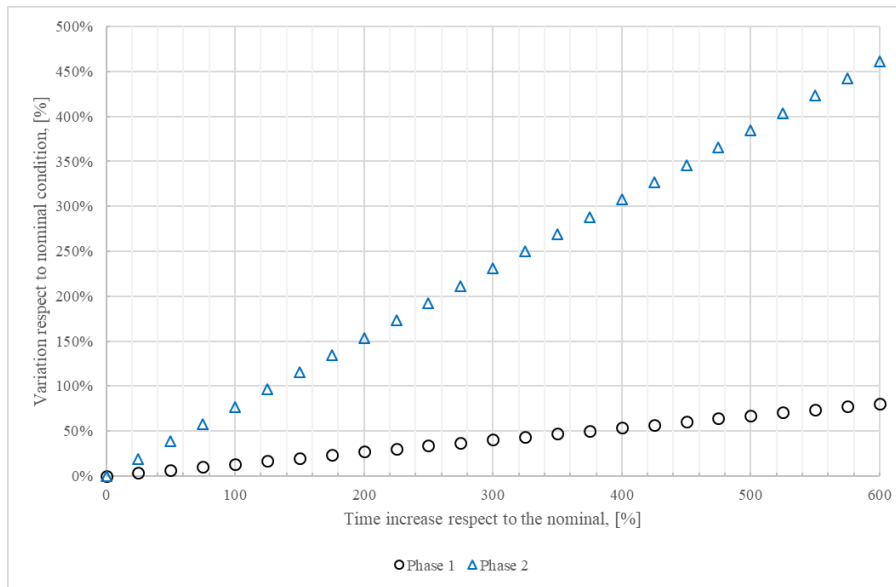


**Figure 175.** Sensitivity analysis of discharged capacity to nominal conditions (good signal coverage) as a function of time increase.

### 9.3.4 Estimation of total daily discharged capacity

In the experimental analysis, different consumptions are identified. Total daily consumption for the four configurations is shown in Figure 176, considering for the communication a value that is representative for the 99% of cases in the case of good signal coverage.

From the calculation, a reduction of the discharged capacity is obtained reducing quantity of data and transmission frequency. Particularly, the configuration 2, 3 and 4 show a reduction respectively of 4.2%, 9.3% and 14.2% respect to existing configuration (= 12.79 mAh/day). In Figure 176 and Figure 177, capacity for configurations 3 and 4 have been reported to the single day even if they communicate every two days in order to simplify the comparison between the different configurations.

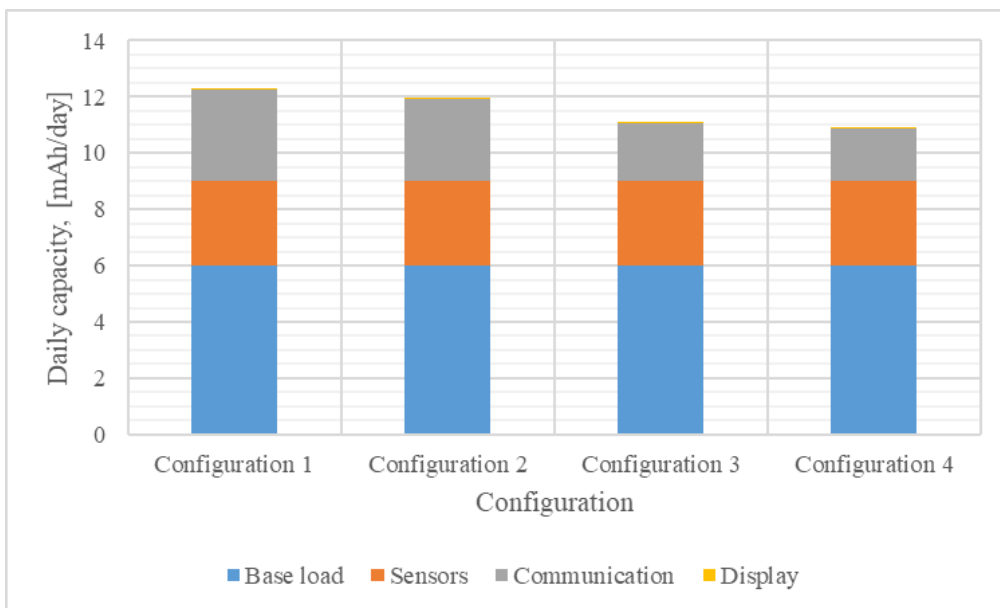


**Figure 176.** Total daily configuration for the four configurations.

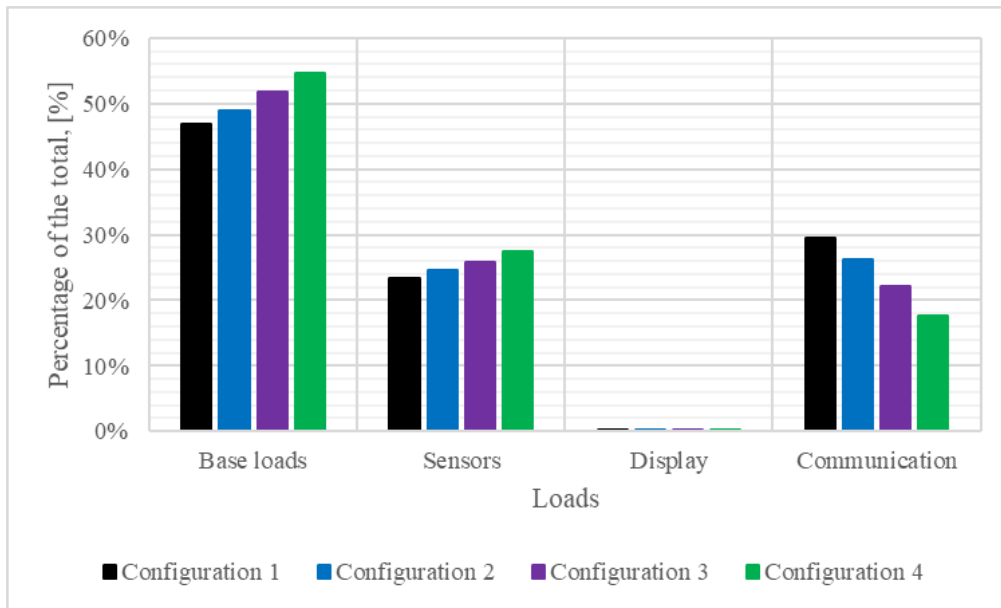


**Figure 177.** Percentage of the total consumption for the electrical loads supplied by the batteries' pack.

From the figures, it is evident that the main part of capacity is supplied to the base load, followed by communication and sensors. Therefore, further activities should be started in order to investigate about the base load or solutions to reduce its impact.

### 9.4 Estimation of the batteries' pack capacity

In order to estimate the available capacity of each battery, the phase 2 of communication has been considered. In fact, this phase is characterized by the greatest values of supplied current and the lowest voltage values were measured at the terminals of the batteries. The identified values of current are reported for the four configurations in Table 101. As shown, a negligible difference is present. For this reason, a representative mean value equal to 440 mA has been considered for the following elaborations.

From Figure 151, capacity has been analysed as a function of operative temperature as reported in Table 102. Coefficient a and b introduced in equation (8-8) have been interpolated obtaining values equal to 84.23 Ah and -655.1 K with a correlation coefficient  $R^2$  equal to 0.9832. It has to be highlighted that the identified values are strictly valid only in the temperature range [-40; 55] °C (Figure 178).

**Table 101.** Representative values for batteries' supplied current during phase 2 for the four configurations.

Configuration	Measured current, [mA]
1	444
2	418
3	444
4	458

**Table 102.** Battery's capacity [Ah] as a function of operative temperature, [°C].

Temperature, [C]	Available capacity, [Ah]	Temperature, [C]	Available capacity, [Ah]
-40	5.2	20	9.5
-20	6	55	11.2

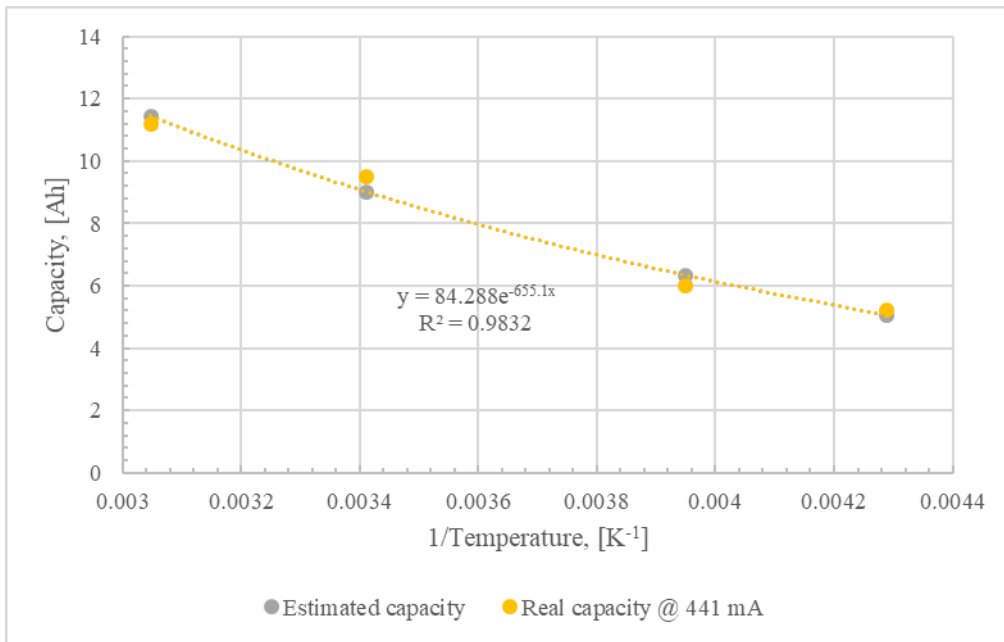


**Figure 178.** Estimated vs real capacity of the battery.

Because of capacity depends on the operative temperature, annual curves of effective available capacity can be designed for all locations. It should be noted, however, that no memory effect that could deteriorate effective battery's performances is present in lithium thionyl battery. For the scope, two different locations representative of extreme cases are considered: location A and location B. Particularly, location A presents an annual mean temperature higher than location B that is therefore representative for cold climates (Figure 179). Considering for the two locations the hourly ambient temperature, it is possible to evaluate the available capacity during the year. In the case that the converter is internally installed a mean ambient temperature equal to 24 °C has been assumed for all the year.

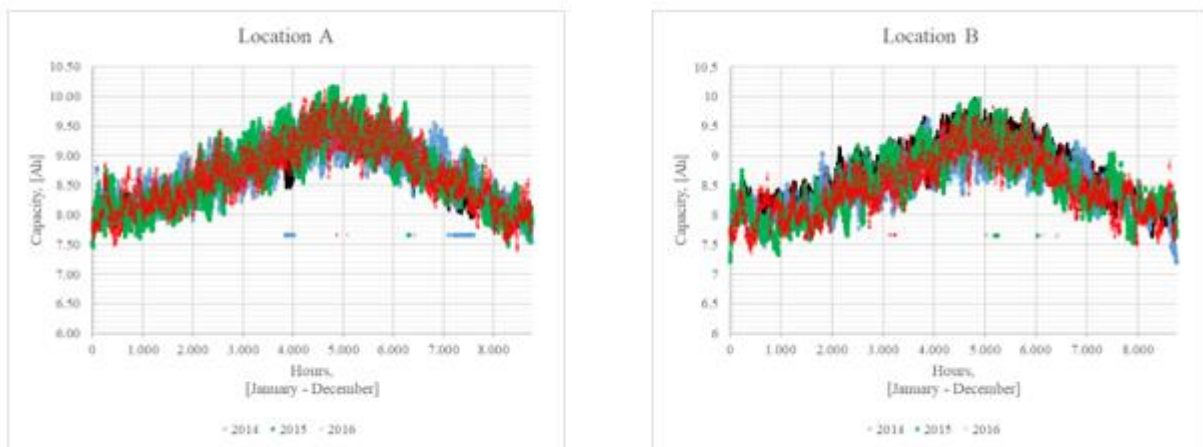


**Figure 179.** Hourly estimated available capacity of the batteries installed in the locations A and B.

For each location, therefore, it is possible to calculate cumulative probability (Figure 180). For the scope, a Gaussian statistical distribution has been considered. Main values of the distribution are reported in Table 103.

**Table 103.** Statistical values of capacity representative of the two locations.

Location	Mean capacity, [Ah]	Standard deviation, [Ah]
Location A	8.7	0.55
Location B	8.5	0.49

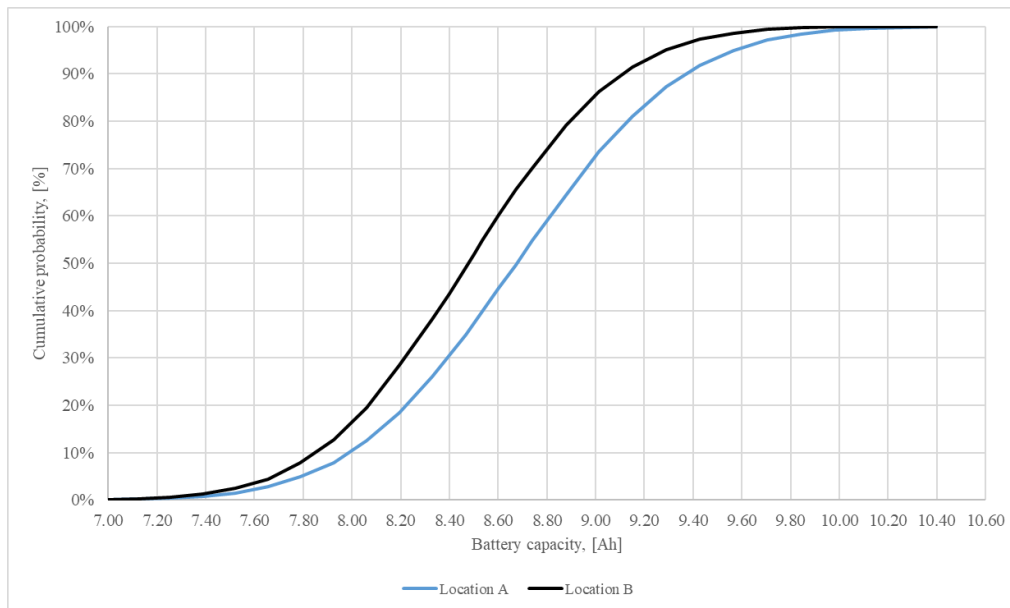


**Figure 180.** Cumulative probability of the battery's capacity for the two identified locations.

From the figure, it can be identified the range within battery's capacity is included during the year. As expected, location A presents a higher probability than location B to present a defined capacity thanks to the higher expected operative temperature. To conclude, a capacity equal to 9.30 Ah is estimated for internal installation. Because of two batteries are installed in the power supply pack, the resulted values have to be multiplied for the factor 2 before to proceed in the calculation of operative life.

### 9.5 Estimation of batteries' operative life

Operative life has been calculated in the case of good signal coverage; for the scope the capacity discharged during single communication has been estimated through a Monte Carlo simulation consisting of 10.000 simulations with as input the mean and the standard deviation calculated in previous paragraphs (Figure 181). This method has been considered in order to avoid conservative results that can derive considering the maximum daily discharge in case of good signal coverage.

However, it should be noted that the reported results represent the best possible condition. In fact, the proposed method ensures the estimation of expected operative life in the case of good signal strength. Instead for the case of a poor signal coverage time duration of the phases 1 and 2 have to be known.

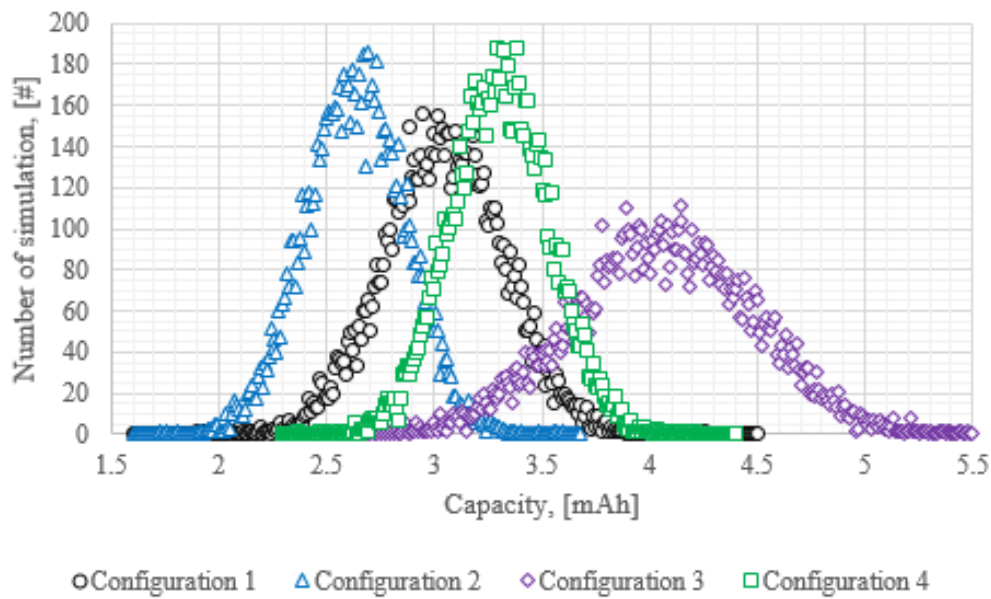


**Figure 181.** Results from the Monte Carlo simulations for the four configurations.

In order to estimate the probability that the power supply pack has an operative life higher than 4 years, the cumulative capacity curve for the battery and the total supplied electrical capacity have to be considered for the two locations. For each value of capacity and so of cumulative probability, an operative life can be calculated in accordance to equation (8-10) and (8-11) for the four configurations. For the scope of estimation, an annual self – discharge has been estimated equal to the 1.5% of existing capacity.

Results are reported in Figure 182 and Figure 183.

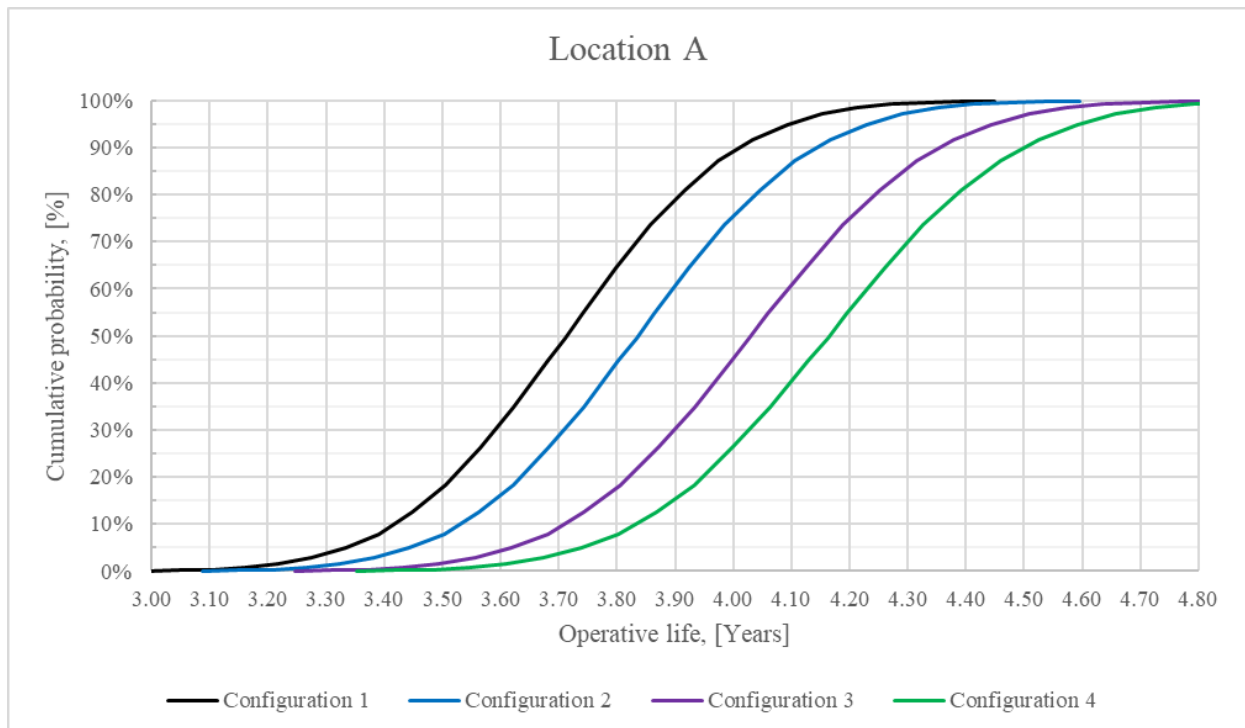


**Figure 182.** Cumulative probability for the estimated operative life in the location A.

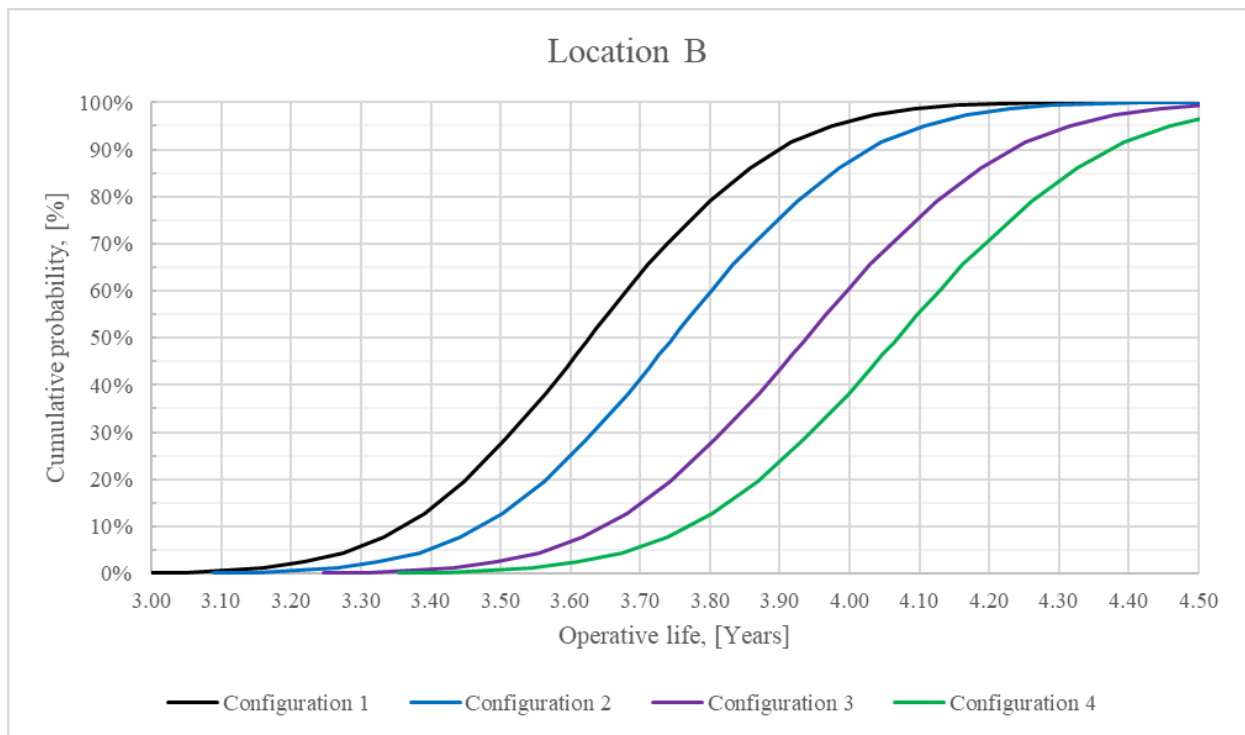


**Figure 183.** Cumulative probability for the estimated operative life in the location B.

As shown, in both the identified localities the probability to reach an operative life longer than 4 years is lower than 10% with the existing configuration, while is slightly higher with the configurations 3 and 4. However, it should be noted that in the case of real installation poor signal coverage can verify reducing the estimated operative life of the power supply pack. For this reason, detailed analysis of real communication condition in specific localities is suggested.

## *Conclusions*

During the three years, several research activities have been performed in order to identify existing lacks and possible improvements to reach better performances in NG distribution. As stated in the introduction to the project, however, many efforts have still to be dedicated to the development of new solutions that can be proposed thank to the increase of available know-how.

In order to improve its effectiveness, the research was principally focused on risk assessment of NG distribution networks and on gas smart metering. Therefore, as made for the thesis, also conclusions about the two topics have been organized separately.

Considering risk assessment in NG distribution, a positive trend is observed about the safety performances of distribution networks as observed by the reduction of the number of accidents, injuries and fatalities occurred in last years both in American and European NG distribution sectors. However, two points have to be immediately highlighted:

- A decreasing rate appears in the last years signifying an always greater complexity in the implementation of dedicated solutions. Therefore, higher investments and resources should be allocated in order to reach higher safety goals. Therefore, assuming that the available budget will remain the same, much time will be necessary to improve company's performances generating a negative perception about the importance attributed to safety and so to the concept of Safety Culture within and outside the Company. Thus, a new safety approach in order to identify dedicated solutions is necessary to overcome this possible obstacle in next future.
- A very poor organization and availability of information is present about NG distribution. Consequently, a dedicated database should be created in order to record data about accident, near missing but also repaired leakages. This will be helpful not only for the Authorities that will have more information in order to take decisions but also for the NG distribution companies that can immediately identify anomalies and take corrective actions.

The availability of data will ensure better decisions. In fact, as reported in the text decisions are usually based on failure frequency and not on risk, that is defined as the product between probability and consequence. For this reason, a new procedure has been proposed because of no internationally accepted method is available in literature. The procedure, consisting of five steps, is improved by the use of available and updated data about the networks that are recorded directly from the field. In order to show the potentials of the proposed method, a case studio has been shown about a NG distribution network installed in Central Italy. As shown, different results appear applying previous and proposed method resulting in a better accuracy in the identification of priorities. Furthermore, NG companies will be more aware of possible consequences resulting in better decisions about interventions thanks to the proposed approach.

The use of real data from the field and not from the calculation of available correlations is an essential step in order to calculate correct results. As shown in chapter 3, in fact, network failure can be caused by an overstress

conditions but also by the reduction of resistance or by a combination of the two depending on the boundary conditions. Furthermore, failures can occur in components for which no correlations are available in literature. Consequently, it is not easy to identify the status of the network through the use of correlations even if they can be used for comparative scopes.

However, waiting the creation and the population of dedicated databases, failure frequency rates have been calculated from PHMSA database about American distribution network. Furthermore, data about leakages occurred in the US distribution networks have been elaborated in order to show the potentials of databases: as shown, critical trends are observed making possible to intervene as soon as possible.

No analogous results can be obtained at the moment in Europe and in other parts of the worlds. Consequently, coordination efforts are required to Authorities, NG companies and interested stakeholders in order to create standardized procedures and universally accepted procedures to record data. In fact, the standardization seems to be required not only to collect but also to elaborate statistics in order to have comparable results. In order to give a preliminary contribution, a possible format for the creation of a database has been proposed considering possible application in a Plan-Do-Check-Act philosophy. Five simple and easy steps have been identified within which data to be recorded have been selected and justified.

About NG smart metering, the importance of the technology is evident from the number of devices to be installed resulting, as highlighted for Italy, in a money allocation greater than 400 M€ only for the installation in 2017 and 2018. Consequently, the success of the technology represents a great challenge for all the sector. Between the technical issues identified, the duration of the power battery is considered as the most important one because of an unexpected increase of operative cost results in the case that the nominal life would not be reached.

For the scope an experimental activity has begun in order to estimate the operative life of the power supply battery pack installed in industrial size meters. With this aim, the supply current has been measured identifying four main loads:

- **Base load:** a current between 0.25 mA and 0.30 mA is continuously present during the day for a total daily discharge equal to 6 mAh/day. Because of no wiring diagrams are available during the experimentation, more research is suggested in order to identify possible solutions to reduce this voice;
- **Sensors:** a mean current of 5 mA for 0.5 seconds every 20 seconds for a total consumption of 3 mAh/day has been measured;
- **Display:** a negligible daily discharge of about 0.025 mAh/day has been calculated;
- **Communication:** discharged capacity depends on the quantity of data sent and on the transmission frequency, as well as on the signal coverage. In optimum conditions, a value between 3 and 4 mAh/day has been measured.

Particularly the following considerations about communication have been made:

- Communication consists of three main phases characterized by different consumption: connection, data transmission and shutdown. In case of good coverage, the transmission phase is responsible for a consumption equal to the 75% - 85% of the total.
- Communication is strongly influenced by signal coverage. Therefore, a sensor should be implemented in order to allow or not the communication if a defined threshold is or not exceeded.
- The connection phase is performed by the converter resulting in a higher consumption for the meter. To reduce it, the connection phase should be assigned to the Central Acquisition System.
- The Master – Slave configuration requires questions (Central Acquisition System) and answers (meters) during data transmission. However, considering the influence of signal coverage on discharge capacity, another protocol should be implemented.
- A timer has to be implemented in the meter in order to automatically stop the tentative of connection.

In order to evaluate the influence of the quantity of transmitted data and of the transmission frequency on the overall discharge four configurations have been analysed. The following results have been obtained:

- In all the configurations, communication is responsible for a daily discharge between the 18% and the 28% of the total.
- In the case of good signal coverage, a daily discharged capacity equal to 3.35 mAh/day has been estimated in the 99.5% of communications for the existing communication configuration.
- The reduction of transmission frequency ensures a capacity saving higher than 38% while the reduction of transmitted data ensures a saving near to the 10%.
- In order to increase the duration of the battery, a reduction of the communication frequency is suggested. This solution has to be evaluated in accordance to other consideration such as the calculation of fiscal bills and the possibility to use data for other scopes.

Even if interesting results have been obtained from the research activity, several efforts are still needed. Particularly, a research activity about the remote controlled valve has begun during the project and is still in progress. In fact, some doubts about its performance during the entire life of the meters and particularly to gas tightness are present.

Consequently, as hoped, a close cooperation and collaboration between universities, research centres, NG companies and Authorities is required in order to obtain the best result in next future.

## References

- [1] D.M. 18/5/2018. Gas combustibile, aggiornamento regola tecnica. 2018.
- [2] UNFCCC. Paris Agreement. 2015.
- [3] Economides MJ, Wood DA. The state of natural gas. *J Nat Gas Sci Eng* 2009;1:1–13.
- [4] British Petroleum. BP Statistical Review of World Energy 2017. 2017.
- [5] Le M. An assessment of the potential for the development of the shale gas industry in countries outside of North America. *Heliyon* 2018:e00516.
- [6] Makogon YF, Holditch SA, Makogon TY. Natural gas-hydrates - A potential energy source for the 21st Century. *J Pet Sci Eng* 2007;56:14–31.
- [7] Eurogas. Statistical Report 2015. Brussels: 2016.
- [8] U.S. Energy Information Administration. International Energy Outlook 2016. 2016.
- [9] U.S. Energy Information Administration. Natural gas 2018. [https://www.eia.gov/dnav/ng/ng\\_enr\\_shalegas\\_dcu\\_NUS\\_a.htm](https://www.eia.gov/dnav/ng/ng_enr_shalegas_dcu_NUS_a.htm) (accessed July 10, 2018).
- [10] U.S. Energy Information Administration. Number of Natural Gas Consumers 2018. [https://www.eia.gov/dnav/ng/ng\\_cons\\_num\\_dcu\\_nus\\_a.htm](https://www.eia.gov/dnav/ng/ng_cons_num_dcu_nus_a.htm) (accessed October 10, 2017).
- [11] Eurogas. Statistical report. 2011.
- [12] Marcogaz. Performance Indicators Report 2008 – 2014. 2017.
- [13] European Network of Transmission System Operators for Gas. The European Natural Gas Network. 2017. [https://www.entsog.eu/public/uploads/files/publications/Maps/2017/ENTSOG\\_CAP\\_2017\\_A0\\_1189x841\\_FULL\\_064.pdf](https://www.entsog.eu/public/uploads/files/publications/Maps/2017/ENTSOG_CAP_2017_A0_1189x841_FULL_064.pdf) (accessed July 10, 2018).
- [14] Pipeline and Hazardous Materials Safety Administration. Pipeline Miles and Facilities 2010+ 2018. <https://hip.phmsa.dot.gov/analyticsSOAP/saw.dll?Portalpages> (accessed December 12, 2017).
- [15] PHMSA. Pipeline Miles and Facilities 2010+ 2018. <https://hip.phmsa.dot.gov/analyticsSOAP/saw.dll?Portalpages>.
- [16] Autorità di Regolazione per Energia Reti e Ambiente (ARERA). Dati statistici 2018. [https://www.arera.it/it/dati/elenco\\_dati.htm](https://www.arera.it/it/dati/elenco_dati.htm) (accessed October 30, 2017).
- [17] Gestore Mercati Energetici (GME). Mercati del gas 2018. <http://www.mercatoelettrico.org/It/>.
- [18] Bianchini A, Pellegrini M, Rossi J, Sacconi C. Biomass and Bioenergy Theoretical model and preliminary design of an innovative wet scrubber for the separation of fine particulate matter produced by biomass combustion in small size boilers. *Biomass and Bioenergy* 2018;116:60–71.
- [19] Bianchini A, Guzzini A, Pellegrini M, Sacconi C. Photovoltaic/thermal (PV/T) solar system: Experimental measurements, performance analysis and economic assessment. *Renew Energy* 2017;111.
- [20] Bianchini A, Donini F, Guzzini A, Pellegrini M, Sacconi C. Natural gas pipelines distribution: Analysis of risk, design and maintenance to improve the safety performance. *Proc. Summer Sch. Fr. Turco, Naples: 2015*, p. 243–8.
- [21] SNAM. Piano decennale di sviluppo delle reti di trasporto di gas naturale 2017-2026. 2017.
- [22] ISO 13623. Petroleum and natural gas industries - Pipeline transportation systems. 2017.
- [23] D.M. 16/04/2008. Regola tecnica per la progettazione, costruzione, collaudo, esercizio e sorveglianza delle opere e degli impianti di trasporto di gas naturale con densità non superiore a 0,8. 2008.
- [24] Hammerschmidt EG. Formation of Gas Hydrates in Natural Gas Transmission Lines. *Ind Eng Chem* 1934:851–5.
- [25] SNAM. Codice di rete 2003.
- [26] ARERA. Zone Climatiche 2009. <https://www.autorita.energia.it/allegati/faq/AggTabellaA.xls> (accessed March 31, 2018).
- [27] ISTAT. Popolazione residente al 1 gennaio 2018. [http://dati.istat.it/Index.aspx?DataSetCode=DCIS\\_POPRES1](http://dati.istat.it/Index.aspx?DataSetCode=DCIS_POPRES1) (accessed March 30, 2018).
- [28] ISTAT. Popolazione e famiglie. 2018.

- [29] UNI-CIG 9034:2004. Condotte di distribuzione del gas con pressione di esercizio minore o uguale a 0,5 MPa (5 bar) - Materiali e sistemi di giunzione. 2004.
- [30] UNI 8827:1/2015. Sistemi di controllo della pressione del gas funzionanti con pressione a monte compresa fra 0,04 bar e 5 bar - Progettazione, costruzione e collaudo - Parte 1: Generalità. 2015.
- [31] UNI 10619:1/2014. Sistemi di controllo della pressione e/o impianti di misurazione del gas naturale funzionanti con pressione a monte massima di 12 bar per utilizzo industriale e civile - Parte 1: Progettazione, costruzione e collaudo - Generalità. 2014.
- [32] UNI 9860:2006. Gas service pipes: Design, construction, testing operation, maintenance and rehabilitation. 2006.
- [33] Legge 6/12/1971, n°1083. Norme per la sicurezza dell'impiego del gas combustibile. 1971.
- [34] Nayyar ML. Piping Handbook. Seventh edition. McGraw-Hill. 2000.
- [35] BS EN 10208-1:2009. Steel pipes for pipelines for combustible fluids — Technical delivery conditions Part 1 : Pipes of requirement class A. United Kingdom: 2009.
- [36] Velaga SK, Rajput G, Murugan S, Ravisankar A, Venugopal S. Comparison of weld characteristics between longitudinal seam and circumferential butt weld joints of cylindrical components. *J Manuf Process* 2015;18:1–11.
- [37] Rosenfeld M, Fassett R. Study of pipelines that ruptured while operating at a hoop stress below 30% SMYS. *Pipeline Pigging Integr. Manag.*, 2013.
- [38] BS EN 10255:2004. Non alloy steel tubes suitable for welding and threading — Technical delivery conditions. 2004.
- [39] Cast Iron Soil Pipe Institute. Cast iron soil pipe and fittings handbook. 2006.
- [40] EN 969:2009. Ductile iron pipes , fittings , accessories and their joints for gas pipelines - Requirements and test methods. 2009.
- [41] Plastic Pipe Institute. Chapter 3: material properties. *Plast. Pipe Inst. Handb. Polyethyl. Pipe.* 2009.
- [42] Farshad M. Plastic pipe systems: failure investigation and diagnosis. Elsevier Science. 2006.
- [43] EN 1555-1:2010. Plastics piping systems for the supply of gaseous fuels - Polyethylene (PE). Part 1: General. 2010.
- [44] EN 1555-2:2010. Plastics piping systems for the supply of gaseous fuels - Polyethylene (PE). Part 2: Pipes. 2010.
- [45] EN 1057:2006 + A1:2010. Copper and copper alloys — Seamless , round copper tubes for water and gas in sanitary and heating applications. vol. 3. 2010.
- [46] American Society of Mechanical Engineers. ASME B31.8-2003. Gas Transmission and Distribution Piping Systems. *Am Society Mech Eng* 2004;552:194.
- [47] ARERA. Parte I dei servizi di distribuzione e misura del gas per il periodo di regolazione 2014-2019 (RQDG). 2017.
- [48] Comitato Italiano Gas (CIG). Linea guida CIG n°13. Linee guida per l'applicazione della normativa sismica nazionale alle attività di progettazione, costruzione e verifica dei sistemi di trasporto e distribuzione del gas combustibile. 2014.
- [49] UNI 9165:2004. Reti di distribuzione del gas con pressioni massime di esercizio minori o uguali a 5 bar. Progettazione, costruzione e collaudo 2004.
- [50] Heldenbrand DW. A Review of Soil Gas Migration in Natural Gas Incidents. *West. Reg. Gas Assoc. Oper. Conf.*, 2017.
- [51] BS ISO 31000:2018. BSI Standards Publication Risk management — Guidelines 2018.
- [52] Montiel H, Vilchez JA, Arnaldos J, Casal J. Historical analysis of accidents in the transportation of natural gas. *J Hazard Mater* 1996;51:77–92.
- [53] Costa Lima GA, Teodoro Filho AM. Economic and risk replacement model for physical assets in a natural gas distribution's system. *Safety, Reliab. Risk Anal. Beyond Horiz.*, 2014, p. 767–73.
- [54] Ahammed M. Probabilistic estimation of remaining life of a pipeline in the presence of active corrosion defects. *Int J Press Vessel Pip* 1998;75:321–9.
- [55] Netto TA, Ferraz US, Estefen SF. The effect of corrosion defects on the burst pressure of pipelines 2005;61:1185–204.

- [56] Caleyó F, Velázquez JC, Valor A, Hallen JM. Markov chain modelling of pitting corrosion in underground pipelines. *Corros Sci* 2009;51:2197–207.
- [57] Alamilla JL, Sosa E. Modelling steel corrosion damage in soil environment. *Corros Sci* 2009;51:2628–38.
- [58] Valor A, Caleyó F, Hallen JM, Velázquez JC. Reliability assessment of buried pipelines based on different corrosion rate models. *Corros Sci* 2013;66:78–87.
- [59] Rajany B, Kleiner Y. Comprehensive review of structural deterioration of water mains: physically based models. *Urban Water* 2001;3:151–64.
- [60] Rajany B, Makar MJ. A methodology to estimate remaining service life of grey cast iron water mains. *Can J Civ Eng* 2000;27:1259–72.
- [61] El-Abbasy MS, Senouci A, Zayed T, Mirahadi F, Parvizedghy L. Artificial neural network model for predicting condition of offshore oil and gas pipeline. *Autom Constr* 2014;45:50–65.
- [62] Sahraoui Y, Khelif R, Chateauneuf A. *International Journal of Pressure Vessels and Piping*. Int J Press Vessel Pip 2013;104:76–82.
- [63] Pesinis K, Tee KF. Bayesian analysis of small probability incidents for corroding energy pipelines. *Eng Struct* 2018;165:264–77.
- [64] ASME B31.8S-2004. Managing system integrity of gas pipelines. 2004.
- [65] Kishawy HA, Gabbar HA. Review of pipeline integrity management practices. *Int J Press Vessel Pip* 2010;87:373–80.
- [66] Xie M, Tian Z. A review on pipeline integrity management utilizing in-line inspection data. *Eng Fail Anal* 2018;92:222–39.
- [67] Nezamian A, Rodrigues C, Nezamian M, WorleyParsons A. Asset integrity management and life extension of gas distribution facilities and pipeline network. *Soc Pet Engineers* 2013.
- [68] Ribeiro PAR. Integrity management program on a Brazilian natural gas distribution company. *Rio Pipeline Conf. Expo.*, 2013.
- [69] Gabetta G, Morrea S, Travaglia F, Cioffi P. Integrity management of pipelines transporting hydrocarbons: an integrated approach. *Soc Pet Engineers* 2015.
- [70] Brito AJ, de Almeida AT. Multi-attribute risk assessment for risk ranking of natural gas pipelines. *Reliab Eng Syst Saf* 2009;94:187–98.
- [71] Palacios V, Simi RG, Von Fischer JC, Mohlin K. Integrating Leak Quantification into Natural Gas Utility Operations. *Public Util Fortn* 2017:1–17.
- [72] Han ZY, Weng WG. Comparison study on qualitative and quantitative risk assessment methods for urban natural gas pipeline network. *J Hazard Mater* 2011;189:509–18.
- [73] Jo Y, Jong B. A method of quantitative risk assessment for transmission pipeline carrying natural gas 2005;123:1–12. doi:10.1016/j.jhazmat.2005.01.034.
- [74] Han ZY, Weng WG. An integrated quantitative risk analysis method for natural gas pipeline network. *J Loss Prev Process Ind* 2010;23:428–36.
- [75] Hao MJ, You QJ, Yue Z. Risk analysis of urban gas pipeline network based on improved bow-tie model Risk analysis of urban gas pipeline network based on improved bow-tie model. *Earth Environ Sci* 2017;93:1–10.
- [76] Bianchini A, Guzzini A, Pellegrini M, Sacconi C. *International Journal of Pressure Vessels and Piping* Natural gas distribution system: A statistical analysis of accidents data. *Int J Press Vessel Pip* 2018;168:24–38.
- [77] Metropolo PL, Brown AEP. Natural gas pipeline accident consequence analysis. *Process Saf Prog* 2004;23:307–10.
- [78] Lam C, Zhou W. Statistical analyses of incidents on onshore gas transmission pipelines based on PHMSA database. *Int J Press Vessel Pip* 2016;145:29–40.
- [79] EGIG. 10th Report of the European Gas Pipeline Incident Data Group (period 1970 – 2016). 2018.
- [80] SVGW. *Statistique technique annuelle Gaz* 2015. 2016.
- [81] Burgherr P, Hirschberg S. Comprehensive Assessment of Energy Systems (GaBE): Comparative Assessment of Natural Gas Accident Risks 2005:53.

- [82] Dietzsch F. Integrated safety concept of DVGW in terms of statistical verification of incidents. *Pipeline Technol J* 2017;16–21.
- [83] Marcogaz. Report on European Gas Safety, Gas Distribution (EGAS B). 2017.
- [84] BS EN 31000:2010. Risk management. Risk assessment techniques. 2010.
- [85] ARERA. Direttiva 574/2013/r/GAS. Italy. 2013.
- [86] UNI TS 11297:2008. Metodologia di valutazione rischi di dispersione gas. 2017.
- [87] Comitato Italiano Gas (CIG). Linee guida CIG n°15: La gestione degli incidenti da gas combustibile distribuito a mezzo di reti e comunicazione delle emissioni in atmosfera. 2017.
- [88] Comitato Italiano Gas (CIG). Linee guida CIG n°4: La gestione delle emergenze da gas combustibile sull'impianto di distribuzione. 2017.
- [89] ISO 16708:2006. Petroleum and natural gas industries. Pipeline transportation systems: Reliability-based limit state methods. n.d.
- [90] Koduro SD, Nessim MA. Review of quantitative reliability methods for onshore oil and gas pipelines. *Risk Reliab. Anal. theory Appl.*, 2017, p. 67–95.
- [91] Moser AP. Buried pipe design. Third edition. The McGraw-Hill Companies. 2008.
- [92] Bruzzone AA, Lonardo PM. Criteria for gas network renewal: Experimental assessment of traffic loads and cast iron joint escapes. *Tunn Undergr Sp Technol* 1996;11:43–51.
- [93] Plastics Pipe Institute (PPI). Design of PE piping systems. *Handb. Polyethyl. Pipe*, 2009, p. 155–264.
- [94] A.B. Change Company. Step 7 – Corrosion Guide 2003:1–18.
- [95] Cole IS, Marney D. The science of pipe corrosion: A review of the literature on the corrosion of ferrous metals in soils. *Corros Sci* 2012;56:5–16.
- [96] Ahammed M, Melchers RE. Reliability of underground pipelines subject to corrosion. *J Transp Eng* 1994;120:989–1002.
- [97] Caleyó F, Velázquez JC, Valor A, Hallen JM. Probability distribution of pitting corrosion depth and rate in underground pipelines: A Monte Carlo study. *Corros Sci* 2009;51:1925–34.
- [98] Rajany B, Kleiner Y. External and internal corrosion of large diameter cast iron mains. *J Infrastruct Syst* 2013;19:486–95.
- [99] UNI EN ISO 15589-1:2017. Industrie del petrolio, petrolchimiche e del gas naturale. Protezione catodica dei sistemi di condotte. Parte 1: Condotte sulla terraferma. 2017.
- [100] Papavinasam S, Attard M, Revie RW. External Polymeric Pipeline Coating Failure Modes. *Mater Perform - Coat Linings* 2006:28–30.
- [101] Beavers JA. Cathodic protection: how it works. *Control pipeline Corros.*, 2001, p. 21–47.
- [102] Baker MJ. Pipeline corrosion: final report. 2008.
- [103] Chen Z, Koleva D, Van Breugel K. A review on stray current-induced steel corrosion in infrastructure. *Corros Rev* 2017;35:397–423.
- [104] Cui G, Li ZL, Yang C, Wang M. The influence of DC stray current on pipeline corrosion. *Pet Sci* 2016;13:135–45.
- [105] Wang X, Tang X, Wang L, Wang C, Guo Z. Corrosion behavior of X80 pipeline steel under coupling effect of stress and stray current. *Int J Electrochem Sci* 2014;9:4574–88.
- [106] Ormellese M, Lazzari L. Interferenza elettrica: definizioni, esempi e criteri di accettabilità. *APCE* 2014:9–12.
- [107] Wen C, Li J, Wang S, Yang Y. Experimental study on stray current corrosion of coated pipeline steel. *J Nat Gas Sci Eng* 2015;27:1555–61.
- [108] Yang C, Cui G, Li Z, Zhao Y, Zhang C. Study the influence of DC stray current on the corrosion of X65 steel using electrochemical method. *Int J Electrochem Sci* 2015;10:10223–31.
- [109] BS EN 50162:2004. Protection against corrosion by stray current from direct current systems. 2004.
- [110] BS EN 50443:2011. Effects of electromagnetic interference on pipelines caused by high voltage a.c. electric traction systems and/or high voltage a.c. power supply systems. 2011.
- [111] Baker MJ. Stress corrosion cracking study. 2005.
- [112] Iverson WP. Graphitization of cast iron as an electro-biochemical process in anaerobic soils. n.d.

- [113] Favier V, Giroud T, Strijko E, Hiver JM, G'Sell C, Hellinckx S, et al. Slow crack propagation in polyethylene under fatigue at controlled stress intensity. *Polymer (Guildf)* 2001;43:1375–82.
- [114] Mamoun M, Maupin J. Plastic pipe failure, risk, and threat analysis. 2009.
- [115] Chen Q, Chebaro MR, Nessim M. Effectiveness of prevention methods for excavation damage. 2006.
- [116] Bianchini A, Guzzini A, Pellegrini M, Saccani C. Earthquake and earth movement monitoring: The possibility to use Natural Gas distribution infrastructure. XXII Summer Sch. “Francesco Turco” - Ind. Syst. Eng., vol. 2017–Septe, Palermo: 2017, p. 143–9.
- [117] O'Rourke MJ, Liu JX. *Seismic Design of Buried and Offshore Pipelines*. 2012.
- [118] Varnes JD. Slope movement types and processes. 1978.
- [119] Cruden DM, Varnes DJ. *Landslide types and processes*. 1993.
- [120] Indian Institute of Technology Kanpur. *Guidelines for seismic design of buried pipelines*. 2007.
- [121] O'Rourke MJ, Liu X, Flores-Berrones R. Steel Pipe Wrinkling due to Longitudinal Permanent Ground Deformation. *J Transp Eng* 1995;121:443–51. doi:10.1061/(ASCE)0733-947X(1995)121:5(443).
- [122] Liu X, O'Rourke MJ. Behaviour of continuous pipeline subject to transverse PGD. *Earthq Eng Struct Dyn* 1997;26:989–1003.
- [123] Abdoun TH, Ha D, O'Rourke MJ, Symans MD, O'Rourke TD, Palmer MC, et al. Factors influencing the behavior of buried pipelines subjected to earthquake faulting. *Soil Dyn Earthq Eng* 2009;29:415–27.
- [124] Choo YW, Abdoun TH, O'Rourke MJ, Ha D. Remediation for buried pipeline systems under permanent ground deformation. *Soil Dyn Earthq Eng* 2007;27:1043–55.
- [125] Kennedy RP, Williamson RA. Fault movement effects on buried oil pipeline. *J Transp Eng* 1977;103:617–33.
- [126] Karamitros DK, Bouckovalas GD, Kouratzis GP. Stress analysis of buried steel pipelines at strike-slip fault crossings. *Soil Dyn Earthq Eng* 2007;27:200–11.
- [127] Ha D, Abdoun TH, O'Rourke MJ, Symans MD, O'Rourke TD, Palmer MC, et al. Centrifuge Modeling of Earthquake Effects on Buried High-Density Polyethylene (HDPE) Pipelines Crossing Fault Zones. *J Geotech Geoenvironmental Eng* 2008;134:1501–15.
- [128] Naeini SA, Mahmoudi E, Shojaedin MM, Misaghian M. Mechanical response of buried high-density polyethylene pipelines under normal fault motions. *KSCE J Civ Eng* 2016;20:2253–61.
- [129] Luo X, Ma J, Zheng J, Shi J. Finite element analysis of buried polyethylene pipe subjected to seismic landslide. *J Press Vessel Technol* 2014;136:031801.
- [130] Esposito S, Giovinazzi S, Elefante L, Iervolino I. Performance of the L'Aquila (central Italy) gas distribution network in the 2009 (Mw6.3) earthquake. *Bull Earthq Eng* 2013;11:2447–66.
- [131] Eidinger JM. Water distribution systems. Loma Prieta, California, Earthq. Oct. 17, 1989 - Lifelines, 1998, p. 63–78.
- [132] O'Rourke TD, Jeon SS, Toprak S, Cubrinovski M, Hughes M, Van Ballegooy S, et al. Earthquake response of underground pipeline networks in Christchurch, NZ. *Earthq Spectra* 2014;30:183–204.
- [133] D.M. 14/01/2008. NTC 2008: Italian Building Code. 2008.
- [134] Lanzano G, Salzano E, De Magistris FS, Fabbrocino G. Seismic vulnerability of natural gas pipelines. *Reliab Eng Syst Saf* 2013;117:73–80.
- [135] American Lifelines Alliance (ALA). *Seismic fragility formulations for water systems*. 2001.
- [136] Lanzano G, Salzano E, De Magistris FS, Fabbrocino G. Vulnerability of pipelines subjected to permanent deformation due to geotechnical co-seismic effects. *Chem Eng Trans* 2013;32:415–20.
- [137] Alzbutas R, Iesmantas T, Povilaitis M, Vitkute J. Risk and uncertainty analysis of gas pipeline failure and gas combustion consequence. *Stoch Environ Res Risk Assess* 2014;28:1431–46.
- [138] Shan X, Liu K, Sun PL. Risk Analysis on Leakage Failure of Natural Gas Pipelines by Fuzzy Bayesian Network with a Bow-Tie Model. *Sci Program* 2017;2017.
- [139] Sklavounos S, Rigas F. Estimation of safety distances in the vicinity of fuel gas pipelines. *J Loss Prev Process Ind* 2006;19:24–31.
- [140] Center for Chemical Process Safety. *Guidelines for chemical process quantitative risk analysis*. 2nd

Editio. New York: 1999.

- [141] API Standard 521. Pressure-relieving and depressuring systems. 1996.
- [142] TNO. Green Book: Methods for the determination of possible damage to people and objects resulting from the release of hazardous materials. 1989.
- [143] Crowl DA, Louvar JF. Chemical process safety fundamentals with application. Second. Prentice Hall PTR; 1990.
- [144] Assael MJ, Kakosimos KE. Vaport Cloud Explosions (VCEs). In: Taylor & Francis Group, editor. Fires, Explos. toxic gas dispersions. Eff. Calc. risk Anal., 2010, p. 149–206.
- [145] Montiel H, Vilchez JA, Casal J, Arnaldos J. Mathematical modelling of accidental gas releases 1998:211–33.
- [146] Moloudi R, Esfahani JA. Journal of Loss Prevention in the Process Industries Modeling of gas release following pipeline rupture: Proposing non-dimensional correlation. J Loss Prev Process Ind 2014;32:207–17.
- [147] Ma L, Li Y, Liang L, Li M, Cheng L. A novel method of quantitative risk assessment based on grid difference of pipeline sections. Saf Sci 2013;59:219–26.
- [148] Vianello C. Risk analysis of gas distribution network. Università degli Studi di Padova. 2011.
- [149] API RP 580. Risk based inspection. 2016.
- [150] BSI EN ISO 14001:2015. Environmental management systems - Requirements with guidance for use. 2015.
- [151] Tavernelli M. Analisi delle rotture nelle tubazioni delle reti acquedottistiche. 2011.
- [152] Bianchini A, Guzzini A, Pellegrini M, Saccani C. Gas smart metering in Italy : state of the art and analysis of potentials and technical issues 2018:49–55.
- [153] Bianchini A, Guzzini A, Pellegrini M, Saccani C. Natural gas distribution system: Overview of leak detection Systems. XXI Summer Sch “Francesco Turco” - Ind Syst Eng 2016;13–15–Sept:123–7.
- [154] AEEGSI. Direttiva 631/2013/r/GAS. 2013.
- [155] AEEGSI. Direttiva 554/2015/r/GAS. 2015.
- [156] UNI TS 11291-6:2013. Dispositivi di misurazione del gas su base oraria. Parte 6: Requisiti per gruppi di misura con portata minore di 10 m<sup>3</sup>/h (contatore < G10). 2013.
- [157] European Commission. Direttiva 2014/34/UE. 2014.
- [158] MISE. Decreto 16/4/2012,. 2012.
- [159] UNI TS 11291-1:2013. Dispositivi di misurazione del gas su base oraria. Parte 1: Caratteristiche generali del sistema di telegestione o telelettura. 2013.
- [160] UNI TS 11291-3:2012. Dispositivi di misurazione del gas su base oraria. Parte 3: Protocollo CTR. 2012.
- [161] Saunders TG. The performance evaluation of lithium thionyl chloride batteries for long-life meter applications. Loughborough Univerisy, 1998.
- [162] Tadiran. Technical brochure LTC-batteries. 2012.
- [163] Erdinc O, Vural B, Uzunoglu M. A dynamic lithium-ion battery model considering the effects of temperature and capacity fading. 2009 Int Conf Clean Electr Power, ICCEP 2009 2009:383–6.
- [164] Pallivathikal M, Yamin H, Zak U. Abstract 82. Electrochem. Soc. Ext. Abstr., Florida: 1989.
- [165] Hoier SN, Eisenmann ET. The Faradaic efficiency of the Lithium-thionyl chloride battery. 1996.
- [166] Zhang Y, Harb JN. Performance characteristics of lithium coin cells for use in wireless sensing systems: Transient behavior during pulse discharge. J Power Sources 2013;229:299–307.
- [167] Zhang Y, Harb JN. Characterization of Battery Behavior for Battery-Aware Design of Wireless Sensing Networks. J Electrochem Soc 2015;162:A820–6.
- [168] Rodrigues LM, Montez C, Moraes R, Portugal P, Vasques F. A temperature-dependent battery model for wireless sensor networks. Sensors (Switzerland) 2017;17:1–24.